SCALABLE DESIGN SYNTHESIS FOR AUTOMOTIVE ASSEMBLY SYSTEM
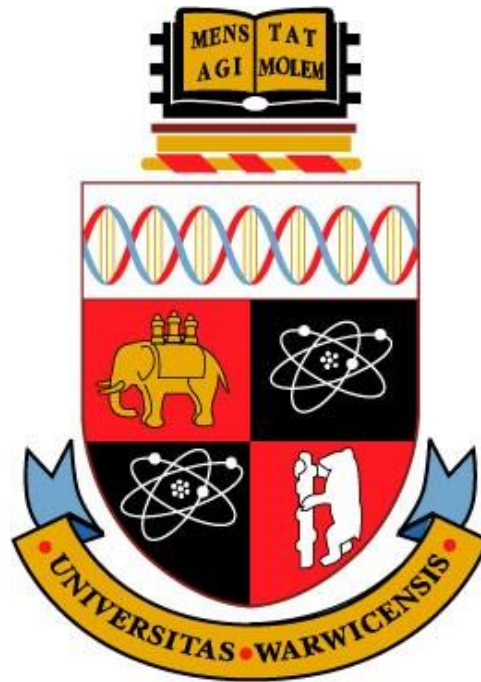
By

Avishek Pal

A thesis submitted in partial fulfillment of the requirements for the degree of

Doctor of Philosophy in Engineering

Warwick Manufacturing Group

University of Warwick

August 2015

DEDICATION

To my parents and my sister for their endless love and support

ABSTRACT

Frequent product model changes have become a characteristic feature in new product development and modern manufacturing. This has triggered a number of requirements such as shortening new product development time and production ramp-up time with simultaneous reduction of avoidable engineering changes and overall vehicle development cost.

One of the most significant challenges when reducing new model development lead time is the large number of engineering changes, that are triggered by failures during production ramp-up stage but are unseen during design. In order to reduce engineering changes during ramp-up stage and also increase Right-First-Time development rate, there is a critical demand for improving quality of integrated product and production system design solutions. Currently, this is obtained by carrying out design synthesis which focuses on design optimization driven by computer simulation and/or physical experimentation.

The design synthesis depends on the quality of the used surrogate models, which integrate critical product variables, (also known as Key Product Characteristics (KPCs)), with key process variables (Key Control Characteristics (KCCs)). However, a major limitation of currently existing surrogate models, used in design synthesis, is that these simply approximate underlying KPC-KCC relations with any deviation between the actual and predicted KPC assumed to be a simple random error with constant variance. Such an assumption raises major challenges in obtaining accurate design solutions for a number of manufacturing processes when: (1) KPCs are deterministic and non-linearity is due to interactions between process variables (KCCs) as is frequently the case in fixture design for assembly processes with compliant parts; (2) KPC stochasticity is either independent of (homo-skedastic) or dependent on (hetero-skedastic) on process variables (KCCs) and there is lack of physics-based models to confirm these behaviour; as can be commonly observed in case of laser joining processes used for automotive sheet metal parts; and, (3) there are large number of KCCs potentially affecting a KPC and dimensionality reduction is required to identify few critical KCCs as commonly required for diagnosis and design adjustment for unwanted dimensional variations of the KPC.

This thesis proposes a generic *Scalable Design Synthesis* framework which involves the development of novel surrogate models which can address a varying scale of the KPC-KCC interrelations as indicated in the aforementioned three challenges. The proposed *Scalable Design Synthesis* framework is developed through three interlinked approaches addressing each aforementioned challenge, respectively:

i. Scalable surrogate model development for *deterministic non-linearity of KPCs characterized by varying number of local maximas and minimas*. *Application*: *Fixture layout optimization for assembly processes with compliant parts.* This is accomplished in this thesis via (1) Greedy Polynomial Kriging (GPK), a novel approach for developing Kriging-based surrogate models for deterministic KPCs focusing on maximization of predictive accuracy on unseen test samples; and, (2) Optimal Multi Response Adaptive Sampling (OMRAS) a novel method of

accelerating the convergence of multiple surrogate models to desired accuracy levels using the same training sample of KCCs. GPK surrogate models are then used for fixture layout optimization for assembly with multiple sheet metal parts.

ii. Scalable surrogate model development for *stochasticity characterized by unknown homo-skedastic or hetero-skedastic behaviour of KPCs*. **Application**: *In-process laser joining processes monitoring and in-process joint quality evaluation*. Scalable surrogate model-driven joining process parameters selection, addressing stochasticity in KPC-KCC relations, is developed. A generic surrogate modelling methodology is proposed to identify and characterize underlying homo- and hetero-skedastic behaviour in KPCs from experimental data. This is achieved by (1) identifying a Polynomial Feature Selection (PFS) driven best-fitting linear model of the KPC; (2) detection of hetero-skedasticity in the linear model; and, (3) enhancement of the linear model upon identification of hetero-skedasticity. The proposed surrogate models estimate the joining KPCs such as weld penetration, weld seam width etc. in Remote Laser Welding (RLW) and their variance as a function of KCCs such as gap between welded parts, welding speed etc. in RLW. This information is then used to identify process window in KCC design space and compute joining process acceptance rate.

iii. Scalable surrogate model development for *high dimensionality of KCCs*. **Application**: *Corrective action of product failures triggered by dimensional variations in KPCs*. Scalable surrogate model-driven corrective action is proposed to address efficient diagnosis and design adjustment of unwanted dimensional variations in KPCs. This is realized via (1) PFS to address high dimensionality of KCCs and identify a few critical ones closely related to the KPC of interest; and (2) surrogate modelling of the KPC in terms of the few critical KCCs identified by PFS; and, (3) two-step design adjustment of KCCs which applies the surrogate models to determine optimal nominal adjustment and tolerance reallocation of the critical KCCs to minimize production of faulty dimensions.

All the aforementioned methodologies are demonstrated through the use of industrial case studies. Comparison of the proposed methods with design synthesis existing for the applications discussed in this thesis, indicate that scalable surrogate models can be utilized as key enablers to conduct accurate design optimization with minimal understanding of the underlying complex KPC-KCC relations by the user. The proposed surrogate model-based Scalable Design Synthesis framework is expected to leverage and complement existing computer simulation/physical experimentation methods to develop fast and accurate solutions for integrated product and production system design.

ACKNOWLEDGEMENTS

DECLARATION

This thesis is presented in accordance with the regulations for the degree of Doctor of Philosophy. It has been written by myself and has not been submitted anywhere else. The work in this thesis has been undertaken by me except where otherwise stated.

TABLE OF CONTENTS

VII

LIST OF TABLES

LIST OF FIGURES

XIV

LIST OF PUBLICATIONS

Conference papers

Pal, A., Franciosa, P., & Ceglarek, D., 2014. Root cause analysis of product service failures in design-A closed-loop lifecycle modelling approach. In Proceedings of 24th CIRP Design Conference, Milan, Italy, pp. 165-170

Pal, A., Franciosa, P., & Ceglarek, D., 2014. Corrective Actions of Product Service Failures via Surrogate Modelling of Dimensional Variations. In Proceedings of the 2014 Industrial and Systems Engineering Research Conference, Institute of Industrial Engineers, Montreal, Canada, pp. 2271-2280

Journal papers

Pal, A., Franciosa, P., Prakash, PKS., & Ceglarek, D., 2015. Surrogate modelling for computer simulations via Greedy Polynomial Kriging and Optimal Multi Response Adaptive Sampling. To be submitted to IEEE Transactions on Systems, Man, and Cybernetics: Systems

Pal, A., Franciosa, P., & Ceglarek, D., 2015, Homo- and hetero-skedastic surrogate modelling for parameter selection in industrial joining processes. To be submitted to The International Journal of Advanced Manufacturing Technology

Pal, A., Franciosa, P., & Ceglarek, D., 2015. Corrective Actions of Product Service Failures through Surrogate Modelling of Dimensional Variations. To be submitted to International Journal of Production Research

ABBREVIATIONS

ARF: Assembly Response Function

BIW   Body-In-White

CA: Corrective Actions

CART: Classification and Regression Trees

DA: Design Adjustments

EGO: Efficient Global Optimization

GBM: Gradient Boosting Machine

GPK: Greedy Polynomial Kriging

KCC: Key Control Characteristic

k-NN: k-Nearest Neighbours

KPC: Key Product Characteristic

KPI: Key Performance Indicator

LTW: Laser Transmission Welding

NN: Neural Network

OK: Ordinary Kriging

O-MRAS: Optimal Multi Response Adaptive Sampling

PFS: Polynomial Feature Selection

RFT: Right-First-Time

RLW: Remote Laser Welding

RSW: Resistance Spot Welding

SDS: Scalable Design Synthesis

SPR: Self-Piercing Riveting

SVM: Support Vector Machine

VSA: Variation Simulation Analysis

URS: Uniform Random Sampling

LAD: Lifecycle Analytics Development

CHAPTER 1
INTRODUCTION

1.1   Motivation

In recent years frequent model changes triggered due to rapidly changing customer preferences have become a prevailing trend in the automotive industry. To remain competitive, automobile manufacturers must accommodate frequent changes not only in an automotive body design but also as a consequence in an automotive body assembly system. Under these requirements, manufacturers strive to maximize their return on investment from every assembly production system by shortening new product development time and production ramp-up time with simultaneous reduction of avoidable engineering changes and overall vehicle development cost.

One of the most significant challenges when reducing new model development lead time is the large number of engineering changes, that are triggered by failures during production ramp-up stage but are unseen during design. This is important as product development time and production ramp-up time strongly depends on the ratio of 'Right-First-Time' strategy, which tries to eliminate additional changes after the design phase. For example, according to a 1999 survey conducted by the University of Michigan, it is estimated that top automotive manufacturers reach up to 80% 'Right-First-Time' during design stage, with many manufacturers in the range of 50%-80% (Ceglarek, *et al*., 2004).   Also, it was reported that in aerospace and automotive industries 67-70% of all design changes are related to product dimensional variation (Shalon, *et al*., 1992; Ceglarek & Shi, 1995).

In order to reduce engineering changes during ramp-up stage and also increase 'Right-First-Time' development rate, there is a critical demand for improving

quality of integrated product and production system design solutions. Currently, this is obtained by carrying out design synthesis which focuses on design optimization driven by computer simulation and/or physical experimentation.

Frequently, the design synthesis approaches uses a functional mapping, which integrate critical product variables (also known as Key Product Characteristics (KPCs)), with key process variables (Key Control Characteristics (KCCs)). The functional mapping from KCCs to KPCs provides a mathematical representation of the physical process through which KPCs are to be achieved by KCCs during production. The main objective of the design synthesis is to optimize selected cost/quality based Key Performance Indicators (KPIs) using the KPC-KCC functional mappings. Additionally, the optimization is constrained by KPC design tolerances which define the range for acceptable product quality and KCC design constraints which define operating limits of process variables in the specific assembly system.

Few notations are introduced as follows before describing an example of an individual design synthesis task for assembly system optimization.

Notations

d	Number of Key Control Characteristics (KCCs)
r	Number of Key Product Characteristics (KPCs)
$\mathbf{x}$	'd' KCCs related to a given design synthesis task $\mathbf{x} = \{x_1, x_2, ..., x_d\}$
$\mathbf{y}$	'r' KPCs related to a design synthesis task $\mathbf{y} = \{y_1, y_2, ..., y_r\}$
y	Any individual KPC related to a design synthesis task such that $y \in \mathbf{y}$
$\boldsymbol{\Phi}$	Key Performance Indicators (KPIs) related to a given design synthesis task and expressed as functions of KCCs and KPCs
$\mathbf{A}$	Assembly response function (ARF) which is a $r \times d$ matrix integrating 'd' KCCs with 'r' KPCs
c_{ij}	Coefficient in ARF integrating i^{th} KPC with j^{th} KCC
$\boldsymbol{\psi}_{\text{KCC}}$	Operating limits of KCCs

$\boldsymbol{\psi}_{\mathrm{KPC}}$	Design tolerances of KPCs
$\mathbf{x}^{*}$	Optimal KCCs obtained after running design synthesis
$\mathbf{y}^{*}$	Optimal KPCs obtained after running design synthesis
n	Number of computer simulations/physical experimentations performed
S_{T}	Training dataset generated by computer simulations/physical experimentations and having 'n' samples of KCCs '$\mathbf{x}$' and a KPC 'y'
$\mathbf{x}_i$	i^{th} sample of KCCs '$\mathbf{x}$' obtained from computer simulation/physical experimentation where $i = \{1,2,...,n\}$
y_i	i^{th} sample of KPC 'y' obtained from computer simulation/physical experimentation where $i = \{1,2,...,n\}$
$\hat{y}_i$	i^{th} value of KPC 'y' predicted by its surrogate model where $i = \{1,2,...,n\}$
$\overline{y}$	Average value of KPC 'y' obtained from 'n' samples *i.e.* $\overline{y} = \dfrac{1}{n}\sum_{i=1}^{n} y_i$
δ_i	Deviance between actual 'y_i' and predicted '$\hat{y}_i$' KPC *i.e.* $\delta_i = y_i - \hat{y}_i$ where $i = \{1,2,...,n\}$
P	Probability distribution followed by δ_i where $i = \{1,2,...,n\}$
$\boldsymbol{\theta}$	Parameters of the probability distribution P such that $\delta_i \sim \mathrm{P}(\boldsymbol{\theta})$
R^2	Degree of determination

An individual design synthesis task for assembly system optimization consists of three components which are:

i. Assembly response function (ARF) model which integrates KPCs with KCCs. Eq. (1.1) shows a linear ARF mapping from 'd' KCCs to 'r' KPCs.

$$\begin{bmatrix} KPC_1 \\ KPC_2 \\ \vdots \\ KPC_r \end{bmatrix}_{r \times 1} = \begin{bmatrix} c_{11} & c_{12} & \cdots & c_{1,d} \\ c_{21} & c_{22} & \cdots & c_{2,d} \\ \vdots & \vdots & \ddots & \vdots \\ c_{r,1} & c_{r,2} & \cdots & c_{r,d} \end{bmatrix}_{r \times d} \begin{bmatrix} KCC_1 \\ KCC_2 \\ \vdots \\ KCC_d \end{bmatrix}_{d \times 1} \quad \text{or } \mathbf{y} = \mathbf{A}\mathbf{x} \qquad (1.1)$$

where $c_{i,j}$ is a constant value derived from analysis of the physical process

through which KPCs are achieved by KCCs. For example Ceglarek and Shi (1996) suggested to link assembly product variables (KPCs) with assembly process variables (KCCs) such as position of fixture locators. This approach was then generalized to Stream-of-Variation Analysis (SOVA) for multi-station assembly processes with rigid parts by Hu (1997), Jin and Shi (1999), Huang, *et al*. (2007a; 2007b), Phoomboplab and Ceglarek (2008) and by Camelio, *et al*. (2003), Wang and Ceglarek (2005) to multi-station assembly processes with compliant parts. In their case, $c_{i,j}$ are the coefficients of linear KPC-KCC models obtained from state-space modelling and analysis of assembly processes with compliant parts.

ii. KPI model is selected as a specific objective function of an individual design task and expressed in terms of KPCs ($\mathbf{x}$) and KCCs ($\mathbf{y}$) as shown in Eq. (1.2)

$$\text{KPI} = \boldsymbol{\Phi}(\mathbf{x}, \mathbf{y}) \tag{1.2}$$

iii. Optimization algorithms to minimize/maximize the selected KPI model to determine optimal KCCs ($\mathbf{x}^*$) and KPCs ($\mathbf{y}^*$). Eq. (1.3) gives a generic representation of the optimization problem.

$$\mathbf{x}^*, \mathbf{y}^* = \underset{\mathbf{x} \in \psi_{KCC}, \mathbf{y} \in \psi_{KPC}}{\arg\min} \boldsymbol{\Phi}(\mathbf{x}, \mathbf{y}) \tag{1.3}$$

where ψ_{KCC} represent design constraints of KCCs and ψ_{KPC} indicate design tolerances of KPCs.

Table 1.1 provides a few examples of design synthesis tasks related to a typical automotive body (Body-in-white (BIW)) assembly system and their corresponding KCCs, KPCs and KPIs.

Table 1.1: Examples of design synthesis and related KCCs, KPCs and KPIs

Design synthesis tasks	Related KCCs	Related KPCs	Related ARF	Related KPIs	Related articles
Product-oriented tolerance synthesis of part fabrication by machining	Component dimensions	Assembly dimensions	Assembly function based on kinematic analysis	- Quality loss due KPC deviance from nominal - Cost of manufacturing required tolerance of KCCs	Chase (1999)
Process-oriented tolerance synthesis of multi-station assembly process	- Part locating layout (position of locators) - Locating layout changes between stations	- Design dimensions of finished assembly - Working dimensions of intermediate workpieces	SOVA state-space model for multi-station assembly process	Cost of tolerance allocation to KCCs	- *2D rigid bodies*: Ding, *et al.* (2005) - *3D rigid bodies*: Huang, *et al.* (2007a; 2007b)
Fixture layout optimization in multi-station assembly	- Part locating layout (position of fixture locators) - Variation in locator positions	Gaps, inclinations between mating parts	SOVA design matrix (Ding, *et al.*, 2005; Huang, *et al.*, 2007 a, b)	Process yield computed as probability of all KPCs within design tolerances	Phoomboplab and Ceglarek (2008)

Abbreviations: KCCs – Key Control Characteristics; KPCs – Key Product Characteristics; KPIs – Key Performance Indicators

As evident from the aforementioned discussion, a key requirement for conducting design synthesis is the development of the ARF which provides the functional mapping between KCCs and KPCs as shown in Eq. (1.1). However, for complex sheet metal assemblies such as those used for automotive BIW, a comprehensive and practically useful ARF for design synthesis is seldom available. Instead, either computer simulation of complex multi-physics based Variation Simulation Analysis (VSA) or physical experimentation is used to study the relationship between KCCs and KPCs as design analysis rather than as design synthesis.

In general, VSA and/or experimentation are generally not sufficient for extensive design synthesis for at least two reasons. First, efficient global optimization and hence, quality of final solution is limited by computationally expensive VSA or resource intensive physical experimentation. Next, fault diagnosis and process adjustment are challenging due to numerical intractability of VSA and/or physical experimentation.

Few studies have been done to address the aforementioned limitations of VSA and physical experimentation that affect design synthesis. These works develop statistical predictive models of KPCs in terms of KCCs. The statistical predictive models, also known as surrogate models of KPCs, are then used in design synthesis as computationally cheap and numerically tractable surrogates for VSA and physical experimentation (Huang, *et al.*, 2009). Typically, surrogate model of a KPC 'y' is

developed by analyzing a training dataset $S_T = \{\mathbf{x}_i, y_i\}_{i=1}^n = \begin{bmatrix} x_{11} & x_{12} & ... & x_{1r} & y_1 \\ x_{21} & x_{22} & ... & x_{2r} & y_2 \\ \vdots & \vdots & \ddots & \vdots & \vdots \\ x_{n1} & x_{n1} & ... & x_{nr} & y_n \end{bmatrix}$

which is generated by running computer simulation or physical experimentation,

where 'n' is the number of simulations or experiments, $\mathbf{x}_i$ are KCCs and y_i is KPC of the ith simulation or experiment.

In design synthesis, currently existing surrogate models, which are developed through data analysis, give an approximation of the underlying interrelation between KPCs and KCCs. Any deviance δ_i between actual (y_i) and predicted ($\hat{y}_i$) KPC is assumed to originate from random numerical error of simulation or measurement error of experimentation. Mathematically, the aforementioned assumption is formulated as a probability distribution, $\delta_i \sim \mathrm{P}(\boldsymbol{\theta})$ whose parameters $\boldsymbol{\theta}$ are considered to be constant and independent of the KCCs. This approach is illustrated by Figure 1.1 in which a black dot represents an actual sample obtained from simulation or experimentation and the blue dotted line is the approximation provided by the surrogate model of KPC 'y'.
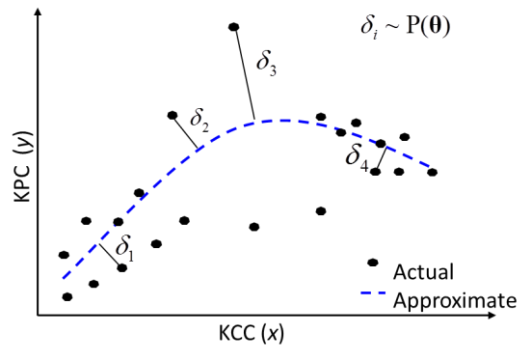
Figure 1.1: Approximation by surrogate model of homogenous deviance

The assumption made by the aforementioned approach raises major challenges in obtaining quality solutions for design synthesis when:

i. *KPCs exhibit varying deterministic non-linearity characterized by varying number of local maximas and minimas*

For computer simulations which have negligible or no numerical error, KPCs

are deterministic and the assumption that the deviance δ_i has a probability distribution with constant parameters $\boldsymbol{\theta}$ has the following issues:

- The assumption is inadequate for developing surrogate models of deterministic KPC-KCC interrelations. In case of deterministic KPC-KCC interrelations, δ_i is not the numerical error of VSA but it is the prediction error of the surrogate model for the ith sample.

- A surrogate model developed with this assumption merely approximates the global trend in the KPC and gives higher prediction error near local maximas/minimas thereby undermining the overall accuracy of the surrogate model.

- Surrogate models developed with this assumption might have acceptable accuracy when there are few maximas and minimas in the KPC-KCC interrelations. However, because these surrogate models approximate only the global trend in the KPC, their accuracy suffers when a large number of local maximas and minimas are present.

Due to the aforementioned issues, current surrogate models for design synthesis cannot cope with varying deterministic non-linearity which is characterized by varying number of local maximas and minimas present in the KPC-KCC interrelations. Current surrogate models' lack of scalability for varying deterministic non-linearity is critical particularly when the design synthesis task requires acceptably accurate surrogate models but the number of local maximas and minimas in the KPC-KCC interrelations, depending on the underlying physical process, varies from case to case and therefore is unforeseen. As an example consider, VSA which models the effect of fixture KCCs such as clamp locations on assembly KPCs such as gap between mating

8

parts. The interaction between KCCs and KPCs in this case is sensitive to dimensional and geometrical variations of the mating parts, also known as part variations and can vary from rigid to compliant. As a result of varying scale of part compliancy, the underlying KPC-KCC interrelations might have an unforeseen number of local maximas and minimas as illustrated by Figure 1.2.
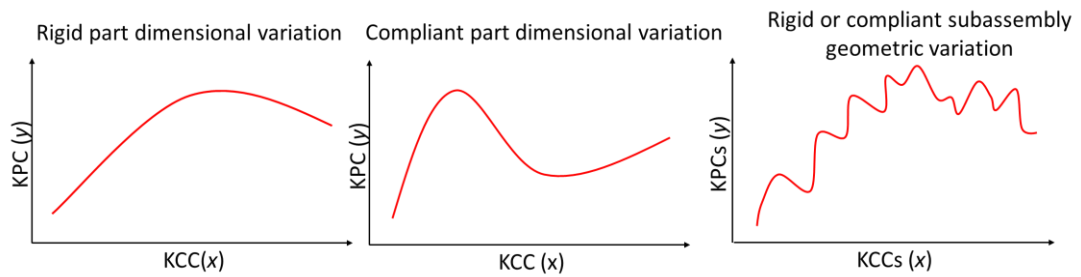
Figure 1.2: Varying non-linearity in KPC-KCC interrelations based on part error type

ii. _KPCs exhibit varying stochasticity characterized by unknown homo- and hetero-skedastic behaviour_

In design synthesis tasks based on physical experimentation, the KPC (y) has stochastic variations which might be homo-skedastic (random noise due to measurement errors and independent of KCCs) or hetero-skedastic (systematic variance and dependent on KCCs). Therefore, current surrogate model based on the assumption of constant θ has the following challenges:

- It ignores underlying hetero-skedastic behaviour associated with a KPC whereby the δ_i is not a random noise but a systematic variance which is dependent on KCCs

- It overlooks mixed behavior where some KPCs are homo-skedastic whereas others are hetero-skedastic.

- Constant θ is a strong assumption, especially if: (1) surrogate modelling is

9

done using experimental data where KPCs are subjected to errors; and, (2) there is lack of comprehensive and useful *first-principle* models, based on physical laws, to confirm the actual KPC behaviour. As an example, there is lack of *first-principle* models for all the industry recommended KPCs related to properties of lap joints produced by Remote Laser Welding (RLW) (Michalos, *et al.*, 2010).

Due to the aforementioned limitations, current surrogate models for design synthesis are not able to address the varying KPC stochasticity, which can be either homo-skedasticity or hetero-skedasticity. This limitation significantly affects the quality of solution for certain design synthesis tasks. For example, for joining process parameter selection, lack of understanding about homo- and hetero-skedasticity of joint KPCs such as weld penetration, weld bead width etc., in case of RLW, would lead to incorrect characterization of control limits of the KPCs and inaccurate computation of joining process acceptance rate (or fallout rate). Figure 1.3 illustrates homo- and hetero-skedasticity in KPCs and their consequence on estimation of KPC control limits.
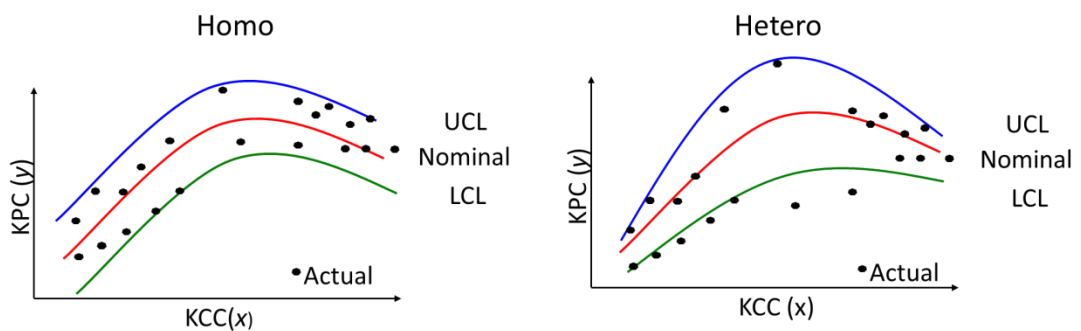
Figure 1.3: Homo- and hetero-skedastic behaviour of KPCs

iii.   *KPC-KCC interrelations exhibit high dimensionality of KCCs and there is*

10

requirement to identify few critical KCCs from a larger set of all given KCCs

In a complex production system involving a large number of KCCs, a KPC might be affected by all the KCCs or by a few critical ones. However, with lack of information about the physical process governing the behaviour of each KPC, the actual number of KCCs closely related to a KPC is unknown. Hence, KPC-KCC interrelations apparently exhibit higher than needed dimensionality of KCCs.

Current surrogate models for design synthesis do not consider dimensionality reduction of KCCs making them unsuitable for design synthesis tasks such as cost-effective corrective action to reduce unwanted variations of KPCs which require identification and adjustment of few critical KCCs related to a particular KPC. Finding critical KCCs can be a challenging task especially with lack of a closed-form analytical assembly transfer function (ARF) linking KPCs and KCCs in complex assemblies where KPCs are estimated from KCCs based on *first-principle* analyses done using VSA software.

Therefore, as evident from the discussion presented in this section, surrogate models are critical for facilitating design synthesis when design optimization has to rely on computer simulation and/or physical experimentation. However, current surrogate models for design synthesis have three major limitations:

- They do not address the capability to cope with varying deterministic non-linearity in KPC-KCC interrelations characterized by varying number of local maximas and minimas
- They lack the capability to identify and characterize varying stochasticity of KPC-KCC interrelations which can be either homo- or hetero-skedastic
- In case of high dimensionality, they do not have capability to identify few critical

11

KCCs closely related to a particular KPC.

This thesis develops three inter-linked approaches each addressing an aforementioned limitation in the context of a design synthesis task.

1.2 Current Requirements and the Proposed Research Framework for Scalable Design Synthesis

The key issue with the state-of-the-art surrogate models for design synthesis is that they do not address varying scales of the following three characteristics of KPC-KCC interrelations: (1) deterministic non-linearity; (2) stochasticity and; (3) high dimensionality of KCCs. Hence for design synthesis, there is need for surrogate modelling, which can identify and model varying scales of the specific characteristic which is most critical to achieving quality solution in a given design synthesis task. To this end, two concepts are proposed in this thesis. Firstly, it introduces the concept of '*scalable surrogate modelling*'. Secondly, *Scalable Design Synthesis* is proposed which is based on integration of resulting scalable surrogate models with optimization routines to realize a specific design synthesis task.

Section 1.2.1 elaborates on the need and objectives of '*scalable surrogate modelling*'. Next, Section 1.2.2 describes the framework for *Scalable Design Synthesis*.

1.2.1 Scalable surrogate modelling

In the context of design synthesis, this thesis defines 'scalable surrogate modelling' as the method of developing surrogate models with capabilities to cope with varying scale of the aforementioned three characteristics that might be present in the KPC-KCC interrelations through data analysis and minimal understanding of the underlying physical process.. The key aspect of 'scalable surrogate modelling' is

'scalability'.

In general terms 'scalability' can be defined as the capability of a system or entity to respond to changes in input in order to generate output while meeting required performance measures or maintaining a low variation in the performance measures. For example, 'scalable' manufacturing systems produce required number of units for varying demand volumes by suitably adjusting manufacturing resources and maintaining a constant or minimal variance lead time (ElMaraghy, 2005; Koren & Shpitalni, 2010). The key aspect of 'scalable' manufacturing systems is the capability to accommodate lesser or greater demand volumes by adjusting production capacity to produce lesser or greater number of units in order to maintain the same lead time of production or incur minimal variance of it. Lead time of production is the performance measure and maintaining it to a constant or minimising its variation between instances of changing demand volumes is the objective of 'scalable' manufacturing systems. Here scalability is achieved by removing or adding manufacturing resources such as machines, operators etc.

Let us now describe '*scalability*' as proposed in the scope of this thesis. In this thesis, '*scalability*' is defined as the algorithmic capability of surrogate modelling methods to generate surrogate models of *acceptable accuracy of prediction* for varying degrees of the following three characteristics:

- deterministic non-linearity which is can vary from single maxima/minima to multiple maximas/minimas
- stochasticity which can vary from homo- to hetero-skedasticity
- dimensionality of KCCs which can vary from few critical KCCs to a large number of KCCs closely related to a KPC of interest

The key expectation of scalable surrogate models is to meet *acceptable*

13

accuracy of prediction under varying conditions of the aforementioned three characteristics. Here *accuracy of prediction* is the performance measure. To quantify *accuracy of prediction*, the degree of determination or R^2 is used in this thesis as a metric of *'goodness'* of the surrogate model. For a dataset $\mathbf{S}=\{\mathbf{x}_i, \mathbf{y}_i\}_{i=1}^{n}$ on 'n' observations of KCCs ($\mathbf{x}$) and a KPC (y), R^2 is defined as follows

$$R^2 = 1 - \frac{\sum_{i=1}^{n}(y_i - \hat{y}_i)^2}{\sum_{i=1}^{n}(y_i - \overline{y})^2} \tag{1.4}$$

where $\overline{y}$ is the average of the KPC 'y' obtained from the 'n' test samples as $\overline{y} = \frac{1}{n}\sum_{i=1}^{n} y_i$. R^2 varies from 0 to 1 where a higher value indicates better model accuracy.

The desired or *acceptable accuracy of prediction* as measured by R^2 is defined by the user and depends on the design synthesis task. For example, surrogate models of computer simulations such as VSA are expected to have high accuracy as the surrogate models will be used as replacement of actual VSA in design synthesis tasks such as fixture layout optimization which requires maintaining part-to-part gaps within tight design tolerances. Deviances between actual and predicted KPCs might introduce costly errors in fixture layout design. Hence R^2 in this case can be set to be greater than 0.90.

In summary, a '*scalable*' surrogate model is expected to achieve desired accuracy as measured by R^2 for KPC-KCC interrelations for which the aforementioned three characteristics is unforeseen and changes from case to case. Figure 4 shows a schematic representation of the concept of scalable surrogate modelling.
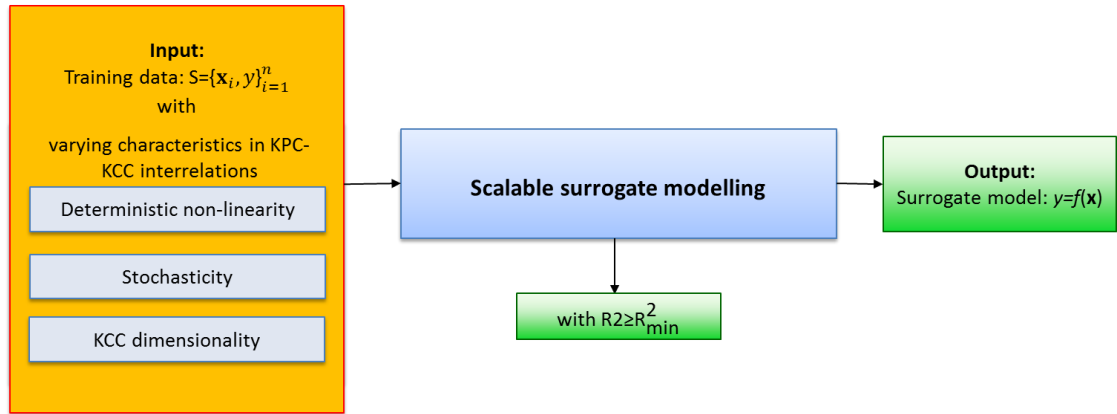
Figure 1.4: Conceptual overview of scalable surrogate modelling

Based on the aforementioned definition, this thesis develops methodologies of 'scalable surrogate modelling' to provide the following algorithmic capabilities:

i. *Scalability for deterministic non-linearity of KPCs characterized by varying number of local maximas and minimas* – For computer-based VSAs, the scale of the deterministic non-linearity of KPCs can vary from having single maxima/minima to multiple maximas/minimas. Therefore, design synthesis tasks, which require accurate surrogate models of KPCs, would benefit from a surrogate modelling method which, irrespective of the actual number of local maximas and minimas present within the KPC-KCC interrelations, can develop surrogate models with acceptable accuracy on *unseen test samples*.

In this thesis, *scalability for deterministic non-linearity of KPCs* is defined as the algorithmic capability to develop surrogate models with *acceptable accuracy* on *unseen samples* for systems with varying non-linearity of KPC-KCC interrelations. The varying non-linearity of KPC-KCC interrelations is measured by the varying number of local *maximas/minimas* present in the data.

Additionally, *scalability for deterministic non-linearity* emphasizes that overfitting a limited sample of points available in the training data, such as through fitting high order polynomial regression, should be avoided to ensure that the surrogate models have acceptable accuracy on *unseen test samples*. Scalability for deterministic non-linearity is addressed in the development of scalable surrogate model for fixture layout optimization presented in Chapter 3.

ii. *Scalability for stochasticity characterized by unknown homo-skedastic or hetero-skedastic behaviour of KPCs* – There is lack of comprehensive and useful *first-principle* based methods to model the relationship between KCCs and KPCs in some joining processes such as resistance spot welding of TRIP steels (Kim, *et al*., 2005) or CO_2 laser welding process of austenitic stainless steel (Benyounis, *et al*., 2005) etc. In such cases, selection of optimal joining process parameters is done by developing surrogate models of joint KPCs from experimental data which is subjected to noise. The noise associated with experimental data might be random KCC independent measurement error or systematic KCC dependent variation.

> This thesis defines *scalability for stochasticity* as the algorithmic capability to identify and characterize varying types of stochasticity in the KPCs by analysing the training data.

Chapter 4 develops scalable surrogate models for joining process parameters selection taking into account different types of stochasticity present in joint KPCs.

iii. *Scalability for high dimensionality of KCCs* – High dimensionality is a common issue in complex assembly systems whereby large number of KCCs can potentially affect variations in a KPC (Shi & Zhou, 2009). Identifying few critical KCCs is required for many of the design synthesis tasks such as root cause diagnosis of unwanted variations of a KPC and subsequent KCC adjustment for example through tolerance reallocation of assembly process.

> In this thesis, *scalability for KCC dimensionality* is defined as the algorithmic capability to identify a few critical KCCs related to a KPC and develop a surrogate model of acceptable accuracy using the identified important KCCs.

Chapter 5 presents methodology for surrogate model driven diagnosis and design adjustment of KCCs to reduce unwanted dimensional variations of KPCs. The developed methodology presents a surrogate model with the capability for handling problems of varying KCC dimensionality (scalability for KCC dimensionality)

1.2.2   Framework for Scalable Design Synthesis

The previous section describes the algorithmic capabilities needed for scalable surrogate modelling. The scalable surrogate models are necessary for many design synthesis tasks as discussed in the previous section. The proposed scalable design synthesis is based on integration of the scalable surrogate model(s) with optimization routines to achieve design objectives.

This section outlines a generic framework for Scalable Design Synthesis which includes: (1) scalable surrogate modelling of KPCs; and, (2) integration of KPC surrogate models with optimization routines to realize the objectives of a particular design task such as: (2A) fixture layout optimization of assembly processes with multiple compliant parts; (2B) assembly joining process parameter selection; and, (2C) corrective action of unwanted dimensional variations in assembly KPCs. The proposed framework provides generic guidelines for developing design synthesis methodologies driven by scalable surrogate models.

Figure 1.5 shows a schematic representation of the proposed framework for Scalable Design Synthesis presented in the context of assembly system. In Step 1, data from computer simulation such as VSA or physical experimentation is used for scalable surrogate modelling. The resulting surrogate models are then used for optimization of KPI in Step 2. KPI, derived as function of KCCs and KPCs, is the objective function for the optimization which is subjected to constraints defined by KPC design tolerances and KCC operating limits.
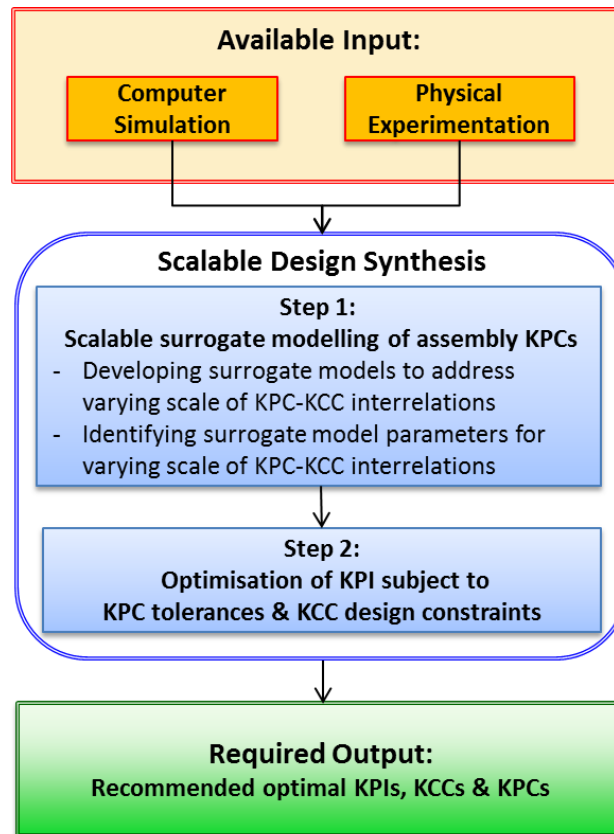
Figure 1.5: Framework of Scalable Design Synthesis for assembly system

The framework of Scalable Design Synthesis is presented in the context of the following applications:

i. *Fixture layout optimization* – Automotive body-in-white or aerospace fuselage and wings are made of deformable sheet metal panels, which are assembled in compliance with part-to-part gap tolerance required by the joining process. Fixtures control the position and orientation of the parts in an assembly process to satisfy geometric and dimensional tolerating (GD&T) of assembly or intermediate requirements as related to a specific assembly process for example, part-to-part gap variation in Remote Laser Welding (RLW). VSA for assembly processes with compliant (deformable) parts are based on deterministic simulation using Finite Element Method (FEM) to model part-to-part gaps (KPCs) for sheet metal assembly for given clamp locating layouts (KCCs)

19

(Rong, *et al*., 2000; Camelio, *et al*., 2003; Franciosa, *et al*., 2011). However, VSA is computationally expensive and causes optimization of fixture locating layout design to be a time consuming process. Hence, there is a very strong need for having surrogate models.

However, surrogate modelling of deterministic KPC-KCC interrelations by using VSA-based simulations of assembly processes with compliant parts is particularly challenging due to at the least the following factors:

- part compliancy or deformability which causes variations in a KPC to be sensitive to variations in multiple KCCs

- part geometry characterised by curvatures which also affects the dependency of variations in a KPC on variations in multiple KCCs (Li, *et al*., 2001; Franciosa, *et al*., 2011)

- initial location and alignment of clamps etc. which are set by the user and varies from case to case (Li, *et al*., 2001; Li & Shiu, 2001; Li, 2002)

As a result, the scale of deterministic non-linearity which can be characterized by varying number local maximas and minimas in KPC-KCC interrelations is unforeseen and differs from case to case. To address the varying scale of deterministic non-linearity through analysis of data from VSA, a scalable surrogate modelling method is developed which can take into consideration varying non-linearity as measured by the number of local maximas and minimas in the underlying KPC-KCC interrelations.

Additionally, the resulting surrogate models can include part-to-part gaps as KPCs and thus can be used in fixture layout optimization to determine optimal clamp locating layout which will minimize the objective function for example KPI related to quality loss due to KPC variations. Chapter 3 presents

the proposed methodology for scalable surrogate modelling driven fixture layout optimization for compliant part assemblies.

ii. *Joining process parameters selection* – KPCs related to assembly joints defines joint quality and in general depend on joining process parameters (KCCs) such as power and speed in case of RLW. Due to lack of reliable *first principle* models characterizing KPC-KCC interrelations for many industrial joining processes such as RLW, KPC-KCC interrelations needs to be developed based on noisy experimental data which includes varying noise types. Therefore, scalable surrogate modelling is required to take into consideration unknown homo- and hetero-skedastic experimental data of KPCs and KCCs. The developed surrogate models can then be used to determine optimal joining process parameters (KCCs) which satisfy the tolerance criteria of KPCs and optimizes KPIs objectives such as process throughput or production yield (Phoomboplab and Ceglarek, 2008). Moreover, estimation of mean and variance of KPCs as function of given KCCs can also be used to identify process window and acceptance rate of making joints of acceptable quality. Chapter 4 describes the methodology for scalable surrogate modelling driven joining process parameters selection.

iii. *Corrective actions of unwanted dimensional variation of KPCs via diagnosis and design adjustment* – The performance of mechanical assemblies depend on functional KPCs such as geometric features like part-to-part gaps, interferences, etc. which directly affect a product functionality required by the user. Unwanted dimensional variations of functional KPCs results in malfunctioning of the assembly. Under these conditions, design adjustment of KCCs affecting the functional KPCs is required and can be achieved via

21

optimal tolerance allocation (Shiu, *et al*., 2003; Huang, *et al*., 2009). Though *first principle* kinematic-based models are useful for estimating KPC-KCC interrelations, there is frequently lack of information allowing identification of a few critical KCCs which require tolerance reallocation for a specific KPCs. This problem is aggravated by high dimensionality of KCCs in complex assemblies where a KPC can be potentially affected by large number of KCCs. Therefore, cost-effective corrective actions require diagnosis of unwanted variation of KPC via identification of few critical KCCs followed by cost-driven design adjustment via tolerance reallocation of the assembly process. Chapter 5 addresses the issue of KCC dimensionality reduction for tolerance allocation by discussing a methodology for scalable surrogate modelling to identify few critical KCCs closely related to a KPC of interest.

1.3 Research Contributions

This thesis proposes a novel framework of Scalable Design Synthesis for assembly system. The proposed methodology is motivated by the requirements of early stage design synthesis of a modern automotive BIW assembly. Currently available advanced VSA-based simulation tools and multi-physics based experimentation, being resource intensive with numerically intractable solutions require development of surrogate models of KPC-KCC interrelations. However, state of the art on surrogate modelling for assembly process design does not sufficiently address the characteristics of KPC-KCC relationships rendering them inadequate for practical use. To address the limitations of existing methods, the main contribution of this thesis is to identify three different characteristics of KPC-KCC interrelations and their degree or scale of significance for developing surrogate models of assembly

KPCs. The three identified characteristics of KPC-KCCs interrelations are as follows:

i. *Deterministic non-linearity of KPCs characterized by varying number of local maximas and minimas*

ii. *Stochasticity of KPCs characterized by unknown homo- and hetero-skedastic behaviour of KPCs*

iii. *High dimensionality of KCCs potentially affecting a given KPC*

Based on the aforementioned characteristics, this thesis proposes scalable surrogate modelling methodologies to address varying scales of characteristics present in the KPC-KCC interrelations of an assembly system. Specifically, the following algorithmic capabilities are proposed for development of scalable surrogate models:

i. *Scalability for deterministic non-linearity of KPCs*

ii. *Scalability for stochasticity of KPCs*

iii. *Scalability for dimensionality of KCCs*

The proposed framework of Scalable Design Synthesis provides a generic guideline for developing scalable surrogate models and utilizing them to solve optimization problems in a design synthesis task. Based on the proposed framework three methodologies are developed, each addressing a relevant problem of assembly system design synthesis task: (1) scalable surrogate modelling for fixture layout optimization exploring varying deterministic non-linearity in KPC-KCC interrelations (Chapter 3); (2) scalable surrogate modelling for joining process parameters selection addressing varying stochasticity in KPC-KCC interrelations (Chapter 4); and, (3) surrogate modelling for corrective actions to reduce unwanted dimensional variations in assembly KPCs dealing with high dimensionality of KCCs (Chapter 5).

The research contributions of the proposed methodologies are as follows:

i. *Scalable surrogate model driven fixture layout optimization:*

- Complexity in fixture related KPC-KCC interrelations due to presence of underlying deterministic non-linearity is addressed through development of scalable surrogate models. The scalable surrogate models can adapt to the underlying non-linearity of KPC-KCC interrelations and generate acceptably accurate predictions without overfitting training data unlike polynomial regression models commonly used for design synthesis tasks.

- Scalable surrogate models for varying deterministic non-linearity is achieved by: (1) Greedy Polynomial Kriging (GPK) with a novel approach of tuning parameters and emphasis on the maximisation of the predictive accuracy for *unseen test samples*; and, (2) Optimal Multi Response Adaptive Sampling (O-MRAS) a novel method of accelerating the convergence of multiple surrogate models to desired accuracy levels using a single training sample.

- Comparison of performance between the developed GPK approach and popular state-of-the-art surrogate models shows higher predictive accuracy for *unseen test samples* obtained using the GPK approach. GPK's predictive accuracy is higher on an average by 30%, 55% and 44% than that of state-of-the-art Kriging, 2nd order polynomial regression and 3rd order polynomial regression, respectively. Moreover, case-studies on well-known benchmark functions are presented to demonstrate that O-MRAS accelerates convergence of surrogate models to desired accuracy levels faster than Uniform Random Sampling (URS). For the same number of simulations, accuracy levels of surrogate models developed via O-MRAS

24

is 35% higher than those trained by URS.

- Overall, a comprehensive methodology for fixture layout optimization for sheet metal assembly has been developed based on GPK surrogate models which are capable of generating accurate and realistic VSA results.

ii. Scalable surrogate model driven joining process parameters selection:

- Contrary to currently existing surrogate modelling of stochastic KPC-KCC interrelations which focuses only on homo-skedastic behaviour of KPCs, the proposed scalable surrogate modelling addresses varying stochastic behaviour of KPCs which can be homo- or hetero-skedastic.

- Training of the homo- and hetero-skedastic surrogate models is accomplished by (1) statistical detection of the actual stochastic behaviour of KPCs; and, (2) development of best-fitting homo- and hetero-skedastic models via Polynomial Feature Selection with a novel approach for identifying critical multiplicative interactions between KCCs and focus on maximizing predictive accuracy on *unseen test samples*.

- The proposed surrogate modelling methodology provides an estimation of both mean and variance of joints KPCs as a function of KCCs. On the other hand, state-of-the-art surrogate models are limited to estimation of only the KPC mean and assume KPC variance to be constant and independent of KCCs.

- The scalable surrogate models have been utilized in joining process parameters selection for the Remote Laser Welding process for BIW assembly. Results attained via the proposed methodology are compared with that obtained from currently existing 2nd order polynomial regression. Differences between the results show overestimation of acceptance rate by

currently existing surrogate models by an average of 41%.

iii. *Scalable surrogate model driven corrective action of product failures due to dimensional variations in KPCs:*

- A scalable surrogate modelling methodology has been developed to address high dimensionality of KCCs in complex assemblies and identify few critical KCCs closely related to a KPC of interest. The proposed methodology provides a data-driven approach which has been utilized for diagnosis of product failures.

- Training of the surrogate models of faulty KPCs in terms of a few critical KCCs has been achieved by Polynomial Feature Selection which identifies few critical KCCs and multiplicative interactions between them.

- Overall, a systematic approach for corrective actions of product failures due to dimensional variations of KPCs is developed by utilizing the surrogate models of faulty KPCs for KCC design adjustment via nominal change and tolerance reallocation.

- The proposed methodology is applied for corrective actions of electro-mechanical failure in an automotive ignition switch caused by unwanted dimensional variations of the KPCs closely related to the fault. Critical KCCs are identified for the faulty KPCs by dimensionality reduction of the complete set of KCCs related to the switch. The number of identified critical KCCs is on average 83% less than the total number of KCCs in the switch assembly. Moreover, design adjustment of KCCs reduces production yield of faulty KPCs by 34 percentage points.

1.4   Organization of the Thesis

Figure 1.6 illustrates the structure of this thesis.

```
┌─────────────────────────────────────────────────────────┐
│                     Chapter 1:                           │
│                     Introduction                         │
└─────────────────────────────────────────────────────────┘
                            │
                            ▼
┌─────────────────────────────────────────────────────────┐
│                     Chapter 2:                           │
│                  Literature Review                       │
└─────────────────────────────────────────────────────────┘
                            │
                            ▼
┌─────────────────────────────────────────────────────────┐
│                     Chapter 3:                           │
│   Scalable surrogate modelling driven fixture layout     │
│                     optimization                         │
└─────────────────────────────────────────────────────────┘
                            │
                            ▼
┌─────────────────────────────────────────────────────────┐
│                     Chapter 4:                           │
│           Scalable surrogate modelling driven            │
│          joining process parameters selection            │
└─────────────────────────────────────────────────────────┘
                            │
                            ▼
┌─────────────────────────────────────────────────────────┐
│                     Chapter 5:                           │
│           Scalable surrogate modelling driven            │
│  corrective action of product failures due to dimensional│
│                   variations in KPCs                     │
└─────────────────────────────────────────────────────────┘
                            │
                            ▼
┌─────────────────────────────────────────────────────────┐
│                     Chapter 6:                           │
│               Conclusions & Future Work                  │
└─────────────────────────────────────────────────────────┘
```

Figure 1.6: Research topics and organization of this thesis

Chapter 2 reviews past research on modelling KPC-KCC relations addressing (1) deterministic non-linearity of KPCs; (2) stochasticity of KPCs; and, (3) high dimensionality of KCCs affecting a KPC.

Chapter 3 describes the methodology for scalable surrogate modelling driven fixture layout optimization. Surrogate models of fixture related KPCs are developed by the proposed GPK and O-MRAS methods. KPC surrogate models are used for fixture layout optimization which minimizes quality loss due to deviance of KPCs from their prescribed design nominal.

Chapter 4 presents scalable surrogate modelling driven joining process parameters selection. Homo- and hetero-skedastic surrogate models of joint KPCs and their variance are developed from noisy experimental data. Using the developed surrogate models process window is identified and computation of process acceptance rate is done.

Chapter 5 addresses the issue high dimensionality of KCCs. Surrogate models of assembly KPCs in terms of few critical KCCs is developed. These surrogate models are applied for effective diagnosis and design adjustment of unwanted variations in KPCs. Design adjustment is achieved by a two-step process: (1) adjustment of design nominal of critical KCCs; and, (2) tolerance reallocation of critical KCCs.

Chapter 6 discusses the overall findings and conclusions derived from the research presented in this thesis and describes possibilities for future work.

CHAPTER 2

LITERATURE REVIEW

2.1 Introduction

In general, surrogate modelling is used to develop computationally efficient and accurate representation of interrelations between KPCs and KCCs for a design synthesis task. To ensure quality of solution in a given design synthesis task, a key requirement for surrogate modelling methods is to identify and model varying scales of specific characteristics in the KPC-KCC interrelations which are the most critical to the design synthesis task. This thesis classifies characteristics of KPC-KCC interrelations as: (1) deterministic non-linearity of KPCs; (2) stochasticity of KPCs; and, (3) high dimensionality of KCCs. Deterministic non-linearity of KPCs estimated by computer-based VSAs with negligible or no numerical error, is characterized by presence of multiple local maximas and minimas. Contrary to deterministic behaviour, KPCs might have stochastic variations manifested as either homo-skedasticity (KCC-independent variance) or hetero-skedasticity (KCC-dependent variance). Lastly, in complex assemblies, a KPC can be affected by potentially a large number of KCCs. Therefore for efficient design synthesis there is need of addressing high dimensionality of KCCs by conducting dimensionality reduction.

This chapter reviews past research on modeling KPC-KCC interrelations. The review discusses how currently existing *first-principle* models and surrogate models address the aforementioned characteristics in the KPC-KCC interrelations. Moreover, limitations of currently existing methods and need for scalable surrogate models, which can address varying scales of the aforementioned characteristics, are highlighted in the context of the following three design synthesis tasks:

i. *Fixture layout optimization of sheet metal assembly processes* which require scalable surrogate models that address varying scale of deterministic non-linearity of assembly KPCs.

ii. *Joining process parameters selection for automotive BIW assembly joining* which require scalable surrogate models that address varying scale of stochasticity of joining process KPCs.

iii. *Corrective action of product failures due to dimensional variations in KPCs* which require scalable surrogate models that address high dimensionality of KCCs affecting the faulty KPC.

The remaining part of this chapter is organized as follows: In Section 2.2, research addressing deterministic non-linearity in KPC-KCC interrelations is discussed. Section 2.3 describes past research on surrogate modelling of stochastic KPCs. Finally, literature review on dimensionality reduction of KCCs is presented in Section 2.4.

2.2 Related work on modelling deterministic non-linearity in KPC-KCC interrelations

An extensive research was done in the past to address deterministic non-linearity in the KPC-KCC interrelations. Initial studies focused on *first-principle* analysis to integrate KPCs with KCCs. Examples include state-space modelling of variation propagation in multi-station assemblies, to estimate critical characteristics and dimensions of the final assembly (KPCs) from dimensions of sub-assemblies and parts and also taking into consideration variations induced by fixture errors and part errors (KCCs), which led to the Stream-of-Variation-Analysis (SOVA) methodology (Ceglarek & Shi, 1996; Hu, 1997; Jin & Shi, 1999; Ding, *et al*., 2000; Ding, *et al*., 2002; Shi, 2006). The SOVA method developed *linear* assembly response functions

(ARFs) which linked KPCs with KCCs. The *linear-structured* SOVA had various applications in multi-station assemblies – variation propagation in rigid body assemblies (Jin & Shi, 1999; Ding, *et al.*, 2002; Huang, *et al.*, 2007), variation propagation in complaint part assembly (Camelio, *et al.*, 2003) and process-oriented tolerance synthesis to assign tolerance to process variables based on minimization of cost of tolerance allocation and subject to design tolerance of final product dimensions (Shiu, *et al.*, 2003; Ding, et al., 2005; Wang & Ceglarek, 2009; Huang, *et al.*, 2009). Linear models such as SOVA are an approximation of the true underlying non-linear relations between KPCs and KCCs (Ren, *et al.*, 2006). Deviation between actual KPCs and their linear approximation, also known as linearization error, can be significant when there are large number of KCCs and errors induced by them is greater than the magnitude of the KPCs. For example, in multi-stage assembly processes, when there is a large number of stations and errors induced by fixture locators are relatively high compared to product tolerances, linearization error due to linear ARFs can be significantly large. To improve the performance of linear models, several approaches were developed to calculate the linearization error. These include analytical adjustment of the linearization error through non-linear mathematical transformations such as Taylor's series expansion of the ARF (Carlson, 2001), homogenous transformation of KCC induced errors to compute error stacking and coupling (Xiong, *et al.*, 2002) and differential representation of kinematic model for fixture designs (Wang, *et al.*, 2003).

The aforementioned works depend on understanding of the underlying physical process to model the linearization error. Recently, *hybrid* approaches, integrating *first-principle* ARFs with surrogate models, have been developed to reduce the required understanding of the underlying physical process and to improve the

quality of solution from existing *first-principle* models. For example Ren, *et al*. (2006) developed multiple additive regression trees for the linearization error left by existing linear models of multi-stage assembly systems. Huang, *et al*. (2009) described a linear regression based surrogate model of process yield taking data from existing SOVA models to perform tolerance synthesis on fixture clamp locations. Zhou, *et al*. (2012) used the Kriging surrogate model for the linearization error on multiple KPCs in multi-stage assembly systems.

The aforementioned research addressing deterministic non-linearity of KPCs can be classified into the following three categories:

  i. *First-principle* methods developing linear ARFs of KPC-KCC interrelations

 ii. *First-principle* methods developing non-linear ARFs of KPCs based on linear ARFs and *analytical* adjustment of linearization error of the linear ARFs by *non-linear* mathematical transformations

iii. *Hybrid* methods developing non-linear ARFs of KPCs based on linear ARFs and *data-driven* adjustment of linearization error of the linear ARFs by surrogate models

It is noteworthy that to develop the ARFs of KPCs through currently existing methods which fall under the aforementioned three categories either complete or partial knowledge of the underlying physical process is required. However, there is a growing demand for *data-driven* approaches which would require no or minimal understanding of the underlying physical processes to develop ARFs of KPCs for design synthesis tasks driven by numerically intractable and computationally expensive computer simulations. For example, fixture layout optimization for assemblies with multiple sheet metal parts depends on advanced computer-based VSA and therefore requires *data-driven* approaches to develop the ARFs of KPCs in terms

of KCCs.

For design synthesis tasks such as fixture layout optimization of sheet metal assembly, the need for *data-driven* approaches to develop KPC ARFs has been spurred particularly by the recent advancements in VSA tools addressing sheet metal mechanical assemblies with complex geometry and complex fixture-to-part interactions. For example, Liao and Wang (2007) and Xie, *et al.* (2007) addressed the fixture-to-part contact problem by solving non-linear FEA approach, which though giving accurate results was computationally expensive. Recently, Franciosa, *et al.* (2014) developed FEA-based approach with an enhanced part meshing and also taking into consideration part-to-part and fixture-to-part surface contact modelling. The methodology conducts computer simulation of the final assembly KPCs by generating part variations and part-to-part gap variations.

With advanced non-linear FEM models capable to simulate more and more complex sheet metal assemblies, there are two new emerging requirements for assessing *data-driven* approaches' capability to generate realistic VSA results:

i. *Acceptable predictive accuracy on unseen test samples for deterministic KPC-KCC interrelations characterized by varying number of local maximas/minimas (varying non-linearity of KPC-KCC interrelations)*

Due to lack of knowledge about underlying system, there is need for surrogate modelling methods which, through data analysis and minimal knowledge about the physical system, can adapt to the scale of underlying non-linearity in KPC-KCC interrelations characterized by varying number of local maximas and minimas and develops surrogate models with acceptable accuracy for unseen test samples.

ii. *Minimal computation time required for generating training data for developing*

To develop the surrogate models, training data needs to be generated by running computationally expensive VSA. Input to VSA is a $n \times d$ design matrix having 'n' samples of 'd' KCCs. To ensure that developed surrogate models achieve acceptable predictive accuracy in fewer simulations, the design matrix of KCCs is chosen by an adaptive sampling strategy to provide maximum predictive information in the training data (Huang, *et al*., 2009; Gorissen, *et al*., 2010). However, currently existing adaptive sampling strategies focus on single response (single KPC) models while most design synthesis applications such as fixture layout optimization for sheet metal assemblies involve multiple KPCs for example part-to-part gaps at multiple assembly joint locations.

To meet the aforementioned requirements, this thesis develops a *scalable surrogate modelling* approach which has the following capabilities:

i. *Acceptable predictive accuracy on unseen test sample via Greedy Polynomial Kriging*, a Kriging based surrogate modelling approach focusing on maximization of predictive accuracy on unseen test samples for deterministic KPC-KCC interrelations with varying number of local maximas/minimas

ii. *Minimal computation time required for generating training data through Optimal Multi Response Adaptive Sampling* to accelerate convergence of multiple surrogate models to desired accuracy levels using a single adaptive sample for multiple KPCs.

Table 2.1 summarizes related research addressing deterministic non-linearity in KPC-KCC interrelations and highlights the contributions of the proposed scalable surrogate modelling approach.

Table 2.1: Related work on modelling deterministic non-linearity in KPC-KCC interrelations

Model type	Related work
First-principle methods for *linear* ARFs of KPCs – Linear KPC-KCC models	Ceglarek & Shi (1996) Hu (1997) Jin & Shi (1999) Ding, *et al.* (2002) Shiu, et al. (2003) Camelio, *et al.* (2003) Ding, *et al.* (2005) Huang & Shi (2004) Huang, *et al.* (2007) Wang & Ceglarek (2009) Huang, *et al.* (2009)
First-principle methods for *non-linear* ARFs of KPCs – Linear KPC-KCC models with analytical adjustment of linearization errors by non-linear mathematical transformations	Carlson (2001) Xiong, *et al.* (2002) Wang, *et al.* (2003)
Hybrid (*first-principle* & *data-driven*) methods for *non-linear* ARFs of KPCs – Linear KPC-KCC models with data-driven adjustment of linearization errors by surrogate models	Kim & Ding (2005) Ren, *et al.* (2006) Huang, *et al.* (2009) Zhou, *et al.* (2012)
Data-driven method for *non-linear* ARFs of KPCs – Scalable surrogate modelling of KPCs with varying scale of deterministic non-linearity based on: • GPK[1] to develop scalable surrogate models • O-MRAS[2] to expedite convergence of GPK surrogate models	***Proposed in this thesis***

[1]GPK: Greedy Polynomial Kriging
[2]O-MRAS: Optimal-Multi Response Adaptive Sampling

The proposed method of scalable surrogate modelling for deterministic non-linearity of KPCs is used to develop an overall approach of <u>*scalable surrogate model driven fixture layout optimization*</u> in sheet metal assemblies which is achieved by the following two interlinked steps:

i. <u>*Scalable surrogate modelling of deterministic assembly KPCs*</u> via GPK and O-MRAS

ii. <u>*Optimization of fixture KCCs*</u> which integrates the GPK surrogate models of fixture KPCs with optimization routine to determine optimal clamp layout in fixtures of sheet metal assembly.

2.3 Related work on modelling stochasticity in KPC-KCC interrelations

Not all design synthesis task can rely on existence of *first-principle* models to provide estimation of KPCs for given KCCs. As an example, in case of laser joining processes such as Remote Laser Welding (RLW), there is lack of comprehensive and accurate *first-principle* models linking joint quality characteristics or joint KPCs with joining process parameters or joining KCCs. Under this condition, design synthesis tasks such as optimal joining process parameter selection rely on analysis of data generated through physical experimentation, which may be subjected to noise such as measurement errors originating from uncontrollable parameters. Therefore, KPCs observed through experiments might exhibit stochastic behaviour which can be due to either KCC-independent homo-skedastic variance or KCC-dependent hetero-skedastic variance. However, due the lack of *first-principle* models, it is challenging to characterize the KPC stochasticity as homo- or hetero- skedastic.

Several researches have been done on development of polynomial surrogate models of stochastic KPCs for design synthesis tasks such as joining process parameters selection for industrial joining processes such as Laser Transmission Welding (LTW), Resistance Spot Welding (RSW), etc. For joining process parameters selection, the polynomial surrogate models of joint KPCs are then used for two design tasks: (1) multi objective optimization to identify optimal joining KCCs which optimize joining process KPIs subject to satisfaction of design tolerances on joint KPCs; and, (2) identification of a process window in the KCC design space which gives a feasible region for achieving satisfactory joint quality determined by compliance of joint KPCs to design tolerances.

In currently exiting methods addressing joining process parameters selection, the polynomial surrogate models of the stochastic joint KPCs are trained

using data generated through conducting physical experimentation. The experiments are designed following various design of experiments approaches such as full-factorial, central composite combinations and others.

However, there are two major limitations of the state-of-the-art on surrogate modelling of stochastic KPCs for design synthesis tasks such as joining process parameters selection:

i. *Assumption of homo-skedasticity of KPCs*

Current methods assume homo-skedasticity or constant variance of the joining KPCs over the KCC design space whereby variance of a KPC is attributed solely to measurement and environmental noise and hence is assumed to be KCC-independent. However, constant variance of all joint KPCs might be a strong assumption especially with the lack of comprehensive and accurate *first principle* models of all joint KPCs to confirm their actual physical behavior. An incorrect constant KPC variance assumption will lead to erroneous joining process parameters selection.

ii. *Lack of approach to select critical interactions between KCCs*

In currently existing methods, the degree of the polynomial surrogate model is selected based on the user's experience. In most cases, a first or second order polynomial surrogate model is used to fit a KPC as a function of KCCs. Higher order polynomials might not be considered to avoid over-fitting on the limited training sample generated by experimentation. However, by restricting to second order polynomials, potential higher order non-linear interactions between KCCs, which can explain the relationship between KPCs and KCCs, might remain unidentified.

To address the aforementioned limitations, this thesis proposes *scalable*

surrogate modelling for KPC stochasticity which has the following capabilities:

i. *A data-driven methodology to address the scale of KPC stochasticity* based on (1) statistical hypothesis testing to detect homo- to hetero-skedastic behaviour of KCCs; and, (2) development of homo- and hetero-skedastic surrogate models based on the detected type of stochasticity.

ii. *Polynomial Feature Selection* (PFS) method to determine critical multiplicative interactions between KCCs which affect a KPC.

Table 2.2 lists research articles related to surrogate modelling of stochastic KPCs related to industrial joining processes.

Table 2.2: Related work on surrogate modelling of stochastic KPCs

Model type	Related work
Homo-skedastic surrogate models of joint KPCs via 1st and 2nd order polynomial regression	*Articles related to LTW*: Olabi, *et al.* (2006) Acherjee, *et al.* (2009) Khan, *et al.* (2011) Zhao, *et al.* (2012) Dongxia, *et al.* (2012) Ghosal & Manna (2013) Wang, *et al.* (2013) *Articles related to RSW*: Darwish & Al-Dekhial (1999) Antony (2001) Kim (2005) Hamedi, *et al.* (2007) Muhammad, *et al.* (2013)
Homo- and *hetero-skedastic* surrogate models of joint KPCs via *Scalable surrogate modelling* for varying KPC stochasticity based on: - Statistical hypothesis testing to detect *homo-* and *hetero-skedastic* behaviour of KPCs - Polynomial Feature Selection of KCCs	***Proposed in this thesis***

The proposed method of scalable surrogate modelling to address KPC stochasticity develops homo- and hetero-skedastic surrogate models of KPCs, which are then used to enhance joining process parameters selection by developing the following novel capabilities:

i. *Multi-objective optimization to optimize KPIs related to joining process (a) efficiency and (b) quality* –

Currently existing methods optimize KPIs only related to joining process efficiency such as speed of welding in case of a LTW process. In this thesis, homo- and hetero-skedastic surrogate models of KPCs are utilized to optimize KPIs related to *joining process efficiency* as well as KPIs related to *joining process quality* such as KCC-dependent variance of joint KPCs.

ii. *Development of process window based on homo- and hetero-skedastic surrogate models of joint KPCs* –

Currently existing methods identify process window in KCC design space based only on the homo-skedastic surrogate models of KPCs. In this thesis, stochastic process window is developed by taking into consideration homo- and hetero-skedastic behaviour of joint KPCs. Additionally, homo- and hetero-skedastic surrogate models of joint KPCs are used to compute process acceptance rate over the process window.

Table 2.3 lists research articles on application of joint KPC surrogate models for tasks in joining process parameters selection such as multi-objective optimization of process KPIs and development of process window.

Table 2.3: Related work on application of surrogate models of joint KPCs for tasks related to joining process parameters selection

Tasks related to joining process parameters selection		Related work
Optimization of KPIs related to joining process	Multi-objective optimization of KPIs related to joining *process efficiency*	*Articles related to LTW*: Acherjee, *et al.* (2009) Padmanaban & Balasubramanian (2010) Khan, *et al.* (2011) Acherjee, *et al.* (2012) Wang, *et al.* (2012) Wang, *et al.* (2013) *Articles related to RSW*: Antony (2001) Kim (2005) Hamedi, *et al.* (2007) Lai, *et al.* (2009) Zhao, *et al.* (2014)
	Multi-objective optimization of KPIs related to joining *process efficiency* and *process quality*	***Proposed in this thesis***
Development of process window	Development of process window based on *homo-skedastic* surrogate models of joint KPCs	*Articles related to LTW*: Khan, *et al.* (2011) Acherjee, *et al.* (2012) *Articles related to RSW*: Fukumoto, *et al.* (2008) Han, *et al.* (2010)
	Development of process window based on *homo-* and *hetero-skedastic* surrogate models of joint KPCs	***Proposed in this thesis***

The proposed method of scalable surrogate modelling for varying stochasticity of KPCs is used to develop an overall approach of *scalable surrogate model driven joining process parameters selection* which is realized through the following two interlinked steps:

i. *Scalable surrogate modelling for homo and hetero skedastic joint KPCs* via: (1) Statistical hypothesis testing to detect homo- and hetero-skedastic behaviour of KPCs; and, (2) Polynomial Feature Selection of KCCs

ii. *Joining process parameters selection* which includes: (1) multi-objective optimization of KPIs related to joining process efficiency and process quality;

and, (2) identification of stochastic process window and computation of acceptance rate

2.4 Related work on modelling for high dimensionality of KCCs

In complex assemblies, there is a large number of KCCs which can potentially affect a KPC and often there is need for addressing high dimensionality of KCCs to identify few critical KCCs which are closely related to a particular KPC of interest. For example, design synthesis tasks such as corrective action of product failures due to unwanted dimensional variations in KPCs require identification of few critical KCCs closely related to the faulty KPC. In general, corrective action to reduce unwanted variations in KPCs can be formulated as the following two interlinked tasks:

i. *Diagnosis of unwanted variations in KPCs* to identify a few critical *KCCs* affecting the faulty KPCs

ii. *Product/process design adjustment of the critical KCCs* to reduce production fallout of faulty KPCs.

It is noteworthy that a critical step in corrective action to reduce unwanted variations of KPCs is the *diagnosis of the unwanted KPC variations.* Methods related to *diagnosis* are required *to address high dimensionality of KCCs* present in the assembly process. Moreover, methods for diagnosis of unwanted KPC variations are required for both type-I and type-II assembly processes. Mantripragada & Whitney (1999) classify assembly processes into two categories: (1) type-I assembly where parts are assembled by part-to-part mating surfaces and characteristics of the final product (KPCs) depend on characteristics of its constituent parts (KCCs); and, (2) type-II assembly, where fixtures position the parts being assembled and characteristics of the final assembly (KPC) depend on assembly

process variables such as layout of fixture locators and clamps (KCCs). Examples of both type-I and type-II assembly processes are shown in Figure 2.1 (a and b).
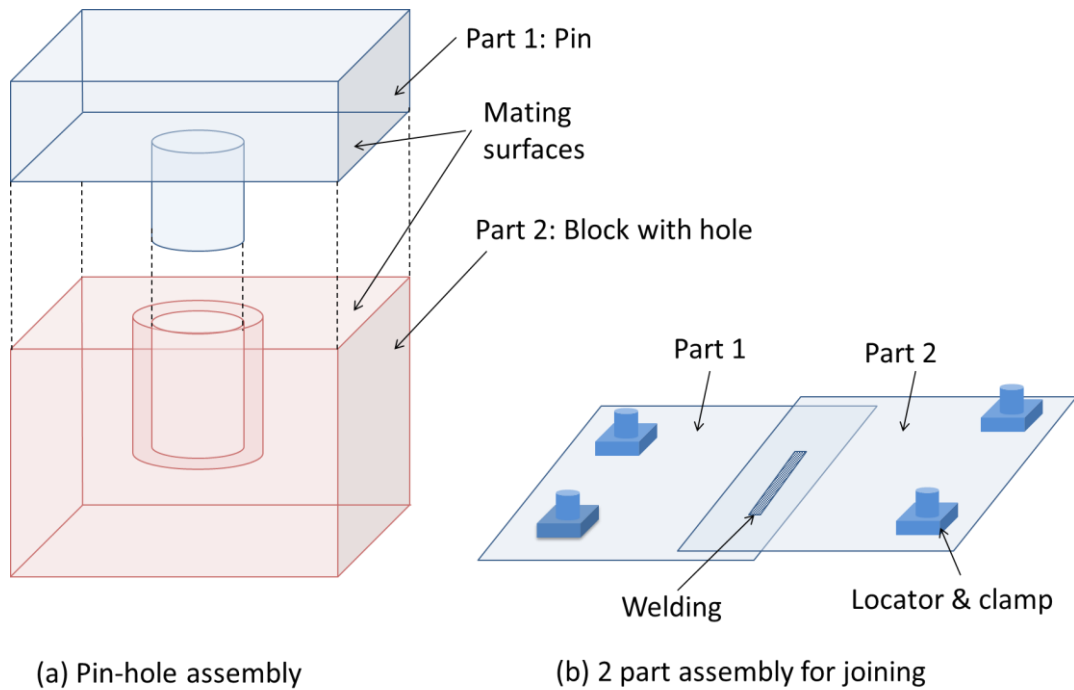
Figure 2.1: (a) Type-I; and, (b) type-II assembly

Let us now review methods on diagnosis of unwanted KPC variations addressing high dimensionality of KCCs for both type-I and type-II assembly processes.

For type-I assembly processes, an extensive research was done in the past to develop mathematical models of KPCs related to the final product based on KCCs of the constituent parts, which are assembled to realize the final product. Wu, *et al.* (2009) classifies these methods as: (1) linear (Chase & Parkinson, 1991); (2) non-linear (Nigam & Turner, 1995); (3) numerical (Varghese, *et al.*, 1996); and, (4) Monte-Carlo simulation based (Skowronski & Turner, 1996; 1997). Some of these methods have been implemented in commercial variation simulation analysis (VSA) softwares (VSA-3D, Pro/Engineer, Sigmetrix's CETOL, and others). With

increase of complexity of assemblies due to large number of individual parts and subassemblies, numerical routines and computer based VSA programs are commonly used for integrating KPCs with KCCs. For example, Sigmetrix's CETOL can simulate the effect of variations in large number of KCCs on variations in KPCs.

The aforementioned VSA-based methods are useful only for forward analysis to evaluate KPCs for given KCCs. They do not address dimensionality reduction of KCCs and hence do not provide diagnostic information such as identification of critical KCCs related to a faulty KPC. This limitation of currently existing VSA-methods is critical particularly in case of complex type-I assemblies which face the following two challenges:

i. *High dimensionality of KCCs* whose variations can potentially cause variations in the faulty KPC

ii. *Numerical intractability* of the underlying physical process governing the KPC-KCC interrelations

To address the aforementioned limitations of VSA-based methods for diagnosis of 6-sigma root causes in type-I assembly processes, there is need for data-driven approaches requiring minimal understanding of underlying process to address issues related to identification of few critical KCCs in type-I assembly processes (Chen, 2001). To this end, this thesis proposes *scalable surrogate modelling* to address high dimensionality of KCCs for diagnosis of unwanted KPC variations. The proposed *scalable surrogate modelling for high dimensionality of KCCs* is based on:

i. *Least squares regression based Polynomial Feature Selection* to determine a subset of a few critical KCCs identified from a larger set of all given KCCs.

ii. *Closed-form analytical models* to represent the relation between the faulty KPC and critical KCC closely related to it.

For type-II assembly processes, several studies addressed the issue of KCC dimensionality for diagnosis of unwanted variations of KPCs by developing analytical approaches. These methods focussed on KCCs related to fixture elements such as locators as source of dimensional variations in the final assembly. Traditionally these methods focused on deriving a manifold of lower dimension from the original KCC space. Based on the manifold of lower dimension, statistical representation of fault patterns was developed. Overall, methods, which generate lower dimensional manifold of KCCs, can be classified into three categories: (1) methods based on principal component analysis (PCA); (2) methods based on correlation clustering (CC); and, (3) methods based on least square regression (LS). Examples of methods based on PCA include single fixture fault diagnosis by mapping variation patterns in KPCs to variations in fixture KCCs such as locators and clamps (Ceglarek & Shi, 1996). This method was further extended to include noise present in in-line measurements of fixture KCCs and assembly KPCs by Optical Co-ordinate Measuring Machine (OCMM) (Ceglarek & Shi, 1999). PCA based fixture fault diagnosis was extended for multi-station assembly by Ding, *et al*. (2002). The aforementioned methods focused on single fault diagnosis whereas in real multi-station assembly system there might be multiple KPCs with unwanted variations and it is important to group the KCCs based on their correlation with KPCs. This issue was addressed by Shiu, *et al*. (1996) by correlation clustering to partition the KCC into groups such that each group is related to a single KPC. Diagnosis in multi-station assemblies was also addressed using least squares regression to correlate observed KPC variations to potential sources of variations such as fixture locator and clamp variations acting as KCCs and derive a measure of significance of each source of variation (Apley & Shi, 1998; Chang & Gossard, 1997; Chang & Gossard, 1998;

Rong, *et al*., 2001). The aforementioned methods uses process data on KPCs and KCCs obtained via in-line measurements taken by OCCM. Recently, hybrid approaches were developed by Camelio and Hu (2004) and Kong, *et al*. (2008) which first derives fault patterns from product and process models and then evaluates the significance of these patterns based on measurement data.

The aforementioned research addresses fault diagnosis in type-II assembly processes through identifying variation patterns in KCC induced errors. However, these methods would not be suitable for identifying critical KCCs in complex type-I assembly processes because of the following two limitations:

i. *Need for in-depth understanding of underlying physical process* − Knowledge about the underlying physical process is critical to model KPCs in terms of KCCs, which in case of the reviewed methods related to fault diagnosis in type-II multi-stage assembly processes, are modelled through *first-principle* based approaches such as SOVA.

ii. *Lack of dimensionality reduction in the original KCC space* − There is lack of explicit dimensionality reduction by building a final analytical model of the faulty KPC in terms of few critical KCCs.

Taking into consideration, the aforementioned challenges in diagnostic methods for type-II assembly processes and numerical intractability of VSA-based methods of type-I assembly processes, the data-driven *scalable surrogate modelling* for high-dimensionality of KCCs has been proposed to address diagnosis of unwanted variations of KPCs in type-I assembly processes.

Table 2.4 summarizes related work on dimensionality reduction of KPCs discussed in this section.

Table 2.4: Related work addrressing dimensionality reduction of KCCs for diagnois of unwanted KPC variations

Approach of KCC dimensionality reduction	Research work	Application
Mathematical transformation of original KCCs to lower dimensional space based on:		
PCA	Ceglarek & Shi (1996) Ceglarek & Shi (1999) Ding, *et al.* (2002)	Diagnosis for *type-II* assembly processes
Correlation Clustering	Shiu, *et al.* (1996)	
Least Squares Regression	Apley & Shi (1998) Chang & Gossard (1998) Rong, *et al.* (2001)	
Designated Component Analysis	Camelio & Hu (2004) Kong, *et al.* (2008)	
Scalable surrogate modelling for KCC dimensionality based on: - Dimensionality reduction in the original KCC space to identify critical KCCs related to faulty KPC - Closed form analytical models of faulty KPCs in terms of critical KCCs	***Proposed in this thesis***	Diagnosis for *type-I* assembly processes

The proposed method of diagnosis of unwanted dimensional variations of KPCs via scalable surrogate modelling for KCC dimensionality is used to develop an overall approach of *scalable surrogate model driven corrective action of product failures due to dimensional variations in KPCs* which is formulated as the following two interlinked tasks:

i. *Diagnosis via scalable surrogate modelling* to identify critical KCCs affecting faulty KPCs

ii. *2-stage design adjustment*: (1) optimal nominal change; and, (2) optimal tolerance re-allocation of the critical *KCCs* to reduce production yield of the faulty KPCs.

2.5 Conclusions

The discussion presented in this chapter shows the limitations of currently existing methods for surrogate modelling in design synthesis for addressing varying scales of deterministic non-linearity of KPCs, stochasticity of KPCs and high dimensionality to KCCs affecting a KPC. Firstly, there is lack of systematic approach of developing surrogate models of deterministic KPCs with varying non-linearity for computer simulation driven design synthesis tasks such as fixture layout optimization for sheet metal assembly. Secondly, though several researches address surrogate modeling based on experimentation data for design synthesis tasks such as assembly joining process parameter selection, modeling stochastic behavior of KCCs characterized by unknown homo- and hetero-skedasticity is not addressed. Lastly, there is need for developing surrogate models which can identify a few critical KCCs closely related to a KPC for design synthesis tasks such as corrective action to reduce unwanted dimensional variations of KPCs.

To address each aforementioned challenge, this thesis proposes *scalable surrogate modelling*.

Based on the idea of *scalable surrogate modelling*, the following three methodologies of scalable surrogate model driven design synthesis are developed:

i. *Scalable surrogate model driven fixture layout optimization* – Chapter 3 develops Greedy Polynomial Kriging (GPK) to develop scalable surrogate models for deterministic KPCs related to sheet metal assembly. GPK is agnostic to the scale of deterministic non-linearity in KPCs and develops surrogate models with acceptable predictive accuracy for unseen test samples. Additionally, Optimal-Multi Response Adaptive Sampling is proposed to accelerate the convergence of multiple surrogate models to desired accuracy

levels. GPK surrogate models are utilised for fixture layout optimization of sheet metal assembly. The GPK surrogate models are integrated with optimization routines to identify optimal fixture layout in sheet metal assembly.

ii. *Scalable surrogate model driven joining process parameter selection* − In Chapter 4, scalable surrogate models addressing homo- and hetero-skedastic behavior of joint KPCs are developed. Statistical hypothesis testing and Polynomial Feature Selection (PFS) has been developed to generate the homo- and hetero-skedastic surrogate models of joint KPCs, which are then utilized for joining parameters selection through optimization of joining process KPIs, identification of process window and computation of process acceptance rate.

iii. *Scalable surrogate model driven corrective action of product failures due to dimensional variations of KPCs* − Chapter 5 develops corrective actions of unwanted dimensional variations in faulty KPCs by scalable surrogate model driven dimensionality reduction of KCCs to identify a few critical KCCs closely related to the faulty KPC. In this chapter, the developed surrogate models are applied in a two-stage design adjustment process to minimize production yield of faulty KPCs through (1) nominal change; and, (2) tolerance re-allocation of the critical KCCs.

CHAPTER 3

SCALABLE SURROGATE MODEL DRIVEN

FIXTURE LAYOUT OPTIMIZATION

3.1 Overview of the chapter

Application of advanced computer-based VSA for design analysis of automotive BIW assembly processes has become a common practice. For example, analyzing effect of fixture layout (KCCs) on part-to-parts gaps (KPCs) in sheet metal assemblies frequently requires Finite Element Method (FEM)-based VSA models (Liao & Wang, 2007; Xie, *et al.*, 2007; Franciosa, *et al.*, 2014; Ceglarek, *et al.*, 2015). However, VSA programs cannot be used effectively for design synthesis because of their: (1) computational expense, which prohibits efficient global optimization within time constraints; and, (2) numerical intractability which makes reverse engineering difficult if not impossible and instead requires experience-based trial-and-error. Therefore, an analytical surrogate model is often required to enhance VSA's practical applicability in design synthesis tasks.

For VSAs with deterministic output, the scale of non-linearity of the KPC-KCC interrelations, characterized by varying number of local maximas/minimas, is unknown due to complex nature of the underlying physical process. Currently, existing approximation techniques in design synthesis such as high order polynomial regressions cease to address the scale of non-linearity of KPC-KCC interrelations without overfitting limited number of samples used for training the surrogate models. However, overfitting training samples leads to poor predictive accuracy for unseen test samples. Therefore, there is a requirement for scalable surrogate modelling methods which can develop surrogate models with *acceptable predictive accuracy for unseen*

test samples for KPC-KCC interrelations which have a *single maxima/minima* as well for those which have *multiple local maximas/minimas*.

To address the aforementioned need, this chapter builds upon the idea of *scalability for deterministic non-linearity* proposed in Chapter 1 as part of the framework of surrogate model driven *Scalable Design Synthesis*. The requirements to achieve *scalability for deterministic non-linearity* are:

i. Develop a surrogate models which can adapt to the scale of deterministic non-linearity present in KPC-KCC interrelations and give *acceptable predictive accuracy for unseen test samples*.

ii. Minimize computational time required for running VSA to generate training data for developing surrogate models of *multiple* KPCs

The aforementioned requirements are addressed in this chapter by developing *scalable surrogate modelling* for deterministic non-linearity of KPCs which includes:

i. Greedy Polynomial Kriging (GPK), a novel approach of training Kriging-based surrogate models of deterministic KPCs by *maximizing predictive accuracy on unseen test samples*

ii. Optimal Multi Response Adaptive Sampling (O-MRAS) a novel method to expedite convergence of multiple surrogate models to desired accuracy level using a single training sample of KCCs.

Furthermore, development and application of the proposed *scalable surrogate modelling* for deterministic non-linearity in KPC-KCC interrelations is discussed in the context of fixture layout optimization for sheet metal assemblies which uses a FEM-based VSA for analysis of assembly KPCs such as gaps between mating parts for given fixture related KCCs such as layout of fixture clamps.

The overall contribution of this chapter is developing a comprehensive methodology of _scalable surrogate model driven fixture layout optimization_ for sheet metal assemblies based on the following two interlinked approaches:

i. _Scalable surrogate modelling of deterministic assembly KPCs_, which develops surrogate models of assembly KPCs using training data generated from VSA

ii. _Optimization of fixture KCCs_ by utilizing the KPC surrogate models to determine optimal fixture KCCs which minimize a cost-based Key Performance Indicator (KPI).

Figure 3.1 highlights the proposed methodology of _scalable surrogate model driven fixture layout optimization_.
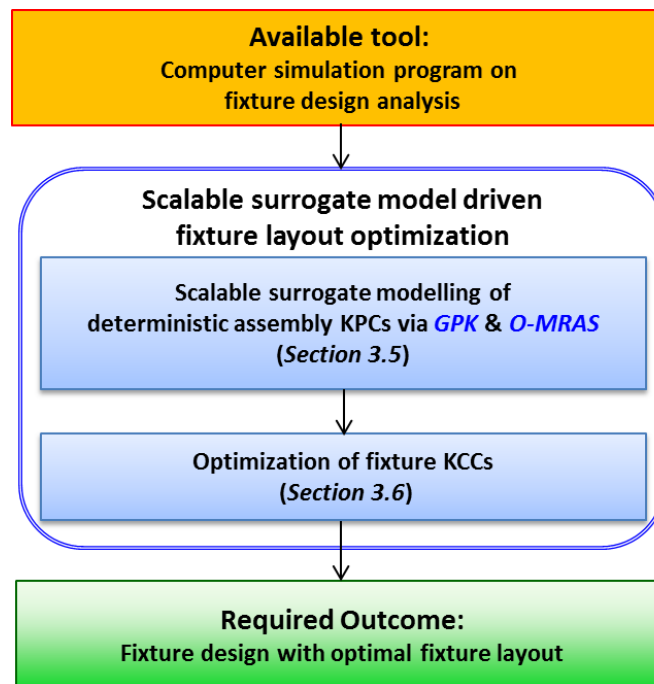
Figure 3.1: Scalable surrogate model driven fixture layout optimization

The proposed methodology of _scalable surrogate model driven fixture layout optimization_ is demonstrated using case studies on sheet metal assemblies from automotive and aerospace industries. Performance of GPK is compared with that of state-of-the-art Kriging and other currently existing surrogate modelling methods.

51

Moreover, performance of O-MRAS is compared with that of state-of-the-art uniform random sampling.

Notations related to the methods developed in this chapter are listed as follows. Notations of KCCs ($\mathbf{x}$) and KPCs ($\mathbf{y}$) used in this chapter are similar to the generic ones introduced in Chapter 1. However, in this chapter KCCs and KCCs are specifically related to fixture layout optimisation for sheet metal assemblies. Hence notations of KCCs and KPCs are redefined in this chapter highlighting their meanings as related to fixture layout optimisation.

Notations

$\mathbf{x}$	Set of *'d'* KCCs $\mathbf{x} = \{x_1, x_2, ..., x_d\}$, where x_i is the ith KCC in $\mathbf{x}$ representing location of the ith clamp in a given fixture layout
y	Set of *'r'* KCCs $\mathbf{y} = \{y_1, y_2, ..., y_r\}$, where y_j is the jth KPC in $\mathbf{y}$ representing part-to-part gap the jth location on the sheet metal assembly where a joint such between the mating parts is to be made
$f(\bullet)$	Surrogate model integrating KCCs ($\mathbf{x}$) with a KPC (y)
θ	Parameters of the surrogate model 'f'
x_j^{lower}	Permissible lower operating limit of jth KCC where $j = 1, 2, ..., d$
x_j^{upper}	Permissible upper operating limit of jth KCC where $j = 1, 2, ..., d$
β	Coefficients of a regression model of the *'d'* KCCs i.e. $\beta = \beta_1, \beta_2 ... \beta_d$
$\mathbf{X}$	Design matrix having *'n'* samples of *'d'* KCCs
$\mathbf{x}_i$	i^{th} sample of *'d'* KCCs i.e. $\mathbf{x}_i = \{x_{i1}, x_{i2}, ..., x_{id}\}$
$\mathbf{y}_i$	i^{th} sample of *'r'* KPCs i.e. $\mathbf{y}_i = \{y_{i1}, y_{i2}, ..., y_{ir}\}$
$\mathbf{S}$	*'n'* training samples generated by running VSA i.e. $\mathbf{S} = \{\mathbf{x}_i, \mathbf{y}_i\}_{i=1}^n$
N	Number of iterations of surrogate modelling performed
$\mathbf{S}_{\text{T}}$	Training matrix where samples generated from each iteration of surrogate modelling is accumulated

t	Number of test samples on KCCs and KPCs used to measure accuracy of the surrogate model 'f' on unseen test samples
$\mathbf{S}_V$	't' test samples on KCCs and KPCs used to measure accuracy of the surrogate model 'f' on unseen test samples *i.e.* $\mathbf{S}_V = \{\mathbf{x}_i, \mathbf{y}_i\}_1^t$
MSE	Measure squared error calculated as average of the square deviances between actual KPCs obtained from VSA and predicted KPCs obtained from the surrogate model 'f'
R^2	Coefficient of determination of the surrogate model 'f'
$\bar{y}_j$	Average of the jth KPC obtained from the 't' test samples
R_j^2	Coefficient of determination of the surrogate model of the jth KPC
R_{avg}^2	Average of the R^2 obtained from individual surrogate models
m	Number of polynomial terms derived from the KCCs
p	Order of the polynomial of the KCCs ($\mathbf{x}$)
$\mathbf{h}(\mathbf{x})$	'm' polynomial terms of $\mathbf{x}$ *i.e.* $\mathbf{h}(\mathbf{x}) = \{h_1(\mathbf{x}), h_2(\mathbf{x}), ..., h_m(\mathbf{x})\}$
$\mathbf{h}'$	Subset of polynomial terms of $\mathbf{x}$ *i.e.* $\mathbf{h}' \subseteq \mathbf{h}$
$\mathbf{h}^D$	Set of polynomial terms of $\mathbf{x}$ arranged in descending order of their correlation with KPC 'y'
$\mathbf{h}^A$	Set of polynomial terms of $\mathbf{x}$ arranged in ascending order of their correlation with KPC 'y'
H	$n \times m$ input matrix of polynomial terms $\mathbf{h}$
ε_i	are deviances of the actual KPC y_i and predicted KPC $\hat{y}_i$ for 'n' training instances where $i = 1, 2, ..., n$
$g(\mathbf{x})$	Regression model of 'm' polynomial terms of KCCs ($\mathbf{x}$)
δ_{ik}	Distance between two points $\mathbf{x}_j$ and $\mathbf{x}_k$ along the jth KCC
$R(\bullet)$	Covariance structure of the Gaussian process regression or *Kriging*
$Z(\mathbf{x})$	Gaussian process used to model local non-linearities
σ^2	Variance of the Gaussian process
γ_j	Sensitivity parameter of jth KCC in covariance structure of *Kriging* where $j = 1, 2, ..., d$

α_j	Smoothing parameter of jth KCC in covariance structure of *Kriging* where $j = 1, 2, ..., d$
$\boldsymbol{\theta}$	All parameters related to the covariance structure of *Kriging i.e.* $\boldsymbol{\theta} = \{\gamma_1, \gamma_2, \ldots, \gamma_d; \alpha_1, \alpha_2 ..., \alpha_d\}$
$L(\bullet)$	Loss function which gives an aggregate measure of the error of the surrogate model
$\xi(\mathbf{h})$	Generalized estimation of the loss function $L(\bullet)$ obtained by the method of *k*-fold cross validation
$\mathbf{h}^*$	Optimal set of polynomial terms of KCCs ($\mathbf{x}$) which minimises $\xi(\mathbf{h})$ and selected by Polynomial Feature Section
$\xi^*(\bullet)$	Optimal value of generalized loss function obtained from optimal set of polynomial terms $\mathbf{h}^*$
p^*	Optimal polynomial order selected by Polynomial Feature Section (PFS)
δ	User-defined convergence tolerance used as stopping criteria of PFS
$\boldsymbol{\theta}^*$	Optimal parameters of the covariance structure of *Kriging*
$\mathbf{X}_C^{(j)}$	Adaptive sample of jth KCC where $j = 1, 2, ..., r$
$\boldsymbol{\upsilon}^{(j)}$	Values of the adaptive sampling criterion assigned to the *'n'* design points in $\mathbf{X}_C^{(j)}$
$\mathbf{X}_C$	A single $\bar{\bar{n}} \times d$ matrix obtained by merging adaptive samples $\mathbf{X}_C^{(1)}, \mathbf{X}_C^{(2)} ... \mathbf{X}_C^{(j)}, ... \mathbf{X}_C^{(r)}$ of *'r'* individual KPCs
$\bar{\bar{n}}$	Number of design points in $\mathbf{X}_C$ after removing duplicate entries
$\mathbf{R}^{(i)}$	Cluster of design points obtained after clustering $\bar{\bar{n}}$ design points in $\mathbf{X}_C$ by *k*-means clustering where *k=n* and $i = 1, 2, ..., n$
$\boldsymbol{\mu}^{(i)}$	Centroid of the points in $\mathbf{R}^{(i)}$
$d^{(i)}(\mathbf{x}_j)$	Distance of the design point $\mathbf{x}_j \in \mathbf{R}^{(i)}$ from the centroid of the cluster $\mathbf{R}^{(i)}$
$d_{\max}^{(i)}$	Distance of the farthest point from the centroid of the cluster $\mathbf{R}^{(i)}$
$\upsilon_{\text{R}}^{(i)}(\mathbf{x}_j)$	The merit of the point $\mathbf{x}_j \in \mathbf{R}^{(i)}$

$\upsilon_{\text{R-max}}^{(i)}$	The highest merit in cluster $\mathbf{R}^{(i)}$
ω_1	User-defined weights assigned to distance criteria
ω_2	User-defined weights assigned to merit criteria
$\mathbf{x}_*^{(i)}$	Optimal point selected from cluster $\mathbf{R}^{(i)}$
$\mathbf{X}_C^*$	Optimal adaptive samples consisting of optimal points each selected from $i = 1, 2, ..., n$ clusters *i.e.* $\mathbf{X}_C^* = [\mathbf{x}_*^{(1)}, \mathbf{x}_*^{(2)}, ..., \mathbf{x}_*^{(n)}]^{\mathrm{T}}$
$[\mathrm{L}_k^{(y)}, \mathrm{U}_k^{(y)}]$	Tolerance limits on KPC y_k where $k = 1, 2, ..., r$
m_k	Nominal of KPC y_k where $k = 1, 2, ..., r$
K_1 and K_2	User-defined Taguchi loss coefficients
$C(y_k)$	Cost of quality loss due to deviation of KPC y_k from nominal where $k = 1, 2, ..., r$
$C(\mathbf{y})$	Total cost of quality loss obtained as a sum of quality losses from 'r' individual KPCs

The remaining part of this chapter is organized as follows: Section 3.2 expands the motivation for the research presented in this chapter by discussing the challenges in fixture layout optimization for sheet metal assemblies. Next, Section 3.3 presents a generic overview of surrogate modelling of KPCs from computer-based VSA and highlights the scope for research on scalable surrogate modelling to address deterministic non-linearity of KPCs. Section 3.4 reviews state-of-the-art Kriging method and currently existing adaptive sampling techniques and discusses their limitations. Next, the proposed methodology for *scalable surrogate model driven fixture layout optimization* is developed through the following two approaches: (1) *scalable surrogate modelling of deterministic assembly KPCs* presented in Section 3.5, which details the GPK and O-MRAS methods; and, (2) *optimization of fixture KCCs* discussed in Section 3.6, which formulates the fixture layout optimization problem using the GPK surrogate models. Section 3.7 demonstrates the proposed

55

methodology with case studies from automotive and aerospace industries. Finally, Section 3.8 summarises the research presented in this chapter.

3.2 Motivation for the research

One of the important design synthesis tasks related to automotive BIW assembly production system is fixture layout optimization for the assembly process. Fixtures play an important role in the assembly process by providing accurate locating of parts to be assembled and hence significantly influence the final dimensional quality of the finished products. Moreover, fixtures also provide accurate clamping to maintain gaps between mating parts of an assembly within specified design tolerances which are critical for making feasible joints between the parts by an industrial joining process. For example, the Remote Laser Welding process requires gap between assembly mating parts to be within 0.05 mm to 0.4 mm at locations where welding is to be done. Therefore, optimal fixture layout optimization is important to ensure acceptable quality of the final assembly.

A significant number of researches have been done in the past on fixture layout optimization for sheet metal assemblies. Research on fixtures can be classified into two areas: (i) fixture design analysis which involves mathematical modelling of the relationship between fixture KCCs and KPCs based on *first principle* or fundamental physical laws from kinematics and finite element methods; and (ii) fixture layout optimization which utilizes the *first principle* mathematical models to determine fixture KCCs which maximize assembly process capability subject to design tolerances of KPCs. For fixture design analysis, a lot of work has been done to model the effect of fixture KCCs for example clamping forces, clamps' locations on the assembly KPCs such as part deformations, gap/contact between mating parts. The

KPC-KCC mathematical models developed through fixture design analysis was then integrated with optimization routines such as linear programming, genetic algorithms etc. to conduct fixture layout optimization (Menassa & DeVries, 1991; Kashyap & DeVries, 1999; Camelio, *et al*., 2002; Chen & Xue, 2008). In the aforementioned cases, efficient optimization of fixture KCCs via direct integration of the KPC-KCC models with optimization routines was possible due to the specific problem scenarios addressed, assumptions made and computationally inexpensive KPC-KCC assembly response functions (ARFs) developed through *first-principle* based modelling. However, in recent years research on compliant part assemblies with specific gap/contact requirements between mating parts, has led to development of advanced VSA methods (Franciosa, *et al*., 2014) which, though able to accurately estimate assembly KPCs for given fixture KCCs, cannot express the KPC-KCC relationships as closed-form and computationally inexpensive analytical functions unlike fixture design analysis methods developed previously. Consequently, efficient global optimization of fixture layout by direct integration of optimization routines with the new generation of fixture design analysis tools has become computationally prohibitive. Moreover, due to numerical intractability of such fixture design analysis tools, deducing critical KCCs for a given KPC is practically infeasible thereby making reverse engineering, required for applications such as fault diagnosis, a trial-and-error based exercise.

Under the aforementioned conditions, surrogate models of KPCs can be used for applications such as fixture layout optimization. To develop surrogate models which can generate realistic VSA results, this chapter proposes *scalable surrogate modelling for deterministic assembly KPCs* which provides the following two capabilities:

i. Acceptable accuracy for unseen test samples in case of deterministic KPC-KCC interrelations whose scale of non-linearity in terms of number of local maximas/minimas is unknown − This is achieved by Greedy Polynomial Kriging (GPK)

ii. Minimal computation time required generating training data for developing surrogate models of multiple assembly KPCs − This is addressed by Optimal-Multi Response Adaptive Sampling (O-MRAS).

3.3 Brief overview of surrogate modelling from computer-based Variation Simulation Analysis (VSA)

This section provides a brief overview of the steps required, in general, for developing surrogate models of deterministic KPCs from computer-based VSA. The discussion is presented without referring to any particular surrogate modelling or adaptive sampling method. The significance of the steps for achieving accurate surrogate models from minimal number of computer simulations is discussed. Furthermore, the scope for research on surrogate modelling and adaptive sampling methods to achieve scalability for deterministic non-linearity is highlighted.

A surrogate model is an analytical function which predicts a KPC for given KCCs. The surrogate model can be expressed as $\hat{y} = f(\mathbf{x})$, where $\hat{y}$ is the predicted value of the KPC and $\mathbf{x} = x_1, x_2 \ldots x_d$ is a d-dimensional input of KCCs. Each KCC is bounded within permissible lower and upper limits: $x_j^{\text{lower}} \leq x_j \leq x_j^{\text{upper}}$, where $j=1,2\ldots d$. The space of all feasible KCCs is called the experiment region or design space and is denoted by D, which is a d-dimensional hyper-rectangle.

The surrogate model 'f' is defined by several parameters (θ), details of which depends on the choice of the surrogate model. For example, regression

58

coefficients $\beta = \beta_1, \beta_2 ... \beta_d$ are parameters in a linear regression model with 'd' KCCs. Similarly, number of hidden layers, learning rate and weight matrix are parameters of a neural network. In general, surrogate modelling of KPCs from VSA involves identifying suitable values of the model parameters 'θ' through the iterative process shown in Figure 3.2.
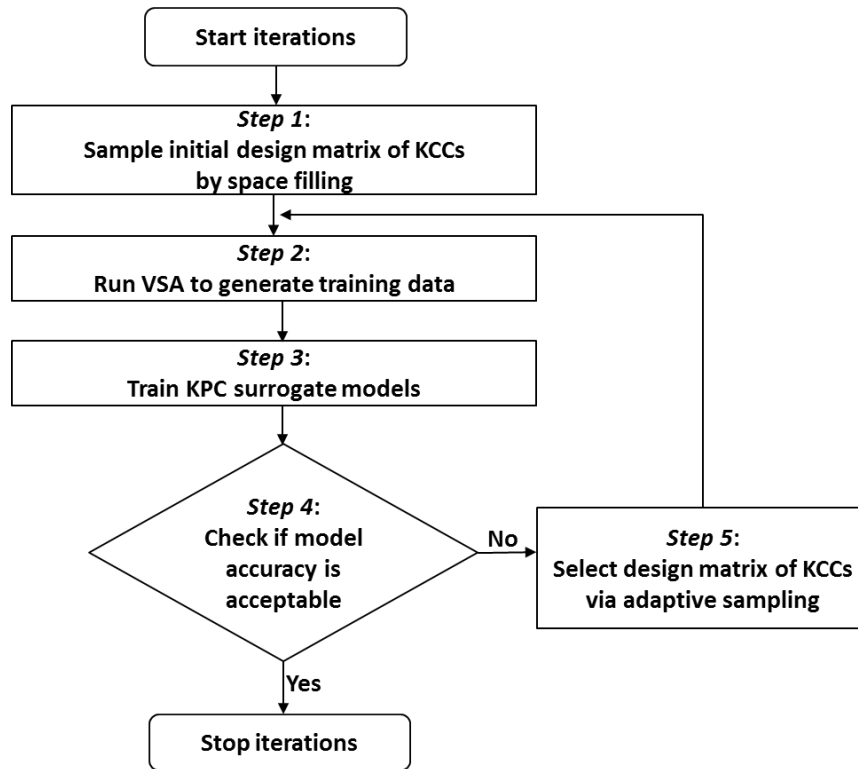
Figure 3.2: Surrogate modelling of KPCs from VSA

The five steps of surrogate modelling of KPCs from VSA, as shown in Figure 3.2, are described as follows:

Step 1: *Sample initial design matrix of KCCs by space filling –*

Input to VSA is a $n \times d$ design matrix $\mathbf{X} = \{\mathbf{x}_i\}_{i=1}^{n}$ having 'n' samples of 'd' KCCs. In the first iteration, the initial design matrix of KCCs is generated based on various design of experiments approaches such as full-factorial, central composite

combinations and others.

Step 2: *Run VSA to generate training data –*

Each row of the $n \times d$ design matrix $\mathbf{X}$ represents a sample fixture layout for the assembly defined by locations of 'd' clamps (KCCs), $\mathbf{x}_i = \{x_{i1}, x_{i2}, ..., x_{id}\}$ where $i = \{1, 2, ..., n\}$. For each fixture layout, FEM-based VSA estimates 'r' assembly KPCs $\mathbf{y}_i = \{y_{i1}, y_{i2}, ..., y_{ir}\}$ which can be for example part-to-part gaps at 'r' welding spots where a permanent joint between the mating parts needs to be made via a joining process such as Resistance Spot Welding (RSW), Remote Laser Welding (RLW) or other joining process.

In each iteration of the surrogate modelling process, shown in Figure 3.2, 'n' training samples $\mathbf{S} = \{\mathbf{x}_i, \mathbf{y}_i\}_{i=1}^n$ on KCCs and KPCs are generated and accumulated in a training matrix $\mathbf{S}_\mathrm{T}$ which is used to develop the surrogate models in that iteration. The number of instances in $\mathbf{S}_\mathrm{T}$ grows as *n, 2n, ...* N*n*, where 'N' is the number of iterations performed.

Step 3: *Train KPC surrogate models –*

During the current iteration, the training matrix $\mathbf{S}_\mathrm{T}$ is used to estimate the parameters (θ) of the surrogate model. The actual method applied to determine θ depends on choice of the surrogate model. For example, least squares method is used to determine the coefficients in case of a linear regression model.

Step 4: *Check if model accuracy is acceptable –*

In this step, test samples $\mathbf{S}_\mathrm{V} = \{\mathbf{x}_i, \mathbf{y}_i\}_1^t$ are used to evaluate the accuracy of the surrogate models, based on a criteria such as mean-squared error (MSE), coefficient of determination (R^2) or others. Mean squared error for the jth KPC is calculated using Eq. (3.1)

$$\text{MSE}_j = \frac{1}{t}\sum_{i=1}^{t}(y_{ij} - \hat{y}_{ij})^2 \tag{3.1}$$

where y_{ij} and $\hat{y}_{ij}$ are the actual and predicted KPCs for the ith test sample and $i = \{1,2,...,t\}$. Coefficient of determination is computed using Eq. (3.2).

$$R_j^2 = 1 - \frac{\displaystyle\sum_{i=1}^{t}(y_{ij} - \hat{y}_{ij})^2}{\displaystyle\sum_{i=1}^{t}(y_{ij} - \overline{y}_j)^2} \tag{3.2}$$

where $\overline{y}_j$ is the average of the jth KPC obtained from the 't' test samples as $\overline{y}_j = \frac{1}{n}\sum_{i=1}^{t}y_{ij}$. The coefficient of determination (R_j^2) measures the accuracy of the surrogate model relative to a naïve model where all predictions are made using the average of the observed values. R_j^2 varies from 0 to 1 where a higher value indicates better model accuracy.

In case of multiple KPCs, average of the accuracy of individual surrogate models, for example $R_{\text{avg}}^2 = \sum_{j=1}^{r}R_j^2 \Big/ r$, is computed to decide the stopping criterion (ψ) of the surrogate modelling process. The stopping criterion can be a user-defined minimum average accuracy required from the surrogate models.

Step 5: *Select design matrix of KCCs via adaptive sampling –*

If the stopping criterion in Step 4 is not met, further iteration needs to be done to generate additional training data by running VSA and enhance the surrogate models. Unlike for the first iteration, design matrix of KCCs for subsequent iterations is generated by an adaptive sampling strategy (Lovison & Rigoni, 2011). Adaptive sampling of KCCs ensure that desired accuracy of the surrogate models can be achieved in as few iterations as possible by selectively sampling KCCs from specific

regions in the KCC-design space. For example, KCCs might be selected from a region where the underlying function of a KPC has a steep slope to ensure that the training data $\mathbf{S}_T$ includes instances from regions of local maximas and minimas. Essentially, adaptive sampling expedites convergence of the surrogate model to desired accuracy level. Simpson, *et al.* (2001) presents a review of different strategies for adaptive sampling and compares its effect on model accuracy with that of uniform random sampling of the input parameters to computer simulation. The design matrix of KCCs generated via adaptive sampling is then fed back to Step 2 where further training data is generated by running VSA.

The two main steps of surrogate modelling of KPCs from VSA are: (1) Step 3 which involves *surrogate model training* using data generated from VSA; and, (2) Step 5 which selects design matrix of KCCs via *adaptive sampling*. Significance of these steps and scope of research on methods for *surrogate model training* and *adaptive sampling* to achieve *scalability for deterministic non-linearity* is discussed as follows:

i. *Training of KPC surrogate models in Step 3* – Surrogate model training involves estimating parameters $\boldsymbol{\theta}$ of the model from the training data generated by VSA. The chosen surrogate modelling technique (for example polynomial regression, kriging, ANN, SVM etc.) has an impact on prediction accuracy and convergence to desired accuracy level. Techniques which can give more accurate surrogate models for deterministic KPCs with varying number of local maximas/minimas in lesser simulations are preferred. This gives the scope to review limitations of currently existing techniques and develop novel ones to achieve scalability for deterministic non-linearity.

ii. *Selecting KCC design matrix via adaptive sampling in Step 5* – Most sheet metal

assemblies in BIW manufacturing involves multiple KPCs which are estimated by VSA for given KCCs. To reduce computation time required to generate training data for developing surrogate models of multiple KPCs, it is desirable to use the same design matrix of KCCs for running VSA. Therefore, adaptive sampling which selects KCC design matrix based on non-linearity of the underlying KPC-KCC interrelation must address multiple KPCs in a single adaptive sample to avoid generating multiple disparate adaptive samples, each for a single KPC. Hence there is a requirement to develop *multi-response* (or multi-KPC) adaptive sampling for Step 5.

3.4 Related work on surrogate modelling from computer-based Variation Simulation Analysis

As discussed in the previous section, surrogate modelling of KPCs from VSA has two main steps: (1) *surrogate model training* which involve estimating the model parameters; and (2) *adaptive sampling* to generate design matrix on KCCs to be given as input to VSA. This section reviews related work on *surrogate model training* and *adaptive sampling*.

This chapter specifically focuses on the Kriging method for training the surrogate models of deterministic KPCs. Section 3.4.1 describes the state-of-the-art Kriging technique. Related work on Kriging is reviewed and their limitations in addressing scalability for deterministic non-linearity are discussed. To address these limitations, Greedy Polynomial Kriging (GPK) is proposed in this chapter. There are other methods for training surrogate models. Examples include polynomial regression, neural network, support vector machine and regression trees. A comprehensive review of different methods applied for training surrogate models from computer simulation for engineering design optimization tasks is given by Simpson, *et al.* (2001), Wang

and Shan (2007) and Chen, *et al*. (2014). Based on the case studies of sheet metal assemblies, this chapter provides comparison of accuracy of GPK, state-of-the-art Kriging (henceforth referred in this thesis as Ordinary Kriging (OK)) and other popular methods for surrogate model training found in the literature.

Section 3.4.2 reviews past research on adaptive sampling and discusses their limitations in the context of multi-KPC or multi-response VSA. To address these limitations, Optimal-Multi Response Adaptive Sampling (O-MRAS) is developed in this chapter to combine multiple adaptive samples each generated for a single response or KPC.

3.4.1 Review of related work on Kriging for surrogate model training

Since its inception in geo-statistics as a distance-weighted predictor of average grades of mineral ores, Kriging has been a popular technique for training surrogate models of deterministic responses obtained from computer-based simulation models. Barton (1998), Simpson, *et al*. (2001), Martin and Simpson (2004), Kleijnen (2009) and Li, *et al*. (2010) showed that the predictive accuracy of Kriging is better than other surrogate modelling methods using well-known benchmark functions.

Kriging is related to polynomial regression. Eq. (3.3) presents a polynomial regression model where a KPC 'y' is predicted from linear regression model of polynomial terms of the KCCs ($\mathbf{x}$). Here $\mathbf{h}(\mathbf{x}) = \{h_1(\mathbf{x}), h_2(\mathbf{x}), ..., h_m(\mathbf{x})\}$ are the polynomial terms of $\mathbf{x}$ and $\boldsymbol{\beta} = \{\beta_1, \beta_2, ..., \beta_m\}$ represents the coefficients of the polynomial terms in $\mathbf{h}(\mathbf{x})$. ε_i for $i=1,2...n$ are deviances of the actual KPC y_i and predicted KPC $\hat{y}_i$ for 'n' training instances.

$$y_i(\mathbf{x}_i) = g(\mathbf{x}_i) + \varepsilon_i = \boldsymbol{\beta}^T \mathbf{h}(\mathbf{x}_i) + \varepsilon_i \quad (i=1,2...n) \tag{3.3}$$

Assuming that deviances ε_i follows an independent and identically

distributed normal density with zero mean and variance σ^2, the coefficients in $\boldsymbol{\beta}$ can be estimated by the method of least squares. However, the normality assumption about the deviances ε_i might not be accurate under the following two conditions: (1) the deviances of the polynomial function from the true values of the KPC cannot be interpreted as random noise in case of VSA which generate deterministic output (Sacks, *et al.*, 1989); and (ii) the deviances might be due to the non-linearity of the underlying physical process (Simpson, *et al.*, 2001). Thus, polynomial regression, though providing a global approximation of the response, is not able to fit local non-linearities, characterized by presence of local maximas and minimas, and hence results in poor accuracy of the surrogate model.

Significant improvement in prediction accuracy over polynomial regression has been achieved by assuming that the deviances originate from a random process. (Blight & Ott, 1975) formulates the deviances ε_i for $i = 1, 2, ..., n$ as 'n' random variables jointly following a multivariate normal or Gaussian distribution of 'n' variables. When the deviances ε_i for $i = 1, 2, ..., n$ are assumed to follow a joint normal or Gaussian distribution in 'n' variables, they are said to be originating from a Gaussian random process (Sacks, *et al.*, 1989). The surrogate modelling method based on this assumption is Kriging, which therefore is also known as *Gaussian process regression*. The covariance structure of the joint Gaussian distribution is given in Eq. (3.4)

$$R_l(\varepsilon_i, \varepsilon_k) = \sigma^2 \left\| \mathbf{x}_i - \mathbf{x}_k \right\|_2^{\alpha} \tag{3.4}$$

where $\left\| \cdot \right\|_2$ represents the L$_2$ norm of $\mathbf{x}_i - \mathbf{x}_k$ or the Euclidean distance between the KCC design points $\mathbf{x}_i$ and $\mathbf{x}_k$. α is the smoothing parameter. Based on the formulation that the deviances ε_i jointly follow a multivariate Gaussian or normal

65

distribution, several works (Sacks, *et al.*, 1989; Koehler & Owen, 1996; Booker, 1996) generalizes the kriging surrogate model as

$$\hat{y}_i = g(\mathbf{x}_i) + Z(\mathbf{x}_i) = \sum_{j=1}^{m} \beta_j h_j(\mathbf{x}_i) + Z(\mathbf{x}_i) \quad (i=1,2\ldots n) \tag{3.5}$$

which includes a regression component $g(\mathbf{x})$ of 'm' basis functions $\mathbf{h}(\mathbf{x}) = \{h_1(\mathbf{x}), h_2(\mathbf{x}),\ldots,h_m(\mathbf{x})\}$ and a Gaussian process $Z(\mathbf{x})$. The regression component $g(\mathbf{x})$ generates a global approximation of the KPC while the Gaussian process $Z(\mathbf{x})$ adjusts the surrogate model for local non-linearities such as local maximas and minimas. The basis functions can be terms from p^{th} order polynomial of $\mathbf{x}$. The random process has mean, $E[Z(\mathbf{x})] = 0$ and covariance, $\text{cov}\big(Z(\mathbf{x}_i), Z(\mathbf{x}_k)\big) = \sigma^2 R(\mathbf{x}_i, \mathbf{x}_k; \boldsymbol{\theta})$. Here, σ^2 is the variance of the Gaussian process and $R(\cdot)$ is the generalized correlation function, which is defined by parameters $\boldsymbol{\theta}$. Frequentist approach exist for finding the best linear unbiased estimators of $\boldsymbol{\beta}$ and σ^2 for a given $\mathbf{h}(\mathbf{x})$ and θ. The correlation function $R(\cdot)$ essentially quantifies the similarity between the points $\mathbf{x}_i$ and $\mathbf{x}_k$. Kleijnen (2009) generalizes the correlation function shown in Eq. (3.4) as a product of 'd' one-dimensional functions expressed as follows

$$R(\mathbf{x}_i, \mathbf{x}_k) = \prod_{j=1}^{d} \varphi(|x_{ij} - x_{kj}|; \theta_j) \tag{3.6}$$

Here $|\cdot|$ represents the absolute value and $\boldsymbol{\theta} = \{\theta_1, \theta_2,\ldots,\theta_d\}$ are the parameters of the correlation function where *j=1,2...d*. A special case of the correlation shown in Eq. (3.6) is the Gaussian correlation function

$R(\mathbf{x}_i, \mathbf{x}_k) = \prod_{j=1}^{d} \exp\left(-\frac{(x_{ij} - x_{ij})^2}{\gamma_j} \right) = \exp(-\sum_{j=1}^{d} \frac{(x_{ij} - x_{ij})^2}{\gamma_j})$ which is based on the

Euclidean distance between the design points $\mathbf{x}_i$ and $\mathbf{x}_k$. In this case, the parameters of the correlation function are $\boldsymbol{\theta} = \{\theta_1, \theta_2, ..., \theta_d\} = \{\gamma_1, \gamma_2, ..., \gamma_d\}$. Moreover, the Gaussian correlation function is a special case of the family of exponential correlation functions given in Eq. (3.7)

$$R(\mathbf{x}_i, \mathbf{x}_k) = \exp(-\sum_{j=1}^{d} \frac{|x_{ij} - x_{kj}|^{\alpha_i}}{\gamma_j}) \tag{3.7}$$

which has parameters $\boldsymbol{\theta} = \{\gamma_1, \gamma_2, \ldots, \gamma_d; \alpha_1, \alpha_2 ..., \alpha_d\}$, where γ_j is the sensitivity parameter which controls how quickly the correlation drops with distance $\delta_{ik} = |x_{ij} - x_{kj}|$ along the jth KCC and α_j is the smoothing parameter which determines the smoothness or differentiability of the surrogate model with respect to the jth KCC. Maximum likelihood estimation is popularly used to estimate parameters $\boldsymbol{\beta}$ and $\boldsymbol{\theta}$ of the Kriging surrogate models.

A lot of work has been done on developing Kriging surrogate models based on the function prescribed in Eq. (3.5). Past research assume that the regression component, $g(\mathbf{x})$ of the Kriging surrogate model is either a constant or a polynomial of $\mathbf{x}$. However, specifying a constant regression component $g(\mathbf{x}) = \beta_0$ is trivial and might not be an accurate global approximation. Moreover when $g(\mathbf{x})$ is a polynomial, the order of the polynomial is often set from the user's knowledge about the underlying physical process, which may not be adequate especially for complex VSA models wherein KPCs are estimated from KCCs based on multiple mathematical formulations and their solutions obtained either analytically or numerically. Furthermore, using all the terms from the user-specified polynomial as features or explanatory variables in the regression component $g(\mathbf{x})$ might lead to overfitting especially for higher order polynomials. Under these conditions, there is need for

67

feature selection which can identify features $\mathbf{h}^*(\mathbf{x})$ to be used in the regression component $g(\mathbf{x})$ of the Kriging surrogate model. Recently, Couckuyt, *et al.* (2012) emphasized the importance of feature selection for Kriging and suggested a Bayesian weighting approach and iterative maximum likelihood to select important features from an initial predefined set of features. However, defining the initial set of features might require knowledge about the underlying physical process. Previously, Wang & Shan (2007) and Kleijnen (2009) and several other suggested that the features can be terms from the pth order multivariate polynomial of $\mathbf{x}$, where 'p' can be suitably chosen by the user. This chapter proposes that 'p' can be algorithmically determined. Choosing the order of the polynomial 'p' and selecting an optimal subset of polynomial terms should be done by optimizing an objective function, which is closely related to the accuracy of the regression model.

At this point, it is noteworthy that in the past, feature selection for kriging focused on variable screening to identify few variables from the original set input parameters. Multiplicative interactions between the input parameters are not considered to generate new features. Related work on variable screening for Kriging was done by (Welch, *et al.*, 1992; Linkletter, *et al.*, 2006) who eliminated unimportant variables from the original set of input parameters ($\mathbf{x}$) based the on scaling parameter γ_j of the variable.

Another important aspect of Kriging surrogate models is the correlation function of the Gaussian process $Z(\mathbf{x})$, which adjusts the model to local non-linearities. The correlation function, also known as *kernel* function in literature, has a significant impact on the prediction error of Kriging surrogate models on unseen test samples (Sacks, *et al.*, 1989). The exponential kernel function is popularly used for developing Kriging surrogate models for engineering design optimization tasks

(Kleijnen, 2009). Most applications use the Gaussian correlation function because it is infinitely differentiable with respect to the input parameters (which are KCCs in the context of fixture layout optimization) and generates smooth response surfaces from the surrogate models. However, the assumption that responses are always smooth to changes in input parameters might not be valid in all applications. Furthermore. maximum likelihood estimation (MLE) has been conventionally applied to determine the parameters $\boldsymbol{\theta} = \{\gamma_1, \gamma_2, \cdots, \gamma_d; \alpha_1, \alpha_2 \ldots, \alpha_d\}$ of the Kriging surrogate models (Kumar, 2006; Wang & Shan, 2007; Ben-Ari & Steinberg, 2007; Kleijnen, 2009; Toal, *et al*., 2011; Chen, *et al*., 2014; Wessing, *et al*., 2014). However, though MLE might give an adequate accuracy on training samples which is used to develop the surrogate model, it might not ensure *minimization of error on unseen test samples*.

Based on the aforementioned discussion, the limitations of state-of-the-art Ordinary Kriging affecting achievement of scalability for deterministic non-linearity are summarized as follows:

i. *Predefined features for regression component* – Currently existing Ordinary Kriging surrogate models require polynomial order for the regression component to be defined by the user. For complex VSA of sheet metal assemblies, defining predefined features might be challenging due to numerical intractability of the VSA.

ii. *Optimization of kernel function by MLE* – State-of-the-art Ordinary Kriging determines parameters $\boldsymbol{\theta}$ of the kernel function through MLE which though providing good accuracy for the training samples, might not ensure acceptable accuracy on unseen test samples.

To address the aforementioned limitations of Ordinary Kriging, this chapter develops the *Greedy Polynomial Kriging* method based on the following two

interlinked approaches:

i. *Polynomial Feature Selection* – To determine optimal order of the polynomial without predefined initialization and select an optimal subset of polynomial terms which maximize predictive accuracy of the regression component $g(\mathbf{x})$, this chapter develops the polynomial feature selection (PFS) approach. Terms from higher order polynomials are iteratively added if addition of a term results in decrease of the generalized prediction error of $g(\mathbf{x})$ till a stopping criterion is reached. The generalized prediction error of the regression component $g(\mathbf{x})$ is a measure of the average model error on unseen test samples. Moreover, to ensure that higher accuracy is reached in fewer computation, polynomial terms are added in a greedy order determined by the correlation of a term with the KPC, where a term with higher correlation with the KPC is evaluated before a term with lower correlation with the KPC.

ii. *Kernel optimization via minimization of generalized model error* – An important requirement for addressing scalability for deterministic non-linearity of assembly KPCs is ensuring acceptable predictive accuracy of the surrogate model on unseen test samples for KPC-KCC interrelations with varying number of local maximas and minimas. Though state-of-the-art Ordinary Kriging method models local maximas and minimas, it does not ensure maximum predictive accuracy on unseen test samples. To address this limitation, this chapter proposes kernel optimization approach based on minimization of the generalized prediction error on unseen test samples to determine optimal $\mathbf{\theta}$ for the exponential kernel function $R(\mathbf{x}_i, \mathbf{x}_k) = \exp(-\sum_{j=1}^{d} \frac{|x_{ij} - x_{ij}|^{\alpha_j}}{\lambda_j})$.

Table 3.1 summarizes related work on state-of-the-art Kriging and

70

highlights the contribution of the proposed GPK method.

Table 3.1: Review of feature selection and kernel optimzation for Kriging surrogate models

	Approach of *feature selection*	Approach of *kernel optimization*	Related work
Ordinary Kriging	*Pre-defined set of features (lack of feature selection)*	Kernel optimization via *maximum likelihood estimation*	Sacks, *et al*. (1989) Odeha, *et al*. (1994) (Booker, 1996) Koehler & Owen (1996 Rajagopalan & Lall (1998) Høst (1999) Lee (2005) Jakumeit, *et al*. (2005) Forsberg & Nilsson (2005) Li, *et al*. (2008) Gao & Wang (2008) Dubourg, *et al*. (2011) Huang, *et al*. (2011) Toal, *et al*. (2011) Luo, et al. (2012) Chen, *et al*. (2014) Wessing, *et al*. (2014)
	Variable screening to identify critical input parameters		Welch, *et al*. (1992) Hoeting, *et al*. (2006) Linkletter, *et al*. (2006)
	Feature selection from predefined set of features		Couckuyt, *et al*. (2012)
GPK	*Polynomial Feature Selection* - Does not require pre-defined set of features - Selects polynomial terms based on minimization of generalized model error	Kernel optimization via *minimization of generalized model error*	***Proposed in this chapter***

Section 3.5 elaborates the proposed GPK method for training scalable surrogate models of deterministic assembly KPCs.

3.4.2 Review of related work on adaptive sampling

Surrogate modelling of KPCs from VSA is an iterative process as shown in Figure 3.2 and in each iteration a KCC design matrix is chosen as input to VSA. In the first iteration, the design matrix of KCCs is chosen based on design of experiment approaches such as full-factorial design of experiments (DOE), fractional-factorial DOE, Latin Hypercube Sampling (LHS), Orthogonal Arrays and other approaches (Simpson, *et al*., 2001). In subsequent iterations, the KCC design matrix is generated

using an adaptive sampling strategy, which analyses the existing training instances and samples points from specific regions of the KCC design space based on the adaptive sampling criteria (Kleijnen, 2009). This section reviews currently existing methods of adaptive sampling. Capabilities and limitations of state-of-the-art methods are discussed in the context of surrogate modelling from VSA which outputs multiple assembly KPCs for fixture related KCCs given as input.

Adaptive sampling focuses on improving the predictive accuracy of a surrogate model over the entire design space of KCCs. (Currin, *et al*., 1991) suggested maximum posterior entropy to generate an entropy-optimal design matrix of KCCs for single-KPC surrogate modelling. Another approach of adaptive sampling for kriging-based surrogate models is to select a new sample point $\mathbf{x}_C$ which has the maximum mean squared error $\mathrm{MSE}\left(\hat{y}(\mathbf{x})\right) = E\left(\hat{y}(\mathbf{x}) - y(\mathbf{x})\right)^2$, estimated from the existing kriging surrogate model (Sacks, *et al*., 1989; Jin, *et al*., 2002). The aforementioned approaches focus on predictive error of the existing surrogate model to identify the adaptive sample. However, they do not consider non-linearity of the underlying input-output interrelations. Kleijnen and Van Beers (2004) suggested an approach of adaptive sampling which takes into consideration non-linearity of the underlying input-output function. Points were sampled from subareas in the design space of the input parameters, where the underlying input-output function has local maximas or minimas. Recently, Lovison and Rigoni (2011) have proposed Lipschitz criteria based adaptive sampling which selects points from subareas having non-linear behaviour of the input/output function. The design space of the input parameters is divided into simplexes by Delaunay triangulation. A local complexity criterion called Lipschitz constant (*L*) is computed for each simplex. Candidate points are generated throughout the design space using a space-filling strategy such as uniform random sampling, full-

factorial design of experiments or others. The merit of each candidate point is calculated as a product of the Lipschitz constant of the point's residential simplex and the Euclidean distance of the point from the nearest vertex of its residential simplex. The top *'n'* points, ranked according to merit, are selected as the adaptive sample $\mathbf{X}_C$ to be used for next batch of simulations. The Lipschitz criteria-based adaptive sampling selects design points, which are near or at the local maximas and minimas of the underlying input/output function. Hence this criteria is preferred for emulating local non-linearities of the underlying input-output function.

The aforementioned sampling approaches provide useful criteria of generating design matrix of KCCs. However, a major limitation of the aforementioned methods is that they are either intended for single-response or single-KPC computer simulations or take union of the individual adaptive samples $\mathbf{X}_C^{(1)}, \mathbf{X}_C^{(2)}, ..., \mathbf{X}_C^{(r)}$ generated independently for *'r'* responses. This limitation is aggravated if the individual adaptive samples have few instances common amongst themselves thereby making simulations for the full set of adaptive sample forbiddingly time-consuming. To address this problem, an Optimal Multi Response Adaptive Sampling (O-MRAS) is developed in Section 3.5. O-MRAS integrates a single-response adaptive sampling criterion with *k*-means clustering and a weighted selection strategy to generate a single adaptive sample from *'r'* disparate adaptive samples. To initially generate the individual adaptive samples $\mathbf{X}_C^{(j)}$ where $j = 1, 2, ..., r$, O-MRAS can be integrated with any state-of-the-art adaptive sampling criteria. Lipschitz criterion is specifically used with O-MRAS for the case-studies discussed in this chapter.

Table 3.2 summarises currently existing methods of adaptive sampling and highlights the capability of the proposed O-MRAS approach.

Table 3.2: Review of state-of-the-art on adaptive sampling

Approach of adaptive sampling	Related work
Single response adaptive sampling	Sacks, *et al*. (1989)
	Currin, *et al*. (1991)
	Jin, *et al*. (2002)
	Kleijnen & Van Beers (2004)
	Lovison & Rigoni (2011)
Multi response adaptive sampling	***Proposed in this chapter***

3.5 Scalable surrogate modelling of assembly KPCs

This section develops scalable surrogate models addressing the deterministic non-linearity of assembly KPCs estimated by computer-based VSA. Figure 3.3 outlines the steps of developing scalable surrogate models from computer-based VSA.
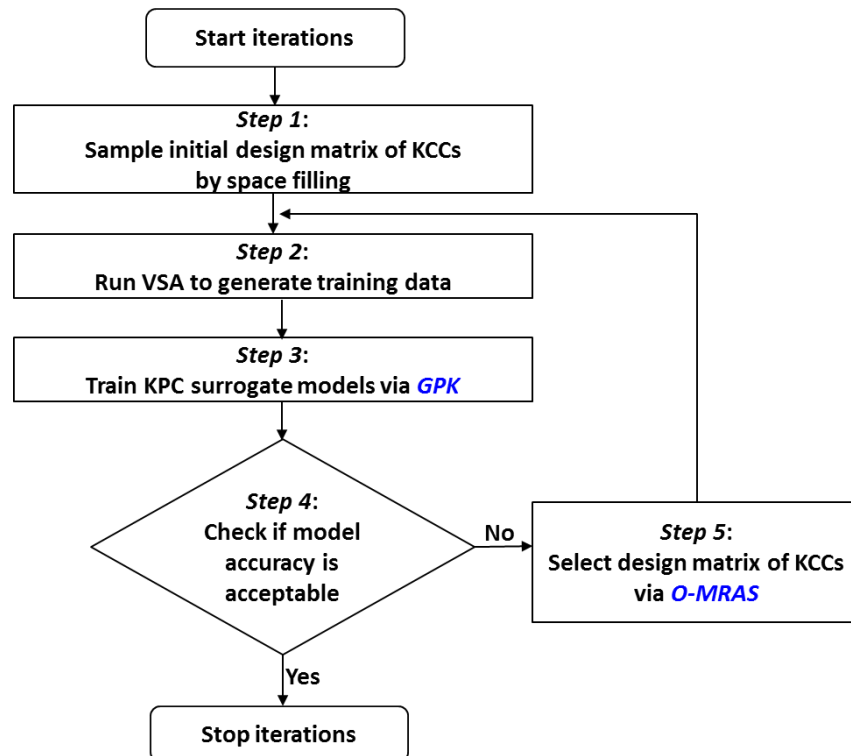
Figure 3.3: Scalable surrogate modelling of assembly KPCs from VSA

The steps of developing the scalable surrogate models, as shown in Figure 3.3, are adapted from the generic approach of surrogate modelling of KPCs described in Section 3.3. The work presented in this section focuses on developing the following two methods (1) GPK for training the KPC surrogate models in Step 3; and, (2) O-MRAS for generating adaptive sample of multiple KPCs in Step 5.

Section 3.5.1 describes GPK and O-MRAS is presented in Section 3.5.2

3.5.1 Greedy Polynomial Kriging (GPK)

A KPC from a computer-based VSA is assumed to be deterministic as same value of the KPC is obtained repeatedly for the same values of KCCs. Any noise in the KPC, due to numerical error of VSA, is considered negligible for practical applications. Figure 3.4 shows the plot of a deterministic KPC (y) with respect to a KCC (x).
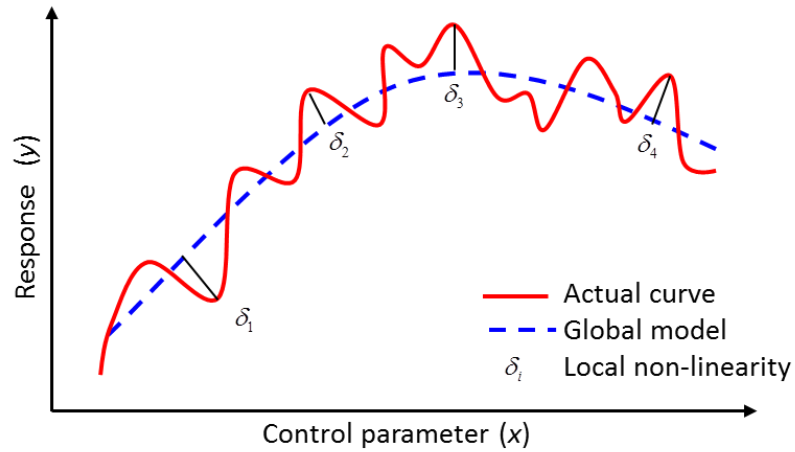
Figure 3.4: Surrogate modelling of determinstic assembly KPCs

Kriging surrogate model of the KPC y is given as

$$\hat{y} = g(\mathbf{x}) + Z(\mathbf{x}) \tag{3.8}$$

whereby the regression component $g(\mathbf{x}) = \sum_{j=1}^{m} \beta_j h_j(\mathbf{x})$ provides a global approximation of the KPC (shown by the blue dashed curve in Figure 3.4). The local non-linearities such as δ_1 through δ_4 are modelled by the Gaussian process $Z(\mathbf{x})$. Details of the regression component, $g(\mathbf{x})$ and the Gaussian process $Z(\mathbf{x})$ are described in Section 3.4.1.

This section proposes Greedy Polynomial Kriging (GPK), a novel approach of developing Kriging surrogate model of deterministic KPC based on the following two methods:

i. *Polynomial Feature Selection* (PFS) which identifies an optimal regression component $g(\mathbf{x})$. PFS is discussed in Section 3.5.1.1.

ii. *Kernel Optimization* (KO) which determines optimal parameters $\boldsymbol{\theta}$ for the exponential correlation function (also commonly known as *kernel* function). KO is described in Section 3.5.1.2.

3.5.1.1 Polynomial Feature Selection

Feature selection identifies the best set of features $\mathbf{h}^* \subseteq \mathbf{h}$ which generates an accurate global approximation of the response. Features are also called basis functions as they can be derived from the control parameters ($\mathbf{x}$). For example, $\mathbf{h}$ can be terms from the pth order polynomial in $\mathbf{x}$ in which case $\mathbf{h}(\mathbf{x}) = \{h_1, h_2, ..., h_m\} = \{x_1^p, x_1^{p-1}x_2, ..., x_d^p\}$ where 'm' is the number of terms in the pth order polynomial.

The approximation done by the regression component is assumed to be a linear combination of features $\mathbf{h} = \{h_1, h_2, ..., h_m\}$ as shown in Eq. (3.9).

$$\hat{y} = \beta_0 + \beta_1 h_1 + \ldots + \beta_m h_m \tag{3.9}$$

The coefficients $\boldsymbol{\beta} = \{\beta_0, \beta_1, \ldots, \beta_m\}$ are determined by the method of least squares and are given as

$$\boldsymbol{\beta} = (\mathrm{H}^{\mathrm{T}}\mathrm{H})^{-1}\mathrm{H}^{\mathrm{T}}\mathbf{y} \tag{3.10}$$

where H is the $n \times m$ input matrix of features $\mathbf{h}$ and $\mathbf{y}$ is $n \times 1$ vector of the KPC obtained from the training dataset $\mathrm{S_T} = \{\mathbf{x}_i, y_i\}_1^n$. The difference between the actual and predicted response can be computed based on the instances in the training dataset $\mathrm{S_T} = \{\mathbf{x}_i, y_i\}_1^n$ as follows

$$\varepsilon_i = y_i - \hat{y}_i \ (i=1,2,\ldots,n) \tag{3.11}$$

Since the errors calculated in Eq. (3.11) are on the individual training samples from the dataset $\mathrm{S_T}$, an aggregate measure of the model's prediction error is required. The aggregate error of the model is calculated as the mean of the squares of the individual errors and is also called mean-squared error (MSE) loss function. The individual errors calculated in Eq. (3.11) depends on the coefficients $\boldsymbol{\beta}$ which in turn depend on the features $\mathbf{h}$ used in the regression component. Therefore, it is apt to consider the MSE loss function as a function of the features $\mathbf{h}$ for the given dataset $\mathrm{S_T}$. Based on this premise the MSE loss function can be expressed as

$$L(\mathbf{h} \mid \mathrm{S_T}) = \frac{1}{n}\sum_{i=1}^{n}\varepsilon_i^2 = \frac{1}{n}\sum_{i=1}^{n}(y_i - \hat{y}_i)^2 \tag{3.12}$$

Feature selection identifies the best subset of features $\mathbf{h}^* \subseteq \mathbf{h}$ which minimizes the MSE loss function. However, it is noteworthy that the loss function in Eq. (3.12) not only depends on the features $\mathbf{h}$ but also on the training dataset $\mathrm{S_T}$ used to compute the individual prediction errors ε_i for $i = 1, 2, \ldots, n$. Therefore, to estimate the prediction error of the regression component which is independent of the training sample, a

77

generalized estimation of the MSE loss function $\xi(\mathbf{h})$ is obtained by the method of k-fold cross validation (Kohavi, 1995), which is described in Appendix A. The generalized MSE loss function $\xi(\mathbf{h})$ is a measure of the regression component's prediction error on unseen test samples.

Polynomial Feature Selection (PFS) identifies the best set of features $\mathbf{h}^* \subseteq \mathbf{h}$ which minimizes the generalized loss function $\xi(\mathbf{h})$. PFS is formalized as the following optimization problem

$$\mathbf{h}^* = \arg\min_{\mathbf{h}' \subseteq \mathbf{h}} \xi(\mathbf{h}') \qquad (3.13)$$

PFS generates a solution to the minimization problem stated in Eq. (3.13). The selected features are used in the regression component of the Kriging surrogate model to develop the best possible global approximation of the underlying non-linear relationship between the KPC y and the KCCs $\mathbf{x}$. To do this, multiplicative interactions between individual KCCs in relation to the KPC are considered in the following two ways:

i. *One-way* interaction – This type of interaction is suggested to model the linear effect of a single KCC on the KPC. *One-way* interactions are represented as $y \sim x_i$, where $i=1, 2,\ldots, d$.

ii. *Generalized n-way* interaction – This type of interaction models the functional dependency of the KPC on multiplicative effects between one or more KCCs. A *generalized n-way* interaction is denoted as $y_j \sim x_1^{p_1} x_2^{p_2} \ldots x_d^{p_d}$ where p_i is an integer. n-way interaction between KCCs can be generated by considering terms from p^{th} order polynomial of the KCCs $\mathbf{x} = \{x_1, x_2,\ldots, x_d\}$. In this case individual interactions are determined by solutions to the Eq. (3.14) given below.

78

$$\sum_{i=1}^{d} p_i = p \text{ where } p_i \in \{0,1,...p\} \text{ for } i = \{1,2,...d\} \tag{3.14}$$

In general, a feature h_k can represent a *generalized n-way* multiplicative interaction between the KCCs. When $n=1$ features denote linear functional dependency $y \sim h_i(\mathbf{x}) = x_i$. For high-order multiplicative interactions between one or more KCCs, the features can be generalized as $h(\mathbf{x}) = x_1^{P_1} x_2^{P_2} ... x_d^{P_d}$ and the subsequent functional dependency with the KPC is $y \sim h(\mathbf{x}) = x_1^{P_1} x_2^{P_2} ... x_d^{P_d}$. The objective of PFS is to determine an optimal polynomial order 'p' and individual polynomial features such as $x_1^{P_1} x_2^{P_2} ... x_d^{P_d}$ which must be included in the regression component of the Kriging model. $\mathbf{h}(\mathbf{x}, p)$ is defined as the set containing the individual terms of the pth order polynomial of $\mathbf{x} = \{x_1, x_2, ..., x_d\}$. $\mathbf{h}(\mathbf{x}, p)$ can be represented as shown in Eq. (3.15).

$$\mathbf{h}(\mathbf{x}, p) = \{x_1^p, x_1^{p-1} x_2, ..., x_d^p\} \tag{3.15}$$

The number of features in $\mathbf{h}(\mathbf{x}, p)$ is the number of unique solutions to Eq. (3.14).

The basic logic of PFS is to: (i) to iteratively increase the order of the polynomial p as 1, 2... and so on over iterations $j =$1, 2... till no satisfactory reduction of generalized MSE loss function $\xi(\mathbf{h})$ is obtained; and, (ii) to identify an optimal subset of features, $\mathbf{h}^*(\mathbf{x}, p) \in \mathbf{h}(\mathbf{x}, p)$ for a given polynomial order 'p' during each iteration.

Initially, the algorithm sets $\mathbf{h}^* = \varnothing$. During j^{th} iteration when $p=j$, a greedy forward selection and backward elimination method is ran to determine subset of $\mathbf{h}^*(\mathbf{x}, p) \in \mathbf{h}(\mathbf{x}, p)$ which must be added to $\mathbf{h}^*$. The criterion for selection and elimination of a term is the decrease in the generalized MSE $\xi(\mathbf{h}^*)$ upon inclusion or exclusion of the term. At any stage of the algorithm, the generalized MSE for $\mathbf{h}^*$ is

calculated by a *k*-fold cross validation process (described in Appendix A). The forward selection process iteratively adds features from $\mathbf{h}(\mathbf{x}, p)$ by decreasing the generalized MSE. Backward elimination runs nested within forward selection and for a set of features already selected in $\mathbf{h}^*$, it attempts to further reduce the generalized MSE by removing those features, whose elimination decreases generalized MSE. The proposed approach of forward selection with nested backward elimination is better in removing sub-optimality from the selected features than only forward selection of features into the initial null set or only backward elimination from a full set of features. The terms are checked for selection and elimination in descending and ascending order of their absolute correlation with the KPC *y*. Selection or elimination of features based on increasing or decreasing correlation of the feature with the KPC induces a *preferential greedy nature* to the algorithm in selecting the polynomial features.

Let us denote the set of features sorted in descending order of their absolute correlation with y as $\mathbf{h}^D(\mathbf{x}, p) = \{h_1^D, h_2^D, ..., h_\eta^D\}$ where h_1^D and h_m^D has the highest and lowest absolute correlation with y respectively. Similarly, let us define the set of features sorted in ascending order as $\mathbf{h}^A(\mathbf{x}, p) = \{h_1^A, h_2^A, ..., h_m^A\}$ where h_1^A and h_m^A hence has the lowest and highest absolute correlation with y respectively.

After the optimal subset of features $\mathbf{h}^*(\mathbf{x}, p)$ are determined, the MSE of $\mathbf{h}^*$ is assigned to $\xi^*(p)$, as a measure of goodness of the polynomial order '*p*'. Iterations are stopped when the percentage drop in $\xi^*(p)$ compared to $\xi^*(p-1)$ is less than an user-defined convergence tolerance 'δ'.

In summary, PFS runs an inner iterative loop to determine optimal terms for a given polynomial order and an outer iterative loop to select a suitable polynomial

order *'p*'*. The final outcome is an optimal set of features $\mathbf{h}^*$ containing selected terms from polynomial of up to order *'p*'*. The feature selection algorithm is summarized in the pseudo code given below.

```
Input: S_T = {x_i, y_i}_1^n  and  δ > 0
Output: h* and p
//selection of order of the polynomial 'p' starts here
let h* and j=0
while true
    let j=j+1
    let h = h(x, j),  η = |h| and h* = ∅

    compute sorted set h^A from h
    let i=0
    //forward selection starts here
    while i ≤ η
        let i=i+1
        compute ξ(h* ∪ {h_i^A})

        if (h* = ∅)

            let h* = {h_i^A}

            let ξ(h*) = ξ({h_i^A})

        elseif (ξ(h*) > ξ(h* ∪ {h_i^A}))

            let h* = h* ∪ {h_i^A}

            let ξ(h*) = ξ(h* ∪ {h_i^A})

        endif
        let η' = |h*|

        compute sorted set h^D from h*
        let k=0
        //backward elimination for each forward selection step starts here
        while k ≤ η'
            let k=k+1
            compute ξ(h* \ {h_k^D})

            if (ξ(h*) > ξ(h* \ {h_k^D}))

                let h* = h* \ {h_k^D}

                let ξ(h*) = ξ(h* \ {h_k^D})

            endif
        end
        //backward elimination for each forward selection step ends here
    end
    //forward selection ends here
    let ξ(j) = ξ(h*)

    let p = j

    if (j > 1) and |ξ(j) − ξ(j − 1)| < [δ * ξ(j)] / 100 break
end
//selection of polynomial feature-mapping parameter 'p' ends here
```

At this stage, it is to be noted that the PFS has the following two

81

contributions towards generating the global approximation for the Kriging model: (1) it generates integral-power transformed KCCs and captures multiplicative interactions between the KCCs; (2) it identifies critical features, which are derived from the original KCCs through power transformation and multiplicative interactions, based on *minimization of generalized prediction error of the regression component on unseen test samples*. In this algorithm, power transformation of KCCs is specifically done with integral powers.

Using the set of critical features $\mathbf{h}^*$ identified by PFS, the GPK surrogate model of KPC y is developed by completing the Kernel Optimization.

3.5.1.2 Kernel Optimization

Using the selected features $\mathbf{h}^*$ the Kriging surrogate model of the KPC y can be written as

$$\hat{y} = \beta_0 + \beta_1 h_1^* + ... + \beta_m h_m^* + Z(\mathbf{x}) \tag{3.16}$$

The Gaussian process $Z(\mathbf{x})$ has mean, $E[Z(\mathbf{x})] = 0$, covariance, $\text{cov}\left(Z(\mathbf{x}_i), Z(\mathbf{x}_k)\right) = \sigma^2 R(\mathbf{x}_i, \mathbf{x}_k; \boldsymbol{\theta})$. Here, σ^2 is the variance and $R(\mathbf{x}_i, \mathbf{x}_k)$ is the exponential correlation function also known as kernel function which measures the similarity between two points. The exponential correlation function can be expressed as

$$R(\mathbf{x}_i, \mathbf{x}_k) = \exp(-\sum_{j=1}^{d} \frac{\left| x_{ij} - x_{kj} \right|^{\alpha_j}}{\gamma_j}) \tag{3.17}$$

which has parameters $\boldsymbol{\theta} = \{\gamma_1, \gamma_2, ..., \gamma_d; \alpha_1, \alpha_2, ..., \alpha_d\}$. The coefficients $\boldsymbol{\beta}$ of the regression component and variance of the Gaussian process σ^2 can be calculated by the method of Best Linear Unbiased Estimation (BLUE) from given training dataset

S_T and $\boldsymbol{\theta}$. The BLUE method is described in Appendix B.

For given S_T and $\boldsymbol{\theta}$, after $\boldsymbol{\beta}$ and σ^2 are determined by BLUE, the Kriging model can be used to predict the KPC from the KCCs. The difference between the actual and predicted KPC can be computed on the dataset $S_T = \{\mathbf{x}_i, y_i\}_1^n$ as follows

$$\varepsilon_i = y_i - \hat{y}_i \ (i=1,2,\dots,n) \tag{3.18}$$

The aggregate error of the model is calculated as the mean of the squares of the individual errors and is also called the mean-squared error (MSE) loss function. The individual errors calculated in Eq. (3.18) and indeed the MSE loss function depend on the coefficients $\boldsymbol{\beta}$, Gaussian process variance σ^2 and correlation parameters $\boldsymbol{\theta}$. Since, $\boldsymbol{\beta}$ and σ^2 can be expressed in terms of $\boldsymbol{\theta}$, it is apt to consider the MSE as a function of $\boldsymbol{\theta}$ for the given dataset S_T. Based on this premise the MSE loss function can be expressed as

$$L(\boldsymbol{\theta} \mid S_T) = \frac{1}{n}\sum_{i=1}^{n}\varepsilon_i^2 = \frac{1}{n}\sum_{i=1}^{n}(y_i - \hat{y}_i)^2 \tag{3.19}$$

The parameters $\boldsymbol{\theta}$ of the correlation function can be pre-defined or estimated by maximum likelihood estimation (MLE) using the training samples. However, MLE though ensuring a good fit on training data might not *minimize the prediction error on unseen test samples*. To address this issue this chapter proposes a kernel optimization method which focuses on the minimization of the generalized MSE $\xi(\boldsymbol{\theta})$ computed by *k*-cross validation. The minimization problem is prescribed in Eq. (3.20).

$$\boldsymbol{\theta}^* = \underset{\boldsymbol{\theta}' \in \mathfrak{R}^d}{\arg\min} \ \xi(\boldsymbol{\theta}') \tag{3.20}$$

To solve the aforementioned minimization problem an adaptive GA is

proposed. The surrogate model is developed over several iterations including generation of training data by running computer simulation of VSA. Over the iterations, size of the training data S_T increases thereby creating a larger space to be searched. To enable search over a larger space the following two parameters of GA are updated over the iterations: (1) number of chromosomes = 10+5(j-1); and, (2) number of generations = 25+10(j-1); where 'j' indicates count of the current iteration. Therefore 5 extra chromosomes are added every iteration and the GA is ran for 10 extra generations. This is suggested to ensure more extensive search by GA to obtain a better solution for optimal $\boldsymbol{\theta}$ as the size of training data increases over iterations of the surrogate modelling process. Additionally, to avoid redundant number of generations and indeed redundant computation time, an early stopping criterion for GA is set whereby if there is no decrease in the global best value of the fitness function $\xi(\boldsymbol{\theta})$ over last 5 generations, then GA is stopped.

In this section, GPK, a novel variant of the popular Kriging method of training surrogate models, has been developed. An important requirement for addressing scalability for deterministic non-linearity is developing surrogate models with *acceptable predictive accuracy on unseen test samples* for varying scale of deterministic non-linearity in KPC-KCC interrelations characterized by presence of varying number of local maximas and minimas. Though ordinary Kriging is preferred for emulating non-linearity of the underlying function, it does not ensure a minimal predictive error (or maximal predictive accuracy) on unseen test samples. Therefore to address scalability for deterministic non-linearity, GPK focuses on *minimization of generalized prediction error* for both feature selection and kernel optimization of the Kriging surrogate model.

3.5.2 Optimal Multi Response Adaptive Sampling (O-MRAS)

Adaptive sampling is used to analyze the existing training samples and suggest the design matrix of KCCs ($\mathbf{x}$) for subsequent batch of simulations. Existing adaptive sampling methods can be used to analyse data on individual KPCs and generate *'r'* disparate adaptive samples $\mathbf{X}_C^{(1)}, \mathbf{X}_C^{(2)}...\mathbf{X}_C^{(j)},...\mathbf{X}_C^{(r)}$ for each KPC individually where $\mathbf{X}_C^{(j)}$ is a $n \times d$ matrix and $j = 1, 2,..., r$.

This section develops Optimal Multi Response Adaptive Sampling (O-MRAS) to aggregate *'r'* disparate adaptive samples, each of which is individually generated by a currently existing single response adaptive sampling method.

The objective of O-MRAS is to select a final sample $\mathbf{X}_C$ which is best representative of all the KPCs. For the adaptive sample $\mathbf{X}_C^{(j)}$ of the jth KPC where $j = 1, 2,..., r$ let us define a $n \times 1$ vector $\mathbf{v}^{(j)}$ having values of the adaptive sampling criterion assigned to the *'n'* design points in $\mathbf{X}_C^{(j)}$ by the single-response adaptive sampling method. $\mathbf{v}^{(j)}$ is henceforth referred in this chapter as the merit vector. For example, if Lipschitz criterion is used to generate the individual adaptive samples then $\mathbf{v}^{(j)}$ is the Lipschitz criterion based merit vector (Lovison & Rigoni, 2011) of *'n'* design points in the adaptive sample $\mathbf{X}_C^{(j)}$.

The O-MRAS is achieved through the following three steps:

A. *Generate adaptive samples for individual KPCs* – Adaptive samples for the individual KPCs can be generated through any currently existing single-response adaptive sampling method. The outcome of this step is '*r*' disparate $n \times d$ adaptive samples $\mathbf{X}_C^{(1)}, \mathbf{X}_C^{(2)}...\mathbf{X}_C^{(j)},...\mathbf{X}_C^{(r)}$ each for a single KPC. Additionally, for each single-KPC adaptive sample, the $n \times 1$ merit vector $\mathbf{v}^{(j)}$ containing values of the adaptive sampling criteria for each point in $\mathbf{X}_C^{(j)}$ is

85

also available.

B. *Perform k-means clustering to identify 'n' groups* – This step starts by merging the points from *'r'* single-KPC adaptive samples into a single $\bar{\bar{n}} \times d$ matrix $\mathbf{X}_C$, where $\bar{\bar{n}}$ is the number of design points after removing duplicate entries. Similarly, the *'r'* independent merit vectors $\mathbf{v}^{(1)}, \mathbf{v}^{(2)},..., \mathbf{v}^{(r)}$ is compiled in a $\bar{\bar{n}} \times 1$ vector $\mathbf{v}_C$. If no duplicate design points are found between the *'r'* individual adaptive samples, then $\bar{\bar{n}} = rn$. On the contrary if all the individual adaptive samples are exactly same then $\bar{\bar{n}} = n$ and $\mathbf{X}_C$ is declared as the final adaptive sample and the algorithm stops. Hence the number of design points $\bar{\bar{n}}$ in the compiled matrix $\mathbf{X}_C$ can take all possible integral values in the range $[n, rn]$ depending on the specific problem being addressed. The strategy of O-MRAS is to distribute the design points in $\mathbf{X}_C$ into *'n'* groups and then select the best representative design point from each group to generate a final sample of *'n'* candidates of KCCs for next batch of computer simulations. *k*-means clustering (Hartigan & Wong, 1979) is used to group the points in $\mathbf{X}_C$ into *'n'* clusters $\mathbf{R}^{(1)}, \mathbf{R}^{(2)},..., \mathbf{R}^{(n)}$. Allocation of points to the clusters is done by minimizing the within cluster sum-of-squared errors as shown in Eq. (3.21).

$$\underset{\mathbf{R}}{\arg\min} \sum_{i=1}^{n} \sum_{\mathbf{x}_j \in \mathbf{R}^{(i)}} \left\| \mathbf{x}_j - \boldsymbol{\mu}^{(i)} \right\|^2 \tag{3.21}$$

where $\mathbf{R} = \{\mathbf{R}^{(1)}, \mathbf{R}^{(2)},..., \mathbf{R}^{(n)}\} = \mathbf{X}_C$ and $\boldsymbol{\mu}^{(i)}$ is the centroid of the points in $\mathbf{R}^{(i)}$. The minimization problem suggested in Eq. (3.21) is solved by the clustering algorithm suggested by Hartigan and Wong (1979).

C. *Identify optimal point from each cluster* – In this step a single point from each cluster is chosen as the best representative of the points in the cluster. One

strategy can be to select the centroid of the cluster. To address the selection of a representative point from each cluster $\mathbf{R}^{(i)}$ where $i = 1, 2, ..., n$ a multi-objective evaluation process is suggested which takes into consideration the following two criteria (1) distance of an individual point from its cluster centroid; and, (2) merit of the point obtained from the single-KPC adaptive sampling method. Based on the results of the k-means clustering the $\bar{\bar{n}} \times 1$ merit vector $\mathbf{v}_C$ is partitioned into 'n' sub-vectors $\mathbf{v}_R^{(1)}, \mathbf{v}_R^{(2)}, ..., \mathbf{v}_R^{(n)}$ where $\mathbf{v}_R^{(i)}$ is the merit vector of the points in cluster $\mathbf{R}^{(i)}$ and $i = 1, 2, ..., n$. The representative design point from the ith cluster is selected by the maximization process suggested in Eq. (3.22).

$$\mathbf{x}_*^{(i)} = \arg\max_{\mathbf{x}_j \in \mathbf{R}^{(i)}} \left(\omega_1 \frac{d_{\max}^{(i)} - d^{(i)}(\mathbf{x}_j)}{d_{\max}^{(i)}} + \omega_2 \frac{\upsilon_R^{(i)}(\mathbf{x}_j)}{\upsilon_{\text{R-max}}^{(i)}} \right) \quad (i = 1, 2, ..., n) \qquad (3.22)$$

where $d^{(i)}(\mathbf{x}_j)$ is the Euclidean distance of the point $\mathbf{x}_j \in \mathbf{R}^{(i)}$ from the centroid of the cluster $\mathbf{R}^{(i)}$, $d_{\max}^{(i)}$ is the distance of the farthest point from the centroid of the cluster $\mathbf{R}^{(i)}$. $\upsilon_R^{(i)}(\mathbf{x}_j)$ is the merit of the point $\mathbf{x}_j \in \mathbf{R}^{(i)}$ and $\upsilon_{\text{R-max}}^{(i)}$ is the highest merit in cluster $\mathbf{R}^{(i)}$. Moreover ω_1 and ω_2 are user-defined weights assigned to the distance criteria and the merit criteria respectively. Solution of Eq. (3.22) can be identified by searching over all points $\mathbf{x}_j \in \mathbf{R}^{(i)}$ and selecting the point which maximizes the objective function. The optimal adaptive sample is $\mathbf{X}_C^* = [\mathbf{x}_*^{(1)}, \mathbf{x}_*^{(2)}, ..., \mathbf{x}_*^{(n)}]^{\text{T}}$, which is the KCC design matrix for the next batch of VSA.

The O-MRAS algorithm is summarized in the pseudo-code given below.

```
Input: X_C^(1), X_C^(2)...X_C^(r) , υ^(1),υ^(2),...,υ^(r) , ω_1 and ω_2
```

Output: $\mathbf{X}_C^* = [\mathbf{x}_*^{(1)}, \mathbf{x}_*^{(2)}, \ldots, \mathbf{x}_*^{(n)}]^{\mathsf{T}}$

```
//optimal multiple-response adaptive sampling starts here
```

Merge $\mathbf{X}_C^{(1)}, \mathbf{X}_C^{(2)}...\mathbf{X}_C^{(r)}$ into a single $\bar{\bar{n}} \times d$ matrix $\mathbf{X}_C$ by removing duplicate points if any

Merge $\mathbf{U}^{(1)}, \mathbf{U}^{(2)}, \ldots, \mathbf{U}^{(r)}$ into a single $\bar{\bar{n}} \times 1$ vector $\mathbf{U}_C$ based on matrix $\mathbf{X}_C$

Partition $\mathbf{R}^{(1)}, \mathbf{R}^{(2)}, \ldots, \mathbf{R}^{(n)}$ into 'n' cluster by *k*-means clustering

Assign the centres of the clusters to $\boldsymbol{\mu} = \{\boldsymbol{\mu}^{(1)}, \boldsymbol{\mu}^{(2)}, \ldots, \boldsymbol{\mu}^{(n)}\}$

Partition $\mathbf{U}_C$ into $\mathbf{U}^{\mathbf{R}^{(1)}}, \mathbf{U}^{\mathbf{R}^{(2)}}, \ldots, \mathbf{U}^{\mathbf{R}^{(n)}}$ based on results of clustering

let *i*=0

while (*i* ≤ *n*)

  let *i*=*i*+1

  let $d^{(i)}(\mathbf{x}_j) = \sqrt{\left\| \mathbf{x}_j - \boldsymbol{\mu}^{(i)} \right\|^2} \;\; \forall \mathbf{x}_j \in \mathbf{R}^{(i)}$

  let $d_{max}^{(i)} = \max\{d^{(i)}(\mathbf{x}_j) \forall \mathbf{x}_j \in \mathbf{R}^{(i)}\}$

  let $\upsilon^{\mathbf{R}^{(i)}}(\mathbf{x}_j) = \upsilon_j^{\mathbf{R}^{(1)}}$

  let $\upsilon_{max}^{\mathbf{R}^{(i)}} = \max\{\upsilon^{\mathbf{R}^{(i)}}(\mathbf{x}_j) \forall \mathbf{x}_j \in \mathbf{R}^{(i)}\}$

  solve $\mathbf{x}_*^{(i)} = \underset{\mathbf{x}_j \in \mathbf{R}^{(i)}}{\arg\max} \left(\omega_1 \dfrac{d_{max}^{(i)} - d^{(i)}(\mathbf{x}_j)}{d_{max}^{(i)}} + \omega_2 \dfrac{\upsilon^{\mathbf{R}^{(i)}}(\mathbf{x}_j)}{\upsilon_{max}^{\mathbf{R}^{(i)}}} \right)$

end

let $\mathbf{X}_C^* = [\mathbf{x}_*^{(1)}, \mathbf{x}_*^{(2)}, \ldots, \mathbf{x}_*^{(n)}]^{\mathsf{T}}$

```
//optimal multiple-response adaptive sampling ends here
```

In the case studies discussed in Section 3.7, Lipschitz criterion is used to generate the *'r'* individual adaptive samples.

3.6 Fixture layout optimization

This section presents the mathematical formulation of the fixture layout optimization using surrogate models of assembly KPCs.

The scalable surrogate modelling methodology described in Section 3.5 can be applied to develop GPK surrogate models of assembly KPCs such as gaps

between mating parts as a function of the fixture KCCs such as the fixture clamping forces, clamp location etc. The data generated by VSA analysis tool is used to train the surrogate models.

Assuming that in a given sheet metal assembly, '*d*' fixture KCCs $\mathbf{x} = \{x_1, x_2, ..., x_d\}$ influence '*r*' assembly KPCs $\mathbf{y} = \{y_1, y_2, ..., y_r\}$, the surrogate model of KPC y_k is given as

$$y_k = f_k(\mathbf{x}) \tag{3.23}$$

Let the allowable tolerance limits for KPC y_k be $[\mathrm{L}_k^{(y)}, \mathrm{U}_k^{(y)}]$ then the cost of quality due to deviation of the KPC from nominal can be described as

$$C(y_k) = \begin{cases} K_1 (y_k - m_k)^2, & y_k \in [\mathrm{L}_k^{(y)}, \mathrm{U}_k^{(y)}] \\ K_2 (y_k - m_k)^2, & y_k \in (-\infty, \mathrm{L}_k^{(y)}) \cup (\mathrm{U}_k^{(y)}, \infty) \end{cases} \tag{3.24}$$

where nominal of KPC y_k is $m_k = \dfrac{\mathrm{L}_k^{(y)} + \mathrm{U}_k^{(y)}}{2}$. K_1 and K_2 are user-defined Taguchi loss coefficients. The cost $C(y_k)$ can be computed for given KCCs by replacing the KPC with its GPK surrogate model. The total cost to be minimized for fixture layout optimization is given by

$$C(\mathbf{y}) = \sum_{k=1}^{r} C(y_k) \tag{3.25}$$

Additionally, the optimization is done subject to design constraints on the KCCs. If KCC x_j is allowed to vary within the limits $[\mathrm{L}_j^{(x)}, \mathrm{U}_j^{(x)}]$ then the fixture design optimization problem is formulated as follows

$$\begin{aligned} &\textit{Minimize} \quad C(\mathbf{y}) \\ &\textit{Subject to} \quad \mathrm{L}_j^{(x)} \leq x_j \leq \mathrm{U}_j^{(x)} \quad \forall j = \{1, 2, ..., d\} \end{aligned} \tag{3.26}$$

The objective function of the fixture layout optimization problem depends

on the KPCs surrogate models. Therefore depending on the surrogate model, the optimization problem can be linear constrained or non-linear constrained optimization and therefore has to be solved by a suitable method. Based on GPK surrogate models, the objective function is non-linear and therefore can be solved by evolutionary optimization methods such as Genetic Algorithm. In the case studies presented in Section 3.7, Genetic Algorithm is used to solve the constrained non-linear optimization.

3.7   Case Studies

This section demonstrates the proposed methodology of scalable surrogate model driven fixture layout optimization using case studies related to sheet assembly in automotive and aerospace Body-In-White (BIW) manufacturing. The case studies consider body panels which consist of two mating parts and are joined by an assembly joining process such as Resistance Spot Welding (RSW), Self-Pierce Riveting (SPR) or Remote Laser Welding (RLW). Typically, a joining process requires a specific alignment or gap control between mating parts to be maintained within tight design tolerances. For example, to make a weld of acceptable quality, RLW requires the part-to-part gap to be between 0.05 mm to 0.4 mm at locations where a weld is to be made. When part-to-part gaps at welding locations are not within the design tolerances there are welding defects such as under-cut, porous weld, poor finishing and corrosion-prone welds. The major challenge in maintaining the part-to-part gaps within design tolerance is the geometrical variation of sheet metal part which is induced during their fabrication process such as forming, stamping or rolling due to material properties, tooling setup and other factors. Geometrical variations in mating parts result in gaps between them. Under these conditions, fixture locators provide proper spatial

alignment of the parts and fixture clamps force mating parts to achieve part-to-part gaps within design tolerances. VSA based on Finite Element Method (FEM) (Franciosa, *et al*., 2014) analyses the non-linear relationship between assembly KPCs such as part-to-part gaps and KCCs such as fixture clamp locations and estimates the KPCs for given KCCs. Figure 3.5 shows KPCs and KCCs of an assembly on which two weld stitches (linear lap joints) are to be made. Clamps are used to control the part-to-part gap (KPC) along a weld stitch. Each clamp is moved between pre-specified initial (P_i) and final (P_f) positions and the Euclidean distance between the current position of a clamp and its initial position is the KCC associated with the clamp (x_j). The part-to-part gap along a weld stitch changes as clamps are moved between their initial and final positions. KCCs associated with the clamp positions are parameterized to vary in the range [0, 1]. The fixture layout is defined by the position of the clamps.
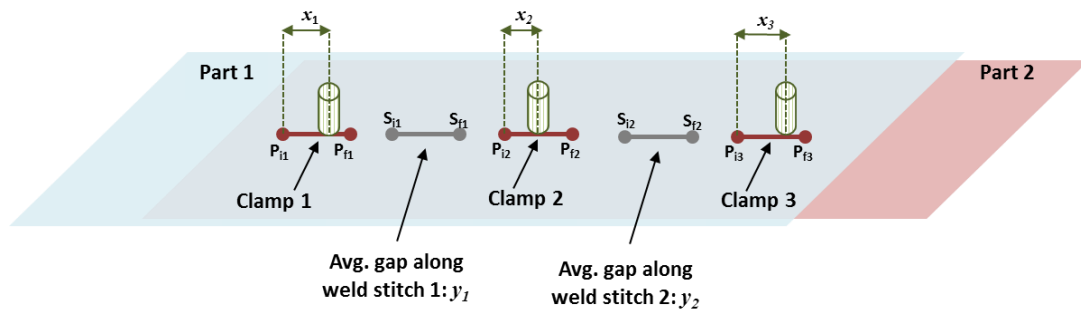
Figure 3.5: Clamp layout of sheet metal assembly for welding

Two case studies on sheet metal assembly are used to demonstrate the methodology of scalable surrogate model driven fixture layout optimization. Table 3.3 summarizes the case studies. Details of each case study are discussed in two parts: (1) scalable surrogate modelling of assembly KPCs which develops surrogate models to integrate part-to-part gaps at weld locations with fixture layout; and, (2) fixture layout optimization which utilizes the KPC surrogate models to minimize cost-based

Key Performance Indicator (KPI) subject to design tolerances of clamp locations.

Table 3.3: Case studies on scalable surrogate model driven fixture layout optimization

Case Study	No. of KCCs (x)	No. of KPCs (y)	Joining Process	Application
Hinge and door inner panel assembly	6	13	Remote Laser Welding	Automotive door assembly
Longitudinal stiffener and skin section assembly	3	11	Self Pierce Riveting	Aircraft wing assembly

The remaining part of this section is organized as follows: Section 3.7.1 presents the hinge and door inner panel assembly followed by discussion on the longitudinal stiffener and skin section assembly in Section 3.7.2. Additional case studies based on well-known benchmark functions are discussed in Section 3.7.3 to demonstrate the performance of GPK surrogate models on non-linear input-output functions with a varying number of local maximas and minimas.

3.7.1 Door inner panel and hinge assembly

The hinge and door inner panel assembly is a part of automotive vehicle door assembly which involves sheet metal parts with complex geometry having multiple planes in different angles and orientations and different material thicknesses. Figure 3.6 shows the hinge and door inner panel assembly. This assembly has 13 RLW stitches and involves 16 clamps to maintain part-to-part gaps at stitch locations within the design tolerance of 0.05 mm to 0.4 mm. Moreover, the clamps are grouped into six clamp panels whereby movement of clamps in the same panel depends on movement of the clamp panel itself. Therefore locations of 6 clamp panels are considered as the KCCs. KPCs are part-to-part gaps at 13 stitch locations. One

instance of FEM-based VSA to estimate 13 KPCs for given KCCs takes 22 minutes on an average. To address the computational expense of VSA, surrogate models of assembly KPCs are used for fixture clamp layout optimization.

Scalable surrogate model driven fixture layout optimization for the door inner panel and hinge assembly is discussed in the following two subsections – Section 3.7.1.1 describes scalable surrogate modelling of the assembly KPCs using the proposed GPK and O-MRAS methods. Next Section 3.7.1.2 discusses the fixture layout optimization using the GPK surrogate models of the assembly KPCs.
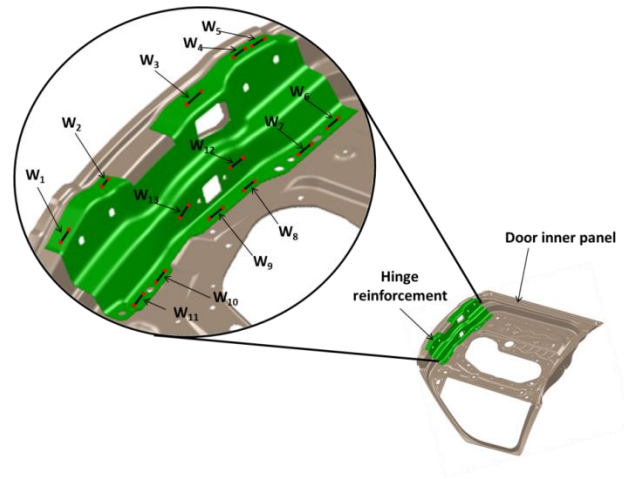
Figure 3.6: Door Inner Panel and hinge assembly having 13 stitches (W_1-W_{13})

3.7.1.1 Scalable surrogate modelling of KPCs in door inner panel and hinge assembly

Scalable surrogate models of the assembly KPCs are developed through several iterations of the following five steps:

Step 1: *Sample initial design matrix of KCCs by space filling* –

The door inner panel and hinge assembly consists of 6 KCCs which are used to control 13 KPCs. A full-factorial DOE with L levels per KCC will require L^6 FEM instances of VSA and approximately $0.37L^6$ hours. For example, full factorial DOE with 4 levels will require over 63 days to complete. Hence to reduce computational time, an initial 100×6 design matrix of KCCs is generated by uniform random sampling which selects $n=100$ points from the KCC design space. The initial design matrix of KCCs is used to run VSA in the first iteration. In subsequent iterations a 100×6 design matrix of KCCs is generated through O-MRAS.

Step 2: *Run VSA to generate training data* –

The 100×6 design matrix of KCCs represents 100 clamp layouts. The KPC design matrix is given as input to VSA which estimates the KPCs for each instance of clamp layout. Additionally, VSA also uses the CAD model of the parts, material properties and geometrical variations of individual parts as input to analyse interactions between KCCs and KPCs. The design matrix of KCCs and the KPC estimation from VSA are compiled in a single training dataset $\mathbf{S} = \{\mathbf{x}_i, \mathbf{y}_i\}_{i=1}^{n=100}$, where $\mathbf{x}_i$ and $\mathbf{y}_i$ are KCCs and KPCs of the ith instance of clamp layout.

Step 3: *Train KPC surrogate models via GPK* –

New training dataset $\mathbf{S} = \{\mathbf{x}_i, \mathbf{y}_i\}_{i=1}^{n=100}$ generated during the current iteration is added to the dataset $\mathbf{S}_\text{T}$ which has which has all the training data generated till the current iteration 'k'. Over the iterations number of training samples in $\mathbf{S}_\text{T}$ grows as $n, 2n, ..., kn$ and so on. During the current iteration, GPK surrogate

models are developed using the dataset $\mathbf{S}_T$, A GPK surrogate model of a KPC 'y' can be represented as

$$\hat{y} = \sum_{j=1}^{m} \beta_j h_j + Z(\mathbf{x}) \tag{3.27}$$

where the regression component $\sum_{j=1}^{m} \beta_j h_j$ models the global behaviour of y and Gaussian process $Z(\mathbf{x})$ captures local non-linearities. Section 3.5.1 describes the regression component and the Gaussian process in details.

The GPK method identifies suitable features $\mathbf{h} = \{h_1, h_2, .., h_m\}$ for the regression component via Polynomial Feature Selection (PFS) and determines parameters $\boldsymbol{\theta} = \{\gamma_1, \gamma_2, ..., \gamma_d, \alpha_1, \alpha_2, ..., \alpha_d\}$ of the exponential correlation function by Kernel Optimization (KO). PFS and KO are described as follows:

A. *Polynomial Feature Selection* – The features $\mathbf{h} = \{h_1, h_2, .., h_m\}$ used in the regression component of GPK are terms from p^{th} order polynomial of the KCCs. PFS identifies suitable polynomial order 'p' and best subset of terms $\mathbf{h}^*$ from the pth order polynomial to be used in the regression part of the GPK model. This is achieved by: (1) iteratively increasing the order of the polynomial p as 1, 2... and so on over iterations j =1, 2... till drop in 5 fold cross validation (CV) Mean Squared Error (MSE) from previous iteration is less than a cutoff of 5%; and, (2) identifying a subset of polynomial terms for a given polynomial order 'p' during each iteration. As an illustration, Figure 3.7 shows the drop of CV MSE over iterations of PFS for KPCs 1, 6 and 13. It is noteworthy from Figure 3.7 that for KPC_6 a higher drop in CV MSE is observed after selecting terms

from 4th order polynomial than after adding terms from 3rd order polynomial. This observed behaviour demonstrates the capability of PFS to identify higher order multiplicative interactions between KCCs in an iterative fashion without pre-specifying the order of the polynomial. Table 3.4 presents a summary of results from PFS for KPCs 1, 6 and 13. The selected features are used for developing the regression component of GPK. Accuracy of the regression component is evaluated by 5 fold cross validation and is expressed as the average degree of determination (R^2) over the cross validation folds. As seen in Table 3.4, a high R^2 of KPC_{13} shows the effectiveness of PFS to identify polynomial terms which can provide an accurate global approximation of the KPC through the regression component.
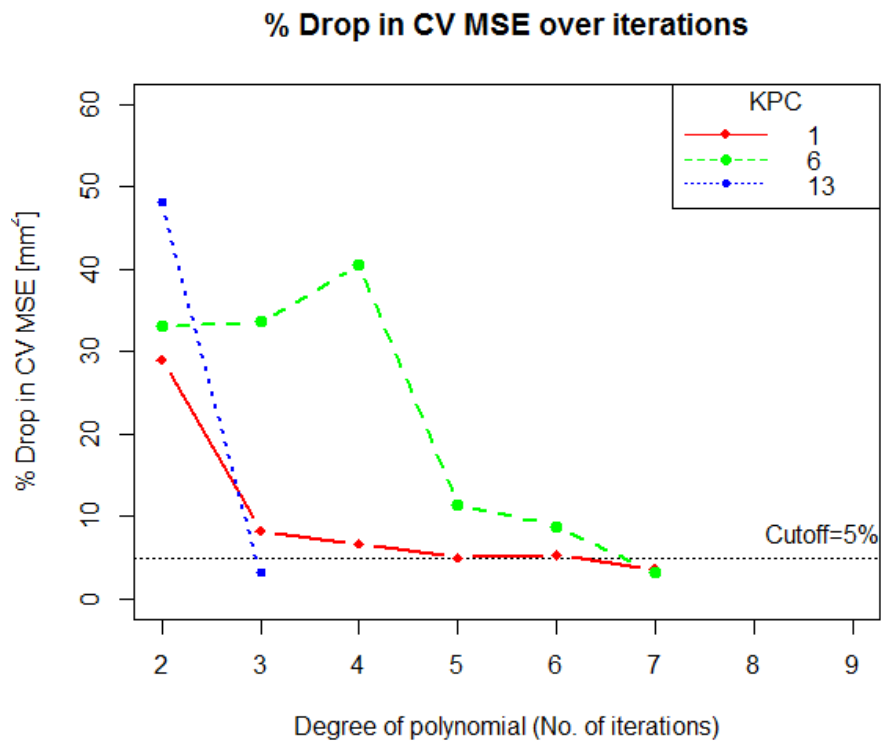
Figure 3.7: Drop in cross-validation MSE over iterations of Polynomial Feature Selection for KPCs in door inner panel and hinge assembly

It is noteworthy that PFS identifies optimal feature set $\mathbf{h}^{*}$ based on *minimization of CV MSE* to ensure that GPK's regression component gives *maximum predictive accuracy on unseen test samples*.

Table 3.4: Summary of results from Polynomial Freature Selection for KPCs 1, 6 and 13 in door inner panel and hinge assembly

KPC Index	Highest polynomial order identified	No. of features in final solution	Average Cross validation $R^{2\,*}$ (Scale: 0-1)
1	7	31	0.86
6	7	15	0.83
13	3	11	0.93

$*R^2$: Degree of determination which varies over a scale of 0-1

B. Kernel Optimization − In GPK surrogate models, the Gaussian process $Z(\mathbf{x})$ captures local non-linearities in the underlying KPC-KCC interrelations. The Gaussian process is characterised by the exponential correlation function also known as kernel function. Kernel Optimization (KO) identifies suitable parameters $\boldsymbol{\theta} = \{\gamma_1, \gamma_2, ..., \gamma_d, \alpha_1, \alpha_2, ..., \alpha_d\}$ of the exponential kernel function. An adaptive Genetic Algorithm (GA) minimizes 5-fold cross validation MSE of the GPK surrogate model to identify optimal $\boldsymbol{\theta}$. In adaptive GA the number of chromosomes and number of generations are set based on number of instances in training dataset $\mathbf{S}_{\mathrm{T}}$ of the current iteration. As the number of instances in $\mathbf{S}_{\mathrm{T}}$ increases over several iterations of the surrogate modelling method, the number of chromosomes and number of generations are adaptively increased to allow more extensive search over a larger search space.

However, if CV MSE does not decrease over last 5 generations, an early stopping criteria terminates GA to avoid redundant computation.

It is noteworthy that *minimization of 5-fold cross validation MSE* in Kernel Optimization ensures that *predictive error of the GPK model on unseen test samples is minimized.*

Figure 3.8 shows the performance of GA over several generations for KPC_2. It is noteworthy that the early stopping criterion has terminated GA due to no decrease in CV MSE.
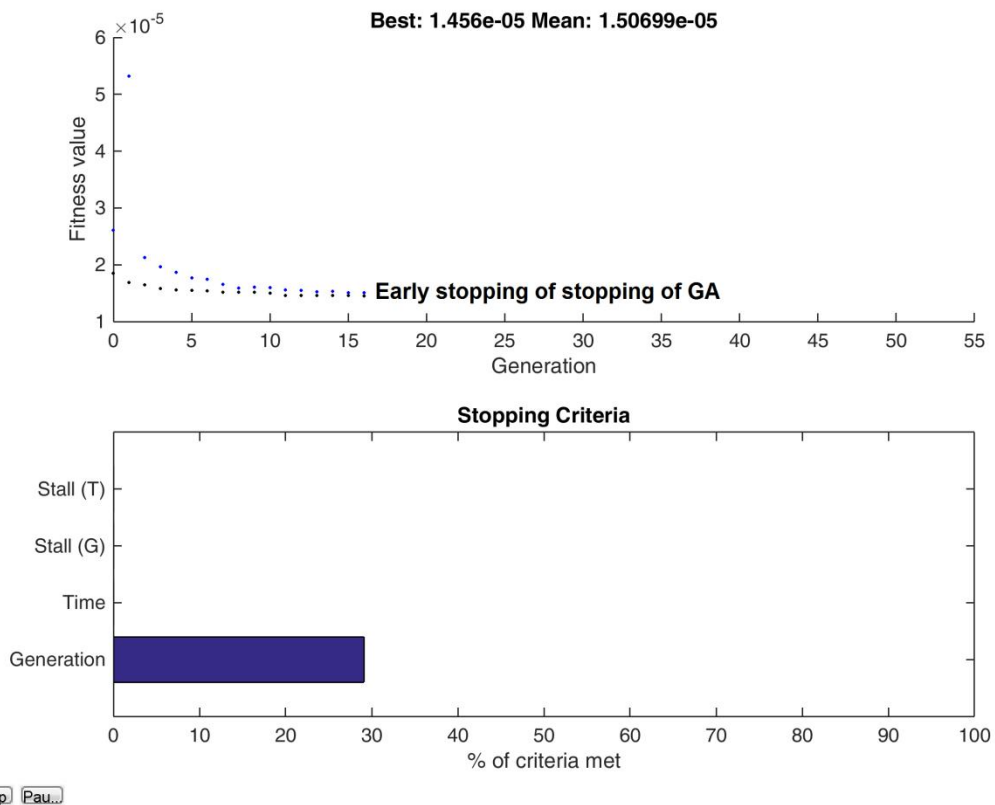
Figure 3.8: Kernel Optimization by adaptive GA for GPK model of KPC_2 in door inner panel and hinge assembly

KO adjusts the global approximation provided by the regression component of GPK for local non-linearities and hence further improves the predictive accuracy of GPK models beyond what has already been

achieved by PFS. Additional improvement in predictive accuracy by KO is demonstrated in Table 3.5 which shows CV R^2 before and after KO is performed for KPCs 1, 6 and 13 of this case study.

Table 3.5: Additonal improvement of CV R^2 by Kernel Optimization for KPCs 1, 6 and 13 in door inner panel and hinge assembly

KPC Index	Cross validation R^2 *before* KO	Cross validation R^2 *after* KO
1	0.86	0.94
6	0.83	0.93
13	0.93	0.98

GPK surrogate models are developed for the 13 KPCs in this case study based on PFS and KO, which have been demonstrated in details in the aforementioned two steps A and B.

Step 4: Check if model accuracy is acceptable –

To check accuracy of the GPK models average degree-of-determination R^2_{avg} over 13 KPCs is calculated using the test data. If $R^2_{avg} \geq 0.9$ then iterations are stopped else further iterations are done to generate more training data from VSA and re-develop the GPK models. For the next iteration, design matrix of KCCs is generated by O-MRAS which is described in Step 5.

Step 5: Select design matrix of KCCs via O-MRAS –

O-MRAS generates design matrix of KCCs through the following three steps:

A. *Generate adaptive samples for individual KPCs* – In this case study adaptive samples for individual KPCs $y_1, y_2, ..., y_6$ are generated using Lipschitz criterion (Lovison & Rigoni, 2011) through the following three sub-steps:

A.1. *Tessellation of the design space*: KCCs in the training sample $\mathbf{S}_T$, are used to partition the KCC design space into simplexes through Delaunay triangulation (Lee & Schachter, 1980). Let us denote the individual simplexes as $u_1, u_2, ..., u_s$. Each simplex has ($d+1$) vertices for a d-dimensional KCC design space. Let us denote the vertices of jth simplex as $\mathbf{X}^{(u_j)}$. In this case study $d=6$ For illustration, Figure 3.9 presents a 2-D Delaunay tessellation of a 5×5 grid of KCC$_1$ (x_1) and KCC$_2$ (x_2). The actual Delaunay triangulation is done in a 6-D space.
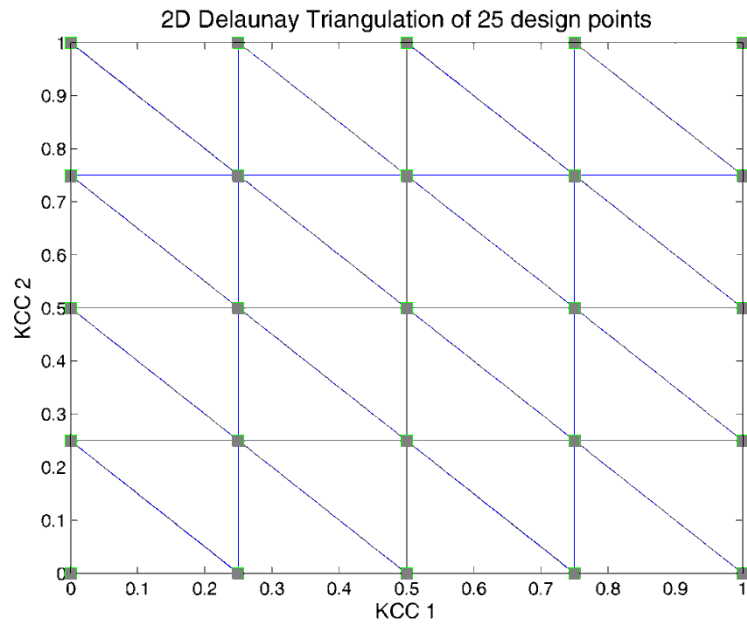
Figure 3.9: 2D Delaunay Triangulation

A.2. *Generation of Candidate Points*: A space-filling strategy is applied to generate Candidate Points (CPs) whose *merit* will be evaluated based on Lipschitz criteria. For the case studies in this chapter, '3n' CPs are generated by uniform random sampling.

Out of '$3n$' CPs, 'n' points will be selected in the final sample. Figure 3.10 shows 75 CPs generated by uniform random sampling. Every CP is assigned to the simplex in which it resides. Let $\mathbf{v}^{(u_j)}$ be the CPs belonging to simplex u_j.
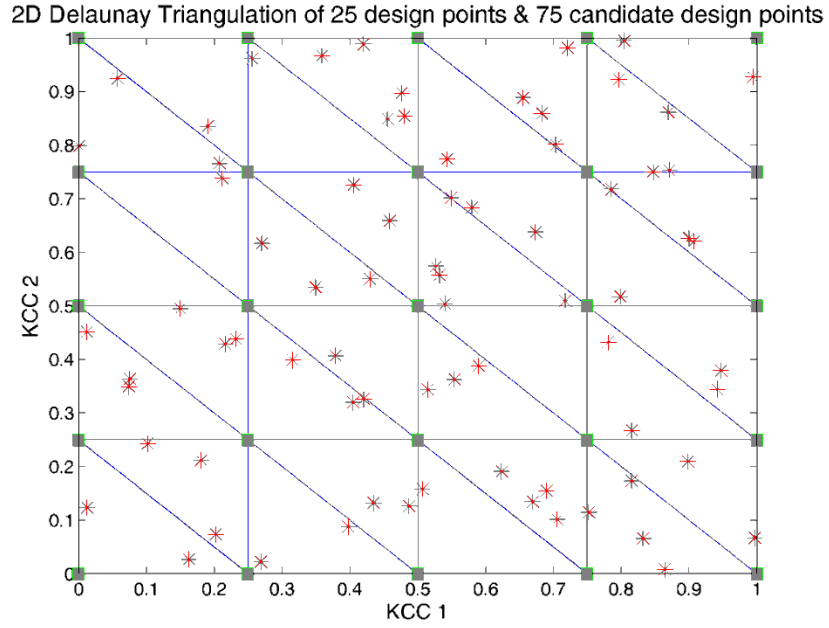
Figure 3.10: 75 candidate points generated by uniform random sampling

A.3. *Selection of adaptive sample from candidate design points*: In this step we evaluate the *merit* of each CP that are generated in the previous step. The merit of the ith CP in $\mathbf{v}^{(u_j)}$ is computed as shown in Eq. (3.28).

$$merit\left(\mathbf{v}_i^{(u_j)}\right) = LC(u_j) \times \min_{\mathbf{x}_k^{(u_j)} \in \mathbf{X}^{(u_j)}} \sqrt{\left\|\mathbf{v}_i^{(u_j)} - \mathbf{x}_k^{(u_j)}\right\|_2} \qquad (3.28)$$

The *merit* of a CP is product of the Lipschitz Constant (*LC*) of its resident simplex and the Euclidean distance between the CP and the nearest vertex of the simplex. LC, which is critical to the

Lipschitz criteria based adaptive sampling, is a measure of non-linearity of a simplex and is determined as suggested by Eq. (3.29).

$$LC(u_j) := \sup_{\substack{\mathbf{x}_i^{(u_j)}, \mathbf{x}_k^{(u_j)} \in \mathbf{X}^{(u_j)} \\ \mathbf{x}_i^{(u_j)} \neq \mathbf{x}_k^{(u_j)}}} \frac{y_l\left(\mathbf{x}_i^{(u_j)}\right) - y_l\left(\mathbf{x}_k^{(u_j)}\right)}{\sqrt{\left\|\mathbf{x}_i^{(u_j)} - \mathbf{x}_k^{(u_j)}\right\|_2}} \qquad (3.29)$$

where $y\left(\mathbf{x}_i^{(u_j)}\right)$ is an actual KPC obtained from VSA for KCC $\mathbf{x}_i^{(u_j)}$. Next the CPs from individual simplexes and their computed merits are flattened into a $3n \times d$ matrix 'V' and $3n \times 1$ vector 'm' respectively. The adaptive sample of the jth $\mathbf{X}_c^{(j)}$ KPC is generated by selecting 'n' CPs from $\mathbf{V}$ having 'n' highest *merit*.

Using Lipschitz criteria 13 adaptive samples $\mathbf{X}_C^{(1)}, \mathbf{X}_C^{(2)}, ..., \mathbf{X}_C^{(13)}$ are generated for the 13 KPCs. At this stage a single adaptive sample $\mathbf{X}_C^*$ will be extracted from the 13 individual adaptive samples.

B. *Perform k-means clustering to identify n=100 groups* – Lipschitz criteria based adaptive sampling have been applied in the previous step to identify 13 individual adaptive samples each having 100 points. Therefore a total of 1300 points have been generated. The individual adaptive samples $\mathbf{X}_C^{(1)}, \mathbf{X}_C^{(2)}, ..., \mathbf{X}_C^{(13)}$ are merged into a single 1300×6 matrix $\mathbf{X}_C$. In this step *k*-means clustering is applied to cluster the 1300 points in 100 groups.

C. *Identify optimal instance from each cluster* – This step identifies an optimal point from each cluster found in the previous step. Individual

points in a cluster are evaluated based on following two criteria: (1) *proximity* of the point to the cluster centroid; and, (2) *merit* of the point obtained from the Lipschitz criteria based single-KPC adaptive sampling. The optimal point in a cluster is chosen by the optimization strategy prescribed in Eq. (3.22). The weights assigned to the *proximity* criteria and *merit* criteria are $\omega_1 = 0.5$ and $\omega_2 = 0.5$ respectively. The point which maximizes the weighted average of *proximity* criteria and *merit* criteria is selected as the optimal point from the cluster.

Overall, O-MRAS identifies a single optimal adaptive sample $\mathbf{X}_C^*$ of 100 instances from 13 individual adaptive samples. $\mathbf{X}_C^*$ is then used as the KCC design matrix for VSA in the next iteration. In this case study, O-MRAS has been ran for 6 KCCs and 13 KPCs. The three steps of O-MRAS namely (1) selection of adaptive sample for individual responses; (2) *k*-means clustering; and, (3) identification of optimal instance from each cluster, are done over the 6-dimensional KCC design space. The O-MRAS is illustrated on 2-dimensional case studies in Appendix C.

Discussion of results from scalable surrogate modelling of KPCs

Results of scalable surrogate modelling of the KPCs related to door inner panel and hinge assembly are discussed as follows:

i. *Achievement of desired predictive accuracy on unseen test samples* – Predictive accuracy of the GPK models is evaluated on unseen test samples which are not used in the model training process. Predictive accuracy is measured in terms of average degree of determination, R^2_{avg} of the GPK models and the desired accuracy level is $R^2_{avg} \geq 0.9$. The GPK models achieve the desired levels in the second iteration. Figure 3.11 shows the performance of GRK and OK models

over four iterations.
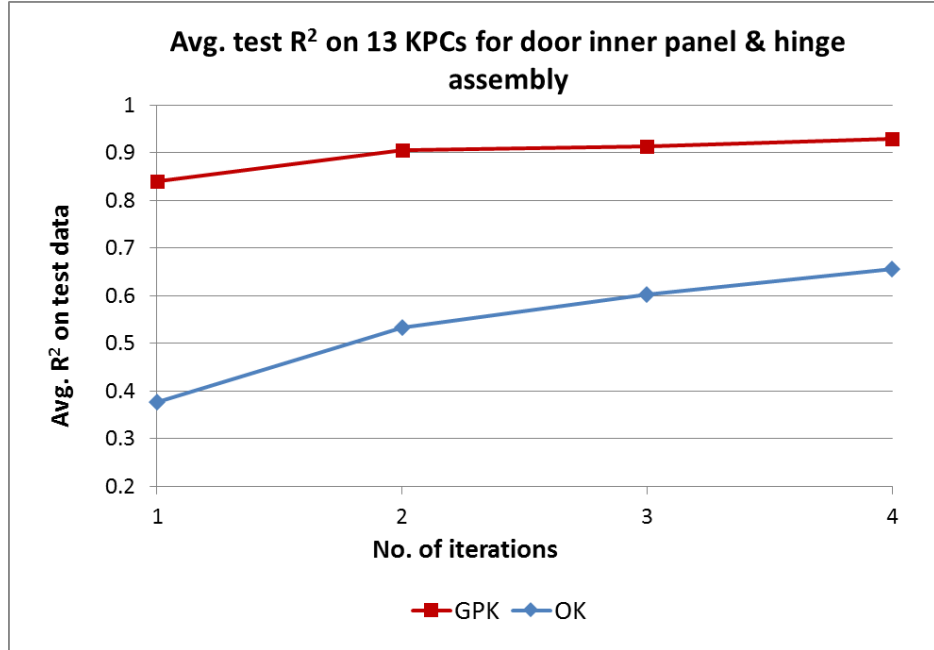
Figure 3.11: Perforamce of GPK and OK surrogate models for door inner panel and hinge assembly

ii. *Comparison of performance with state-of-the-art Ordinary Kriging* – Ordinary Kriging (OK) models are developed using the same training data, which is used for developing GPK models. The OK models are characterized by constant regression component and parameters of correlation function determined by maximum likelihood estimation (MLE). As shown in Figure 3.11, R^2_{avg} of GPK models after four iterations is higher than R^2_{avg} of OK surrogate models by 42 %. This highlights that GPK's PFS and KO based on minimization of generalized model error, which is estimated by 5-fold cross validation, has imparted better accuracy to the surrogate models in lesser number of iterations.

iii. *Scalability for deterministic non-linearity* – Learning the *scale of non-linearity* present in the underlying KPC-KCC interrelations through data analysis has been proposed as a capability of GPK models. Non-linearity of a KPC with

104

respect to KCC$_j$ can be understood in terms of smoothness of the KPC surrogate model along KCC$_j$. Smoothness with respect to KCC$_j$ is controlled by the corresponding smoothing parameter α_j in the exponential correlation function of the Gaussian process. The proposed Kernel Optimization (KO) for GPK focuses on identifying a suitable α_j which represents the underlying non-linearity in the KPC-KCC$_j$ interrelation without compromising the surrogate model's overall accuracy on unseen test samples. It is also expected that α_j will be different for different KCCs depending on the interaction between the KCC and the KPC. As an example, in the GPK model of KPC$_2$, the smoothing parameters determined by KO are [1.28, 2, 1.37, 2, 0.43, 2] for KCCs 1 to 6 for R^2=0.975 on unseen test samples. This shows that GPK has been able to identify different scales of non-linearities at an acceptable test R^2 for KPC$_2$. In this particular case, KPC$_2$ is smooth and infinitely differentiable with respect to KCCs 2, 4 and 6. Figure 3.12 shows smooth response surface of KPC$_2$ with respect to KCC$_2$ and KCC$_4$. Figure 3.13 shows a smooth profile diagram of KPC$_2$ with respect to KCC$_2$ and has a single global maxima and minima. On the other hand, KPC$_2$ is rough and non-differential with respect KCCs 1, 3 and 5 as shown in the response surface in Figure 3.14 and profile diagram in Figure 3.15 which has multiple local maximas and minimas.

2D Response Surface of GPK Surrogate Model of KPC$_2$
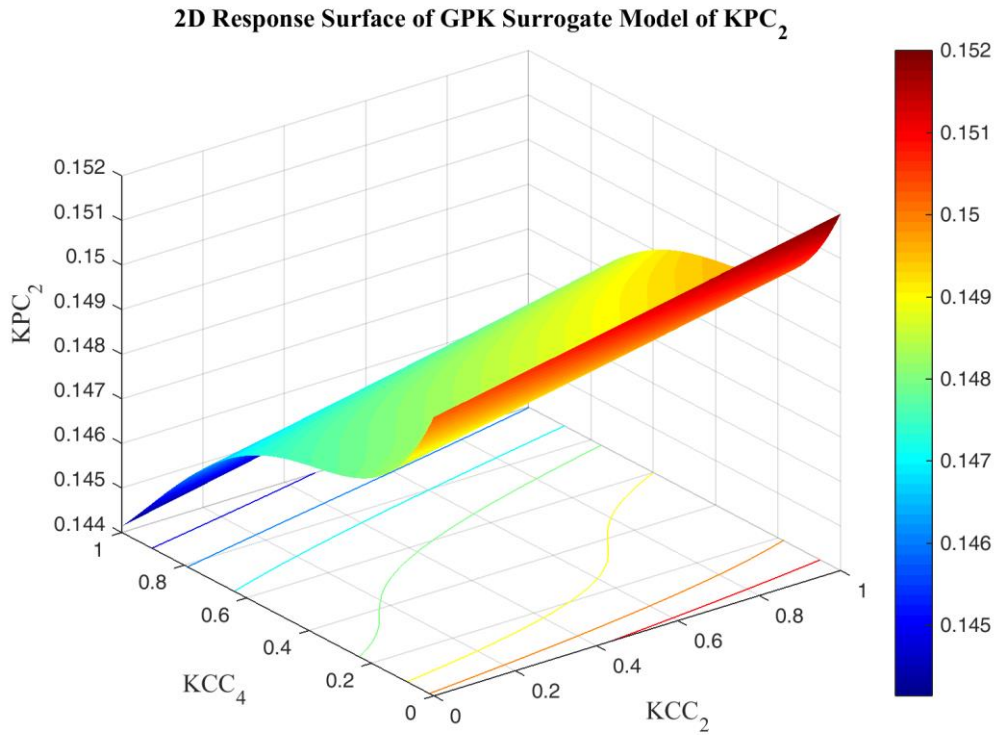
Figure 3.12: 2D response surface of GPK model of KPC$_2$ with respect to KCC$_2$ and KCC$_4$ in door inner panel and hinge assembly

Profile of KPC$_2$ along KCC$_4$
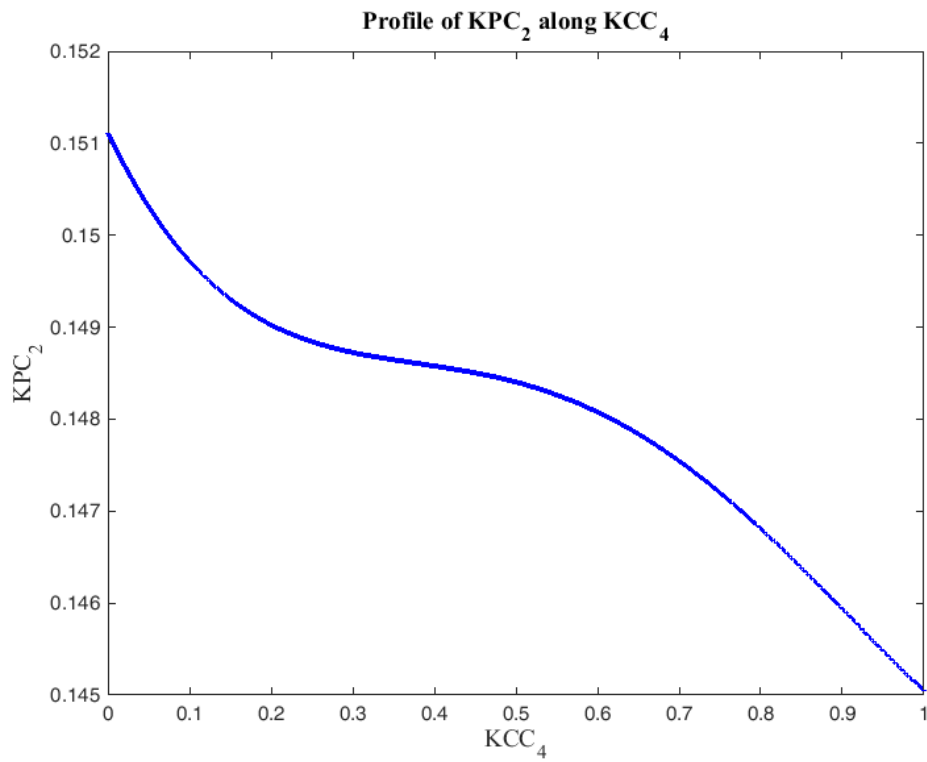
Figure 3.13: Profile of KPC$_2$ with respect to KCC$_4$ in door inner panel and hinge assembly

106
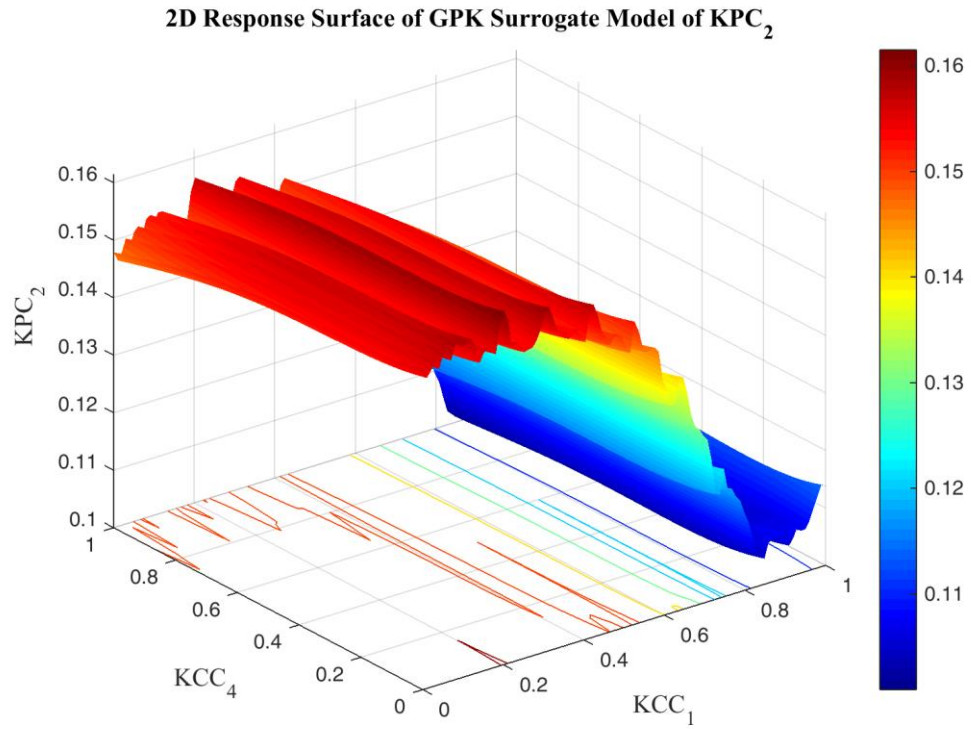
Figure 3.14: 2D response surface of GPK surrogate model of KPC_2 with respect to KCC_1 and KCC_4 in in door inner panel and hinge assembly
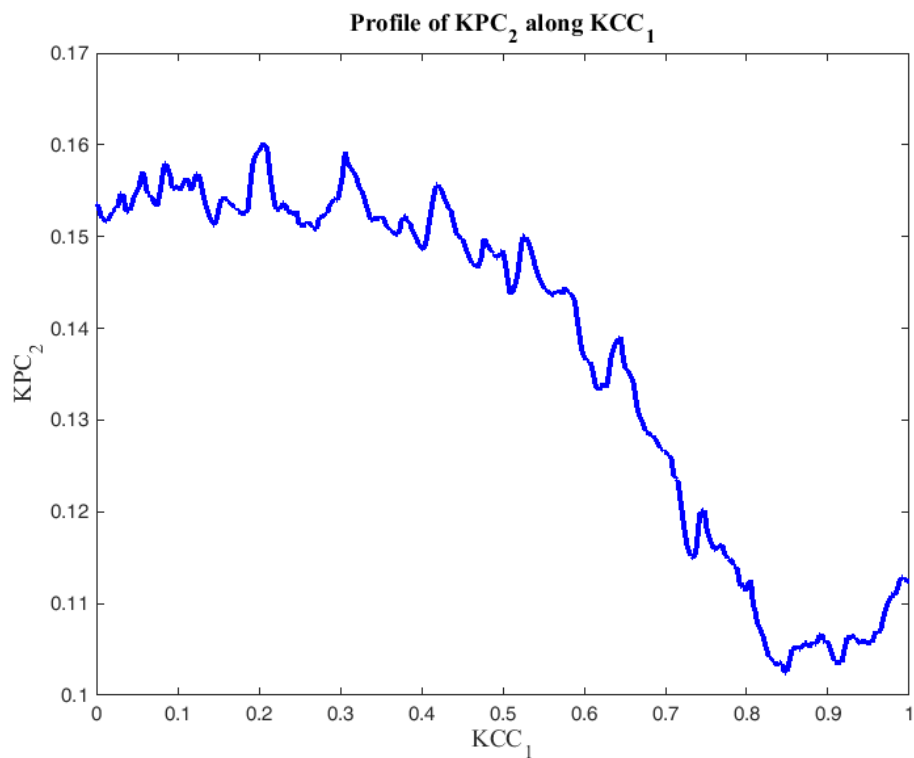
Figure 3.15: Profile of KPC_2 with respect to KCC_1 in in door inner panel and hinge assembly

iv. Comparisons with other state-of-the-art-surrogate models – Using the same training data, surrogate models are trained by five other well-known state of the art methods which are frequently used to address non-linearity in the output. These methods are Neural Network (NN), Support Vector Machine (SVM), Gradient Boosting Machine (GBM), *k*-nearest neighbours (*k*-NN) and Classification and Regression Trees (CART). Parameters of these methods are tuned based on 5-fold cross validation. Moreover, 1st, 2nd and 3rd order polynomial regressions, which are frequently used for surrogate modelling in design synthesis are also included in the comparative study. Figure 3.16 shows comparison of performance between GPK and other methods. As evident GPK has performed better than state-of-the-art methods.
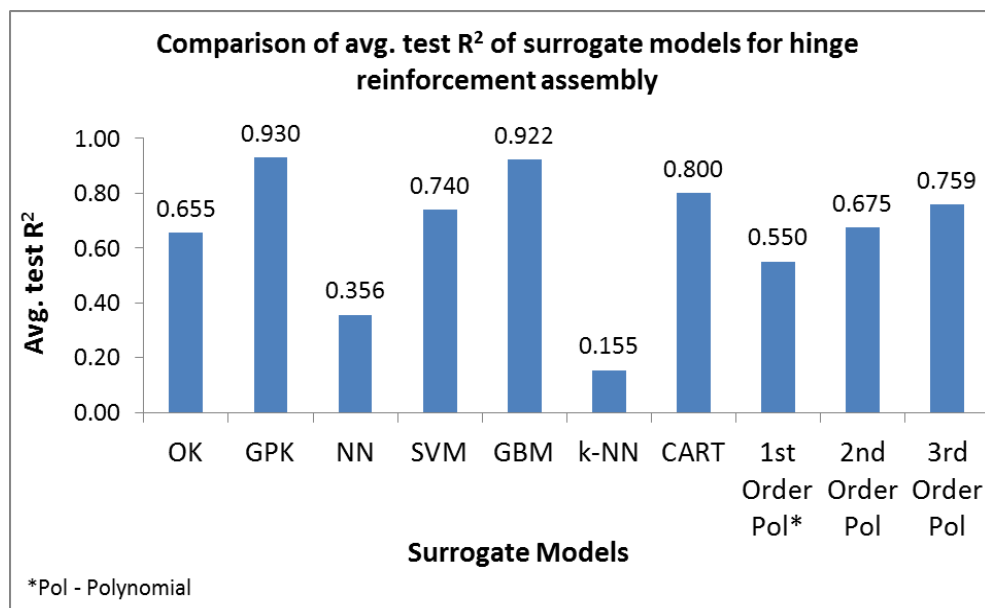
Figure 3.16: Comparison of peformance between GPK and state of the art methods for hinge reinforcement assembly

3.7.1.2 Fixture layout optimization for door inner panel and hinge assembly

The surrogate models developed in the previous section are utilized for fixture layout optimization in the door inner panel and hinge assembly. The GPK surrogate models of the assembly KPCs are represented as

$$y_k = f_k(\mathbf{x}) \tag{3.30}$$

where $k=1,2,\ldots 13$.

The weld stitches in this assembly are created by Remote Laser Welding which requires part-to-part gap to be within 0.05 mm to 0.40 mm at weld locations. Therefore, the allowable tolerance limits on KPC y_k are $[\mathrm{L}_k^{(y)}, \mathrm{U}_k^{(y)}] = [0.05 \text{ mm}, 0.40 \text{ mm}]$. The cost of quality due to deviation of the KPC 'y_k' from nominal can be described as

$$C(y_k) = \begin{cases} K_1\left(y_k - m_k\right)^2, y_k \in [\mathrm{L}_k^{(y)}, \mathrm{U}_k^{(y)}] \\ K_2\left(y_k - m_k\right)^2, y_k \in (-\infty, \mathrm{L}_k^{(y)}) \cup (\mathrm{U}_k^{(y)}, \infty) \end{cases} \tag{3.31}$$

where nominal of KPC y_k is $m_k = \dfrac{0.05 + 0.40}{2} = 0.225 \text{ mm}$. $K_1 = 100$ units/mm and $K_2 = 1000$ units/mm are Taguchi loss coefficients. A higher penalty is assigned to out-of-tolerance deviance to deter identification of clamp locations (KCCs) which generate an unacceptable gap between mating parts (KPCs). The cost $C(y_k)$ can be computed by replacing the KPC 'y_k' with its surrogate model. The total cost to be minimized for fixture layout optimization is given by

$$C(\mathbf{y}) = \sum_{k=1}^{13} C(y_k) \tag{3.32}$$

Moreover, the optimization is subject to design constraints on the KCCs. Based on the clamp parameterization described in Figure 3.5, all KCCs x_j for

j=1,2,…,6 are allowed to be within limits $[L_j^{(x)}, U_j^{(x)}]$=[0,1]. Therefore, the fixture layout optimization problem is given as follows

$$
\begin{aligned}
&Min \quad C(\mathbf{y}) \\
&Subject \quad to \quad 0 \le x_j \le 1 \quad \forall j = \{1,2,...,6\}
\end{aligned}
\tag{3.33}
$$

Genetic algorithm is applied to solve the aforementioned optimization. Settings of the GA are as follows:

    i.   Size of chromosome pool – 20

    ii.   Number of generations – 50

    iii.   Crossover probability – 0.60

    iv.   Mutation – 0.1

The optimal solution after 50 generations of GA is described as follows:

    i.   Optimal fixture clamp parameters (KCCs) – $(x_1, x_2, x_3, x_4, x_5, x_6) =$ (0.3123, 0.3253, 0.0009, 0.0029, 0.9063, 0.6296)

    ii.   Optimal part-to-part gaps at 13 weld locations (KPCs) in mm – $(y_1, y_2, y_3, y_4, y_5, y_6, y_7, y_8, y_9, y_{10}, y_{11}, y_{12}, y_{13}) =$(0.2225,   0.1595,   0.1643, 0.3691, 0.1847, 0.3674, 0.3021, 0.2831, 0.2202, 0.1283, 0.0670, 0.1776, 0.2099)

    iii.   Optimal cost of quality due to deviation of KPCs from nominal – 9.6766 units

As evident from the results, all optimal KPCs are within desired tolerance limits of $[L^{(y)}, U^{(y)}]$ = [0.05 mm, 0.40 mm].

3.7.2 Longitudinal stiffener and skin section assembly

This case study is a part of aircraft wing assembly. The assembly, as shown in Figure 3.17, consists of the following two parts: (1) skin-section of the fuselage and (2) longitudinal stiffener which attaches the wing with the fuselage. The skin-section and longitudinal stiffener is a sub-assembly of the overall aircraft wing assembly. The joining process for this assembly is Self-Piercing Riveting (SPR) which requires part-to-part gaps at riveting locations to be within 0.05-1 mm. Riveting for this assembly is done at 11 spots. Part-to-part gaps at the riveting locations are controlled by 3 clamps. Figure 3.18 shows the riveting spots and clamps which are used to maintain part-to-part gaps at the riveting locations.

Longitudinal stiffener-
skin section
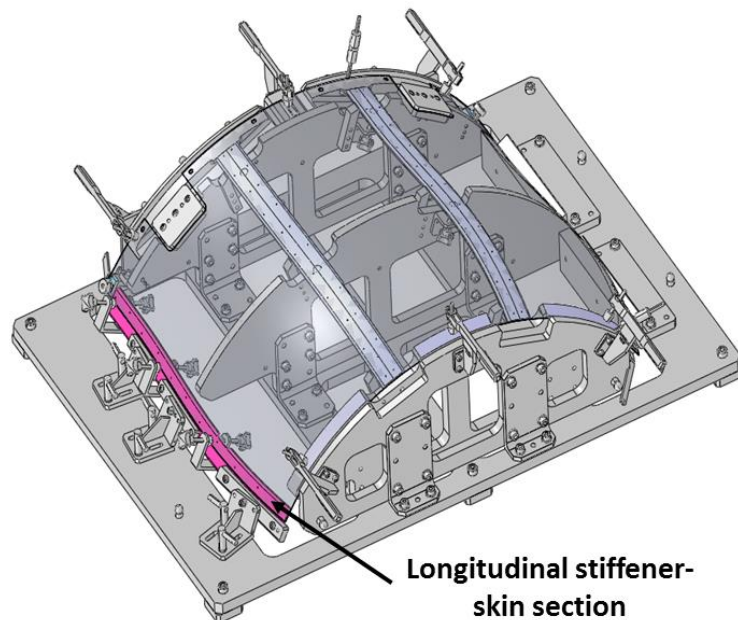
Figure 3.17: Longitudinal stiffener and skin section assembly
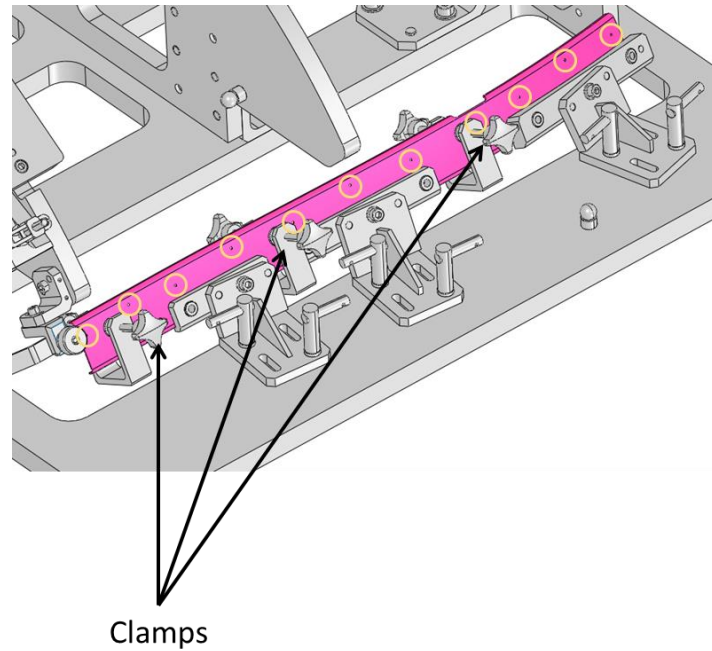
Figure 3.18: KPCs (gaps at riveting locations) and KCCs (clamp positions) in longitudinal stiffener and skin section assembly

Positions of the three clamps (KCCs 1 to 3) determine the fixture layout. For a given fixture layout, FEM-based VSA estimates part-to-part gaps (KPCs) at 11 riveting locations. A single instance of VSA takes 7 minutes on an average for this assembly.

Scalable surrogate models for deterministic non-linearity of KPCs are developed using the proposed GPK and O-MRAS methods. The surrogate models are then used to conduct fixture layout optimization. The remaining part of the case study is described as follows: Section 3.7.2.1 describes the scalable surrogate modelling of the assembly KPCs. Next, Section 3.7.2.2 discusses fixture layout optimization using the KPC surrogate models.

3.7.2.1 Scalable surrogate modelling of KPCs in longitudinal stiffener and skin section assembly

The scalable surrogate models of the assembly KPCs are developed

through the following five steps:

Step 1:   *Sample initial design matrix of KCCs by space filling* −

Design matrix of KCCs for the first iteration consists of $n=50$ points generated through uniform random sampling. For subsequent iterations, design matrix having 50 points is generated through O-MRAS.

Step 2:   *Run VSA to generate training data* − Each row of the KCC design matrix represent a fixture layout. The design matrix of KCCs is given as input to VSA which estimates KPCs for n instances of fixture layout present in the KCC design matrix.

Step 3: *Train surrogate models via GPK* − The GPK surrogate models are developed using the training data $\mathbf{S}_T$ which has all the data generated till the current iteration. GPK surrogate model of KPC 'y' is developed based on Polynomial Feature Selection (PFS) and Kernel Optimization (KO) which are described as follows:

A.   *Polynomial Feature selection* − PFS identifies optimal features for the regression component of GPK surrogate model based on minimization of 5-fold CV MSE. As an illustration, Figure 3.19 shows the drop of CV MSE over iterations of PFS for KPCs 1, 6 and 11. Table 3.6 presents a summary of results of PFS for KPCs 1, 6 and 11. From the results, it is evident, that a high CV R^2 (0.96) for KPC_1 after PFS indicates that the global approximation by the regression component has an acceptable predictive accuracy. However, a low R^2 (0.34) of the regression component of KPC_{11} indicates requirement for further improvement by KO.
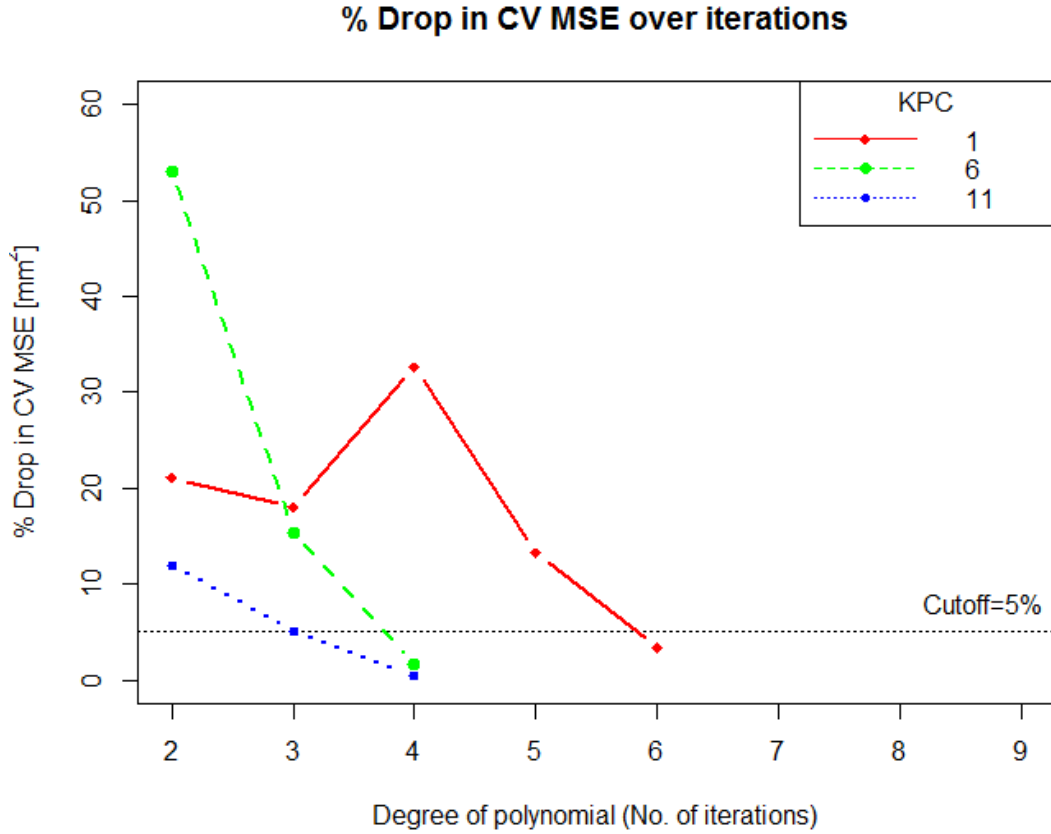
Figure 3.19: Drop in cross-validation MSE over iterations of feature selection for KPCs 1, 6 and 11 longitudinal stiffener and skin section assembly

Table 3.6: Summary of feature selection for KPCs 1, 6 and 11 of longitudinal stiffener and skin section assembly

KPC Index	Highest polynomial order identified	No. of features in final solution	Cross validation degree of determination (CV R^2)
1	6	8	0.96
6	4	6	0.84
11	4	5	0.34

    B. *Kernel Optimization* – This is applied to determine the parameters $\boldsymbol{\theta}$ of the correlation or kernel function of the Gaussian process based on minimization of generalized prediction error of the GPK model. The search for optimal $\boldsymbol{\theta}$ is done by the adaptive GA method. Figure 3.20 shows the performance of the adaptive GA for kernel optimization of KPC_1. It is noteworthy that though depending on number of instances in the training

114

data, the number of generations of GA was set as 75, the early stopping criterion terminated GA thereby avoiding redundant search.
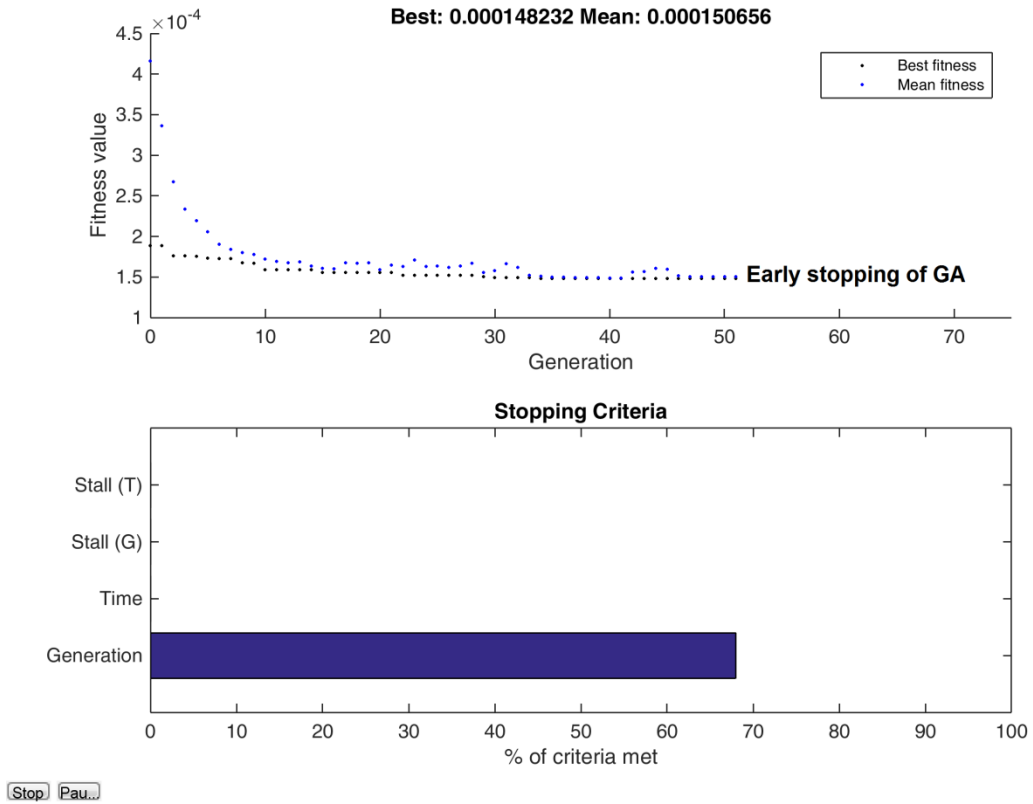
Figure 3.20: Kernel Optimization by adaptive GA for GPK model of KPC_1 in longitudinal stiffener and skin section assembly

KO further improves the predictive accuracy of the GPK models on unseen test samples beyond what has already been achieved by PFS. Table 3.7 summarizes the additional improvement in CV R^2 achieved by KO.

Table 3.7: Additonal improvement of CV R^2 by Kernel Optimization for KPCs 1, 6 and 12 in longitudinal stiffener and skin section assembly

KPC Index	Cross validation R^2 *before* KO	Cross validation R^2 *after* KO
1	0.96	0.99
6	0.84	0.97
13	0.34	0.90

Based on PFS and KO, GPK surrogate models are developed for the 11 KPCs related to the longitudinal stiffener and skin section assembly.

Step 4: <u>Check if model accuracy is acceptable</u> –

Model accuracy is measured by average degree-of-determination R^2_{avg} on the test samples for 11 KPCs. Surrogate modelling is stopped if $R^2_{avg} \geq 0.9$ else further iterations are conducted to generate model training data and re-develop the GPK models. Design matrix of KCCs for VSA in subsequent iterations is generated by O-MRAS, which is described in Step 5.

Step 5: Select design matrix of KCCs via O-MRAS –

Design matrix of KCCs is generated by O-MRAS through the following three steps:

A. *Generate adaptive samples for individual KPCs* – In this case study adaptive samples for individual KPCs $y_1, y_2, ..., y_{11}$ are generated using Lipschitz criterion (Lovison & Rigoni, 2011). Each adaptive sample contain *n*=50 instances of KCCs. This is done by the following three sub-steps which are same as those in the case study on door inner panel and hinge assembly discussed in Section 3.7.1:

B. *Perform k-means clustering to identify n=50 groups* – Using Lipschitz criteria based adaptive sampling 11 single-KPC adaptive samples each having 50 instances of KCCs have been generated. The individual adaptive samples $\mathbf{X}_C^{(1)}, \mathbf{X}_C^{(2)}, ..., \mathbf{X}_C^{(13)}$ are merged into a single 550×3 matrix $\mathbf{X}_C$. *k*-means clustering is applied to divide the 550 instances into 50 groups.

C. *Identify optimal instance from each cluster* – An optimal instance from each of the 50 clusters is chosen by a weighted selected strategy which takes in consideration the following two criteria: (1) proximity of CPs from cluster centroids; and, (2) merit of the CPs as obtained from Lipschitz criteria based single-KPC adaptive sampling. Weights assigned to the aforementioned two criteria are: $\omega_1 = 0.5$ and $\omega_2 = 0.5$.

Overall, O-MRAS identifies a single optimal adaptive sample $\mathbf{X}_C^*$ of 50 instances from 11 individual adaptive samples. In this case study, O-MRAS has been done over 3-dimensional space. The O-MRAS is further illustrated on 2-dimensional case studies in Appendix C.

Discussion of results from scalable surrogate modelling of KPCs

Results of surrogate modelling of the KPCs related to longitudinal stiffener and skin section assembly are discussed as follows:

i. *Achievement of desired predictive accuracy on unseen test samples* – The desired predictive accuracy on unseen test samples is evaluated by R_{avg}^2, which

is computed on the test dataset. Figure 3.21 shows GRK models have achieved $R^2_{avg} > 0.9$ in six iterations.
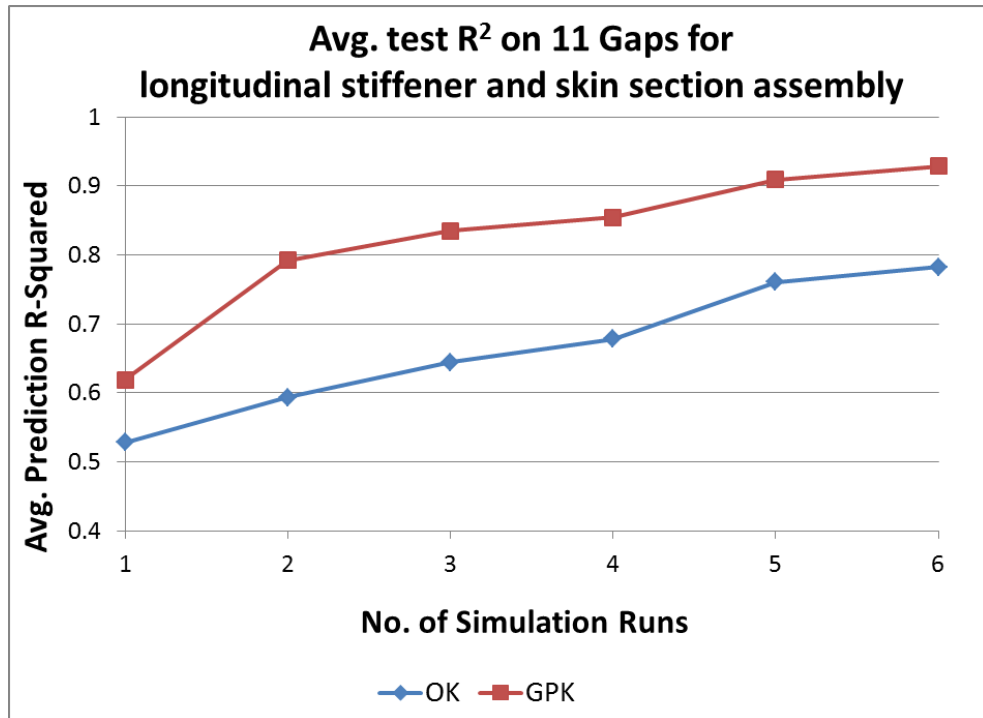
Figure 3.21: Performance of GPK and OK surrogate models for longitudinal stiffener and skin section assembly

ii. *Comparison of performance with state-of-the-art Ordinary Kriging –* Figure 3.21 highlights that GPK's PFS and KO based on minimization of generalized model predictive error has developed more accurate surrogate models in lesser number of iterations as compared to OK.

iii. *Scalability for deterministic non-linearity –* KO identifies suitable smoothing parameters α_j for KCC$_j$ based on minimization of generalized model predictive error. A suitable smoothing parameter should manifest the non-linearity in the underlying KPC-KCC relations as well maximize accuracy of the surrogate model on unseen training samples. For instance, in this case study smoothing parameters of KCCs 1 to 3 for KPC$_2$ determined by KO are

[2, 2, 2] at a R^2=0.975 on unseen test samples. This shows that GPK has been able to identify a smooth and differentiable relationship between KPC_2 and KCCs 1 to 3 at an acceptable test R^2. Figure 3.22 shows the 2D response surface of KPC_2 with respect to KCC_1 and KCC_2. Figure 3.23 presents the profile of KPC_2 with respect to KCC_1 which has a single global maxima and minima. On the other hand, for KPC_1, smoothing parameters determined by kernel optimization are [1, 1.4, 2] for KCCs 1 to 3 at R^2=0.989 on unseen test samples. This implies that KPC_1 is smooth and infinitely differentiable with respect to KCC_3 and has single global maxima. However KPC_1 is rough with respect to KCC_1 and KCC_2 and has multiple local maximas and minimas. For illustration, 2D response surface of KPC_1 with respect to KCC_1 and KCC_3 is shown Figure 3.24 while profile of KPC_1 with respect to KCC_1 is shown in Figure 3.25.
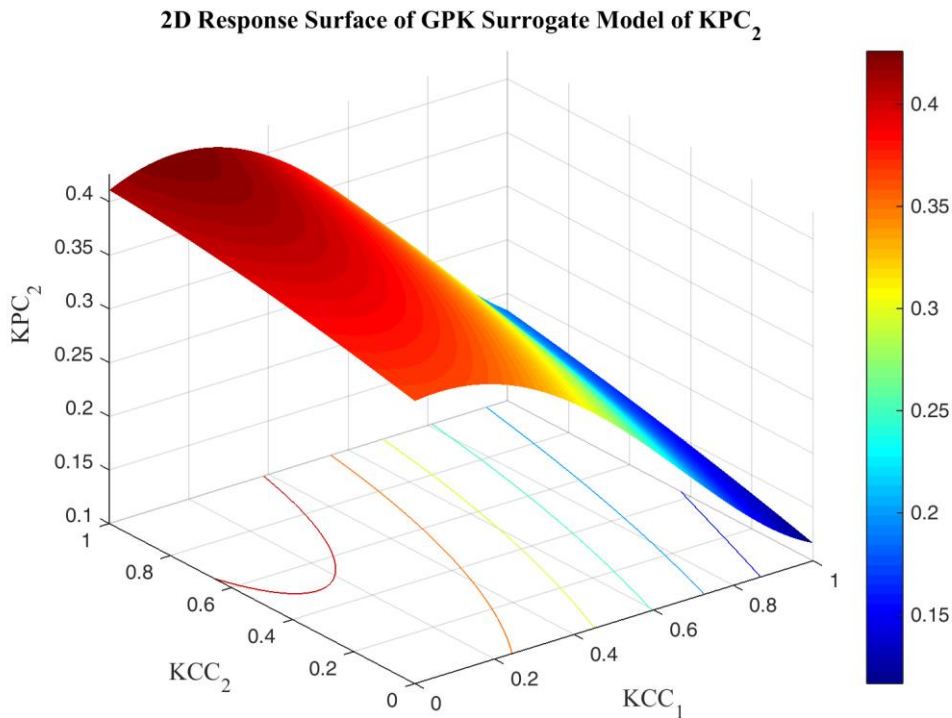
Figure 3.22: 2D response surface of GPK surrogate model of KPC_2 with respect to KCC_1 and KCC_2 in longitudinal stiffener and skin section assembly
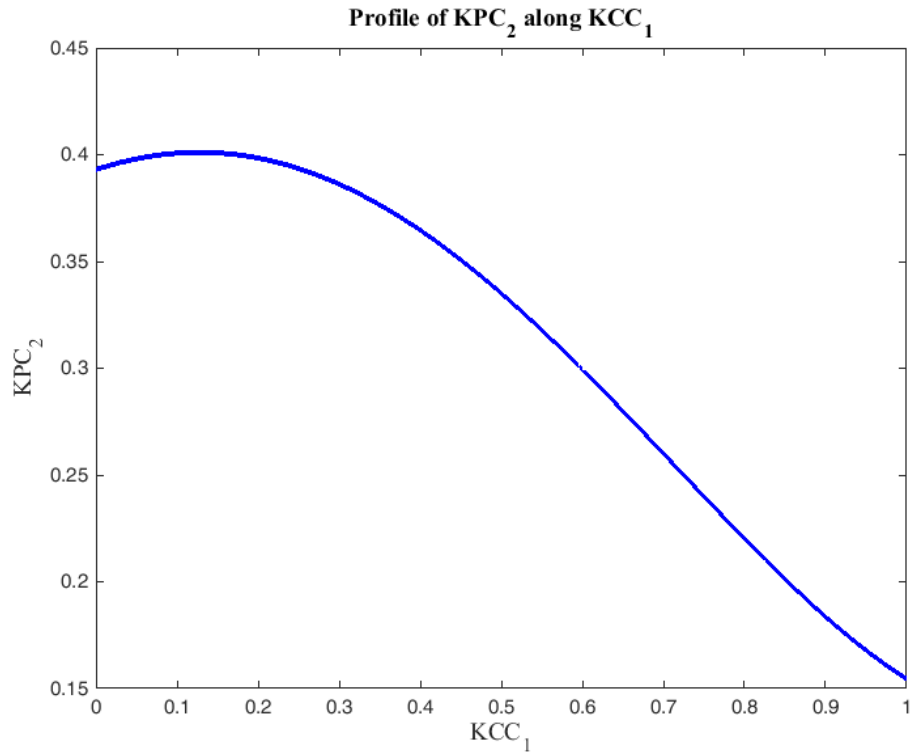
Figure 3.23: Profile of KPC_2 with respect to KCC_2 in longitudinal stiffener and skin section assembly
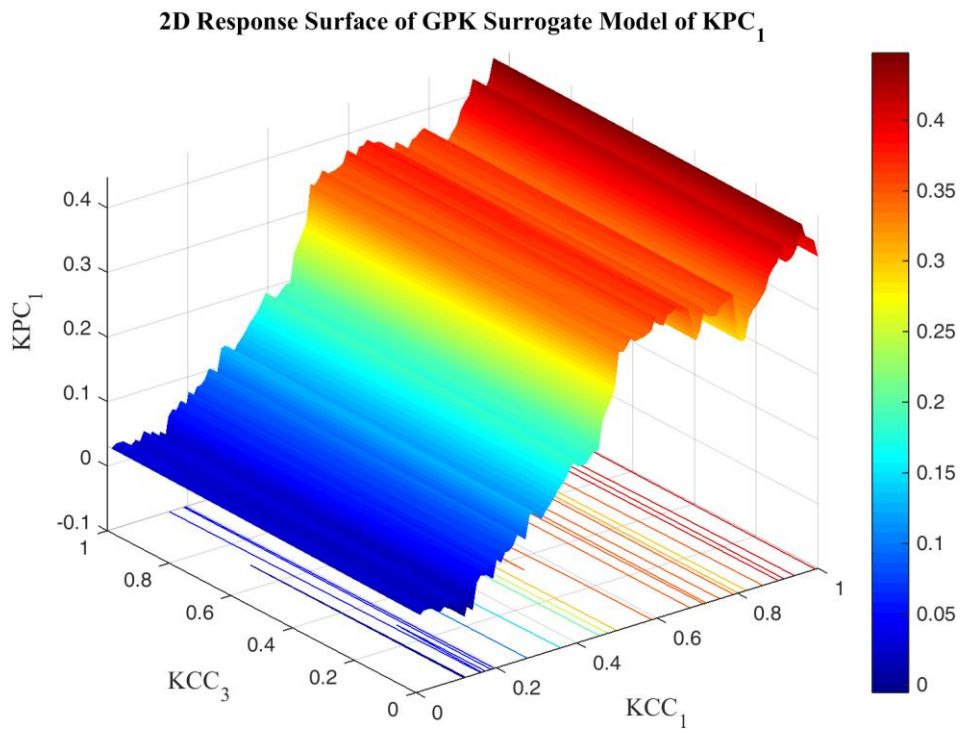
Figure 3.24: 2D response surface of GPK surrogate model of KPC_1 with respect to KCC_1 and KCC_3 in longitudinal stiffener and skin section assembly
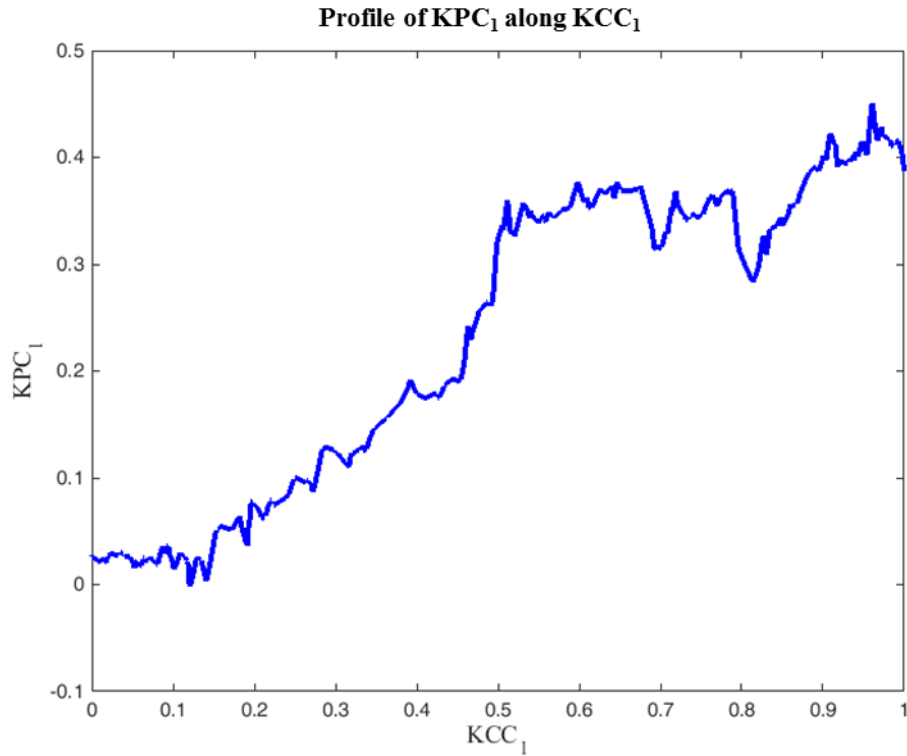
Figure 3.25: Profile of KPC_1 with respect to KCC_1 in longitudinal stiffener and skin section assembly

iv. Comparison with other state-of-the-art surrogate models − Performance of GPK is compared with the following state-of-the-art methods − Neural Network (NN), Support Vector Machine (SVM), Gradient Boosting Machine (GBM), *k*-nearest neighbours (*k*-NN) and Classification and Regression Trees (CART) which are frequently used to model non-linearity in input-output interrelations. For each of these methods, parameter tuning is done by 5-fold cross validation. Moreover, 1st, 2nd and 3rd order polynomial regressions are also included in the comparative study. Figure 3.26 shows comparison of performance between GPK and other methods. As evident GPK has performed better than these methods.
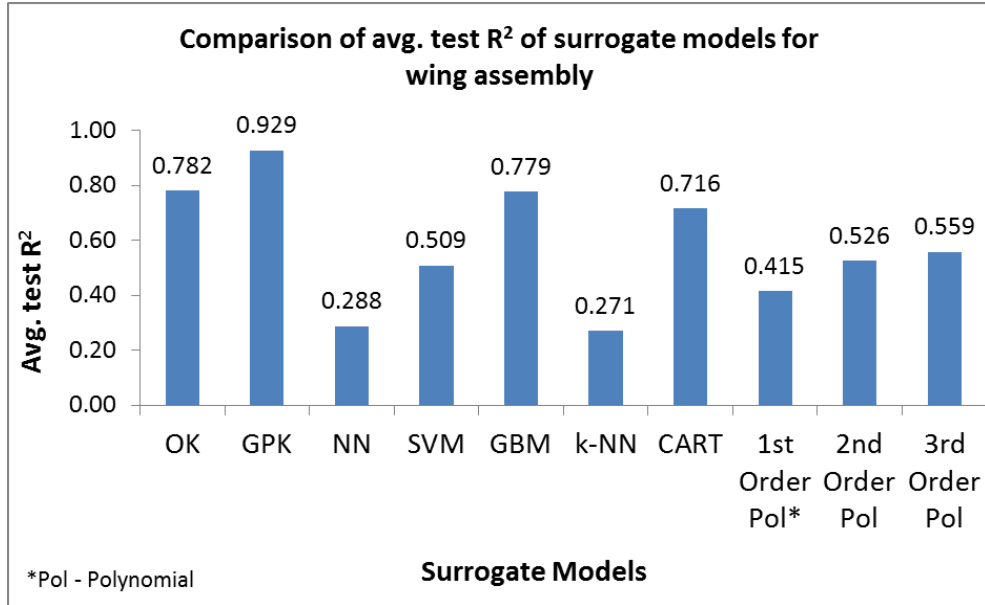
Figure 3.26: Comparison of peformance between GPK and state of the art methods for longitudinal stiffener and skin section assembly

3.7.2.2 Fixture design optimization for longitudinal stiffener and skin section assembly

The GPK models developed in the previous section are used for fixture layout optimization for this assembly. A cost based KPI which depends on the deviation of the assembly KPCs from nominal is minimized subject to design tolerances on assembly KCCs. The parameters of the optimization problem are as follows:

i. Tolerance limits of KPCs − $[L_k^{(y)}, U_k^{(y)}]$ = [0.05 mm, 0.40 mm] for k=1,2,…,11.

ii. Nominal of KPCs, $m_k = \dfrac{0.05 + 1}{2} = 0.5025$ mm for k=1,2,…,11.

iii. Taguchi loss coefficients − In-tolerance loss coefficient, $K_1 = 100$ units/mm and out-of-tolerance loss coefficient, $K_2 = 1000$ units/mm

iv. Design tolerance of KCCs −$[L_j^{(x)}, U_j^{(x)}]$=[0,1] for j=1,2 and 3.

Cost of quality due to a KPC's deviation from nominal is given as

$$C(y_k) = \begin{cases} K_1\left(y_k - m_k\right)^2, \; y_k \in [\mathrm{L}_k^{(y)}, \mathrm{U}_k^{(y)}] \\ K_2\left(y_k - m_k\right)^2, \; y_k \in (-\infty, \mathrm{L}_k^{(y)}) \cup (\mathrm{U}_k^{(y)}, \infty) \end{cases} \tag{3.34}$$

Fixture layout optimization minimizes total cost given as follows.

$$C(\mathbf{y}) = \sum_{k=1}^{11} C(y_k) \tag{3.35}$$

subject to $0 \le x_j \le 1$ for $j = 1, 2, 3$.

Genetic algorithm is applied to solve the optimization. Settings of the GA are as follows:

i.   Size of chromosome pool – 20

ii. Number of generations – 50

iii. Crossover probability – 0.60

iv. Mutation – 0.1

The optimal solution after 50 generations of GA is described as follows:

i.   Optimal fixture clamp parameters (KCCs) – $(x_1, x_2, x_3) =$ (0.6749, 0.1886, 0.4208)

ii. Optimal part-to-part gaps at 13 weld locations (KPCs) in mm – $(y_1, y_2, y_3, y_4, y_5, y_6, y_7, y_8, y_9, y_{10}, y_{11}) = $(0.3463, 0.1639, 0.0801, 0.0432, 0.1751, 0.9849, 0.9398, 0.0650, 0.5982, 0.6201, 1.9135) mm.

iii. Optimal cost of quality due to deviation of KPCs from nominal – 2125 units

As evident from the results, all optimal KPCs are within desired tolerance limits of $[\mathrm{L}_k^{(y)}, \mathrm{U}_k^{(y)}] = [0.05 \text{ mm}, 1 \text{ mm}]$ except KPC$_{11}$. Out-of-tolerance gap for KPC$_{11}$ in the optimal clamp layout indicates the need for additional clamps

for this assembly.

3.7.3 Additional case studies

Greedy Polynomial Kriging (GPK) is developed in this chapter as a scalable surrogate modelling method for deterministic KPCs estimated by VSA of sheet metal assemblies. It is expected that GPK should provide an *acceptable prediction accuracy on unseen test samples* for the scale of non-linearity in underlying KPC-KCC interrelations characterized by varying number of local maximas and minimas. To demonstrate the capability of GPK to address scale of deterministic non-linearity, it is used to develop surrogate models of seven well-known benchmark functions: (1) two unimodal functions having single maxima or minima; and, (2) five multimodal functions having multiple local maximas and minimas. Accuracy of GPK is evaluated by computing R^2 on unseen test samples and is compared with that obtained from Ordinary Kriging (OK).

For comparative study using a benchmark function, surrogate models using both GPK and OK are developed based on the iterative surrogate modelling method outlined in Figure 3.2. During each iteration, a design matrix of $\mathbf{x}$ is generated by selecting 25 points via uniform random sampling from the domain of $\mathbf{x}$. The response at these 25 points is calculated by the benchmark function. A training dataset $\mathbf{S_T} = \{\mathbf{x}, y\}_{i=1}^{n}$ stores all the training data generated till the current iteration. The number of samples in S_T increases as 25, 50… over the iterations. OK and GPK surrogate models are developed and their R^2 is determined on an unseen test dataset $\mathbf{S_V} = \{\mathbf{x}, y\}_{i=1}^{40000}$ which is not used in training the surrogate models. $\mathbf{S_V}$ is generated by using a 200×200 grid on the domain of $\mathbf{x}$ as the design matrix and computing the response y using the benchmark function. The stopping criteria of iterations is

124

$R^2 \geq 0.90$ on the test sample.

The seven benchmark functions used for the comparative study are as follows:

i. Branin function – *unimodal* and evaluated in $x_1 \in [-5,10]$ and $x_2 \in [0,15]$

$$(x_2 - \frac{5.1}{4\pi} x_1^2 + \frac{5}{\pi} x_1 - 6)^2 + 10(1 - \frac{1}{8\pi}) \cos(x_1) + 10 \qquad (3.36)$$

ii. Booth function – *unimodal* and evaluated in $x_i \in [-10,10]$

$$(x_1 + 2x_2 - 7)^2 + (2x_1 + x_2 - 5)^2 \qquad (3.37)$$

iii. Rastrigin function – *multi-modal* and evaluated in $x_i \in [-5.12, 5.12]$

$$20 + x_1^2 - 10\cos(2\pi x_1) + x_2^2 - 10\cos(2\pi x_2) \qquad (3.38)$$

iv. Cross-in-tray fuction – *multi-modal* and evaluated in $x_i \in [-10,10]$

$$-0.0001\left(\left|\sin(x_1)\sin(x_2)\exp\left(\left|100 - \frac{\sqrt{x_1^2 + x_2^2}}{\pi}\right|\right)\right| + 1\right)^{0.1} \qquad (3.39)$$

v. Schwefel function – *multi-modal* and evaluated in $x_i \in [-500, 500]$

$$837.9658 - \left(x_1 \sin\sqrt{|x_1|} + x_2 \sin\sqrt{|x_2|}\right) \qquad (3.40)$$

vi. Griewank function– *multi-modal* and evaluated in $x_i \in [-10,10]$

$$\frac{x_1^2}{4000} + \frac{x_2^2}{4000} - \cos(x_1)\cos\left(\frac{x_1}{\sqrt{2}}\right) + 1 \qquad (3.41)$$

vii. Shubert function– *multi-modal* and evaluated in $x_i \in [-2,2]$

$$y = \left(\sum_{i=1}^{5} i\cos\left((i+1)x_1 + i\right)\right)\left(\sum_{i=1}^{5} i\cos\left((i+1)x_2 + i\right)\right) \qquad (3.42)$$

Surjanovic and Bingham (2013) provides detailed description about the aforementioned benchmark functions. 2D plots of these functions are given in Appendix D.

Comparison of R^2 on unseen test sample obtained from OK and GPK for the aforementioned seven benchmark functions is shown in Figures 3.27 to 3.33.
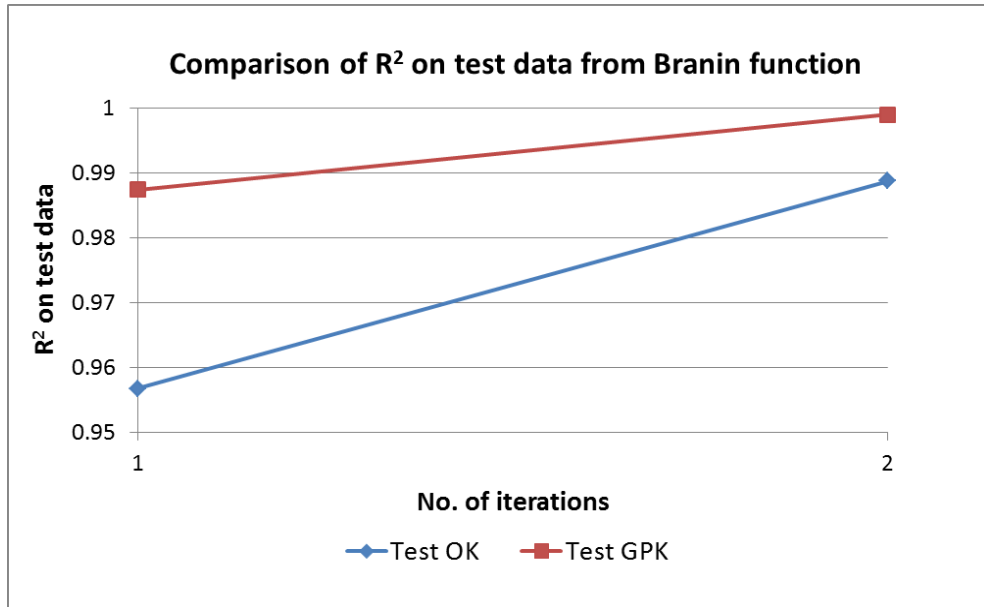
Figure 3.27: Performance of GPK and OK surrogate models for Branin function
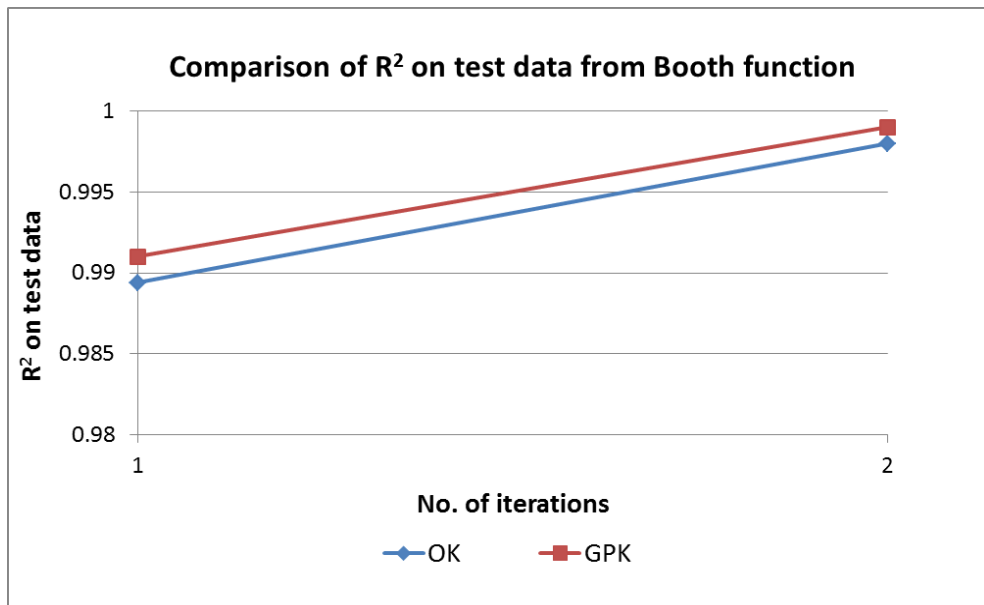
Figure 3.28: Performance of GPK and OK surrogate models for Booth function
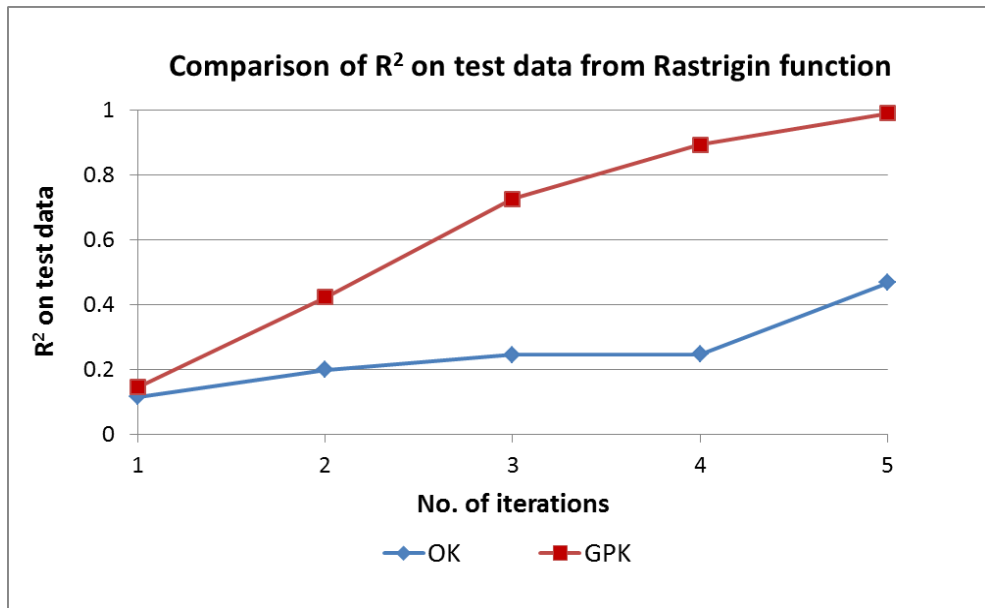
Figure 3.29: Performance of GPK and OK surrogate models for Rastrigin function
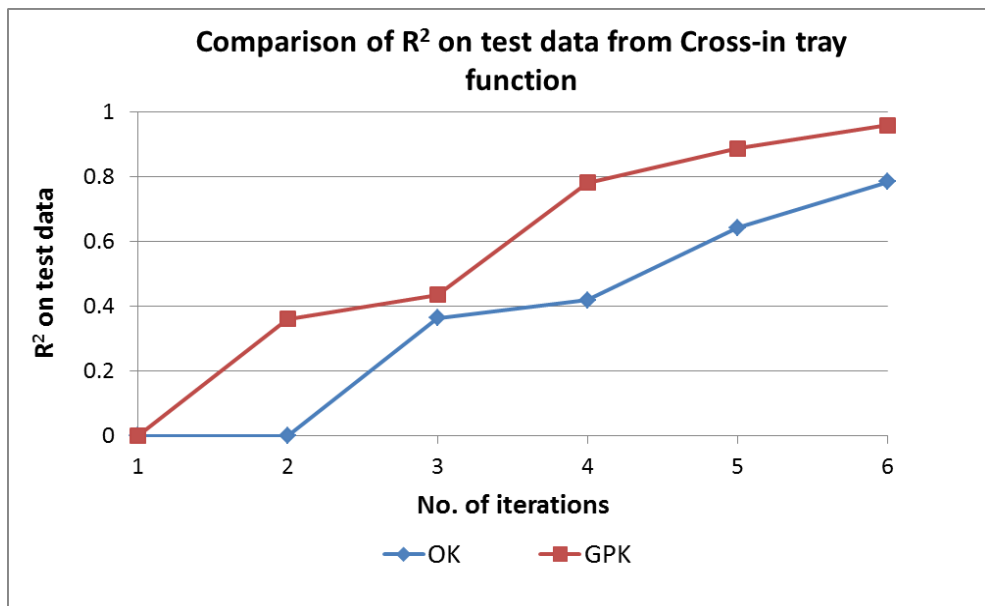
Figure 3.30: Performance of GPK and OK surrogate models for Cross-in-tray function
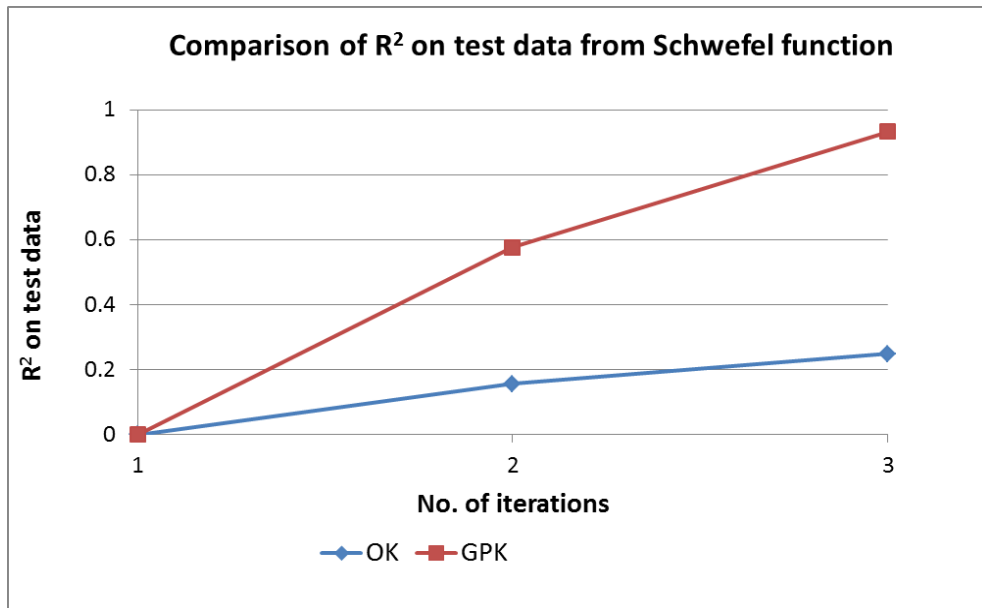
Figure 3.31: Performance of GPK and OK surrogate models for Cross-in-tray function
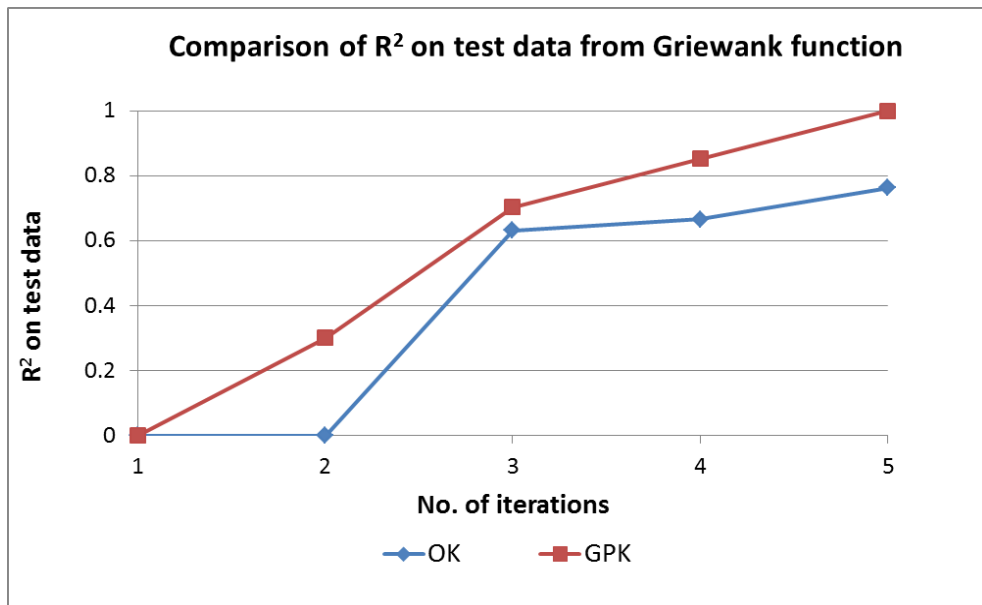
Figure 3.32: Performance of GPK and OK surrogate models for Griewank function
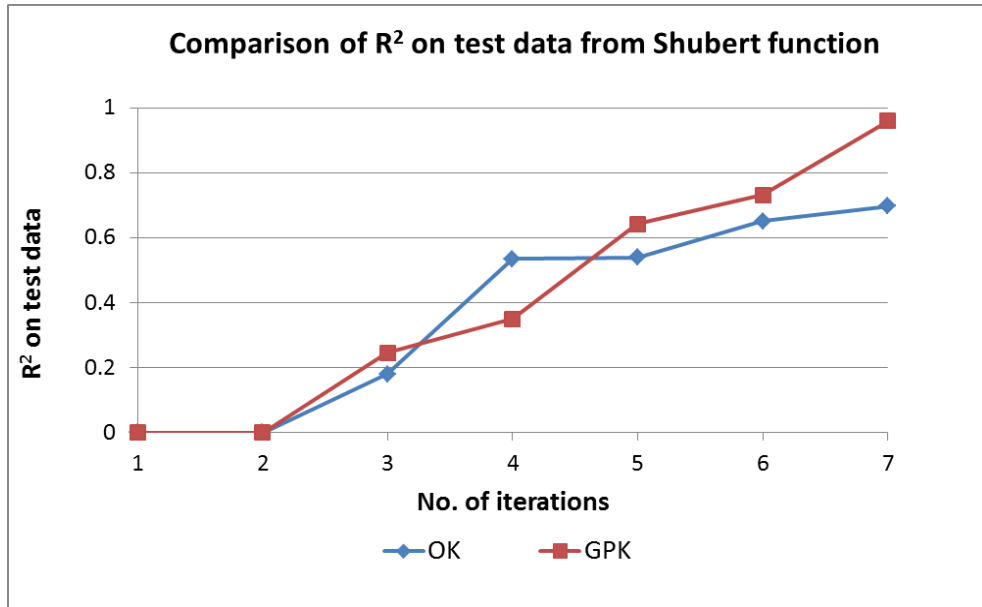
Figure 3.33: Performance of GPK and OK surrogate models for Shubert function

GPK is expected to learn the scale non-linearity in the underlying input-output interrelations characterized by varying number of local maximas and minimas. GPK's capability to emulate non-linearity in output-input interrelations can be verified by visualising and comparing the actual and GPK-predicted profiles of the response (y) with respect to one of the input parameters ($\mathbf{x}$). To this end, Figures 3.34 to 3.40 shows the actual and GPK-predicted profiles of 'y' with respect to x_1 for each of the seven benchmark functions discussed in this section. Additionally, profile predicted by OK is also included in the plots.
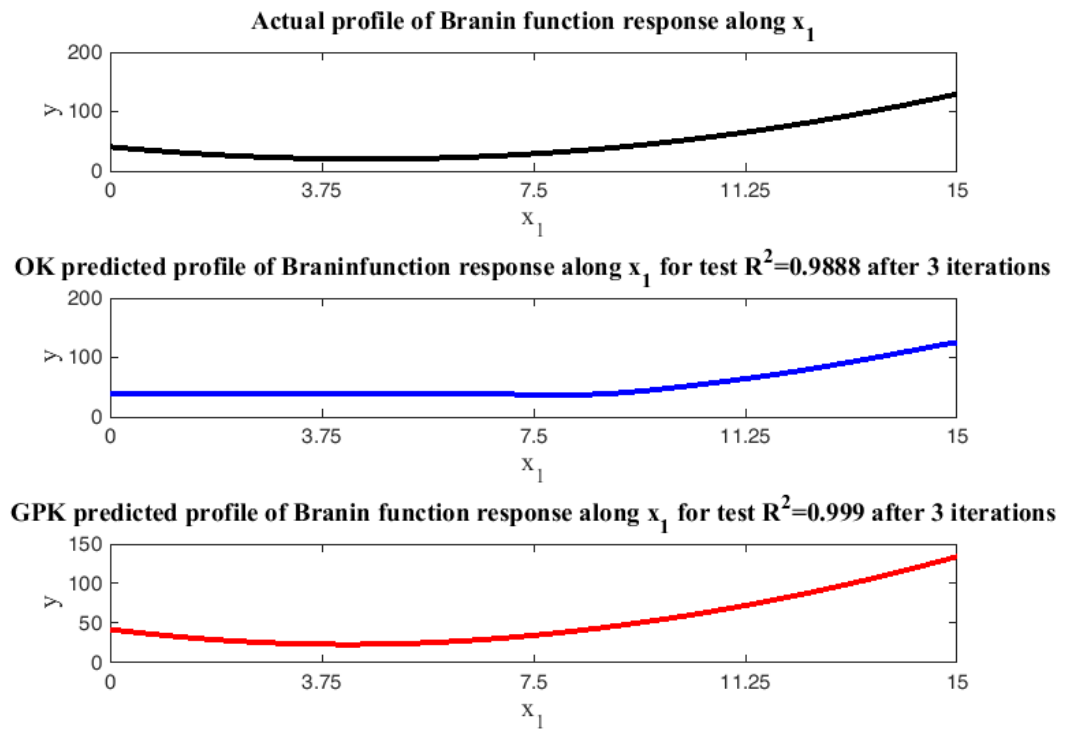
Figure 3.34: Actual, OK- and GPK-predicted profiles of Branin function
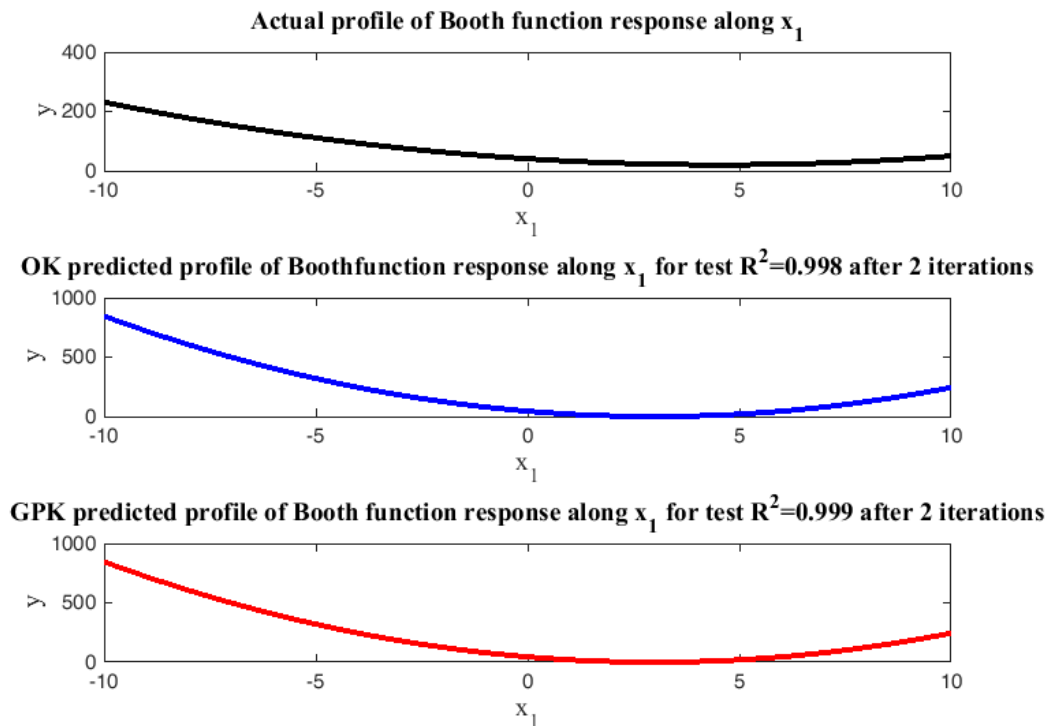
Figure 3.35: Actual, OK- and GPK-predicted profiles of Booth function
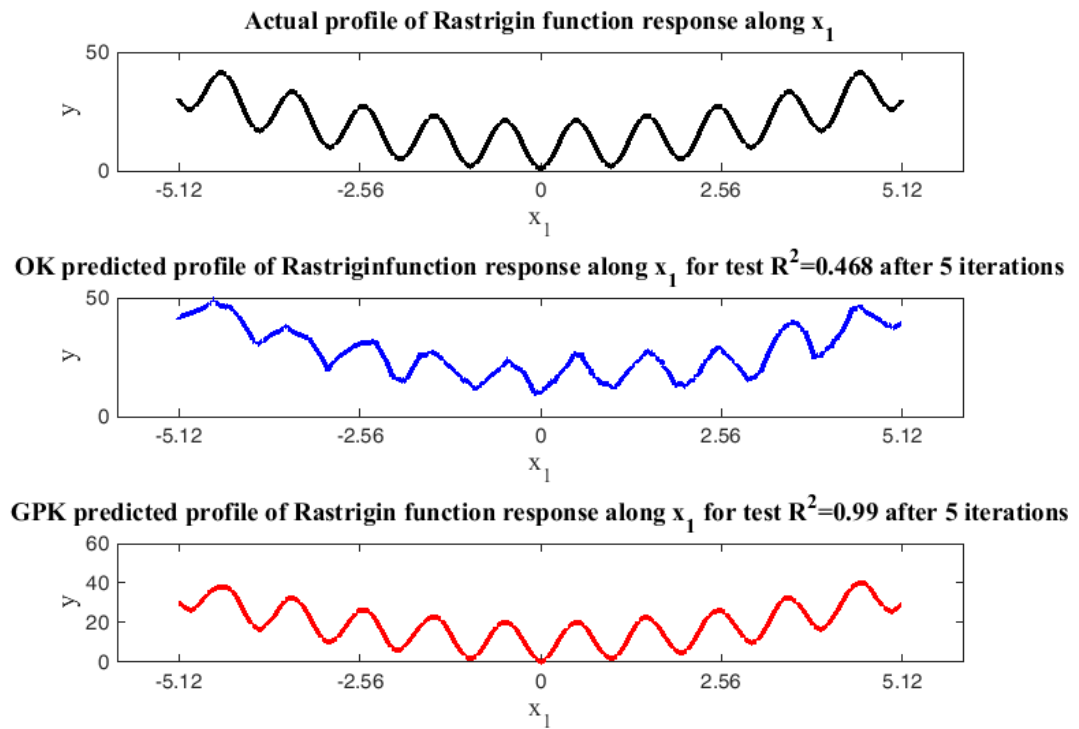
Figure 3.36: Actual, OK- and GPK-predicted profiles of Rastrigin function
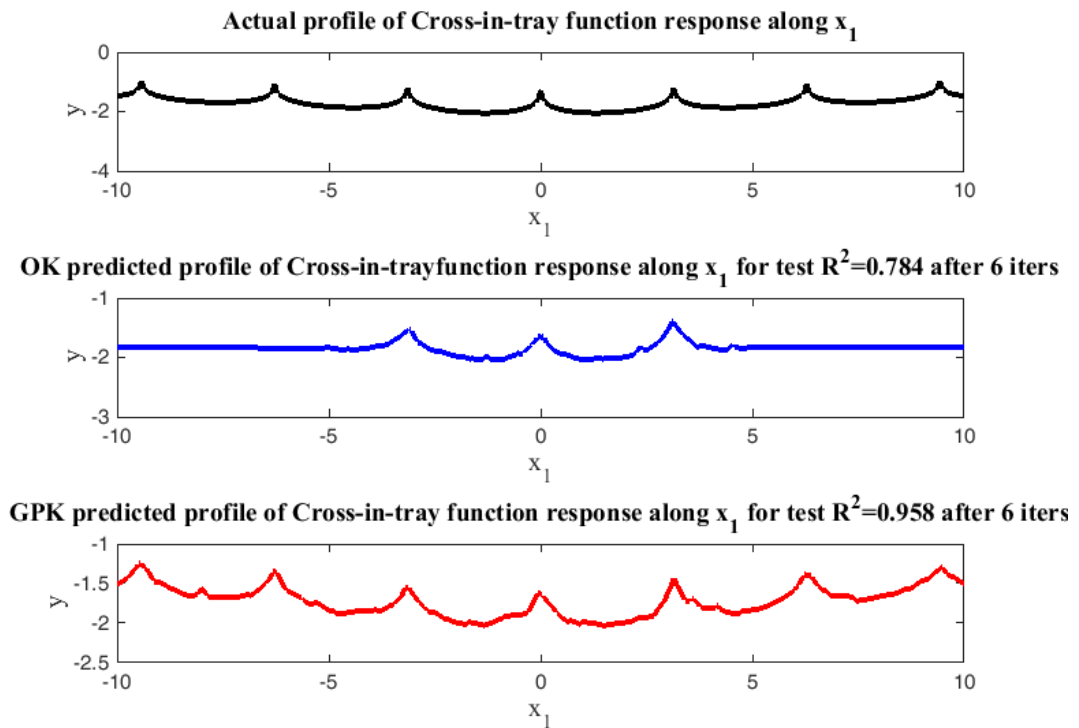
Figure 3.37: Actual, OK- and GPK-predicted profiles of Cross-in-try function
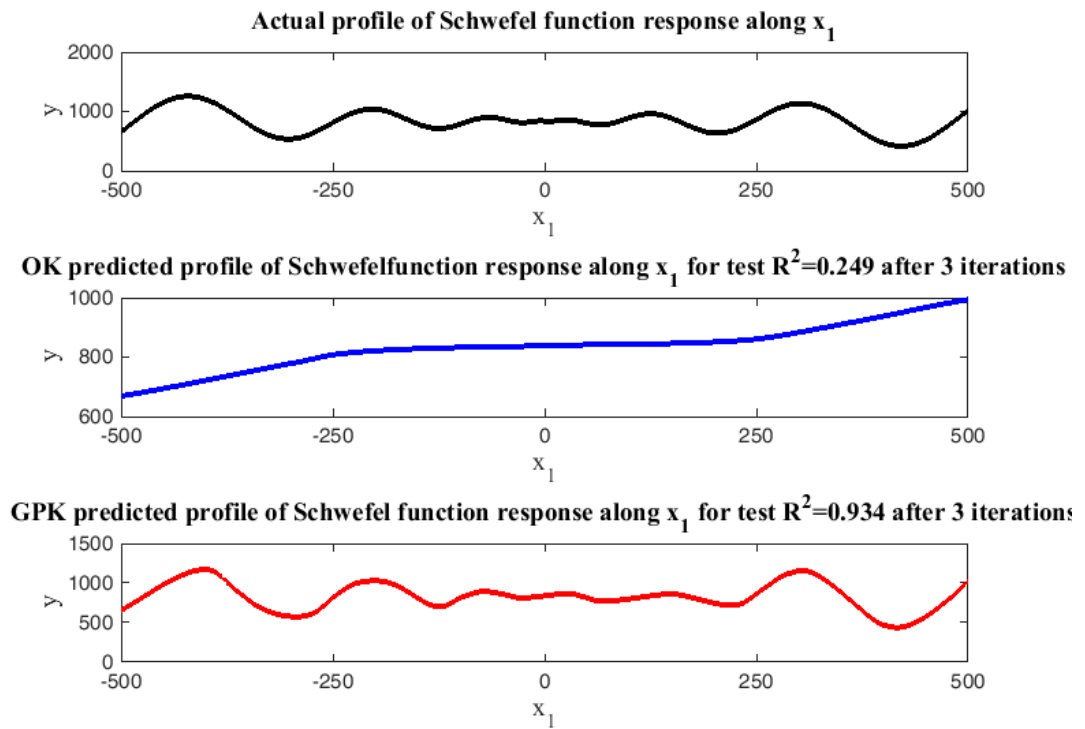
Figure 3.38: Actual, OK- and GPK-predicted profiles of Schwefel function
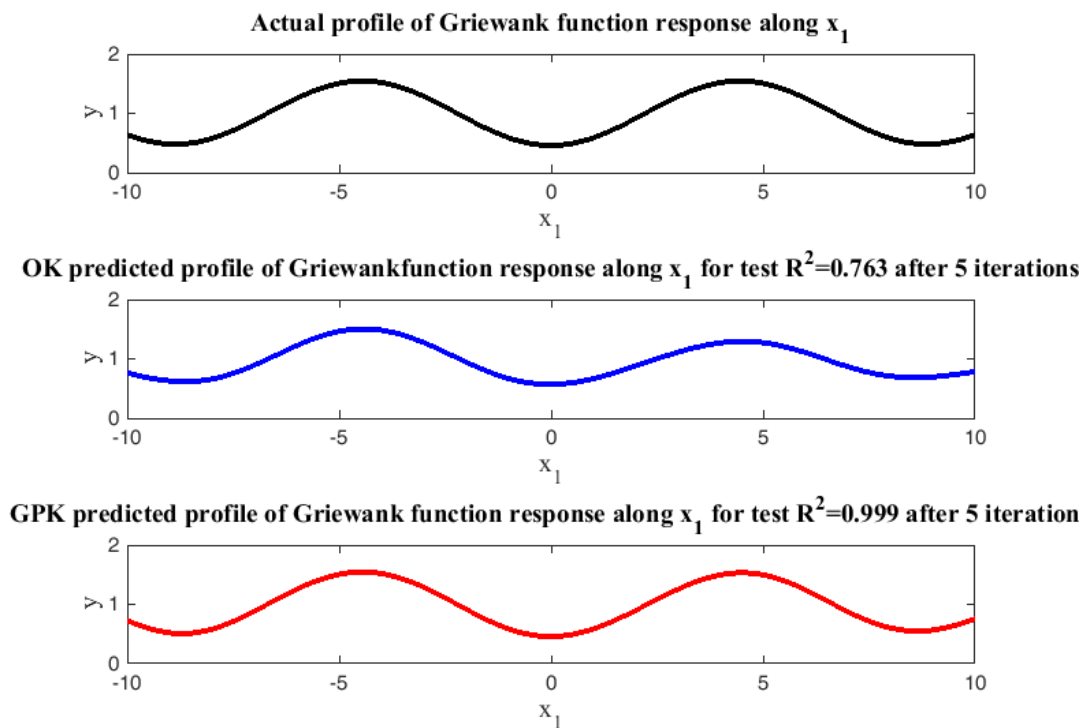
Figure 3.39: Actual, OK- and GPK-predicted profiles of Griewank function
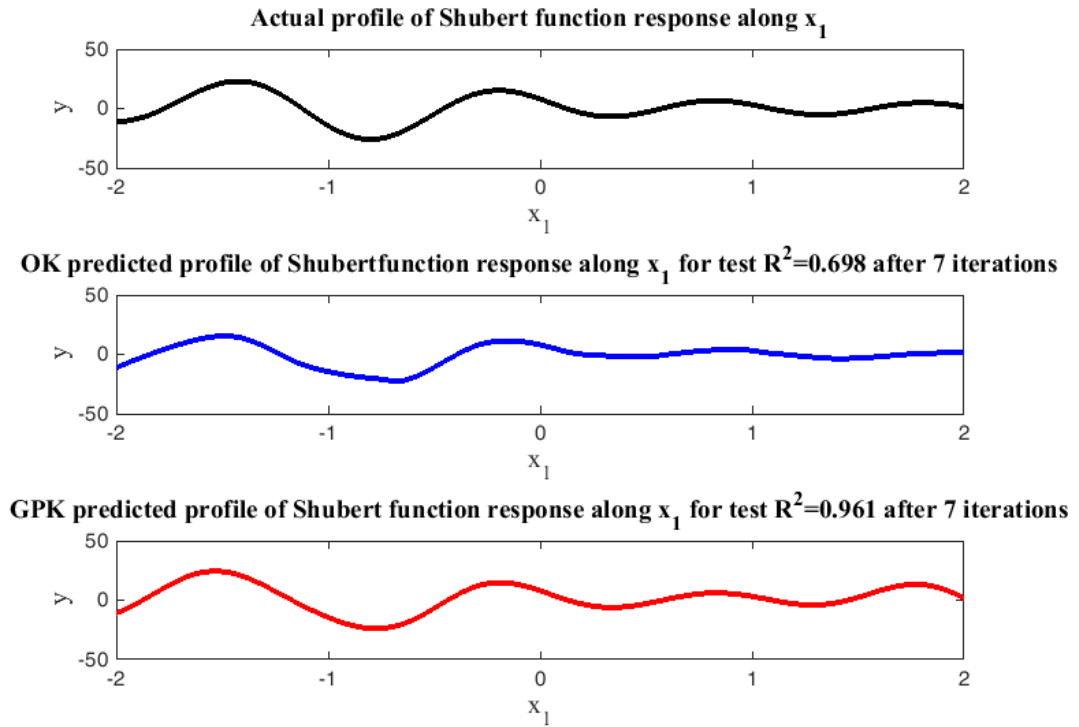
Figure 3.40: Actual, OK- and GPK-predicted profiles of Shubert function

Discussion of results – Significance of the results obtained in this section is discussed based on the following two aspects:

i.*Comparison of R^2 on unseen test samples* – As evident from the results, both OK and GPK give comparatively high R^2 for the unimodal Branin and Booth functions. However, for the multimodal functions, GPK's Polynomial Feature Selection and Kernel Optimization done based on minimization of generalized model error have helped it to achieve higher R^2 on unseen test samples with a smaller training dataset having lesser number of training instances. GPK's capability to achieve an acceptable predictive accuracy on unseen test samples with minimal number of training instances is a significant advantage for developing acceptably accurate surrogate models from computationally expensive VSA models in minimal computation time to generate training data.

ii. Addressing scale of deterministic non-linearity in output-input interrelations – To address scalability of deterministic non-linearity, the following two criteria needs to be taken into consideration: (1) emulation of non-linearity in output-input interrelations characterized by presence of maximas and minimas; and, (2) acceptable predictive accuracy on unseen test samples. Currently existing methods of surrogate modeling such as polynomial regression which are frequently used for design synthesis emulate non-linearity in output-input interrelations at the expense of overfitting training samples and giving low predictive accuracy on unseen test samples.

GPK focuses on achieving scalability for deterministic non-linearity by addressing the aforementioned two criteria in a non-conflicting manner whereby GPK surrogate models emulate non-linearity in output-input interrelations while generating acceptably accurate prediction on unseen test samples. Figures 3.34 to 3.40, showing comparison between actual and GPK predicted profiles of the benchmark functions, demonstrate GPK's capability to achieve scalability for deterministic non-linearity by emulating non-linearity in underlying KPC-KCC interrelations at acceptable predictive accuracy on unseen test samples.

3.8 Summary

This chapter focuses on developing scalable surrogate models having *acceptable accuracy on unseen test samples* for deterministic and non-linear KPCs whose scale of non-linearity is characterized by varying number of local maximas and minimas present in the underlying KPC-KCC interrelations. The consideration

of scale of non-linearity in deterministic KPCs is critical for developing accurate surrogate models which can generate realistic Variation Simulation Analysis (VSA) results in design synthesis tasks such as fixture layout optimization for sheet metal assemblies which require surrogate models of computationally expensive VSA for efficient global optimization within limited time resources. Currently existing surrogate models such as high order polynomial regression, frequently used in design synthesis, cease to address non-linearity in KPC-KCC interrelations without overfitting training samples.

In order to address this problem, this chapter developed *scalable surrogate modelling for deterministic assembly KPCs* based on the following two interlinked methods: (1) Greedy Polynomial Kriging (GPK) which generates acceptably accurate predictions for output-input interrelations having single maxima or minima as well as for those having multiple local maximas and minimas; and, (2) Optimal-Multi Response Adaptive Sampling (O-MRAS) which accelerates the convergence of multiple surrogate models to reduce time required for generating training samples from computationally expensive VSA.

The two main steps in GPK are: (1) Polynomial Feature Selection (PFS) which identifies features for the regression component of GPK models; and, (2) Kernel Optimization (KO) which determines optimal parameters of the correlation or kernel function of GPK models. Both PFS and KO focus on minimization of generalized prediction error of the model to identify features and correlation parameters respectively.

To expedite the convergence of a surrogate model an adaptive sampling method is used to generate design matrix of KCCs to be given as input to VSA. Currently existing adaptive sampling methods focus on single response whereas

sheet metal assemblies in automotive Body-In-White (BIW) manufacturing have multiple KPCs. To address this challenge, O-MRAS combines multiple adaptive samples generated for individual KPCs using a currently existing single-response adaptive sampling criteria. This is achieved by following three steps: (1) generating 'r' individual adaptive samples and merging them in a common design matrix; (2) clustering the common design matrix into 'r' groups; and, (3) selecting a point from each group based on an optimization strategy.

Furthermore, the proposed *scalable surrogate modelling for deterministic assembly KPCs* has been developed in the context of fixture layout optimization for sheet metal assemblies. This has led to the development of a comprehensive methodology of *scalable surrogate model driven fixture layout optimization* which has the following two interlinked approaches: (1) *scalable surrogate modelling for deterministic assembly KPCs* to develop GPK surrogate models of assembly KPCs; and, (2) *optimization of fixture KCCs* which utilizes the GPK surrogate models to determine optimal fixture layout.

Scalable surrogate model driven fixture layout optimization has been demonstrated using case studies on sheet metal assemblies from automotive and aerospace industries.

Acknowledgements

CHAPTER 4

SCALABLE SURROGATE MODEL DRIVEN

JOINING PROCESS PARAMETERS SELECTION

4.1 Overview of the chapter

Not all design synthesis tasks related to automotive BIW production system are supported by *first-principle* based Variation Simulation Analysis (VSA). In such cases, design synthesis tasks addressing optimal characterization of KCCs and KPCs to optimize Key Performance Indicators (KPIs) rely on data generated from physical experiments or in-line measurements taken by sensors. For example, there is a lack of useful and accurate *first-principle* models of all joint KPCs for sheet metal assembly joining made by Remote Laser Welding (RLW) process. Therefore, design synthesis task like joining process parameters selection to determine optimal joining process KCCs and KPCs depend on analysis of data from physical experiments or in-line measurements taken by sensors.

The data on KPCs obtained from experiments or in-line measurements are often subjected to stochastic deviations which can be random homo-skedastic noise due to measurement error or uncontrollable factors or can be KCC-dependent hetero-skedastic variance. Accurate characterization and quantification of the KPC stochasticity is critical for identification of KPC control limits and computation of process acceptance rate. However, currently existing surrogate models of stochastic KPCs, such as 1st and 2nd order polynomial regressions, focus only on homo-skedastic noise. Therefore currently existing surrogate models of stochastic KPCs are not sufficient for addressing the scale of KPC stochasticity which can vary from homo- to hetero-skedasticity.

To address the aforementioned challenge this chapter expands the idea of *scalability for stochasticity* proposed under the framework of *Scalable Design Synthesis* in Chapter 1. *Scalability for stochasticity* requires identification and characterization of underlying homo- and hetero-skedastic behaviour in KPCs from experimental data. This is achieved by developing data-driven *scalable surrogate modelling of homo- and hetero-skedastic KPCs* which provides the following three capabilities:

i. *Developing best fitting homo-skedastic surrogate models of stochastic KPCs* based on minimization of generalized prediction error of the models

ii. *Statistical hypothesis testing to detect hetero-skedasticity* in the best-fitting linear model

iii. *Enhancement of the linear models to characterize hetero-skedasticity* based on minimization of generalized prediction error of the models

Polynomial Feature Selection (PFS) described in the previous chapter is adapted here for building the best-fitting homo- and hetero-skedastic surrogate models of KPCs.

Furthermore, *scalable surrogate modelling for homo- and hetero-skedastic KPCs* is developed in this chapter to address joining process parameters selection for industrial joining processes used in automotive BIW assembly production. The homo- and hetero-skedastic surrogate models of joint KPCs are utilized to conduct *joining process parameters selection* which provides the following two capabilities: (1) Multi-objective optimization of KPIs related to joining process efficiency and process quality; and, (2) Development of process window and computation of process acceptance rates based on homo- and hetero-skedastic surrogate models of joint KPCs.

Overall, the main contribution of this chapter is developing a

comprehensive methodology of _scalable surrogate model driven joining process parameters selection_ based on the following two interlinked approaches:

i. _Scalable surrogate modelling for homo- and hetero-skedastic joint KPCs_

ii. _Joining process parameters selection_ based on homo- and hetero-skedastic surrogate models of joint KPCs.

Figure 4.1 highlights the main approaches involved in the proposed methodology of _scalable surrogate model driven joining process parameters selection_.

The proposed methodology is applied to characterize the RLW process of joining sheet metal assemblies for automotive BIW production. Comparison of results with those obtained from currently existing surrogate models is also presented.
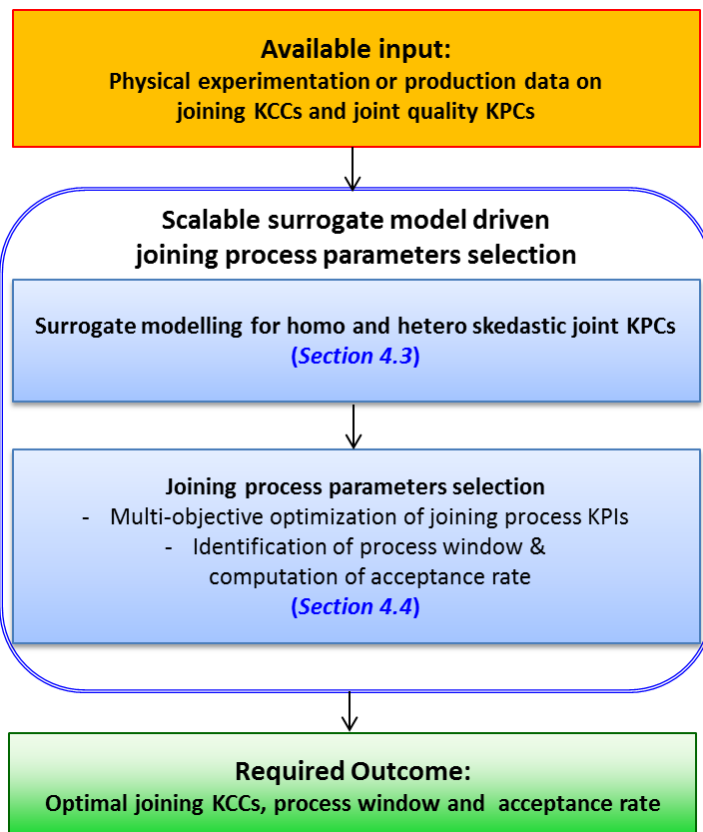
Figure 4.1: Scalable surrogate model driven joining process parameters selection

The rest of the chapter is organized as follows: Section 4.2 outlines the motivation for the research presented in this chapter. Next the methodology of *scalable surrogate modelling for joining process parameters selection* is developed through the following two approaches: (1) *scalable surrogate modelling for homo- and hetero-skedastic joint KPCs*, which is described in Section 4.3; and, (2) *joining process parameters selection*, which is discussed in Section 4.4. This is followed by an industrial case study on RLW joining process for automotive BIW assembly production in Section 4.5. The significance of the results from the case study is also discussed. The chapter ends with a summary of work done in Section 4.6.

4.2   Motivation for the research

An important aspect of BIW assembly production for automotive vehicles is the joining process whereby mating parts in the assembly are permanently linked by mechanical joints such as welds, rivets and others.

Joining technologies such as Resistance Spot Welding (RSW), Self-Piercing Riveting (SPR) etc. have been used and recently Remote Laser Welding (RLW), because of its economic advantages (Bea, et al., 2011), is being implemented for joining in BIW assembly production. Effective and systematic implementation of a new joining process in industrial production requires *joining process parameters selection*. A critical element in addressing the aforementioned two requirements for joining process parameters selection is an analytical model integrating joint KPCs with joining process KCCs.

Several researches have been done on developing surrogate models of joint KPCs in terms of joining process KCCs. The joint KPC surrogate models are trained using data generated through experiments. However, the major limitation of

currently existing surrogate models is the assumption that variance of joint KPCs is due to homo-skedastic measurement error or uncontrollable parameters and is independent of the KCCs. Under the assumption of homo-skedasticity, though KPCs change as functions of KCCs, their variance remains constant over the design space of KCCs. Figure 4.2 shows a homo-skedastic model with constant KPC variance.
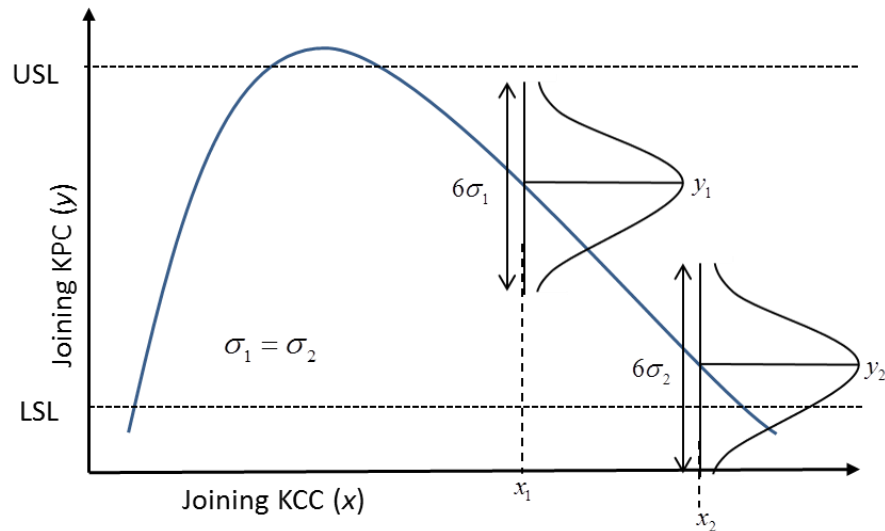
Figure 4.2: Constant variance surrogate model of joining KPC

The major challenge of homo-skedasticity assumption is that it might lead to inaccurate characterization of the process window and computation of acceptance rate. For example, in the homo-skedastic scenario shown in Figure 4.2, acceptance rate is higher at (KCC, KPC)=(x_1, y_1) than at (KCC, KPC)=(x_2, y_2) because KPC=y_1 is further away from the nearest specification limit. However, if the KPC variance is actually hetero-skedastic as shown in Figure 4.3, acceptance rate at (KCC, KPC)=(x_1, y_1) is lower than at (KCC, KPC)=(x_2, y_2) though KPC=y_1 is further away from the nearest specification limit. This is because KPC variance, σ_1 being higher than σ_2 causes higher fallout. Therefore, as illustrated by Figures 4.1 and 4.2, computation of acceptance rate is affected by erroneous characterization of

KPC stochasticity.
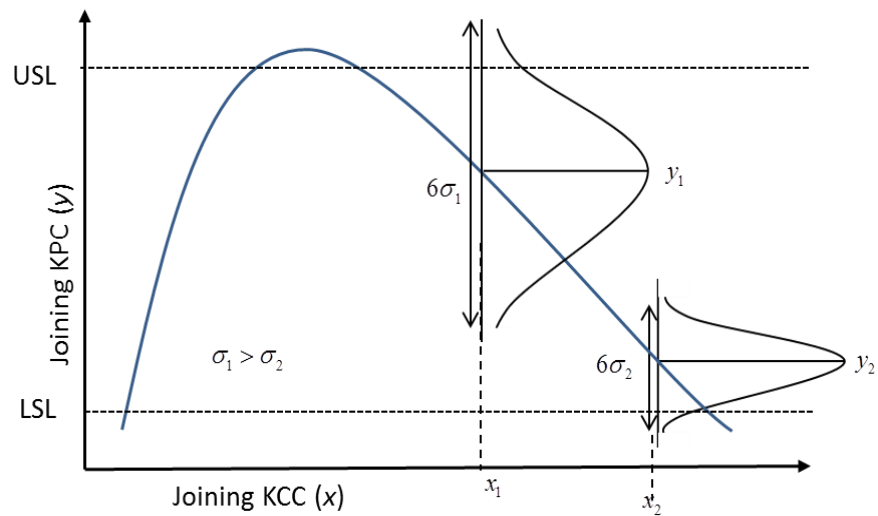
Figure 4.3: Hetero-skedastic surrogate model of joining KPC

Taking into consideration the aforementioned limitation of homo-skedastic models, joining process parameters selection will significantly benefit from a data-driven method which is agnostic to the actual relationship between joining process KCCs and joint KPCs and can address the scale of stochasticity in joint KPCs, which can vary from *homo-* to *hetero-skedasticity*, through data analysis. To address this need, this chapter proposes *scalable surrogate modelling for homo- and hetero-skedastic joint KPCs*.

4.3 Scalable surrogate modelling for homo- and hetero-skedastic joint Key Product Characteristics

The three main steps of scalable surrogate modelling for homo- and hetero-skedastic joint KPCs, as shown in Figure 4.4, are:

Step A – Develop homo-skedastic surrogate model of joint KPC

Step B – Detect hetero-skedasticity via statistical hypothesis testing

Step C – Enhance homo-skedastic surrogate model to characterize hetero-skedasticity

Additionally, the best-fitting surrogate models in *Steps A* and *B* are generated via Polynomial Feature Selection (PFS) method developed in Chapter 3. PFS develops the best-fitting surrogate models of the joint KPCs based on minimization of generalized model error
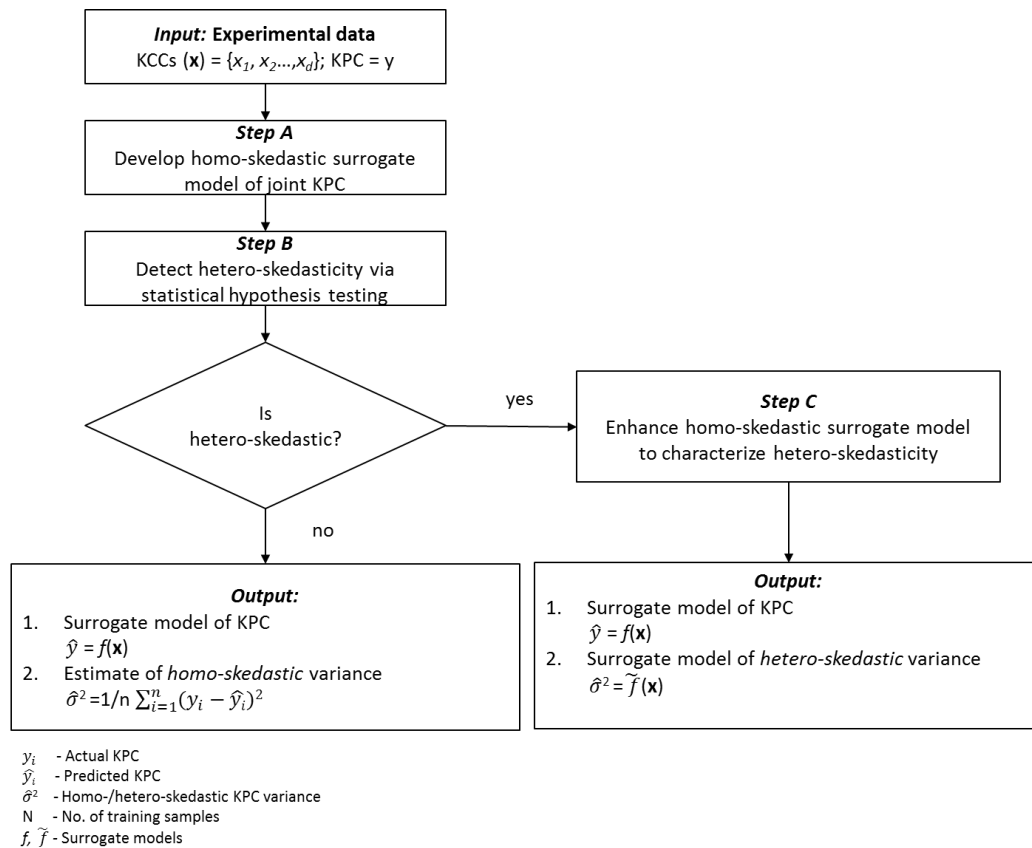
Figure 4.4: Scalable surrogate modelling for homo- and hetero-skedastic joint KPCs

Few notations are introduced below before describing the aforementioned three steps in details.

Notations

x	Set of *'d'* KCCs $\mathbf{x} = \{x_1, x_2, ..., x_d\}$, where x_i is the ith KCC in x representing the ith KCC of joining process
y	Joining process KPC for surrogate modelling
x'	Subset of *'d' '* KCCs $\mathbf{x'} = \{x'_1, x'_2, ..., x'_{d'}\} \in \mathbf{x}$, where x'_i is the ith KCC in subset **x'**
h	Set of *'m'* features or basis functions for the KPC where $\mathbf{h} = \{h_1, h_2, ..., h_m\}$ are derived from the original KCCs (**x**)
f	Surrogate model of the KPC
β	Coefficients of the surrogate model *i.e.* $\boldsymbol{\beta} = \{\beta_0, \beta_1, ..., \beta_m\}$
$\hat{y}$	Estimated KPC from surrogate model *i.e.* $\hat{y} = f(h_1, h_2, ..., h_m) = \beta_0 + \beta_1 h_1 + \beta_2 h_2 + ... + \beta_m h_m$
$\tilde{\mathbf{h}}$	Set of *'$\tilde{m}$'* features or basis functions for the variance of KPC where $\tilde{\mathbf{h}} = \{\tilde{h}_1, \tilde{h}_2, ..., \tilde{h}_{\tilde{m}}\}$ are derived from the original KCCs (**x**)
$\tilde{f}$	Surrogate model of the variance of KPC
$\tilde{\boldsymbol{\beta}}$	Coefficients of the surrogate model *i.e.* $\tilde{\boldsymbol{\beta}} = \{\tilde{\beta}_0, \tilde{\beta}_1, ..., \tilde{\beta}_{\tilde{m}}\}$
$\hat{\sigma}^2$	Estimated variance of KPC from surrogate model *i.e.* $\hat{\sigma}^2 = \tilde{f}(\tilde{h}_1, \tilde{h}_2, ..., \tilde{h}_{\tilde{m}}) = \tilde{\beta}_0 + \tilde{\beta}_1 \tilde{h}_1 + \tilde{\beta}_2 \tilde{h}_2 + ... + \tilde{\beta}_{\tilde{m}} \tilde{h}_{\tilde{m}}$
$y \sim x_i$	~ indicates functional dependency of *y* on x_i.
n	Number of experiments performed
$\mathbf{S}_T$	Training data which is a design matrix of *'n'* observations on *'d+1'* variables (*'d'* KCCs and one KPC): $\mathbf{S}_T = \{\mathbf{x}_i, y_i\}_1^n$
MSE	Mean squared error of the surrogate model *f* measures the discrepancy between actual and predicted values and is calculated as $MSE = \dfrac{1}{n}\sum_{i=1}^{n}(y_i - \hat{y}_i)^2$

The remaining part of this section is organized as follows: Section 4.3.1 describes PFS in the context of joining process KCCs and joint KPCs. Section 4.3.2 describes the *Steps A* to *C* of developing homo- and hetero-skedastic surrogate models of joint KPCs. Section 4.3.3 summarizes the major outputs of the proposed

scalable surrogate modelling of joint KPCs.

4.3.1 Polynomial Feature Selection

In this chapter PFS is used to develop best-fitting surrogate models of joint KPCs. Moreover, when hetero-skedasticity is detected, PFS is also used to develop the best-fitting surrogate model of the hetero-skedastic KPC variance. Best-fitting surrogate models maximize predictive accuracy through minimization of generalized model prediction error on unseen test samples. In this chapter PFS determines optimal polynomial interactions between joining process KCCs $\mathbf{x} = \{x_1, x_2, ..., x_d\}$ to develop the best-fitting surrogate model of joint KPC 'to develop the best-fitting surrogate model of joint KPC 'y'. The PFS algorithm has been developed in Chapter 3. In this chapter PFS has been adapted from Chapter 3 where it has been applied to determine optimal polynomial interactions between fixture related KCCs such as clamp locations to develop best-fitting global model of KPCs such as part-to-part gaps between mating parts of an assembly. For detailed description of the PFS algorithm, the reader is suggested to refer Section 3.5.1.1 of Chapter 3.

4.3.2 Homo- and hetero-skedastic surrogate models of joint KPCs

The three main steps of scalable surrogate modelling (shown in Figure 4.4) to address stochastic behaviour of a joint KPC are described as follows:

***Step A** – Develop homo-skedastic surrogate model of joint KPC*

This step fits the best-fitting surrogate model of the joint KPC assuming that the noise associated with the joint KPC is homo-skedastic noise originating from measurement errors and/or uncontrollable factors. PFS (as described in Section

4.3.1) is applied to identify an optimal polynomial order p^* and set of multiplicative features $\mathbf{h}^* = \{h_1^*, h_2^*, ..., h_{m^*}^*\}$. The homo-skedastic model is developed based on the features identified by PFS and can be represented as follows

$$\hat{y} = \beta_0^* + \beta_1^* h_1^* + \beta_2^* h_2^* + ... + \beta_m^* h_{m^*}^* \tag{4.3}$$

where $\boldsymbol{\beta}^* = \{\beta_0^*, \beta_2^*, ..., \beta_{m^*}^*\}$ are coefficients of the regression model and determined through the method of least squares. Based on the homo-skedastic model, deviances between the actual and predicted KPC can be calculated as follows:

$$\varepsilon_i = y_i - \hat{y}_i \quad (i = 1, 2, ...n) \tag{4.4}$$

where 'n' is the number of samples in the training data, y_i and $\hat{y}_i = \beta_0^* + \beta_1^* h_{i1}^* + \beta_2^* h_{i2}^* + ... + \beta_m^* h_{im^*}^*$ are the actual and predicted KPC respectively for the ith sample.

***Step B** – Detect hetero-skedasticity via statistical hypothesis testing*

In this step, hetero-skedastic behaviour of the KPC is assessed by the Breusch-Pagan (BP) test (Koenker, 1981). The BP test detects hetero-skedasticity in the KPC by assessing functional dependency between the variance of the KPC and the features ($\mathbf{h}^*$) used to develop the homo-skedastic model of the KPC shown in Eq. (4.3). If the actual variance at the 'n' design points of the experiment are $\sigma_1^2, \sigma_2^2 ... \sigma_i^2, ..., \sigma_n^2$ then hetero-skedasticity as a function of $\mathbf{h}^*$ can be represented as

$$\sigma_i^2 = \tilde{\beta}_0 + \tilde{\beta}_1 h_{i1}^* + \tilde{\beta}_2 h_{i2}^* + ... + \tilde{\beta}_{m^*} h_{im^*}^* \tag{4.5}$$

In absence of information about the actual variance at the 'n' training points, the least squares residuals as obtained from Eq. (4.4) are used as estimates $\hat{\sigma}_i^2 = \varepsilon_i^2$ and a model of the hetero-skedastic variance is developed as follows

$$\hat{\varepsilon}_i^2 = \tilde{\beta}_0 + \tilde{\beta}_1 h_{i1}^* + \tilde{\beta}_2 h_{i2}^* + ... + \tilde{\beta}_{m^*} h_{im^*}^* \tag{4.6}$$

The null hypothesis (H₀) of the BP test of hetero-skedasticity states

$$H_0 : \tilde{\beta}_1 = \tilde{\beta}_2 = ... = \tilde{\beta}_{m^*} = 0 \tag{4.7}$$

Therefore the alternate hypothesis (H₁) states:

$$H_1 : \tilde{\beta}_1 \neq \tilde{\beta}_2 \neq ... \neq \tilde{\beta}_{m^*} \neq 0 \tag{4.8}$$

The coefficients ($\tilde{\beta}$) of the model in Eq. (4.6) is determined using the method of least squares and the degree of determination of the fitted model is calculated as follows:

$$R^2_{\hat{\sigma}^2} = 1 - \frac{(\varepsilon_i^2 - \hat{\varepsilon}_i^2)^2}{(\varepsilon_i^2 - \frac{1}{n}\sum_{i=1}^{n}\varepsilon_i^2)^2} \tag{4.9}$$

where the estimated residual is $\hat{\varepsilon}_i^2 = \tilde{\beta}_0 + \tilde{\beta}_1 h_{i1}^* + \tilde{\beta}_2 h_{i2}^* + ... + \tilde{\beta}_{m^*} h_{im^*}^*$. The test statistic of the BP test is $nR^2_{\hat{\sigma}^2}$, which under the assumption of the null hypothesis follows Chi-square distribution with 'm^*' degrees of freedom $i.e.\ nR^2_{\hat{\sigma}^2} \sim \chi^2_{m^*}$. For a chosen level of statistical significance 'α', H_0 is rejected if the p-value or the probability ($t \geq nR^2_{\hat{\sigma}^2}$) is less than or equal to α, where $t \sim \chi^2_{m^*}$. In case H_0 is true, hetero-skedasticity in the observed data for KPC y is not detected and final surrogate model of the joint KPC is given as

$$\hat{y} = \tilde{\beta}_0^* + \tilde{\beta}_1^* h_1^* + \tilde{\beta}_2^* h_2^* + ... + \tilde{\beta}_{m^*}^* h_{m^*}^* \tag{4.10}$$

Eq. (4.10) also represents the estimated conditional mean of the KPC $\hat{\mu}_x$ as a function of the joining process KCCs. KPC variance is constant over the design space of the KCCs and is estimated from the residuals obtained in Eq. (4.4) as follows

$$\hat{\sigma}^2 = \frac{1}{n}\sum_{i=1}^{n}\varepsilon_i^2 \tag{4.11}$$

For joining process parameter optimization and process window selection, the joint KPC is considered to be normally distributed as $y \sim N(\hat{\mu}_{\mathbf{x}}, \hat{\sigma}^2)$, which has a *KCC-dependent* mean $\hat{\mu}_{\mathbf{x}}$ and *constant* variance $\hat{\sigma}^2$.

If H_0 is rejected at the chosen level of significance 'α', Step C is performed to update the surrogate model of the KPC with hetero-skedasticity and to develop a surrogate model for the hetero-skedastic KPC variance using PFS.

***Step 3**: Enhance homo-skedastic surrogate models to characterize hetero-skedasticity*

The homo-skedastic model of the KPC obtained in Eq. (4.3) assumes that the residuals ε_i for $i = 1, 2, ..., n$ are independent and identically distributed Gaussian white noise and hence can be represented $\varepsilon_i \sim N(0, \sigma^2)$. Under this assumption, the least squares estimate of the model coefficients $\boldsymbol{\beta}^* = \{\beta_0^*, \beta_2^*, ..., \beta_{m^*}^*\}$ is given by

$$\boldsymbol{\beta}^* = (H^T H)^{-1} H^T \mathbf{y} \tag{4.12}$$

where H is $n \times (m^* + 1)$ feature matrix derived from the original design matrix of KCCs and $\mathbf{y}$ is $n \times 1$ vector of observations on KPC y. However, if BP test in *Step B* detects presence of hetero-skedasticity, the normal distribution of the residuals needs to be modified as $\varepsilon_i \sim N(0, \sigma_i^2)$ where σ_i^2 is the variance at the ith design point. Under this condition, the model in Eq. (4.3) can be transformed as,

$$\frac{\hat{y}_i}{\sigma_i} = \frac{1}{\sigma_i}(\beta_0^* + \beta_1^* h_{i1}^* + \beta_2^* h_{i2}^* + ... + \beta_m^* h_{im}^*) + \frac{\varepsilon_i}{\sigma_i}$$

or
$$\hat{y}_i = \widehat{\beta}^T \widehat{\mathbf{h}}_i + \widehat{\varepsilon}_i \tag{4.13}$$

The variance of the transformed residuals is $Var(\widehat{\varepsilon}_i) = 1$ and therefore the transformed model is homo-skedastic. The data for the transformed model can be

represented as $\hat{\mathbf{y}} = W\mathbf{y}$ and $\hat{H} = WH$ where W is a $n \times n$ weight matrix as shown in Eq. (4.14).

$$W = \begin{bmatrix} \sqrt{w_1} & \cdots & 0 \\ \vdots & \ddots & \vdots \\ 0 & \cdots & \sqrt{w_n} \end{bmatrix}$$ (4.14)

where $w_i = 1 / \sigma_i^2$. In absence of information about the actual variance σ_i^2 at the ith design point, the residuals of the initial homo-skedastic model can be used as White consistent estimator $\hat{\sigma}_i^2 = \varepsilon_i^2$ (White, 1980). The coefficients $\boldsymbol{\beta}^*$ are now updated using the weighted data $\hat{H}$ and $\hat{\mathbf{y}}$ as follows

$$\hat{\boldsymbol{\beta}}^* = (\hat{H}^T \hat{H})^{-1} \hat{H}^T \mathbf{y}$$

or $$\hat{\boldsymbol{\beta}}^* = \left((WH)^T (WH) \right)^{-1} (WH)^T W\mathbf{y}$$

which can be simplified as follows

$$\hat{\boldsymbol{\beta}}^* = (H^T WH)^{-1} H^T W\mathbf{y}$$ (4.15)

Using the new coefficients, the surrogate model of the KPC is updated as follows

$$\hat{y} = \hat{\beta}_0^* + \hat{\beta}_1^* h_1^* + \hat{\beta}_2^* h_2^* + ... + \hat{\beta}_m^* h_m^*$$ (4.16)

As the variance of the KPC has been found to be hetero-skedastic and dependent on the KCCs, this step also develops the best-fitting surrogate model of the hetero-skedastic KPC variance. PFS (as described in Section 4.3.1) is applied to identify an optimal polynomial order '$\tilde{p}^*$' and set of multiplicative features $\tilde{\mathbf{h}}^*$. The model developed for the KPC variance through PFS is represented as

$$\hat{\sigma}^2 = \tilde{\beta}_0^* + \tilde{\beta}_1^* \tilde{h}_1^* + \tilde{\beta}_2^* \tilde{h}_2^* + ... + \tilde{\beta}_m^* \tilde{h}_m^*$$ (4.17)

Overall, the output from *Step C* are surrogate models of *KCC-dependent* mean ($\hat{\mu}_\mathbf{x}$) and *KCC-dependent* variance ($\hat{\sigma}_\mathbf{x}^2$) of the hetero-skedastic joint KPC as functions of

the process KCCs. For joining process parameter optimization and process window selection, the hetero-skedastic KPC is considered to be normally distributed as $y \sim N(\hat{\mu}_{\mathbf{x}}, \hat{\sigma}_{\mathbf{x}}^2)$, which has a *KCC-dependent* mean $\hat{\mu}_{\mathbf{x}}$ and *KCC-dependent* variance $\hat{\sigma}_{\mathbf{x}}^2$.

4.4 Joining process parameters selection

Joining process parameters selection focuses on the following two aspects: (1) multi-objective optimization to optimize process KPIs subject to design tolerances on joint KPCs and joining process KCCs; and, (2) identification of process window in the KCC design space and computation of process acceptance rate.

4.4.1 Multi-objective optimization of joining process Key Performance Indicators

Key Performance Indicators (KPIs) related to the joining process can be classified into the following two types:

i. *KPIs related to process efficiency* − The efficiency of a joining process can be evaluated based on KPIs such as cycle time, throughput, number of units produced per shift and others. KPIs related to process efficiency are closely related to joining process KCCs. For example, in case of RLW, welding cycle time can be expressed as a function of the speed of welding, which is a critical KCC affecting joining process efficiency related KPIs such as cycle time. In general, '*PE*' process efficiency related KPIs $\mathbf{\Phi}_{KCC}(\mathbf{x}) = \left\{ \begin{array}{c} \Phi_{KCC}^{(1)}(\mathbf{x}) \\ \Phi_{KCC}^{(2)}(\mathbf{x}) \\ \vdots \\ \Phi_{KCC}^{(PE)}(\mathbf{x}) \end{array} \right\}$ can be

represented as functions of the KCCs $\mathbf{x} = \{x_1, x_2, ..., x_d\}$.

ii. *KPIs related to process quality* – Joint quality is determined by joint KPCs such as penetration, weld bead width, weld surface concavities and others which must satisfy pre-defined design tolerances. To produce acceptable joint quality, joining process KCCs must be within process window (discussed in detail in Section 4.4.2). However, even though KCCs are within process window, KPCs might violate required design tolerances because of their variance which can be KCC-dependent hetero-skedastic variance. Under these conditions, it important to identify KCCs which optimizes process quality related KPIs such as quality loss due to hetero-skedastic KPC variance. In general, '*PQ*' process quality

related KPIs $\mathbf{\Phi}_{\mathrm{KPC}}(\hat{\mathbf{\mu}}_\mathbf{x}, \hat{\mathbf{\sigma}}_\mathbf{x}) = \begin{Bmatrix} \Phi_{\mathrm{KPC}}^{(1)}(\hat{\mathbf{\mu}}_\mathbf{x}, \hat{\mathbf{\sigma}}_\mathbf{x}) \\ \Phi_{\mathrm{KPC}}^{(2)}(\hat{\mathbf{\mu}}_\mathbf{x}, \hat{\mathbf{\sigma}}_\mathbf{x}) \\ \vdots \\ \Phi_{\mathrm{KPC}}^{(PQ)}(\hat{\mathbf{\mu}}_\mathbf{x}, \hat{\mathbf{\sigma}}_\mathbf{x}) \end{Bmatrix}$ can be represented as functions of

KCC-dependent mean ($\hat{\mathbf{\mu}}_\mathbf{x}$) and variance ($\hat{\mathbf{\sigma}}_\mathbf{x}$) of the KPCs where $\hat{\mathbf{\mu}}_\mathbf{x}$ and $\hat{\mathbf{\sigma}}_\mathbf{x}$ represent '*r*' KCC-dependent mean and variance of '*r*' joint KPCs.

The multi-objective optimization to optimize *process-efficiency* and *process quality* related KPIs is formalized as follows

$$\mathbf{x}^* = \underset{\mathbf{x} \in D}{\arg\min} \begin{Bmatrix} \mathbf{\Phi}_{\mathrm{KCC}}(\mathbf{x}) \\ \mathbf{\Phi}_{\mathrm{KPC}}(\hat{\mathbf{\mu}}_\mathbf{x}, \hat{\mathbf{\sigma}}_\mathbf{x}) \end{Bmatrix} \text{ subject to } \mathbf{y} \leq \mathbf{\psi}_{\mathrm{KPC}} \text{ and } \mathbf{x} \leq \mathbf{\psi}_{\mathrm{KCC}} \quad (4.18)$$

where *D* is *d*-dimensional design space of KCCs and $\mathbf{\psi}_{\mathrm{KPC}}$ represent design tolerances of joint KPCs. The design tolerances define the range for KPCs which make a joint of acceptable quality. $\mathbf{\psi}_{\mathrm{KCC}}$ are operating limits on joining process KCCs which also define the boundaries of the KCC design space *D*. The optimization in Eq. (4.18) can be solved by meta-heuristic search algorithms such as Genetic Algorithms.

4.4.2 Identification of process window and computation of acceptance rate

The process window defines a region in the KCC design space where joining process parameters will produce acceptable joints within required design tolerances $\mathbf{\psi}_{KPC}$ for 'r' KPCs. A design tolerance can be one of the following two types (1) *one-sided* (lesser or greater than a limit); or, (2) *bounded* (between specified lower and upper limits). The KCC process window is derived by mapping the KPC design tolerances to the KCC design space D via the surrogate models linking KPCs with KCCs. Moreover, KPC design tolerances and surrogate models can also be used to compute the acceptance rate or probability of making an acceptable joint at any point $\mathbf{x}$ inside the KCC process window.

This chapter proposes the following two types of analyses for the identification of the process window and the computation of acceptance rate:

i. *Mean only analysis* – In this case only the KPC mean is taken into consideration to derive the process window in the KCC design space and compute acceptance rate. In this type of analysis homo- or hetero-skedastic KPC variance is not used for deriving the process window and computing the acceptance rate. For KPC 'y' with a *one-sided* design tolerance $y \leq \psi_{max}$, the KCC process window (*PW*) is determined as follows

$$PW = \{\mathbf{x} \in D \mid \hat{\mu}_{\mathbf{x}} \leq \psi_{max}\} \tag{4.19}$$

where $\hat{\mu}_{\mathbf{x}} = f(\mathbf{x})$ is the KCC-dependent mean of the KPC and $\mid$ indicates 'such that' in set theory notation. In this case, the acceptance rate (*AR*) at a point $\mathbf{x}$ inside the process window can be computed as

$$AR = Prob(0 \leq y \leq \psi_{max}) \tag{4.20}$$

here KPC 'y' follows a normal distribution $y \sim N(\mu, \hat{\sigma}_{\mathbf{x}})$. For homo-skedastic

KPCs, the variance $\hat{\sigma}_{\mathbf{x}}$ is constant $\hat{\sigma}^2$ whereas for hetero-skedastic KPCs, the variance $\hat{\sigma}_{\mathbf{x}}$ is KCC-dependent function $\tilde{f}(\mathbf{x})$.

ii. *Worst-case analysis* – Joint KPCs exhibit stochastic variation which can be attributed to either measurement error (homo-skedastic) or systematic deviance (hetero-skedastic) due to complex underlying interrelations between joint KPCs and joining process KCCs. The worst-case analysis takes into consideration the variation of the KPC within '$\pm q$' sigma levels where 'q' is specified by the user. When the KPC variance is hetero-skedastic, the process window is determined not only by the design constraints on the KPCs but also by the KCC-dependent variance. As a result, the acceptance rate varies over the process window as a function of the *KCC-dependent* hetero-skedastic variance hence leading to a *stochastic* process window. For a KPC 'y' with *one-sided* design tolerance $y \leq \psi_{max}$, the KCC process window (PW) and acceptance rate (AR) at point $\mathbf{x}$ inside the process window are determined as shown in Eq. (4.21) and Eq. (4.22), respectively.

$$PW = \{\mathbf{x} \in D \,|\, \hat{\mu}_{\mathbf{x}} + q\hat{\sigma}_{\mathbf{x}} \leq \psi_{max}\} \tag{4.21}$$

$$AR = Prob(0 \leq y \leq \psi_{max}) \tag{4.22}$$

where KPC 'y' follows normal distribution $y \sim N(\mu, \hat{\sigma}_{\mathbf{x}})$ which a constant homo-skedastic variance $\hat{\sigma}_{\mathbf{x}} = \hat{\sigma}^2$ or a KCC-dependent hetero-skedastic variance $\hat{\sigma}_{\mathbf{x}} = \tilde{f}(\mathbf{x})$.

Table 4.1 enumerates all possible cases for '*mean only*' and '*worst-case*' analyses of the process window and computation of the acceptance rate for each of the two types of design tolerances (*one-sided* and *bounded*) with respect to a single joint KPC 'y'.

Table 4.1: Process window and probability of acceptable joint with respect to KPC '*y*'

Analyses of process window ⟋ Design Tolerance		*Mean only* analysis		*Worst-case* analysis at '$\pm q$' sigma levels	
		Process Window (*PW*)	Acceptance Rate (*AR*)	Process Window (*PW*)	Acceptance Rate (*AR*)
One sided	*Lesser than* $y \le \psi_{max}$	$\{\mathbf{x} \in D \mid^* \hat{\mu}_{\mathbf{x}} \le \psi_{max}\}$	$Prob(0 \le y^{***} \le \psi_{max})$	$\hat{\mu}_{\mathbf{x}} + q\hat{\sigma}_{\mathbf{x}} \le \psi_{max}$	$Prob(0 \le y \le \psi_{max})$
	Greater than $\psi_{min} \ge y$	$\{\mathbf{x} \in D \mid \hat{\mu}_{\mathbf{x}} \ge \psi_{min}\}$	$Prob(y \ge \psi_{min})$	$\hat{\mu}_{\mathbf{x}} - q\hat{\sigma}_{\mathbf{x}} \ge \psi_{min}$	$Prob(y \ge \psi_{min})$
Bounded	$\psi_{min} \le y \le \psi_{max}$	$\{\mathbf{x} \in D \mid \psi_{min} \le \hat{\mu}_{\mathbf{x}} \le \psi_{max}\}$	$Prob(\psi_{min} \le y \le \psi_{max})$	$\{\mathbf{x} \in D \mid \hat{\mu}_{\mathbf{x}} + q\hat{\sigma}_{\mathbf{x}} \le \psi_{max}\}$ $\cap^{**}$ $\{\mathbf{x} \in D \mid \hat{\mu}_{\mathbf{x}} - q\hat{\sigma}_{\mathbf{x}} \ge \psi_{min}\}$	$Prob(\psi_{min} \le y \le \psi_{max})$

* | indicates 'such that' in set theory notation; ** $\cap$ indicates intersection of two sets; *** $y \sim N(\mu, \hat{\sigma}_{\mathbf{x}})$

The quality of a joint is assessed by multiple joint KPCs $\mathbf{y} = \{y_1, y_2, ..., y_j, ...y_r\}$. For KPC '$j$', where $j = 1, 2, ..., r$, the identification of the process window (PW_j) and the computation of the acceptance rate (AR_j) is done using the guidelines given in Table 4.1. The final process window and acceptance rate, taking into consideration all KPCs, is obtained from Eq. (4.23) and Eq. (4.24) respectively.

$$PW = \bigcap_{j=1}^{r} PW_j \qquad (4.23)$$

$$AR = \prod_{j=1}^{r} AR_j \qquad (4.24)$$

It is noteworthy that the final process window (PW) is an intersection of the individual process windows PW_j and the final acceptance rate AR is a product of the individual acceptance rates AR_j where $j = \{1, 2, ..., r\}$.

4.5 Case study

In this section, the proposed methodology of scalable surrogate model driven joining process parameters selection is applied to characterize the KCCs and KPCs of the RLW joining process for automotive BIW assembly production. Starting from experimental data as shown in Figure 4.1, full-factorial design of experiment for the joining process KPCs is developed to conduct physical experimentation. For each experiment, the joint KPCs are measured by microscopic imaging.

This section is organized in the following three subsections: Section 4.5.1 describes the joint KPCs, joining process KCCs and experimental setup related to the RLW case study. Next, the scalable surrogate model driven joining process

parameters selection is demonstrated in two parts. Firstly, in Section 4.5.2, a step by step demonstration of the scalable surrogate modelling of homo- and hetero-skedastic joint KPCs is presented based on one of the joint KPCs. This subsection also summarizes the results of the surrogate modelling for all the other KPCs. Next, Section 4.5.3 utilizes the surrogate models of the joint KPCs to conduct the joining parameters selection in the following two parts: (1) optimization of the joining process KPIs; and (2) analyses of the process window and computation of acceptance rate.

4.5.1 Case study description and experimental setup

In RLW for BIW assembly production, the welding between two mating parts of galvanized steel sheet metal assembly is made in the lap joint configuration, shown in Figure 4.5. However, contrary to a conventional lap joint, a minimum gap of 0.05 mm has to be maintained between the mating parts being welded to allow zinc vapours to escape. The requirement for minimum gap of 0.05 mm between the mating parts is critical for RLW because sheet metal panels, being made of galvanized steel, have outer coating of zinc which evaporates during welding and non-removal of zinc vapours creates porosity and cracks in the weld. The minimum gap is achieved by creating humps or dimples on the mating surfaces by dimpling process (Gu, 2010).

Moreover, the maximum gap between mating parts which allows formation of a weld is 0.40 mm. If, due to geometric variations of the mating sheet metal parts, the gap is more than 0.40 mm at the weld locations, fixture clamps are used to achieve a smaller gap. Chapter 3 has discussed fixture layout optimization for sheet metal assemblies to maintain gaps between mating parts within specific limits.
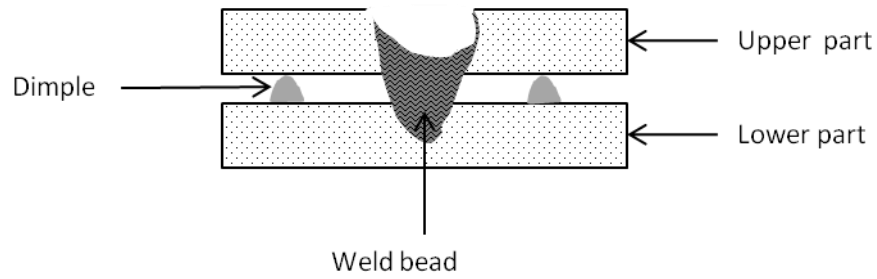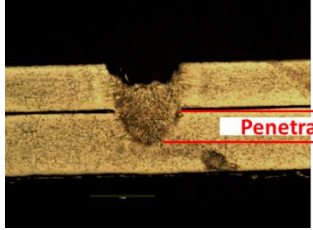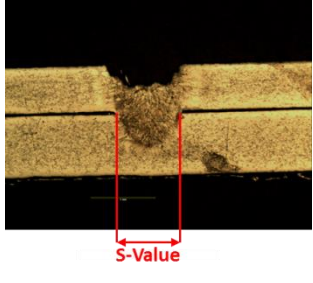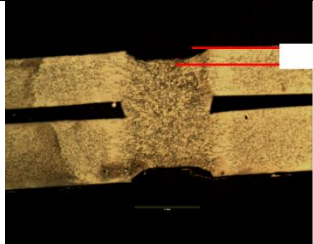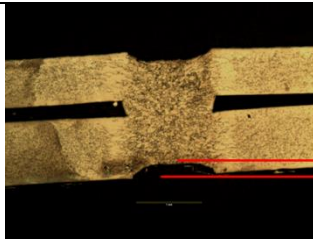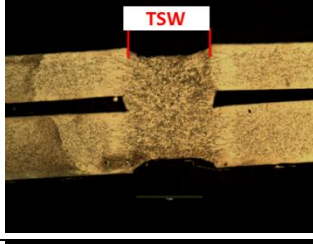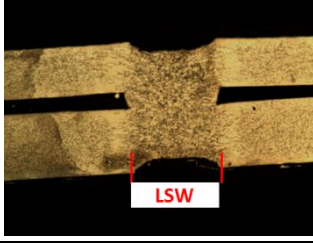
Figure 4.5: Cross-sectional view of lap joint with gap between welded parts

An extensive research has been done in the past on developing *first-principle* models for KPCs and KCCs of laser welding process in lap joint and other configurations. However, there is lack of accurate *first-principle* models for the specific case of making a lap joint by laser welding where there is a gap between welded parts. Therefore, data-driven surrogate modelling has been proposed in this chapter to develop analytical functions integrating RLW joint KPCs with RLW process KCCs.

The following joint quality KPCs are taken into consideration to determine quality of welds made by RLW as suggested by Ford (2010): (1) penetration; (2) interface width (s-value); (3) Top Surface Concavity (TSC); (4) Bottom Surface Concavity (BSC); (5) Top Seam Width (TSW); and, (6) Bottom Seam Width (BSW). The different KPCs and their design tolerances are shown in Table 4.2. Thickness of the lower and upper parts involved in the welding process are denoted as T_{lower} and T_{upper} respectively.

Table 4.2: Weld quality KPCs for RLW joining

Weld KPCs (y)	Design Constraints	Micro-section image
Penetration	$0.3T_{lower} \leq y \leq T_{lower}$	
Interface width (S-Value)	$y \geq 0.9 \min(T_{lower}, T_{upper})$	
Top surface concavity (TSC)	$y \leq 0.5T_{upper}$	
Bottom Surface Concavity (BSC)	$y \leq 0.5T_{lower}$	
Top seam width (TSW)	NA	
Lower seam width (LSW)	$y \leq T_{lower}$	

The KPCs related to weld quality produced by RLW are briefly

explained as follows. Weld bead '*penetration*' directly affects mechanical strength of the weld. According to ANSI/American Welding Society (ANSI/American Welding Society, 1989) standards, '*penetration*' is defined as the distance the weld extends only in the lower part. Several researches relate weld strength to weld interface width, also referred as s-value (Benyounis, *et al.*, 2005). '*Top surface concavity*' (TSC) is the depression of the weld's top surface that extends below the top surface of the upper sheet (ANSI/American Welding Society, 1989). TSC reduces '*s-value*' and mechanical strength of the weld. Similarly, '*bottom surface concavity*' (BSC) also reduces mechanical strength of the weld

Additionally, '*top surface seam width*' (TSW) and '*lower surface seam width*' (LSW) are also analyzed in this study as both of these KPCs are related to aesthetics of the weld bead.

In RLW process, KCCs which affect the joint KPCs are laser power, welding speed, part-to-part gap, upper material thickness and lower material thickness. Table 4.3 presents full-specification of the experimental setup. The objective of this research is to study the effect of welding speed and part-to-part gap (KCCs) on the joint KPCs. Variations in parameters such as laser source power, material thicknesses (upper and lower) are assumed to contribute to random noise in the KPCs.

Table 4.3: Experimental setup for study of KPCs and KCCs in RLW joining process

Parameters	Allowable Value	Controllable
Weld bead length (L_s)	18.0 mm	NA (constant)
Lower thickness (ψ_{lower})	1.0 ± 0.016 mm	No
Upper thickness (ψ_{upper})	0.75 ± 0.04 mm	No
Laser power (P)	2.3 ± 0.0078 kW	No
Welding speed (s)	$[1.0 \div 4.0]$ m/min	Yes
Part-to-part gap (g)	$[0.05 \div 0.4]$ mm	Yes

Experiments were performed on 12 cm × 4 cm overlapping metal strips, known as coupons, having same alloy and thickness specifications as the sheet metal parts of the actual assembly. Transverse linear welds of 18 mm are welded by RLW on the coupons in lap joint configuration. Gap between the welded parts is created using metal strips of required thickness. Figure 4.6 shows an RLW weld made on overlapping coupons.

Figure 4.6: Transverse linear weld by RLW on overlapping coupons

The operating limit of welding speed (s) is [1.0 ÷ 4.0] m/min and that of part-to-part gap (g) is [0.05 ÷ 0.4] mm. Based on the operating limits of welding speed and part-to-part gaps, design space *D* for the KCCs is generated and a full factorial design of experiments is setup with four levels of welding speed (1, 2, 3 and 4 m/min) and seven levels of part-to-part gap (0.05, 0.1, 0.15, 0.2, 0.25, 0.30, 0.4 mm). Two replications are performed for each combination of speed and gap. Table 4.4 and 4.5 presents the micro-section images of the weld beads for experiments in replications 1 and 2, respectively.

Table 4.4: Micro-section images of RLW stitches in replication 1

Rep. 1		Gap [mm]						
		0.05	0.1	0.15	0.2	0.25	0.3	0.4
Speed [m/min]	1.0							
	2.0							
	3.0							
	4.0							No WELD

Table 4.5: Micro-section images of RLW stitches in replication 2

Rep. 2		Gap [mm]						
		0.05	0.1	0.15	0.2	0.25	0.3	0.4
Speed [m/min]	1.0							
	2.0	NA						
	3.0							
	4.0							No WELD

For each experiment, post-processing of the weld is conducted to measure the six KPCs listed in Table 4.2. A cross-sectional cut at 9mm is made across the weld bead (as illustrated in Figure 4.7).
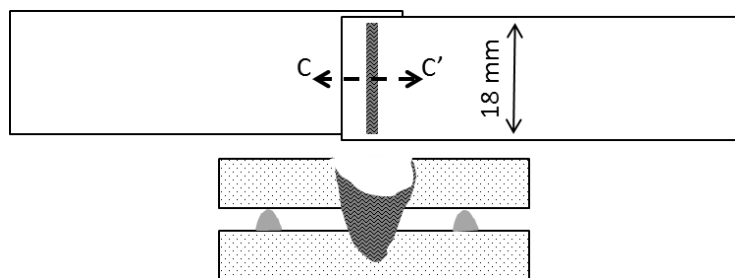
Figure 4.7: Cross-section cut of RLW stitch for measurement of KPCs

161

The cut samples are subjected to metallographic inspection and then analysed using an optical microscope attached to a camera. Figure 4.8 shows an image generated during the post-processing of the cut samples. Initially, 56 experiments (28 sets and 2 replications per set) are performed. 3 experiments are rejected due lack of weld formation. Therefore, *n*=53 experiments are used for analyses in this case study.
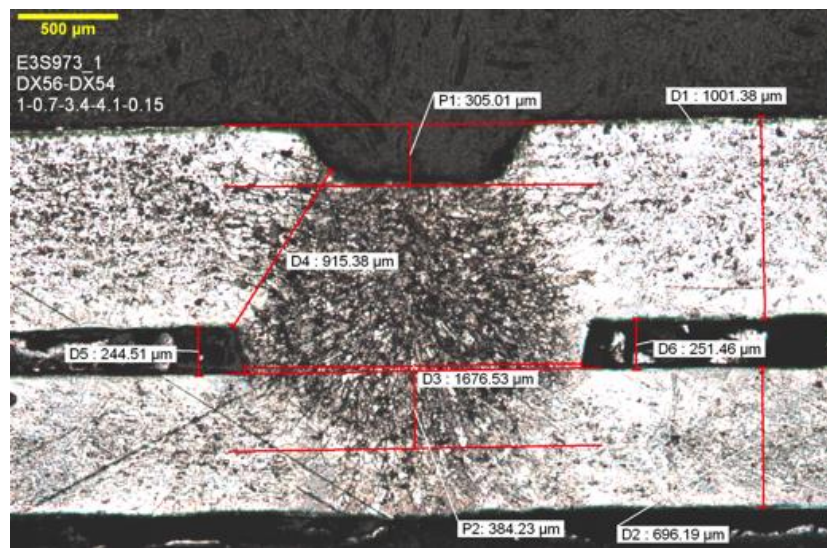
Figure 4.8: Micro-section image with measurements of KPCs

4.5.2 Scalable surrogate modelling for homo- and hetero-skedastic joint KPCs

This section demonstrates the three steps of scalable surrogate modelling with respect to KPC '*penetration*'. A summary of results for all the other KPCs is also given. The three steps of scalable surrogate modelling are described as follows:

Step A *– Develop homo-skedastic surrogate model of joint KPC*

Polynomial Feature Selection (PFS) is ran to determine optimal polynomial order (p^*) and features ($\mathbf{h}^*$) for '*penetration*'. Initially the algorithm sets $\mathbf{h}^* = \varnothing$. Multiplicative features from polynomial of order p=1,2,3… and so on

are iteratively added to $\mathbf{h}^*$ based on reduction of cross validation (CV) mean squared error (MSE) $\xi(\mathbf{h}^*)$, which is estimated by 5 fold cross-validation. During iterations over $p=1,2,3\ldots$, the '*goodness*' of the current polynomial order '*p*' is $\xi(p)$, which is the same as $\xi(\mathbf{h}^*)$, where $\mathbf{h}^*$ are the features selected till the current polynomial order. The algorithm stops if $\dfrac{\xi(p)-\xi(p-1)}{\xi(p)}\times100\le\delta$, where $\delta=1\%$ is a user-defined convergence tolerance. Figure 4.9 shows the CV MSE ($\xi(\mathbf{h}^*)$) obtained for polynomial order $p=1,2,3$ and 4. The plot in Figure 4.10 shows the percentage drop in CV MSE over increasing the order of the polynomial. In this case the algorithm stops after $p=4$ as no further reduction of CV MSE is observed. Table 4.6 presents a summary of the selected features $\mathbf{h}^*$.
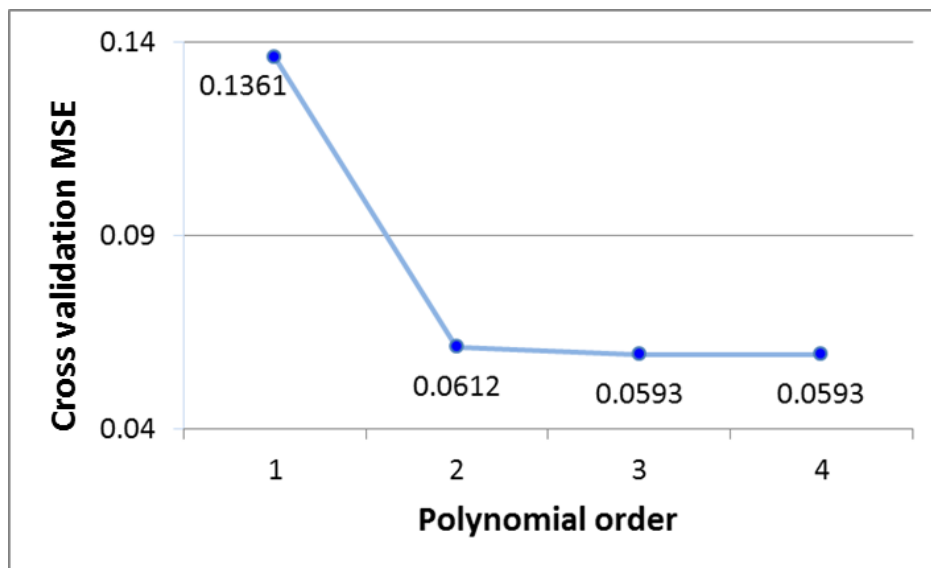
Figure 4.9: Drop in cross validation mean squared error during polynomial feature selection
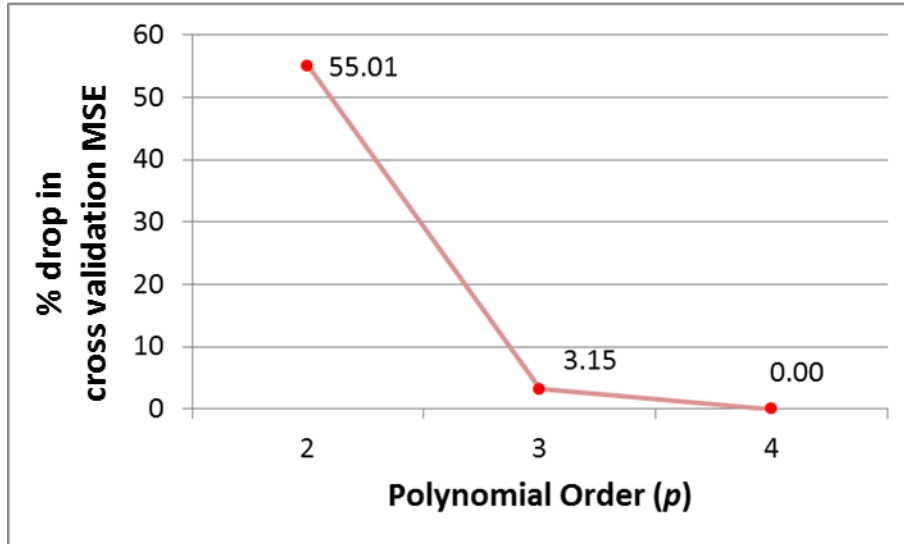
Figure 4.10: % drop in cross-validation mean squared error during polynomial feature selection

Table 4.6: Summary of features selected for penetration

Selected features (h_j)	Regression coefficient (θ_j)	Coefficient p-value prob ($\theta_j = 0$)
S	0.77165	4.33e-10
s^2	-0.17701	7.18e-12
g^3	-3.19781	0.00472

The homo-skedastic surrogate model fitted for '*penetration*' is given in Eq. (4.25).

$$\hat{\mu}_{penetration}(s, g) = 0.1206 + 0.7717s - 0.1770s^2 - 3.1978g^3 \qquad (4.25)$$

The coefficient of determination (R^2) of the surrogate model in Eq. (4.25) is 0.7078. At this stage the surrogate model is fitted assuming that it is homo-skedastic and therefore an estimate of the constant variance of penetration is calculated from the residuals of the fitted model. The estimated constant variance is $\hat{\sigma}^2_{penetration} = 0.0188$. Table 4.7 summarizes the results of *Step A* for all six welding KPCs addressed in this case study.

Table 4.7: Summary of homo-skedastic surrogate models of joint KPCs

Weld KPC	Feature selected (h_j)	Regression coefficient (β_j)	Coefficient p-value prob($\beta_j = 0$)	R^2	Surrogate model of KPC mean ($\hat{\mu}_y$) [mm]	Constant homoscedastic KPC variance ($\hat{\sigma}_y^2$) [mm^2]
Penetration	S	0.77165	4.33e-10	0.7078	$\hat{\mu}_{penetration} = 0.1206 + 0.7717s$ $-0.1770s^2 - 3.1978g^3$	0.0188
	s^2	-0.17701	7.18e-12			
	g^3	-3.19781	0.00472			
S-Value	S	-1.1380	1.50e-10	0.8531	$\hat{\mu}_{s-value} = 2.6596 - 1.1380s$ $+3.9703g + 0.1576s^2$ $-6.4457g^2$	0.0366
	G	3.9703	0.0006			
	s^2	0.1576	8.32e-07			
	g^2	-6.4457	0.0112			
TSC	g^2s	0.9205	1.13e-10	0.568	$\hat{\mu}_{tsc} = 0.1356 + 0.9205g^2s$	0.0082
BSC	S	-0.1654	4.41e-08	0.73	$\hat{\mu}_{bsc} = 0.5045 - 0.1654s$ $+0.0006s^4$	0.0067
	s^4	0.0006	0.0476			
TSW	S	-2.3124	7.08e-05	0.8823	$\hat{\mu}_{tsw} = 3.7128 - 2.3124s$ $+0.7136s^2 - 0.1742gs$ $-0.0737s^3$	0.0209
	s^2	0.7136	0.0038			
	Gs	-0.1742	0.0389			
	s^3	-0.0737	0.0222			
BSW	s^3	-0.1058	<2e-16	0.9716	$\hat{\mu}_{bsw} = 1.6969 - 0.1058s^3$ $+0.0050s^5$	0.0137
	s^5	0.0050	<2e-16			

Step B *– Detect hetero-skedasticity via statistical hypothesis testing*

The homo-skedastic model of '*penetration*' obtained in Eq. (4.25) is tested for hetero-skedasticity in this step using the Bruesch-Pagan (BP) test.

The optimal polynomial order and features identified for '*penetration*' are $p^* = 3$ and $\mathbf{h}^* = \{s, s^2, g^3\}$ respectively. The BP test fits a surrogate model on the residuals of the homo-skedastic model:

$$\hat{\varepsilon}_i^2 = \tilde{\beta}_0 + \tilde{\beta}_1 s_i + \tilde{\beta}_2 s_i^2 + \tilde{\beta}_3 g_i^3 + v_i \;; (i = 1, 2, ..., 53) \qquad (4.26)$$

The null hypothesis (H_0) of the BP test assumes homo-skedasticity. The test statistic is $nR_{\hat{\sigma}^2}^2 = 10.5155$, where n is the number of experiments and $R_{\hat{\sigma}^2}^2$ is coefficient of determination of the model fitted in Eq. (4.26). The test statistic follows Chi-Square distribution with 3 degrees of freedom i.e. $nR_{\hat{\sigma}^2}^2 \sim \chi_3^2$. The p-value of the test is 0.01466. Therefore at $\alpha = 0.05$ level of significance, H_0 is false and hetero-skedasticity is detected for '*penetration*'. Based on hetero-skedasticity, the homo-skedastic model of '*penetration*' will be updated by weighed least squares regression in *Step C*, which will also develop a surrogate model for the hetero-skedastic variance of '*penetration*' using PFS. Table 4.8 summarizes the results of the BP test for all the six KPC analyzed in this case study.

Table 4.8: Summary of results of Breusch-Pagan test of hetero-skedasticity

Welding KPC	Chi-Square distribution d.o.f[*] for test statistic	Test statistic	p-value	H_0 (homo-skedasticity) is True/False	*Step C* required (Yes/No)
Penetration	3	10.5160	0.0147	False	Yes
S-Value	4	11.1510	0.0249	False	Yes
TSC	1	0.4683	0.4938	True	No
BSC	2	2.9939	0.2238	True	No
TSW	4	12.4400	0.0144	False	Yes
BSW	2	2.9213	0.2320	True	No

[*]d.o.f – Degrees of freedom

Step C – *Enhance homo-skedastic surrogate models to characterize hetero-skedasticity*

The homo-skedastic model of '*penetration*' is updated by weighted least squares regression in this step. The weight matrix $W = diag(1/\sigma_1^2, 1/\sigma_2^2, ..., 1/\sigma_{53}^2)$ is a 53×53 diagonal matrix where σ_i^2 is the variance of '*penetration*' at the ith design point, where $i=1,2,...,53$. Since, actual σ_i^2 is unknown, the residuals obtained from the homo-skedastic model in Eq. (4.25) are used as White consistent estimates of '*penetration*' variance $\hat{\sigma}_i^2 = \varepsilon_i^2$. Therefore, the weight matrix is given as $W = diag(1/\varepsilon_1^2, 1/\varepsilon_2^2, ..., 1/\varepsilon_{53}^2)$.

W is now used to update the coefficients of the homo-skedastic model of '*penetration*' using the weighted least squares method. The updated hetero-skedastic surrogate model of '*penetration*' is as follows.

$$\hat{\mu}_{penetration}(s,g) = 0.0858 + 0.8117s - 0.1860s^2 - 3.1488g^3 \tag{4.27}$$

This step also determines a surrogate model for the hetero-skedastic variance of '*penetration*' through PFS. The fitted model for KPC variance is shown in Eq. (4.28).

$$\hat{\sigma}_{penetration}^2(s,g) = 0.1514 - 0.2570s + 0.1294s^2 - 0.0184s^3 \tag{4.28}$$
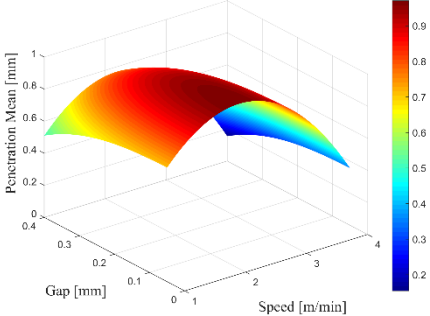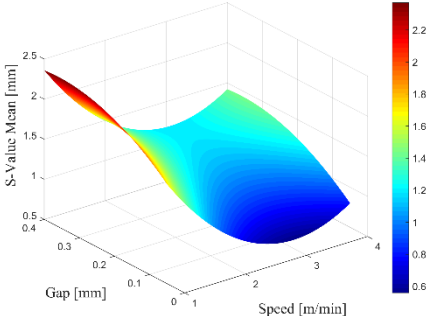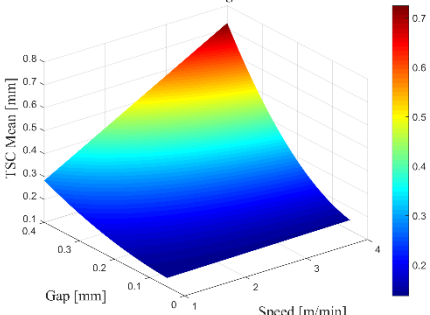
Table 4.9 summarizes the final homo- and hetero-skedastic surrogate models developed for the joint KPCs analyzed in this case study. 2-D plots of the homo- and hetero-skedastic surrogate models of KPC mean ($\hat{\mu}_y$) and variance ($\hat{\sigma}_y^2$) are shown in Table 4.10 and Table 4.11.

Appendix E describes an experimental verification of the surrogate models developed in this section.

Table 4.9: Summary of final homo- and hetero-skedastic surrogate models of RLW joint KPCs

	Weld KPC	Feature selected (h_j)	Regression coefficient (β_j)	Coefficient p-value [prob($\theta_j = 0$)]	R^2	Surrogate model of KPC mean ($\hat{\mu}_y$) [mm]	KPC variance ($\hat{\sigma}_y^2$) [mm^2]
Hetero-skedastic	Penetration	s	0.8117	< 2e-16	0.9950	$\hat{\mu}_{penetration} = 0.0858 + 0.8117s$ $-0.1860s^2 - 3.1488g^3$	$\hat{\sigma}_{penetration}^2 = 0.1514 - 0.2570s$ $+0.1294s^2 - 0.0184s^3$
		s^2	-0.1860	< 2e-16			
		g^3	-3.1488	< 2e-16			
	S-Value	s	-1.6923	2.35e-11	0.9081	$\hat{\mu}_{s-value} = 2.9350 - 1.6923s$ $+4.7311g + 0.2759s^2$ $-6.5696g^2$	$\hat{\sigma}_{s-value}^2 = -0.0035 + 0.2530sg$ $-0.0589s^2g$
		g	4.7311	0.0074			
		s^2	0.2759	5.13e-08			
		g^2	-6.5696	0.0373			
	TSW	s	-3.9907	0.2385	0.9158	$\hat{\mu}_{tsw} = 4.6274 - 3.9907s$ $+1.3927s^2 + 0.4666gs$ $-0.1581s^3$	$\hat{\sigma}_{tsw}^2 = 0.1480 - 0.0519s$ $-0.2239g + 0.0174s^2g$ $+0.0008s^3$
		s^2	1.3927	0.4036			
		gs	0.4666	0.0090			
		s^3	-0.1581	0.5041			
Homo-skedastic	TSC	g^2s	0.9205	1.13e-10	0.868	$\hat{\mu}_{tsc} = 0.1356 + 0.9205g^2s$	0.0082
	BSC	s	-0.1654	4.41e-08	0.835	$\hat{\mu}_{bsc} = 0.5045 - 0.1654s$ $+0.0006s^4$	0.0067
		s^4	0.0006	0.0476			
	BSW	s^3	-0.1058	<2e-16	0.9716	$\hat{\mu}_{bsw} = 1.6969 - 0.1058s^3$ $+0.0050s^5$	0.0137
		s^5	0.0050	<2e-16			

Table 4.10: 2D plots of homo- and hetero-skedastic surrogate models of KPC mean

Welding KPC	Plot of KPC Mean Surrogate Model
Penetration	
S-Value	
TSC	
BSC	

Continues to next page…

TSW	
BSW	
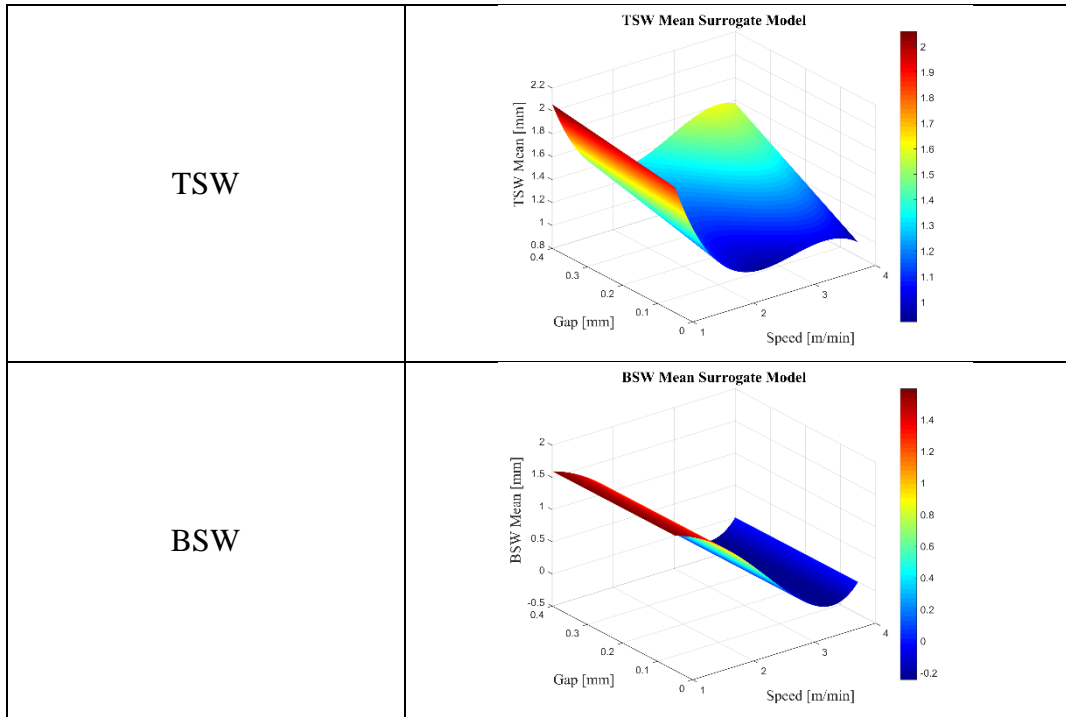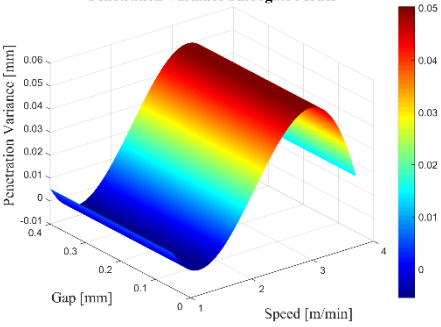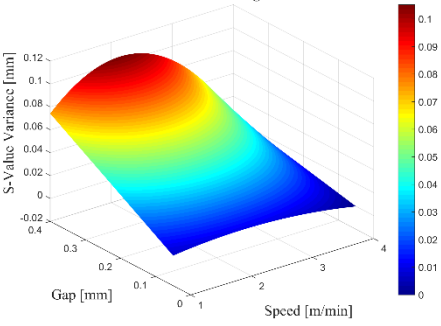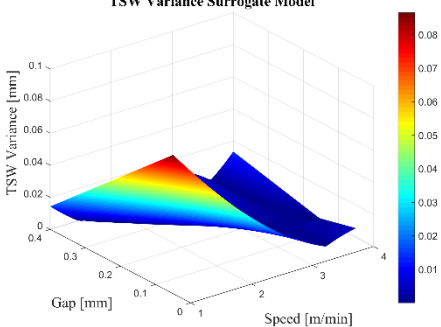
Table 4.11: 2D plots of homo- and hetero-skedastic surrogate models of KPC variance

Welding KPC	Plot of KPC Variance Surrogate Model
Penetration	
S-Value	
TSC	*Constant Variance*
BSC	*Constant Variance*
TSW	
BSW	*Constant Variance*

4.5.3 Joining process parameters selection

The homo- and hetero-skedastic surrogate models of the joint KPCs developed in Section 4.5.2 are utilized to conduct the joining process parameters selection in two parts: (i) multi-objective optimization of the joining process KPIs (*Section 4.5.3.1*); and, (ii) identification of the stochastic process window and

computation of the acceptance rate (*Section 4.5.3.2*).

4.5.3.1 Multi-objective optimization of joining process Key Performance Indicators

In this case study a bi-objective optimization is conducted to optimize the following two KPIs:

i. *Process efficiency related KPI* – The process efficiency related KPI taken into consideration in this case study is '*welding cycle time*' which needs to be *minimized*. The 'w*elding cycle time*' is inversely related to the welding speed (s) which is a KCC of the RLW process. In this case study, the '*welding cycle time*' is modelled as negative of the welding speed $(-s)$.

ii. *Process quality related KPI* – In this case study, the hetero-skedastic variance of the '*penetration*' $\hat{\sigma}^2_{penetration}(s, g)$ is considered as a process quality related KPI. The bi-objective optimization problem solved in this section focuses on the *minimization* of $\hat{\sigma}^2_{penetration}(s, g)$ to identify the welding speed (s) and part-to-part gap (g) which give minimum variance of the '*penetration*'.

Based on the aforementioned two KPIs, the bi-objective optimization problem optimizes the KPIs shown in Eq. (4.29).

$$\text{KPIs} = \begin{cases} \text{KPI}_1 = cycle\_time = -s \\ \text{KPI}_2 = \hat{\sigma}^2_{penetration}(s, g) = 0.1514 - 0.2570s + 0.1294s^2 - 0.0184s^3 \end{cases} \quad (4.29)$$
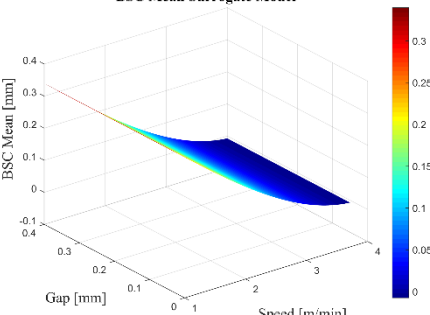
Here KPI_1 is related to *process efficiency* while KPI_2 is indicative of *process quality*.

The design tolerances of the weld KPCs, as shown in Table 4.3 are constraints in the bi-objective optimization problem. Given the thickness of the lower material, $T_{lower} = 1.0$ mm and thickness of the upper material, $T_{upper} = 0.75$ mm, the formulation of the constrained bi-objective optimization is prescribed as follows.

$$[s,g]^* = \underset{[s,g] \in D}{\arg\min} \begin{cases} -s \\ 0.1514 - 0.2570s + 0.1294s^2 - 0.0184s^3 \end{cases} \quad (4.30)$$

subject to,

Penetration: $\qquad 0.30 \leq 0.0858 + 0.8117s - 0.1860s^2 - 3.1488g^3 \leq 1.00$

S-Value: $\qquad 2.9350 - 1.6923s + 4.7311g + 0.2759s^2 - 6.5696g^2 \geq 0.90$

TSC: $\qquad\qquad 0.1356 + 0.9205g^2 s \leq 0.375$

BSC: $\qquad\qquad 0.5045 - 0.1654s + 0.0006s^4 \leq 0.50$

BSW: $\qquad\qquad 1.6969 - 0.1058s^3 + 0.0050s^5 \leq 1.00$

where the KCC design space is $D = \{1.0 \leq s \leq 4.0\} \times \{0.05 \leq g \leq 0.40\}$.

The aforementioned optimization problem is solved by the Fast Elitist Non-Dominated Sorting Genetic Algorithm (also known as NSGA II) (Deb, *et al.*, 2002). NSGA II is a computationally efficient solver of multi-objective optimization problems. For this case study, NSGA-II implementation in the Multiple Criteria Optimization ("mco") package of R Statistical Computing platform is used. Table 4.12 lists the parameters of NSGA-II used in this case study.

Table 4.12: Parameters of NSGA-II algorithm

Algorithm parameter	Value used
Population size	20
Number of generations	50
Cross-over probability	0.70
Mutation probability	0.20

Figure 4.13 shows the optimal Pareto front of feasible solutions. As evident, *lesser welding cycle time* or *higher process efficiency* (KPI_1) can be achieved at the expense of *higher variance of 'penetration'* or *lower process quality* (KPI_2) and vice versa. Table 4.13 lists the KPIs from the optimal Pareto front and the corresponding joining process parameters.
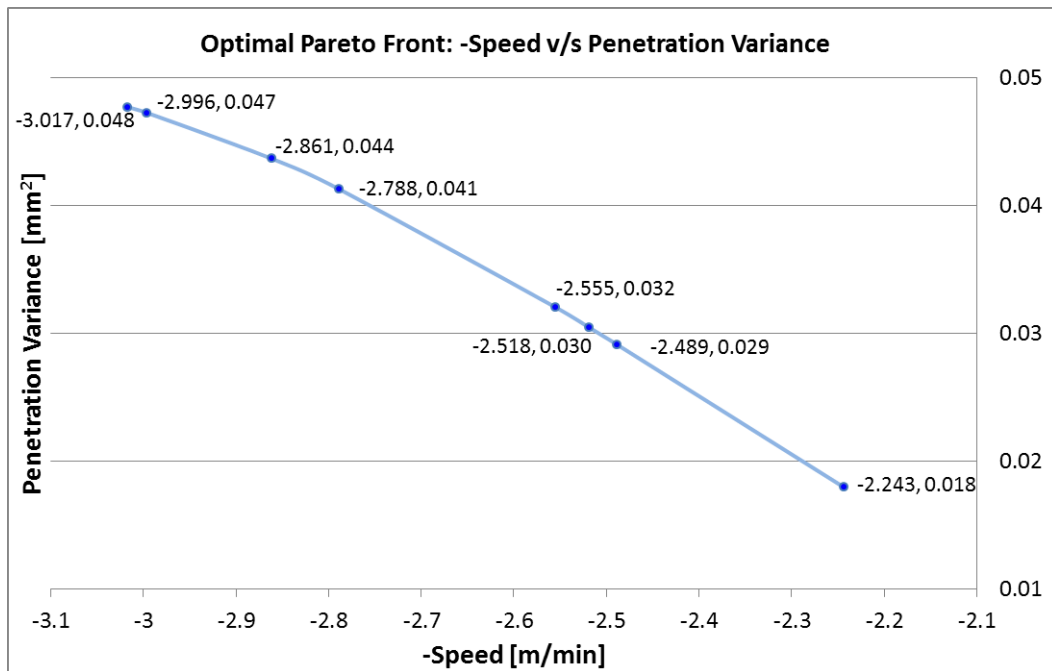
Figure 4.11: Optimal Pareto front for bi-objective optimization of RLW joining proess Key Performance Indicators

Table 4.13: KPIs from optimal Pareto front and
corresponding joining process parameters

KPI_1 (-*Speed*)	KPI_2 ($\hat{\sigma}^2_{penetration}$)	Welding Speed (*s*)	Part-to-part gap (*g*)
Best -3.017	*Worst* 0.048	3.017	0.104
-2.996	0.047	2.996	0.095
-2.861	0.044	2.861	0.098
-2.788	0.041	2.788	0.097
-2.555	0.032	2.555	0.070
-2.518	0.030	2.518	0.070
-2.489	0.029	2.489	0.068
Worst -2.243	*Best* 0.018	2.243	0.052

Discussion of results – As evident from both Figure 4.13 and Table 4.13, the process efficiency, measured in terms of the welding cycle time, can be increased at the expense of the process quality measured here by the variance of penetration (KPI_2). The optimal Pareto front shown in Figure 4.13 can be used as a decision making guideline to set appropriate joining process parameters.

It is noteworthy that the bi-objective optimization described in this

section has been enabled by the proposed scalable surrogate modelling of homo- and hetero-skedastic joint KPCs which detects relevant hetero-skedastic behaviour of joint KPCs and develops analytical functions of both KCC-dependent mean and variance of the joint KPCs.

4.5.3.2 Identification of process window and computation of acceptance rate

The process window defines the feasible region in the 2-D design space of the joining process KCCs welding speed and part-to-part gap.

Moreover, identification of process window and computation of acceptance rate is done based on each of the following types of analysis:

i. *Mean only analysis* whereby variation of the KPCs is not considered

ii. *Worst-case analysis* whereby KPCs variance is taken into consideration and upper and lower '$q=1$' sigma limits are used to determine compliance to KPC design tolerance.

In this case study, the process window is graphically generated over a 100×100 mesh grid of the two KCCs. The conditions defined in Table 4.1 are used to find the process window for each KPC. The final process window which satisfies design tolerances of all six joint KPCs is obtained by taking the intersection of the individual process windows. A MATLAB program has been developed to generate the individual process windows and the final process window.

The acceptance rate is computed in terms of the probability of an acceptable weld at each design point inside the process window using the formulae listed in Table 4.1.

Table 4.14 shows the 2D plot of process window, 3D surface plot of the acceptance rate and 2D contour plot of the acceptance rate for the *'mean only'* and '*worst-case*' analysis.

175

Furthermore, mean and $\pm$ one sigma control limits of the six joint KPCs, analysed in this case study, are shown in Figure 4.12 to illustrate the effect of homo- and hetero-skedasticity on the estimation of the control limits. As evident from Figure 4.12, for homo-skedastic KPCs such as TSC, BSC and BSW, width between the control limits is constant over the process window of welding speed (KCC) due to their constant KCC-independent variances. On the other hand, for hetero-skedastic KPCs such as penetration, s-value and TSW, the width between the control limits varies over the process window of the welding speed due to their changeable KPC-dependent variances.

Table 4.14: Process window and acceptance rate for RLW joining process

Process window analyses	2D plot of process Window	3D surface plot of acceptance rate	3D surface plot of acceptance rate
Mean only			
Worst-case at q=1 sigma limits			
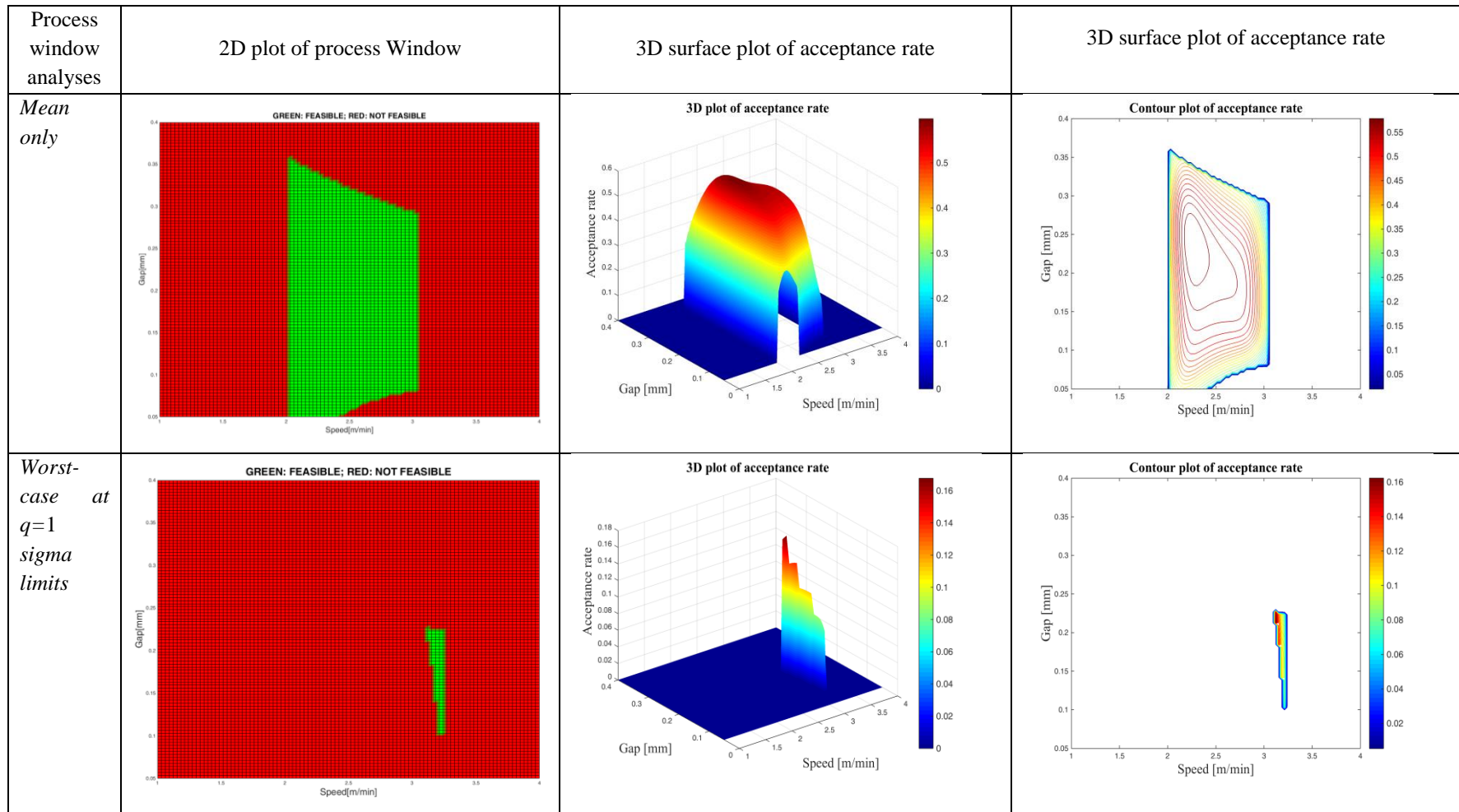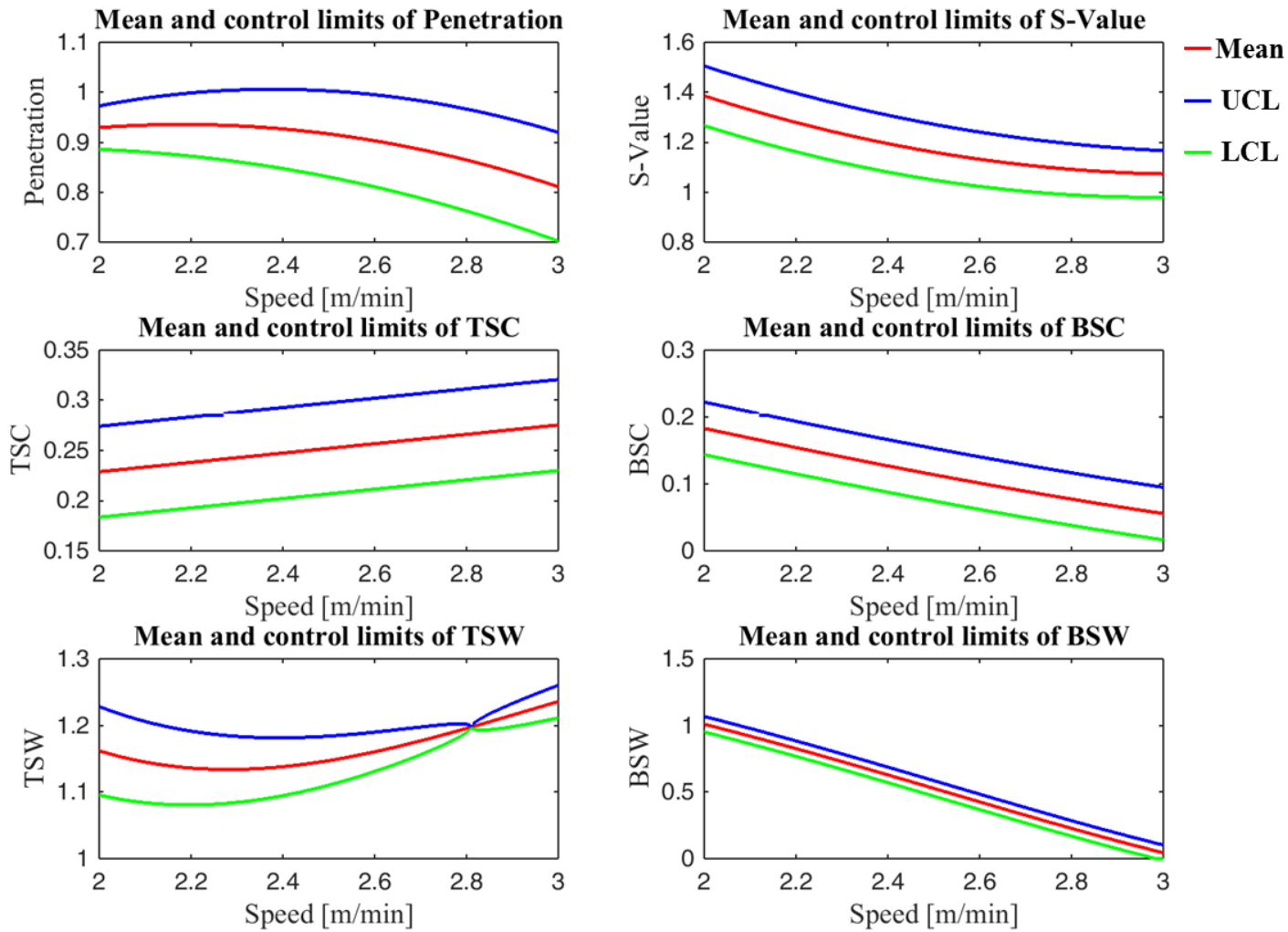
Figure 4.12: Mean and one sigma control limits of joint KPCs

Discussion of results – The significance of the results obtained from the case study on RLW joining process is discussed based on the following two aspects:

i. *Trade-off between process efficiency and process quality –* There can be trade-off between the process efficiency and the process quality related KPIs of the joining process. In case of a trade-off, the optimal process efficiency is obtained at the expense of process quality. Results from the case study illustrate the trade-off between the process efficiency and the process quality in the RLW joining process as explained here.

In this case study, the process efficiency is related to the welding cycle time which is modelled as negative of the welding speed ($-s$), where higher process efficiency is achieved at a lower negative welding speed. On the other hand, the process quality is represented by the hetero-skedastic variance of '*penetration*' $\hat{\sigma}^2_{penetration}(s, g)$ where higher process quality is achieved at lower $\hat{\sigma}^2_{penetration}(s, g)$. The results from the bi-objective optimization show that higher process efficiency (lower $-s$) is attained at lower process quality (higher $\hat{\sigma}^2_{penetration}(s, g)$). This is illustrated by a summary of the best and worst results obtained by solving the bi-objective optimization problem, as shown in Table 4.15 given below.

Table 4.15: Best and worst Key Performance Indicators obtained from bi-objective optimization for joining process parameters selection

		Key Performance Indicators	
		Process efficiency (*higher* process efficiency is from lower $-s$)	Process quality (*higher* process quality is from lower $\hat{\sigma}^2_{penetration}$)
Quality of solution		*Best* - 3.017 m/min	*Worst* 0.048 mm^2
		Worst -2.243 m/min	*Best* 0.018 mm^2

Another important measure of process quality is the acceptance rate (AR) which is the probability of making a joint of acceptable quality at a design point inside the KCC process window. The computation of AR has been enabled by the surrogate models of KCC-dependent mean and variance of the joint KPCs. Within the process window, the acceptance rate is varying as illustrated in Table 4.14. The variation of the process acceptance rate can cause a trade-off between the process efficiency and the process quality when a monotonic increase in the process efficiency, evaluated by welding speed, is not accompanied by a monotonic increase in process quality, measured by acceptance rate, over the process window, as illustrated in Figure 4.13. Consequently, the maximum process efficiency does not correspond to the maximum process quality. For example, consider the process window and acceptance rate computed for the '*mean only*' analysis shown in Table 4.14. The *maximum* welding speed at which a feasible weld can be made is 3.03 m/s however acceptance rate at this speed is 0.31 (or 31 %). The *maximum* achievable acceptance rate is 0.60 (or 60 %) which is achieved at a lower welding speed of 2.27 m/s.
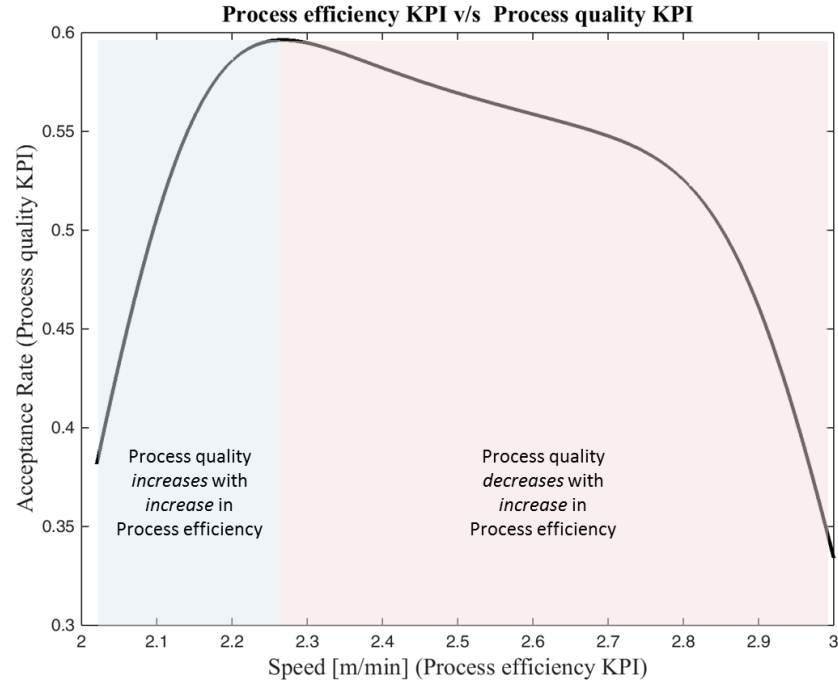
Figure 4.13: Non-monotonic change of process quality for monotonic change of process efficiency

ii. *Impact of homo- and hetero-skedastic models on identification of process window and computation of acceptance rate* – The scalable surrogate modelling proposed in this chapter allows the identification and characterization of homo- and hetero-skedastic behaviour of joint KPCs through data analysis. Characterization of hetero-skedastic behaviour leads to identification of a process window and computation of an acceptance rate which is expected to be significantly different than that obtained from currently existing surrogate models which address only homo-skedastic behaviour of joint KPCs.

To compare results obtained from the proposed method and state-of-the-art surrogate models, the case study presented in this section is analyzed using second order polynomial regression models which assume homo-skedasticity of all KPCs. The following four joining process characteristics are derived from the results: (1) maximum feasible welding speed giving welds of

acceptable quality (s_{max}); (2) acceptance rate at maximum welding speed (AR-s_{max}); (3) maximum acceptance rate over the process window (AR_{max}); and, (4) welding speed at which maximum acceptance is obtained (s-AR_{max}). The comparison of the aforementioned four process characteristics derived from the state-of-the-art 2nd order homo-skedastic polynomial regression (Acherjee, *et al.*, 2009) versus those obtained from the proposed homo- and hetero-skedastic models is given in Table 4.16. The results highlighted in the dotted red, blue and green boxes on Table 4.16 shows significant differences in the results obtained from the proposed and currently existing surrogate models of joint KPCs as explained below.

Table 4.16: Comparison of process window analyses
by state-of-the-art 2nd order homo-skedastic polynomial model and proposed methodology

Process window analyses	Methodology	s_{max}	AR-s_{max}	AR_{max}	s-AR_{max}	Actual AR
Mean only	State-of-the-art	3.03	0.36	0.64	2.70	0.56
	Proposed	3.03	0.31	0.60	2.27	NA
Worst-case at 1-σ limits	State-of-the-art	3.21	0.10	0.62	2.79	Infeasible
	Proposed	3.21	0.09	0.17	3.12	NA

s_{max} - Maximum feasible welding speed; AR-s_{max} - Acceptance rate at maximum welding speed
AR_{max} - Maximum acceptance rate over the process window; s-AR_{max} - Welding speed at which maximum acceptance is obtained

Table 4.16 indicates that the currently existing surrogate models which assume that all joint KPCs are homo-skedastic, lead to erroneous joining process parameters selection as highlighted in the following three significant instances:

A. *Erroneous estimation of maximum acceptance rate* (AR_{max}) *in 'mean-only'*

analysis –

The state-of-the-art surrogate models estimate a maximum acceptance rate (AR_{max}) of 0.64 (or 64 %) at 2.70 m/min of the welding speed; however actual acceptance rate at this welding speed as computed by proposed methodology is 0.56 (or 56 %). Hence, currently existing methods overestimate AR_{max} by 8% points. This case is highlighted by the red-dotted box in Table 4.16.

B. *Erroneous estimation of maximum acceptance rate (AR_{max}) in 'mean-only' analysis –*

For the worst case analysis of the process window and the computation of acceptance rate at 1-σ limits', the currently existing methods overestimate AR_{max} by 45 % points as indicated in the blue dotted box in Table 4.16.

C. *Erroneous estimation of welding speed for maximum acceptance rate (s - AR_{max}) in 'mean-only' analysis –*

For the worst case analysis of the process window and the computation of the acceptance rate at 1-σ limits', the currently existing methods identify the welding speed at which maximum acceptance is obtained (s-AR_{max}) as 2.79 m/min, which is an infeasible welding speed according to process window developed through the proposed methodology. This case is highlighted by the green-dotted box in Table 4.16.

4.6 Summary

The successful implementation of a new joining process in automotive Body-In-White (BIW) assembly production depends on accurate joining process parameters selection. The quality of the solution in joining process parameters selection critically depends on the capability of the surrogate models, integrating joining process KCCs with stochastic joint KPCs, in addressing the scale of KPC stochasticity which varies from homo- to hetero-skedasticity. However, currently existing homo-skedastic surrogate models of joint KPCs do not address the scale of stochasticity in joint KPCs and therefore might lead to inaccurate results for joining process parameters selection.

To address the aforementioned challenge, this chapter has developed an approach for *scalable surrogate modelling of homo- and hetero-skedastic joint KPCs* which identifies and characterizes appropriate stochasticity of joint KPCs through data analysis. Data from physical experimentation is given as input to the proposed method which models the homo- and hetero-skedastic noise in the joint KPCs based on the following three steps: (1) development of homo-skedastic surrogate model of joint KPC; (2) detection of hetero-skedasticity via statistical hypothesis testing; and, (3) enhancement of homo-skedastic surrogate models to characterize hetero-skedasticity. As output, surrogate models of KCC-dependent mean and variance of joint KPCs are obtained.

Based on the homo- and hetero-skedastic surrogate models of joint KPCs, this chapter has developed a comprehensive approach of *joining process parameters selection* which focuses on the following two design synthesis tasks: (1) identification of optimal KCCs which optimize process KPIs subject to design tolerances on KPCs and operating limits of KCCs; and, (2) identification of process window and

computation of acceptance rate.

Overall, this chapter has developed a comprehensive methodology of *scalable surrogate model driven joining process parameters selection* based on the aforementioned two interlinked approaches namely: (1) *scalable surrogate modelling of homo- and hetero-skedastic joint KPCs*; and, (2) of *joining process parameters selection* based on homo- and hetero-skedastic surrogate models of joint KPCs.

The proposed methodology of *scalable surrogate model driven joining process parameters selection* has been applied for characterization of KCCs and KPCs in the Remote Laser Welding joining process for sheet metal assembly. The results have been compared with those obtained from state-of-the-art homo-skedastic models of joint KPCs. Significant differences between the results demonstrate the usefulness of the proposed methodology as a data-driven approach of addressing design synthesis tasks, such as joining process parameters selection in BIW assembly production, which rely on noisy experimental data in the absence of accurate *first-principle* models.

Acknowledgements

CHAPTER 5 [1]

SCALABLE SURROGATE MODEL DRIVEN CORRECTIVE ACTION OF PRODUCT FAILURES DUE TO DIMENSIONAL VARIATIONS OF KEY PRODUCT CHARACTERISTICS

5.1 Overview of the chapter

In mechanical assemblies, product failures can be triggered by unwanted dimensional variations in KPCs. In complex assemblies there can be a large number of KCCs which can potentially influence a KPC. Therefore, dimensionality reduction of of KCCs is critical for design synthesis tasks such as corrective action of product failures which require diagnosis of unwanted variations in KPCs (Shi and Zhou, 2009). For diagnosis it is necessary to identify few critical KCCs closely related to the faulty KPCs.

Currently existing methods of KCC dimensionality reduction focus on identifying statistical fault patterns by deriving a lower dimensional manifold as a function of the original KCCs and depend on *first-principle* models to formulate an initial analytical model linking KPCs with KCCs. Methods based on the aforementioned approach exist for diagnosis of fixture induced errors in multi-station type-II assembly processes.

However, there are two limitations of the aforementioned state-of-the-art diagnosis methods: (1) lack of dimensionality reduction in the original KCC space; and, (2) need for knowledge about the physical process governing the KPC-KCC

---

[1] Based on papers (1) Pal, A., Franciosa, P., & Ceglarek, D., 2014. Root cause analysis of product service failures in design-A closed-loop lifecycle modelling approach. In Proceedings of 24th CIRP Design Conference, Milan, Italy, pp. 165-170; and, (2) Pal, A., Franciosa, P., & Ceglarek, D., 2014. Corrective Actions of Product Service Failures via Surrogate Modelling of Dimensional Variations. In Proceedings of the 2014 Industrial and Systems Engineering Research Conference, Institute of Industrial Engineers, Montreal, Canada, pp. 2271-2280.

interrelations. The aforementioned limitations are critical particularly for complex type-I assemblies which face the following two challenges: (1) variation in a KPC can be affected by potentially a large number of KCCs; and, (2) KPC-KCC interrelations are modelled by numerically intractable Variation Simulation Analysis (VSA).

To address the aforementioned challenges, this chapter builds upon the idea of *scalability for KCC dimensionality* introduced in Chapter 1 under the proposed framework of *Scalable Design Synthesis*. *Scalability for KCC dimensionality* has the following two requirements:

i. *Dimensionality reduction of KCCs with minimal knowledge about underlying causality between dimensional variations in the faulty KPC and the assembly KCCs*

ii. *Closed-form analytical model of the faulty KPC in terms of few critical KCCs*

To meet the aforementioned requirements, this chapter develops *scalable surrogate modelling for KCC dimensionality*, as a data-driven approach for diagnosis of unwanted variations in KPCs, which provides the following two key capabilities:

i. *Identification of few critical KCCs and their interactions closely related to the faulty KPC* based on Polynomial Feature Selection (PFS) which has been adapted in this chapter to address KCC dimensionality

ii. *Surrogate model of the faulty KPC* in terms of critical KCCs and their interactions

Furthermore, *scalable surrogate modelling for KCC dimensionality* is discussed in this chapter in the context of a corrective action (CA) to reduce unwanted variations in faulty assembly dimensions (KPCs) in type-I assembly processes. A corrective action of unwanted variations in faulty KPCs requires diagnosis to identify few critical KCCs closely related to the faulty KPCs. In this chapter, diagnosis is

187

achieved by *scalable surrogate modelling for KCC dimensionality* which determines the critical KCCs related to the faulty KPCs and develops surrogate models of the faulty KPCs in terms of the identified critical KCCs. The surrogate models of faulty KPCs are then utilized in a *two-step design adjustment* process which minimizes production yield of the faulty KPCs via: (1) optimal nominal change; and, (2) tolerance re-allocation of subassembly dimensions (KCCs).

Overall, this chapter develops a systematic methodology of <u>*scalable surrogate model driven corrective action for product failures due to unwanted dimensional variations of KPCs*</u> based on the following two interlinked approaches:

  i. *Diagnosis via scalable surrogate modelling for KCC dimensionality*

  ii. *Two-step design adjustment* to reduce production yield of faulty KPCs

The outcome of the corrective action is recommend engineering changes such as adjusted nominal and tolerance of the critical KCCs related to the faulty KPCs. Additionally, a cost-benefit analysis is presented to show the increase in cost of manufacturing due to the adjusted KCC tolerances versus reduction in cost of quality loss due to unwanted variation in KPC.

Figure 5.1 highlights the main approaches involved in the proposed methodology of corrective action of product failures due to unwanted dimensional variations of KPCs.
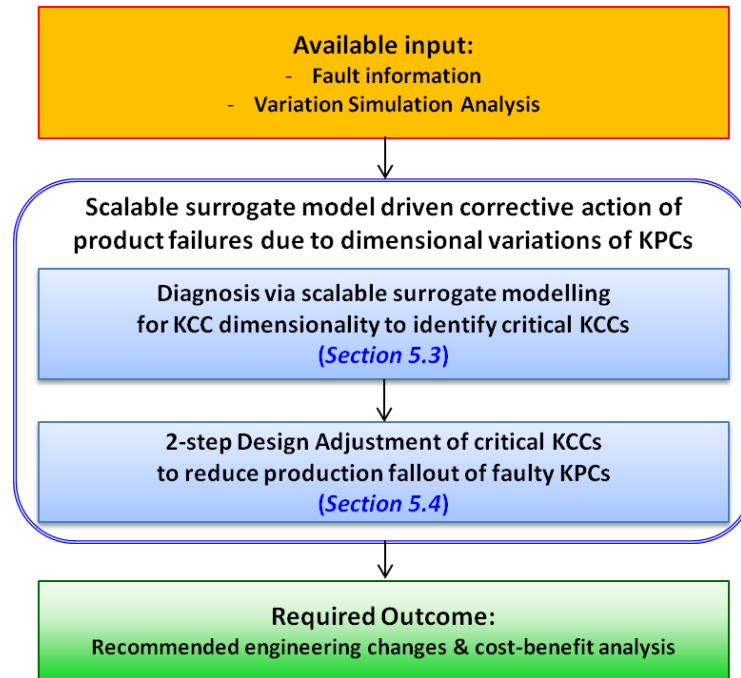
Figure 5.1: Scalable surrogate model driven corrective action of product failures due to dimensional variations of KPCs

The proposed methodology is applied to address warranty failures in an automotive ignition switch assembly.

The remaining part of this chapter is organized as follows: Section 5.2 outlines the motivation for the research presented in this chapter. Next, the proposed methodology of *scalable surrogate model driven corrective action of product failures due to dimensional variations of KPCs* is developed in Section 5.3 based on the following two methods: (1) *diagnosis via scalable surrogate modelling for KCC dimensionality*; and, (2) *two-step design adjustment*. Next, Section 5.4 demonstrates the proposed methodology through an industrial case study of automotive ignition switch assembly. Finally, summary of the research done in this chapter is presented in Section 5.5.

Notations related to the methods developed in this chapter are listed as follows. Notations of KCCs ($\mathbf{x}$) and KPCs ($\mathbf{y}$) used in this chapter are similar to the

generic ones introduced in Chapter 1. However, in this chapter KCCs and KCCs are specifically related to corrective actions of product failures due of unwanted variations in assembly dimensions (KPCs) caused by variation in individual part dimensions (KCCs). Hence notations of KCCs and KPCs are redefined in this chapter highlighting their meanings as related to corrective actions of product failures.

Notations

$\mathbf{x}$	Set of 'd' KCCs $\mathbf{x} = \{x_1, x_2, ..., x_d\}$, where x_i is the ith KCC in $\mathbf{x}$ representing the ith individual part dimension
$\mathbf{y}$	Set of 'r' KCCs $\mathbf{y} = \{y_1, y_2, ..., y_r\}$, where y_j is the jth KPC in $\mathbf{y}$ representing the jth faulty KPC
N	Number of times Variation Simulation Analysis is performed to generate training data which is used for developing surrogate models of faulty KPCs
$\mathbf{x}^*$	Critical KCCs closely related to the faulty KPC 'y'
$\mathbf{h}^*$	Optimal set of polynomial features obtained from the critical KCCs $\mathbf{x}^*$
$f(\bullet)$	Regression based surrogate model of the faulty KPC 'y' in terms of critical KCCs $\mathbf{x}^*$ closely related to it
$\boldsymbol{\beta}^*$	Coefficients of the regression model of optimal set of polynomial features $\mathbf{h}^*$
FR$_i$	Failure region related to the ith faulty KPC where $i = 1, 2, ..., r$
LFL$_i$, UFL$_i$	Lower and upper failure levels respectively of FR$_i$
$g_i(y_i)$	Manufacturing probability distribution of the ith faulty KPC where $i = 1, 2, ..., r$
M_i	Production fallout of the ith faulty KPC where $i = 1, 2, ..., r$
μ_j	Initial design nominal of the jth KCC x_j where $j = 1, 2, ..., d$
T_j	Tolerance of the jth KCC x_j where $j = 1, 2, ..., d$
C_{p_k}	Process capability of manufacturing the jth KCC x_j where $j = 1, 2, ..., d$

δ_j	Nominal change applied to the jth KCC x_j where $j = 1, 2, ..., d$
δ_j^{lower}, δ_j^{upper}	Allowable lower and upper limits respectively of nominal change due to manufacturing constraints on the jth KCC x_j where $j = 1, 2, ..., d$
C_j	cost of tolerancing required to achieve a tolerance T_j of KCC$_j$ where $j = 1, 2, ..., d$
$\mathbf{A}_j$, $\mathbf{B}_j$	User-defined constants for the tolerancing cost model
Cw	Cost of quality loss is proportional to the fallout of the faulty KPCs
a_j	Binary variable indicating whether the jth KCC x_j where $j = 1, 2, ..., d$ is selected as a critical KCC. $a_j = 1$ if the jth KCC is selected as a critical KCC else $a_j = 0$
δ_j^{opt}	Optimal nominal change of applied to the jth KCC x_j
M_i'	Production fallout of the ith faulty KPC after optimal nominal adjustment where $i = 1, 2, ..., r$

5.2 Motivation for the research

Type-I assembly products are frequently found in components and sub-components of an automotive vehicle. An example of type-I assembly is the electro-mechanical automotive ignition switch operated using a key. Components such as the ignition switch are complex and assembled from multiple individual parts. The final assembly dimensions (KPCs) are related to a large number of individual part dimensions (KCCs). Coupling between KCCs and stack-up of their variations can potentially cause unwanted variations in the final assembly KPCs.

Unwanted variations in assembly KPCs which are closely related to normal functionality of the assembly can trigger product failures such as warranty failures in service which results in warranty costs, customer dissatisfaction and safety

issues. Hence corrective action to reduce unwanted dimensional variations in assembly KPCs is of paramount importance.

In electro-mechanical components, failures are related to faulty KPCs such as misalignment between mating surfaces causing electrical malfunctioning. Tolerances are allocated to KPCs based on the requirement for normal functionality of the component. Failure occurs when the KPC is out-of-tolerance due to uncontrolled manufacturing variations of KCCs. Out-of-tolerance KPCs are triggered as result of challenges in design such as sensitivity of a KPC on a large number of KCCs due to ill-conditioned design, stack-up of variations from individual KCCs and lack of process-oriented tolerance allocation, which leads to low yield from manufacturing (Ding, *et al.*, 2005; Ceglarek & Prakash, 2012). Also, failures related to warranty are caused, though less expected, by the presence of failure regions inside the defined design tolerances (in-tolerance failures), which occur due to erroneous characterization of customer attributes during early product development, and unexplored interactions during the design phase (Mannar, *et al.*, 2006). Such interactions may go unnoticed by designers due to the increasing complexity of product and production systems as well as reduced time for new product development. Hence failures due to out-of-tolerance or in-tolerance KCCs may be caused by a variety of complex underlying root causes. Under these conditions, corrective action will significantly benefit from a methodology that is agnostic to the underlying failure root causes but can recommend engineering changes and provide a cost-benefit analysis.

Current tools for VSA which estimate KPCs for given KCCs based on *first-principle* analysis are necessary but not sufficient for corrective action due to their lack of information about few critical KCCs closely related to the faulty KPC and due to absence of an analytical model of their specific relationship with the latter. This

makes corrective actions costly, time-consuming and case-specific reverse engineering requiring knowledge about underlying root causes which can potentially cause malfunctioning of the product.

To eliminate the dependency on case-by-case heuristic analysis, this chapter develops *scalable surrogate model driven corrective action of product failures due to dimensional variations of KPCs* based on (1) *diagnosis via scalable surrogate modelling for KCC dimensionality*; and, (2) *two-step design adjustment* to reduce production yield of faulty KPCs.

5.3 Scalable surrogate model driven corrective action of product failures due to dimensional variations in KPCs

Failures in type-I assembly products can be caused by unwanted dimensional variations of assembly KPCs. The proposed method of diagnosis via scalable surrogate modelling for KCC dimensionality focuses on addressing direct or consequential failures caused by unwanted dimensional variations in assembly KPCs. Failures are caused by a product malfunctioning which critically depends on dimensional variations of KPCs such as gaps, contacts or inclination between mating surfaces. Assembly KPCs depend on dimensions of individual parts and sub-assemblies (KCCs). When KPCs do not meet the tolerance required for normal functioning of the product, failures occur. For example, if a clearance or contact between two mating surfaces is required for normal functioning, then interference between the two surfaces will cause failure.

The proposed methodology first diagnoses few critical KCCs whose dimensional variations are closely related to the faulty KPCs. A surrogate model of the faulty KPCs as a function of the critical KCCs is also developed. This is followed by a two-step design adjustment process using the surrogate models of faulty KPCs to

determine an optimal nominal change and tolerance reallocation of the critical KCCs which minimizes production fallout of faulty KPCs. The steps of scalable surrogate model driven corrective action are elaborated in Figure 5.2.
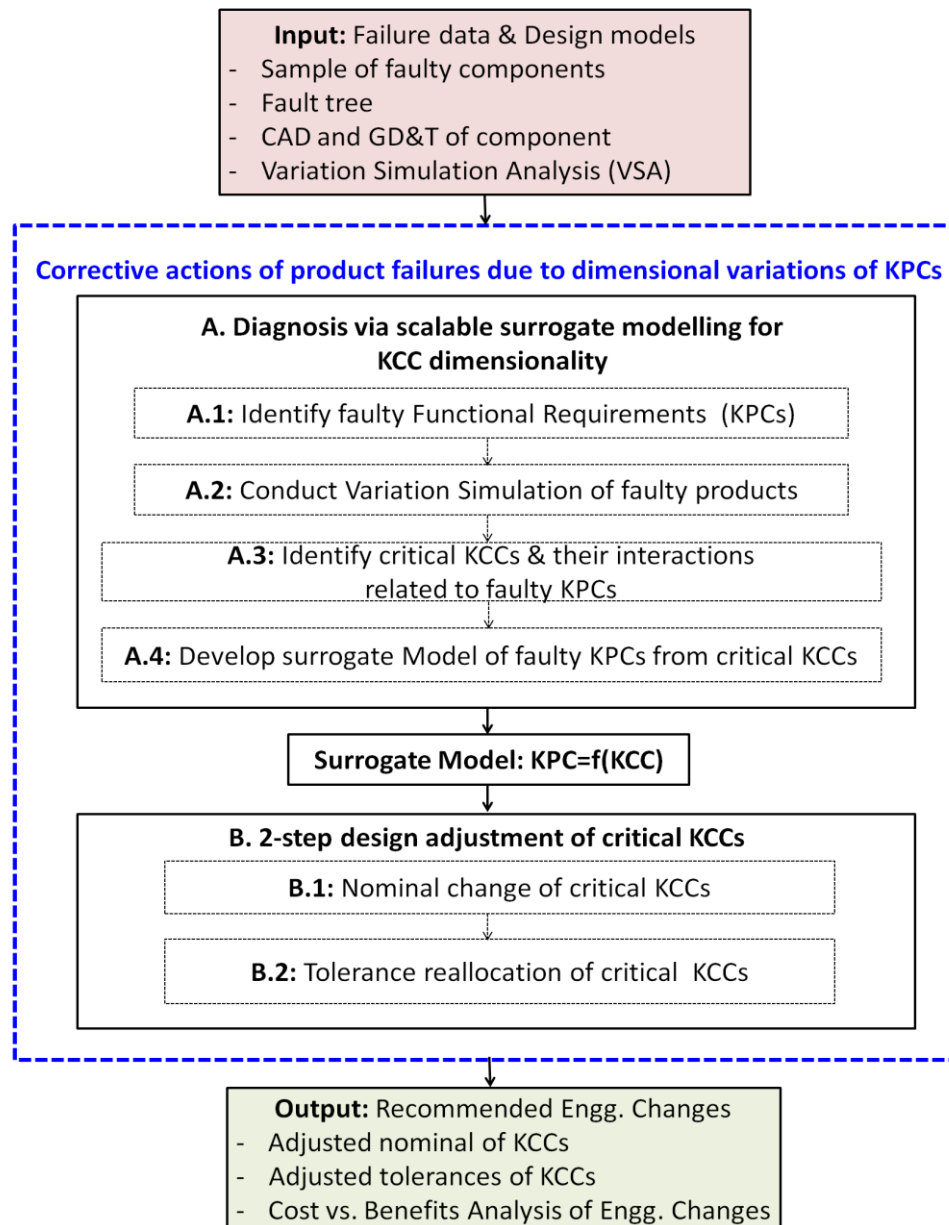
Figure 5.2: Corrective action of product failures due to dimensional variations of KPCs

The two major components of the methodology are described as follows:

A. Diagnosis via scalable surrogate modelling for KCC dimensionality – Steps A.1 through A.4 is done to identify few critical KCCs relates to the faulty KPC:

- **Step A.1: Identify faulty KPCs** – Fault tree diagram is used to map the failure mode to dimensional KPCs, such as gaps, contacts between mating surfaces. Moreover, a sample of failed parts is subjected to inspection and measurement to confirm that the faulty KPCs, which are identified from analyzing the fault tree, do not satisfy the tolerance required for the normal functioning of the component.

- **Step A.2: Conduct Variation Simulation Analysis of faulty KPCs** – Data from VSA is analyzed to identify critical KCCs related to the faulty KPCs and develop surrogate models of the latter. Data is generated by simulating dimensional variation of KCCs and faulty KPCs through the following two steps:

  A.2.1. *Setup input to VSA* – Datum Flow Chain (DFC) technique (Whitney, 2004) is applied to nominal CAD of the component to determine individual parts whose dimensional variation are the KCCs in this case. Nominal, tolerance and probability distribution are defined for the KCCs. Next assembly constraints are introduced between the KCCs to define mating surfaces.

  A.2.2. *Run VSA for 'N' times* –VSA generates KCCs by random sampling based on the nominal, tolerance and probability distribution defined in the previous step. Based on *first-principle* analysis, such as kinematic analysis, VSA determines the optimal assembly configuration for given KCCs and KPCs of interest are estimated by measuring the related geometric features such as clearance or inclination between mating surfaces. VSA is run for 'N' times and KCCs and KPCs are recorded

for each run. Data generated by simulation is used to train the surrogate model.

- **Step A.3: Identify critical KCCs and their interactions related to faulty KPCs –** In complex assemblies, variations in a large number of KCCs can potentially affect variations in the faulty KPCs. This step addresses the high dimensionality of KCCs to identify the few ones closely related to the faulty KPCs. The main objective is to develop the best fitting surrogate model of a faulty KPC based on minimization of the generalized prediction error of the model. KCCs selected to achieve the best fitting model are considered as the critical KCCs related to the faulty KPC.

  The aforementioned best fitting surrogate model of a faulty KPC in terms of critical KCCs is achieved by Polynomial Feature Selection (PFS), which is adapted from Chapters 3 and 4 to selectively identify critical KCCs and multiplicative interactions between them which accurately models the faulty KPCs.

  In this section, PFS is adapted in the context of surrogate modelling for dimensionality reduction to address identification of critical KCCs. Variations in 'd' KCCs, $\mathbf{x} = \{x_1, x_2, ... x_d\}$ are considered to develop surrogate model of a KPC 'y'. The surrogate model of the KPC is based on critical KCCs $\mathbf{x}^* \subseteq \mathbf{x}$ which is a subset of the full set of KCCs. The surrogate model is represented as

$$y = f(\mathbf{x}^*) \tag{5.1}$$

Since KCCs interact non-linearly to affect variations in KPCs, the objective of PFS is to analytically model the underlying non-linear relationship between the faulty KPC and the critical KCCs.

In this chapter critical KCCs ($\mathbf{x}^*$) and their polynomial interactions ($\mathbf{h}^*$) affecting faulty KPCs is identified using the Polynomial Feature Selection (PFS) algorithm. The PFS algorithm has been developed in Chapter 3. In this chapter PFS has been adapted from Chapter 3 where it has been applied to determine optimal polynomial interactions between fixture related KCCs such as clamp locations to develop best-fitting global model of KPCs such as part-to-part gaps between mating parts of an assembly. For detailed description of the PFS algorithm, the reader is suggested to refer Section 3.5.1.1 of Chapter 3.

- **Step A.4: Develop surrogate model of faulty KPCs from critical KCCs -** Critical KCCs and their interactions are determined in the previous step. The final surrogate model is built on the full training data using the polynomial terms $\mathbf{h}^*$. The final surrogate model is represented in Eq. (5.4).

$$y = \beta_0^* + \beta_1^* h_1 + \beta_2^* h_2 + ... + \beta_{m^*}^* h_{m^*} \qquad (5.4)$$

where m^* are number of features in $\mathbf{h}^* = \{h_1^*, h_2^*, ..., h_{m^*}^*\}$ and $\boldsymbol{\beta}^* = \{\beta_1^*, \beta_2^*, ..., \beta_{m^*}^*\}$ are coefficients of the surrogate model determined by the method of least squares.

B. 2-step design adjustment of critical KCCs – The 2-step design adjustment focuses on reducing production fallout of faulty components at minimal increase in costs of manufacturing due to adjusted tolerance of critical KCCs. KPCs such as gaps or inclinations between mating parts are required for normal functioning of the product. Faulty KPC, such as interference instead of clearance, lead to malfunctioning of the component. A range of dimensions for KPC$_i$ liable to cause

product malfunctioning is defined as a failure region $FR_i=[LFL_i, UFL_i]$ where the lower and upper failure levels are LFL_i and UFL_i respectively.

In this step, adjustment of the nominal and tolerances of critical KCCs is done to reduce production fallout of KPC_i within the failure region FR_i. To address this, a two-step design adjustment is suggested: (1) nominal change of critical KCCs; and (2) tolerance reallocation of critical KCCs based on the adjusted nominal.

Furthermore, it is assumed that the nominal change of KCCs can be achieved at no additional cost of manufacturing while tolerance reallocation is accompanied by an increase in cost of manufacturing.

The critical elements in the 2-step design adjustment are the surrogate models of faulty KPCs developed by *diagnosis via scalable surrogate modelling for KCC dimensionality*. The surrogate models links faulty KPCs with few critical KCCs closely related to the faulty KPCs.

The two steps of the proposed design adjustment process are described as follows:

- **Step B.1: Nominal change of KCCs** – Nominal adjustment of KCCs is performed to minimize the total production yields of faulty KPCs. Let g_i be the probability distribution of the dimensional variations of ith faulty KPC y_i. The production fallout of KPC y_i is obtained as

$$M_i = \int_{LFL_i}^{UFL_i} g_i(y_i) dy_i \tag{5.5}$$

The constrained optimization problem to minimize total production yield of all the faulty KPCs is described as follows:

$$\text{Minimize,} \sum_{i=1}^{r} M_i \text{ , Subject to } \quad \begin{array}{c} x_j \sim N(\mu_j + \delta_j, \dfrac{T_j}{6C_{p_k}}) \\[3mm] \delta_j^{lower} \leq \delta_j \leq \delta_j^{upper} \end{array} \qquad (5.6)$$

Here, μ_j =Initial design nominal of x_j

T_j = Tolerance of x_j

C_{p_k} = Process capability of manufacturing x_j

δ_j = Nominal change applied to x_j

δ_j^{lower} and δ_j^{upper} =Allowable lower and upper limits of nominal change due to manufacturing constraints.

KCCs are assumed to follow normal distribution. The probability distribution g_i of the faulty KPC$_i$ depends on the probability distribution of the critical KCCs and can be derived as a function of the probability distribution of the individual KCCs. The mapping of the probability distribution of KPC$_i$ from the probability distributions of the individual KCCs is enabled by the surrogate model of KPC$_i$. Since the surrogate model might have a higher order polynomial and multiplicative terms, KPC$_i$ is not a linear combination of the critical KCCs related to it. In this case, g_i might not be derivable as a closed-form function of the normal distributions of the individual KCCs. Therefore, kernel density estimation (KDE) is applied to approximate the integral in Equation (5.5).

The optimization problem prescribed in Eq. (5.6) can be solved by meta-heuristic search techniques such as Genetic Algorithm. Let M_i' be the reduced production yield of faulty KPC$_i$ after nominal change of the critical KCCs.

- **Step B.2: Tolerance reallocation of KCCs -** Adjustment of tolerance is accompanied by change in cost of manufacturing. The cost of manufacturing particularly related to tolerance reallocation of assembly KCCs is referred to as cost of tolerancing. A tighter tolerance with less variation requires higher cost of tolerancing. Chase (1999) suggests several methods to calculate the cost of tolerancing from tolerance of individual assembly dimensions. In this chapter, cost of tolerancing is modelled using the reciprocal squared relationship between the cost and the required tolerance of KCC. The cost of tolerancing required to achieve a tolerance T_j of KCC_j is calculated as,

$$C_j = A_j + \frac{B_j}{T_j^2} \qquad (5.7)$$

where A_j and B_j are user-defined constants for the tolerancing cost model.

Moreover in this step, cost of quality loss due to unwanted variations in KPCs, such as warranty cost, is also taken into consideration. The cost of quality loss (C_W) is proportional to fallout of faulty KPCs and is given by,

$$C_W = D \times \sum_{i=1}^{n} M_i' \qquad (5.8)$$

where D is the cost of quality loss per failure.

The optimization problem of determining tolerance reallocation of critical KCCs focus on minimization of the total cost incurred due to cost of tolerancing and the cost of quality loss. Eq. (5.9) formulates the tolerance reallocation.

Minimize, Total Cost $= \sum_{j=1}^{d} a_j C_j + C_W$, Subject to $x_j \sim N(\mu_j + \delta_j^{opt}, \frac{T_j}{6 C_{p_k}})$ (5.9)

Here, $a_j=0$ if j^{th} KCC is selected as a critical one for at least of the else $a_j=1$ if not. δ_j^{opt} is the optimal nominal change of x_j determined in *Step B.1*. A_j and B_j are constants which determine fixed and variable costs of producing tolerance T_j. Rest of the variables has same meaning as in the nominal change optimization problem formulated in Eq. (5.6).

The optimization problems in *Steps B.1* and *B.2* are solved by Genetic Algorithm with settings as follows: (1) Population size: 20 chromosomes; (2) No. of generations: 150; (3) Crossover rate: 0.80; and (4) Mutation rate: 0.20.

5.4 Case Study

The proposed methodology for corrective action of product failures due to dimensional variations of KPCs is demonstrated with an industrial case study of automotive ignition switch. Corrective action is suggested for a warranty failure related to the ignition switch. Figure 5.3 presents an exploded view of the ignition switch showing individual components 1-5.
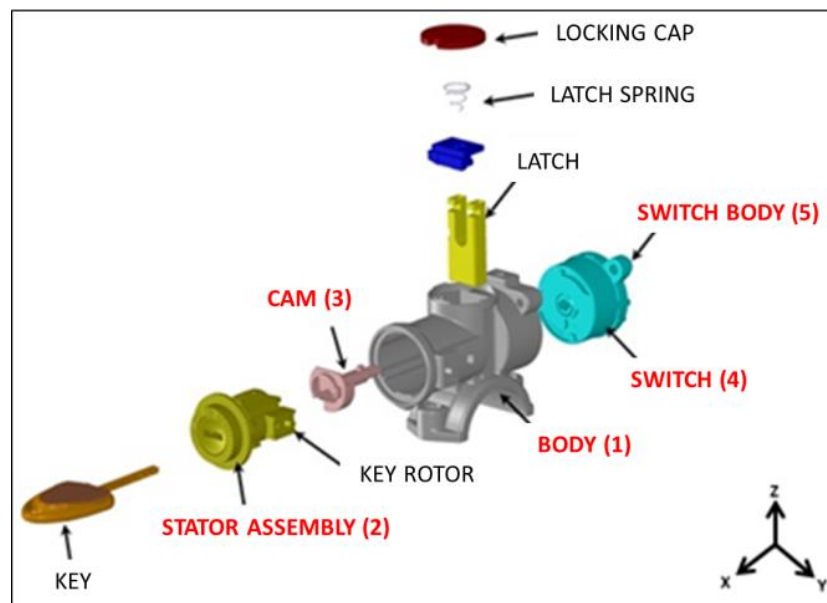
Figure 5.3: Exploded view of automotive ignition switch with individual parts

A warranty failure directly related to ignition switch is *'Sticky key'* whereby when the key is turned from *Ignition* to *Start* position, the ignition switch malfunctions and the key is incapable of returning to *Ignition* position by an internal spring-back action due to interference between mating surfaces of individual parts.

Moreover, there is a consequential warranty failure caused by the aforementioned malfunction. Overstay of the key at the *Start* position allows excessive current to flow through starter motor resulting in *'Starter motor burnout'*, which is an electro-mechanical failure *i.e.* consequential electrical failure caused by dimensional variations of internal components of the ignition switch which is a type-I mechanical assembly.

Results of the case study are presented in two parts as follows: (A) diagnosis via scalable surrogate modeling for KCC dimensionality; and, (B) 2-step design adjustment via nominal change followed by tolerance reallocation of critical KCCs. The results are detailed as follows:

- **Case study results of part A:** Diagnosis via scalable surrogate modelling for KCC dimensionality is described in the following four steps:

  - *Step A.1: Identify faulty KPCs* - Warranty data is analysed to find 'Sticky Key' and 'Start motor burnout' incidents reported by customers. The ignition switch is found to be replaced for both failures. The fault tree diagram of 'Sticky key' problem as shown in Figure 5.4 identifies that the misalignment of stator within the body of the ignition switch is a potential cause of the failure.
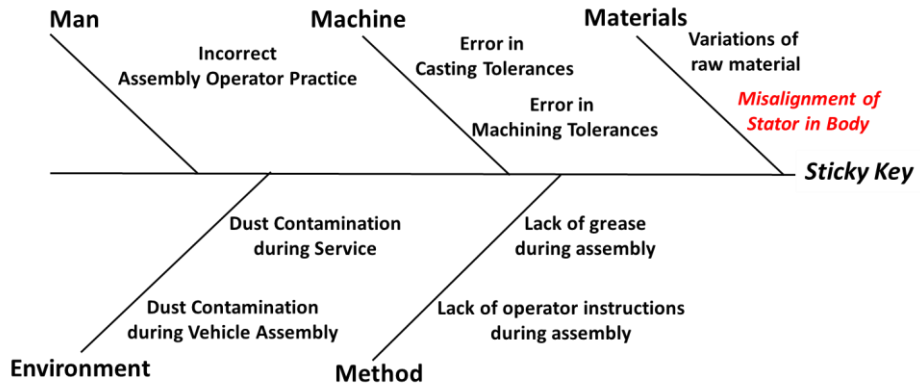
Figure 5.4: Fault tree diagram of 'Sticky key' failure in ignition switch

X-Ray Computer Tomography (CT) scanning of faulty ignition switches shows that misalignment of the stator within the body causes interference between the lock and the cam. This is illustrated in Figure 5.5.
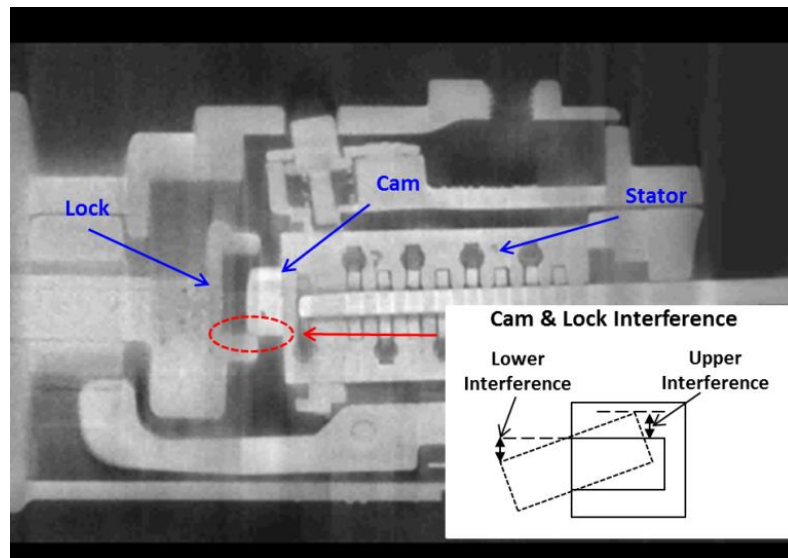
Figure 5.5: Lock & cam interference due to stator

In this case study, the gap between the lock and the cam is taken into consideration as KPC, which in the case of clearance allows free rotation of the cam inside the lock but in case of interference causes the '*Sticky key*' failure. Measurements from a sample of failed ignition

switches show interferences of more than 0.02 mm has caused both *'Sticky key'* and *'Starter motor burnout'* failures. Hence, the objective of this case study is to reduce production fallout of ignition switches with lock-cam interference of more than 0.02 mm. The KPCs required for the free movement of the key are clearance at both upper and lower ends of the cam and lock contact. Therefore, the KPCs are KPC_1=Upper Clearance and KPC_2=Lower Clearance. *'Sticky Key'* occurs in case of interference or faulty KPCs at either end.

o ***Step A.2: Conduct Variation Simulation Analysis of faulty KPCs*** *-* Datum flow chain (DFC) of the ignition switch is prepared from the nominal CAD of the ignition switch. Joints J_1-J_8 are the mating surfaces as shown in Figure 5.6. The cam and lock mating surface is indicated by joint J_4 . The VSA model used in this case study is Statistical Variation Analysis for Tolerancing (SVA-TOL) (Franciosa, *et al.*, 2010). KCCs are of two types: (i) Rotational-α, β and γ for rotations about x, y and z axis respectively; and (ii) Translational - Δx, Δy and Δz for movement along x, y and z axis respectively. A total of 24 KCCs can affect variation in the KPCs. All KCCs represent deviations from the original dimensions and therefore have a nominal of zero. SVA-TOL is run N=3000 times to generate the data for developing the surrogate models.
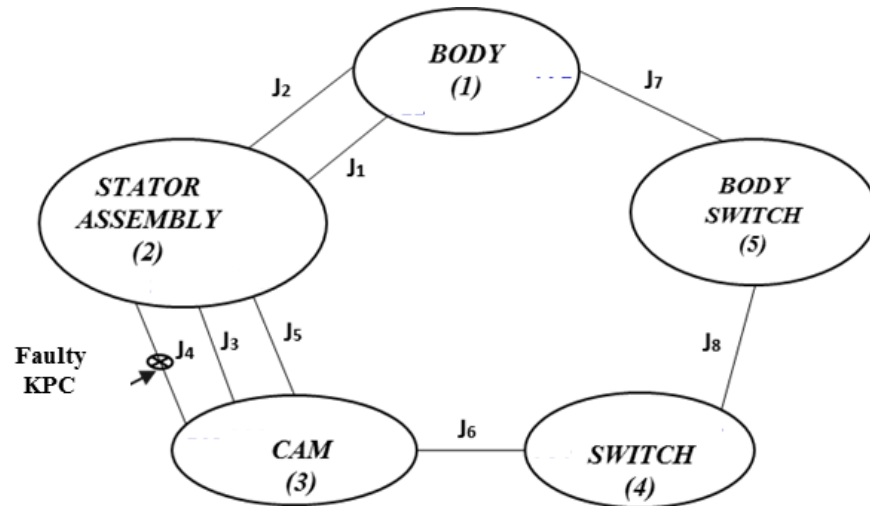
Figure 5.6: Datum Flow Chain of Ignition Switch

o *Step A.3: Identify critical KCCs and their interactions related to faulty KPCs* - The optimal order of the polynomial identified by PFS for both KPCs is $p^*=3$ in this case study. The Forward Selection-Backward Elimination algorithm selects the critical KPCs by fitting 1st, 2nd and 3rd order surrogate models successively. 5 fold cross validation is performed to determine selection or elimination of a feature. The total number of candidate polynomial terms with multiplicative interaction is $24+24^2+24^3=14424$ out of which 4 critical terms are identified by PFS for each KPC. Critical KCCs present in these terms are 3 and 5 at model $R^2 = 0.901$ and 0.923 for KPC_1 and KPC_2 respectively. Table 5.1 summarizes the results of PFS.

Table 5.1: Results of Polynomial Feature Selection for diagosis
to identify critical KCCs

Initial design nominal	Total no. of KCCs	No. of critical KCCs	Critical KCCs
Upper clearance (KPC$_1$)	24	3	$\beta_2, \beta_3 \,\&\, \beta_{11}$
Lower clearance (KPC$_2$)	24	5	$\beta_2, \beta_3, \beta_{11}, \Delta x_{F21} \,\&\, \Delta x_{23}$

- o **Step A.4: Develop Surrogate Model of faulty KPCs from critical KCCs** - Based on the critical KCCs identified in the previous step, the final surrogate model is built using the full training data. The final surrogate models are as follows:

$$FR_1 = 1.16 \times 10^{-5} + 1.61\beta_{F42} - 1.63\beta_{F43} + \beta_{F43}(2.47\beta_{F11} - 4.66\beta_{F43}) \quad (5.10)$$

$$FR_2 = -4.22 \times 10^{-4} - 1.58\beta_{F42} + 1.56\beta_{F43}$$
$$+ \beta_{F11}\Delta x_{F21}(37.01\Delta x_{F21} - 45.91\Delta x_{F53}) \quad (5.11)$$

3-D plots of the surrogate models are shown in Figures 5.7 (a) and (b).
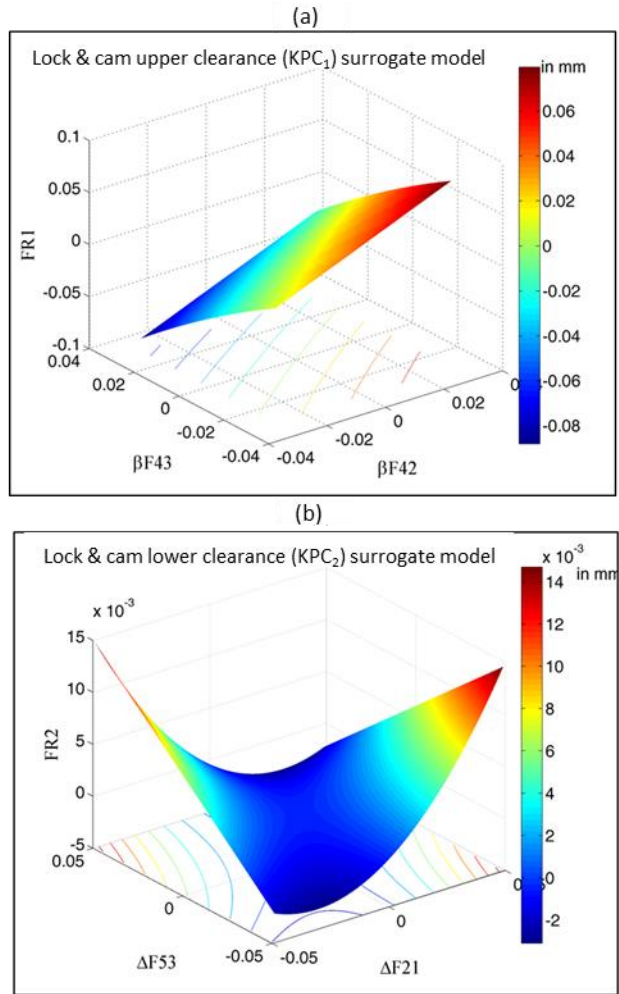
Figure 5.7: Surrogate models of (a) Upper; and (b) Lower Clearance

- **Case Study Results Part (B): 2-step design adjustment of critical KCCs** – The surrogate models developed in the previous step are used for the two step design adjustment to reduce production yield of faulty KPCs. The input to the optimization models related to the design adjustment process are listed in Table 5.2.

Table 5.2: Input to two-step design adjustment

Input to GA / KCCs	Initial Tolerance (T_{KCC}) (in radians or mm**)	LB-UB* for Nominal change (radians or mm)	Process Capability	Fixed Cost of Tolerancing (A) (in monetary units)	Variable Cost of Tolerancing (B) (in monetary units)
β_{F42}	0.08			6.75	1.20
β_{F43}	0.08			2.80	2.75
β_{F11}	0.20	0-0.1	1.33	4.50	0.88
Δ_{F21}	0.13			2.80	2.75
Δ_{F53}	0.13			2.80	2.75

*LB – Lower Bound & UB – Upper Bound ; **radians for rotational KCCs & mm for translational KCCs

Results of nominal change and tolerance reallocation of KCCs are detailed as follows:

- o *Step B.1: Nominal adjustments of critical KCCs* – The nominals of the critical KCCs are adjusted to minimize the total fallout of faulty KPCs. In this stage, minimization is done by keeping the tolerance constant. Therefore manufacturing costs related to nominal change is assumed to be negligible. Due to the manufacturing constraints upper and lower bounds of the nominal change of each KCC is specified.

    The nominal change in this step reduces *'Sticky key'* cases from 38.82% to 13.34%.

- o *Step B.2: Tolerance reallocation of critical KCCs* – In this case study, the cost of quality loss due to unwanted dimensional variations of KPCs is derived from the cost of warranty failure of the ignition switch. To demonstrate the impact of the tolerance reallocation on failures and related costs, this step in done in the following two ways – (1) only tolerance reallocation assuming nominal change have not been done; and, (2) tolerance reallocation following nominal change. As shown by

results in Table 5.3, only tolerance reallocation reduces percentage of *'Sticky Key'* cases from 38.82% from 7.97% but at a total cost which is highest among the three types of design adjustments.

Summary of results

Summary of results is presented as follows: Table 5.3 presents a summary of the adjusted nominal and tolerance of the critical KCCs and associated cost of warranty and cost of tolerancing. Figure 5.8 shows percentage of faulty KPC_1 and KPC_2 before and after the corrective action (CA). Next Figure 5.9 shows cost of tolerancing and cost of warranty before and after CA. Furthermore, *cost-benefit* analyses are shown in Figure 5.10 for the following three types of CA: (1) Nominal change; (2) Tolerance reallocation; and (3) Nominal change followed by tolerance reallocation. For *cost-benefit* analysis in case of each of the three aforementioned types of corrective action, cost of tolerancing is the "*cost*" component and decrease in cost of warranty after performing the corrective action is the "*benefit*" component.

Table 5.3: Summary of results of corrective actions of warranty failure in automotive ignition switch

CAs / Results	Before CA	After CA		
		Only Nominal Change	Only Tolerance Reallocation	Nominal Change & Tolerance Reallocation
Nominals of KCCs $[\beta_{F42}, \beta_{F43}, \beta_{Fl1}, \Delta_{F21}\Delta_{F53}]$ (in radians or mm)	[0, 0, 0, 0, 0]	[0.025, 0.014, 0.1, 0.1, 0]	[0, 0, 0, 0, 0]	[0.024, 0.0142, 0.10, 0.10, 0]
Std. Dev. of DPs $[\beta_{F42}, \beta_{F43}, \beta_{Fl1}, \Delta_{F21}\Delta_{F53}]$ (in radians or mm)	[0.08, 0.08, 0.20, 0.13, 0.13]	[0.08, 0.08, 0.20, 0.13, 0.13]	[0.005, 0.005, 0.024, 0.016, 0.016]	[0.007, 0.008, 0.019, 0.015, 0.016]
% of Faulty FR_1	19.68	6.36	4.13	1.64
% of Faulty FR_2	19.14	6.98	3.84	2.76
% of *'Sticky Key'*	38.82	13.34	7.97	6.39
Cost of Tolerancing (in monetary units)	997	997	2822	1584
Cost of Warranty (in monetary units)	5775	1980	1190	648
Total Cost (in monetary units)	6772	2977	4012	2232
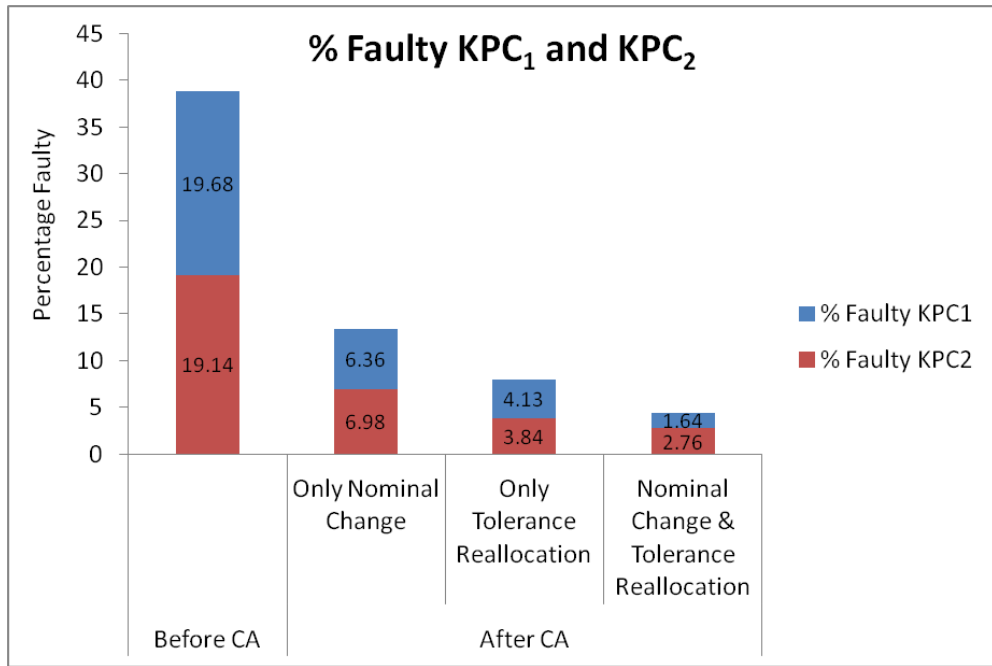
Figure 5.8: Percentage faulty KPC_1 and KPC_2 before and after corrective action
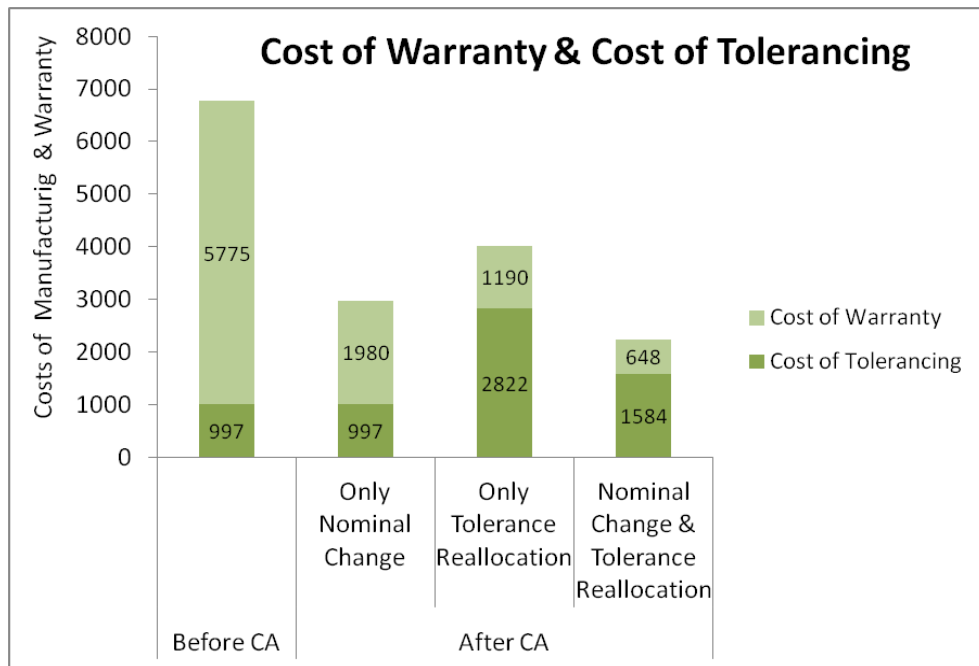
Figure 5.9: Cost of tolerancing and warranty before and after corrective action

211
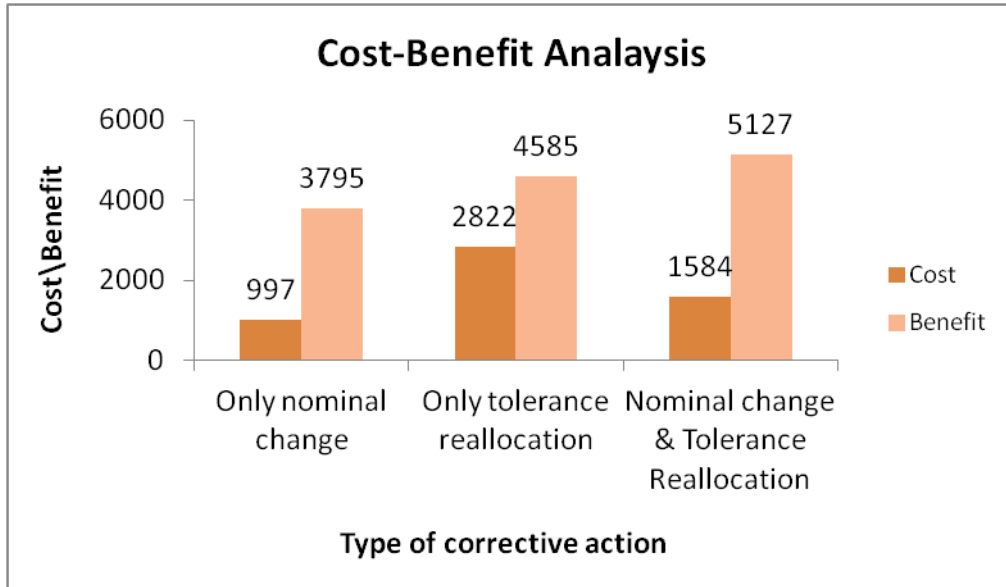
Figure 5.10: Cost-benefit analysis of corrective actions

Discussion of Results – The significance of results from the case study is discussed based on the following three aspects:

i. *Dimensionality reduction for identification of critical KCCs affecting faulty KPCs* – The scalable surrogate modelling approach identified 3 and 5 critical KCCs from a total of 24 for KPC_1 and KPC_2 respectively. Reducing the number of KCCs is crucial as tolerance re-allocation incurs cost, which will be lesser when fewer KCCs are adjusted.

ii. *Sensitivity Analysis of faulty KPCs with respect to critical KCCs* – The surrogate models expresses the faulty KPCs as analytical response functions of critical KCCs. For complex assemblies analyzed by numerically intractable VSA models, the KPC surrogate models can be utilized as closed-form assembly response functions (ARF) integrating KPCs with KCCs. Availability of ARF enables sensitivity analysis of the KPCs with respect the KCCs which

is crucial for traditional approaches of tolerance allocation (Chase, 1999) during type-I assembly process design.

iii. *Corrective action of product failures* – Overall, the surrogate models have expressed faulty KPCs as analytical response of critical KCCs and their interactions. Closed-form relations between faulty KPCs and critical KCCs have been used in determining production fallout of faulty KPCs, which is then minimized by the proposed two-step design adjustment. As indicated in the results, the best approach for corrective action to achieve minimization of fallout of faulty KPCs, in this case, is nominal change followed by tolerance reallocation. This approach minimizes both the fallout of faulty KPCs and total the cost given by the sum of warranty and tolerancing costs.

It is noteworthy from Figure 5.8 that the total percentage of faulty KPCs is over 38 %. This high initial percentage of faulty cases can be explained by the ill-conditioned design of the ignition switch assembly wherein variations of lock and cam upper and lower clearances (KPC_1 and KPC_2) is affected by variations of critical KCCs (β_2, β_3 and β_{11}) which affects both the KPCs. When two KPCs share multiple critical KCCs the assembly design is ill-conditioned. Under ill-conditioned design, the total percentage of faulty KPCs is high (Phoomboplab and Ceglarek, 2008; Huang, *et al.*, 2009)

5.5   Summary

In complex assemblies, dimensional variations in a KPC can be affected by variations in a large number of KCCs. Addressing the dimensionality of KCCs is crucial for design synthesis tasks such as the diagnosis of unwanted variations in KPCs by identification of few critical KCCs closely related to the KPC of interest.

Currently existing methods for the diagnosis of KPC variations have the following two limitations: (1) they do not address the dimensionality reduction of the original set of KCCs to identify fewer critical KCCs; and, (2) they rely on the in-depth understanding of the physical process governing the KPC-KCC interrelations through closed form *first-principle* models.

To address the aforementioned limitations, this chapter has developed an approach for the *diagnosis of unwanted variations in KPCs via scalable surrogate modelling for KCC dimensionalit*y. The proposed method is data-driven and is independent of the actual physical process through which variations in KCCs lead to variations in faulty KPCs. The critical KCCs are identified by Polynomial Feature Selection which searches through the original set of KCCs to determine a few critical KCCs and their multiplicative interactions through development of best fitting surrogate models linking the faulty KPCs with the critical KCCs.

Furthermore, *scalable surrogate modelling for KPC dimensionality* is developed in this chapter to address the corrective action of product failures triggered by dimensional variations of KPCs. Such failures occur in type-I assembly products, for which, though advanced Variation Simulation Analysis (VSA) models exist for estimating KPCs from KCCs, there is lack of systematic approach of corrective action of failures due to unwanted variations in KPCs which are closely related to the normal functionality of the assembly. To address this need, a systematic methodology of *scalable surrogate model driven corrective action* has been developed based on the following two interlinked approaches: (1) *diagnosis via scalable surrogate modelling for KPC dimensionality* to develop surrogate models of faulty KPCs in terms of few critical KCCs; and, (2) *two-step design adjustment* which utilizes the surrogate models to minimize production fallout of the faulty KPCs via nominal change followed by

214

tolerance reallocation of the critical KCCs.

The proposed methodology was demonstrated through an industrial case study on the warranty failures related to an automotive ignition switch. The results indicate a successful dimensionality reduction of KCCs from an initial set of twenty four KCCs to the final sets of three and five critical KCCs for KPC_1 and KPC_2, respectively. Furthermore, as a result of the proposed corrective actions, the total production yield of faulty KPCs is reduced from 38.82 % to 7.97 %.

Acknowledgements

CHAPTER 6
CONCLUSIONS, CRITICAL REVIEW AND FUTURE WORK

This chapter summarizes the methodologies developed in this thesis and discusses the conclusions and overall findings derived from the research presented in the previous chapters. Moreover, a critical review of the proposed methods in terms of advantages and limitations is presented. A discussion on the computational effort required for developing scalable surrogate models is also given. Broader impact of the research in terms of engineering relevance and applications is also discussed. Furthermore, future work based on the current research is discussed.

6.1 Summary

In automotive industry, there is a growing expectation to improve the quality of integrated product and production system design solutions by design synthesis in order to reduce failures and subsequent engineering changes during ramp and consequential delays to launch of full-production. Design synthesis of automotive body-in-white (BIW) assembly system focuses on determining optimal Key Control Characteristics (KCCs) and Key Product Characteristics (KPCs) which optimize Key Performance Indicators (KPIs) related to the assembly system subject to design tolerances of KPCs and operating limits of KCCs. A critical element of design synthesis is the assembly response function (ARF) integrating KPCs with KCCs interrelations. However, design synthesis tasks driven by computer-based Variation Simulation Analysis (VSA) or physical experimentation involve two challenges: (1) lack of analytical ARF between KPCs and KCCs interrelations; and, (2) resource intensive simulation and experimentation.

Few studies were done in the past to address the aforementioned

challenges by surrogate models. However, there is lack of systematic approach to develop surrogate models which can adequately address the following three crucial characteristics of KPC-KCC interrelations: (1) varying deterministic non-linearity of KPCs as measured by number of local maximas and minimas; (2) varying stochasticity of KPC-KCC interrelations which can be measured by homo- to hetero-skedastic behaviour; and, (3) KCC dimensionality affecting a KPC of interest. The aforementioned challenges contribute to the fundamental requirements of many design synthesis tasks related to assembly system in automotive and aerospace industries.

To address the aforementioned challenges, this thesis proposed three fundamental methodological enablers for surrogate model development in design synthesis tasks in order to address the KPC-KCC interrelations with minimal knowledge about the underlying physical processes. The three proposed methodological enablers are: (1) *scalability for deterministic non-linearity of KPCs*; (2) *scalability for stochasticity of KPCs*; and, (3) *scalability for KCC dimensionality affecting variations in a KPC*.

The aforementioned three methodological enablers are developed in this thesis for *Scalable Design Synthesis* (SDS). The SDS framework is based on the following two interlinked approaches: (1) scalable surrogate models addressing the aforementioned three characteristic of KPC-KCC interrelations; and, (2) integration of the scalable surrogate models with optimization routines to determine optimal KPCs and KCCs for the given design synthesis task.

Based on the SDS framework three methodologies are developed each addressing a characteristic of the KPC-KCC interrelations.

Firstly, *scalable surrogate model driven fixture layout optimization* for sheet part assemblies addresses varying *deterministic non-linearity* of assembly KPCs

such as part-to-part gaps which are estimated by VSA for given fixture clamp locating layout (KCCs). The KPC surrogate models are utilized to determine optimal clamp layout.

Secondly, *scalable surrogate model driven joining process parameters selection* develops surrogate models of assembly joining KPC-KCC interrelations which can vary from homo-to hetero-skedastic behaviour. The homo- and hetero-skedastic surrogate models are then used for the following two tasks (1) multi-objective optimization of process efficiency and quality; and, (2) identification of process window and computation of acceptance rate.

Lastly, *scalable surrogate model driven corrective action for product failures* addresses the issue of *high dimensionality* of KCCs. Efficient diagnosis of failures due to dimensional variations of KPCs is achieved through dimensionality reduction of KCCs which identifies few critical KCCs closely related to the faulty KPCs. Surrogate models integrating the faulty KPCs with the identified critical KCCs are developed. The surrogate models are used for KCC adjustment to reduce production yield of faulty KPCs.

6.2 Conclusions

The Scalable Design Synthesis framework is expected to leverage and complement the capabilities of currently existing VSA softwares and physical experimentation to deliver quality design solutions within time constraints for design synthesis tasks related to assembly system. To this end, the major achievements of this thesis are summarized as follows:

i. *Scalable surrogate model driven fixture layout optimization*

The major achievement of this methodology is enabling the application of advanced VSA softwares in efficient design synthesis tasks such as fixture

218

layout optimization for sheet metal assemblies. The crucial element is development of scalable surrogate models of KPC-KCC interrelations from VSA. The proposed scalable surrogate models generate realistic VSA results for underlying KPC-KCC interrelations which have varying deterministic non-linearity. To achieve this, *scalable surrogate modelling for deterministic non-linearity* has been developed based on the following two novel methods:

A. *Greedy Polynomial Kriging* (*GPK*) − This method develops a novel approach of training Kriging surrogate models focusing on minimization of generalized prediction error on *unseen test samples*

B. *Optimal Multi Response Adaptive Sampling* (*O-MRAS*) − To reduce computation required for generating training data from VSA, O-MRAS provides a novel approach of accelerating convergence of *multiple* surrogate models using a *single* training sample

Optimization of fixture KCCs is done by utilizing the GPK surrogate models of part-to-part gaps (KPCs) to determine optimal fixture layout (KCCs).

The proposed methodology is applied to industrial case studies of sheet metal assemblies from automotive and aerospace industries. Comparison with state-of-the-art methods shows that predictive accuracy of GPK is on an average 55% higher than 2nd order polynomial regression, which is most commonly used for surrogate modelling in design synthesis. Moreover, O-MRAS accelerates convergence of multiple surrogate models faster than currently existing Uniform Random Sampling (URS) as demonstrated by the fact that surrogate models trained by O-MRAS are 35% more accurate than those trained by URS in same number of simulations.

ii. *Scalable surrogate model driven joining process parameters selection*

The main achievement of this methodology is enabling efficient use of physical experimentation for design synthesis tasks which lack *first-principle* based VSA models of KPC-KCC interrelations. The proposed methodology allows accurate characterization of stochastic behaviour of KPCs frequently observed in physical experimentation. This is achieved by *scalable surrogate modelling for KPC stochasticity* which identifies and characterizes varying stochasticity of KPC-KCC interrelations in design synthesis tasks such as joining process parameters selection.

Scalable surrogate modelling for KPC stochasticity is achieved by the following three steps:

A. *Development of homo-skedastic model of KPCs*

B. *Detection of hetero-skedasticity in the homo-skedastic models* via statistical hypothesis testing

C. *Enhancement of homo-skedastic models to characterize the hetero-skedastic behaviour* of KPCs detected by statistical hypothesis testing

Moreover, best fitting homo- and hetero-skedastic models are developed by Polynomial Feature Selection which focuses on minimization of generalized prediction error on *unseen test samples*.

Homo- and hetero-skedastic surrogate models are developed for joint KPCs of Body-in-White (BIW) assembly joining processes. The surrogate models are utilized in joining process parameters selection which includes the following two capabilities: (1) multi-objective optimization, which contrary to state-of-the-art methods on Laser Transmission Welding and Resistance Spot Welding, not only optimizes joining KPIs related to process efficiency such as cycle time, welding speed etc. in case of laser welding but also minimizes KPIs

related to process quality such as KCC-dependent hetero-skedastic variance in joint quality; and, (2) identification of process window and acceptance rate of the joining process taking into consideration homo- and hetero-skedasticity of joining process KPC-KCC interrelations.

The proposed methodology is applied to characterize the Remote Laser Welding (RLW) process for BIW assembly joining. Results from the case study provide the following two important insights about the RLW process:

A. *Presence of both homo- and hetero-skedastic KPCs* − Scalable surrogate modelling for the RLW joint KPCs shows that both homo- and hetero-skedastic joint KPCs are present in the RLW joining process. The presence of hetero-skedastic KPCs having KCC-dependent variance contributes to the results of joining process parameters selection being significantly different from that obtained from currently existing homo-skedastic surrogate models. For example, acceptance rate estimated by state-of-the-art 2nd order polynomial regression is on an average 41% higher than that computed using the proposed scalable surrogate models.

B. *Trade-off between process efficiency and process quality* – The major impact of presence of hetero-skedastic KPCs is the non-monotonic change in process quality over a monotonic change in process efficiency. This is illustrated by the variation of acceptance rate over the process window as explained below.

The process window determines the operating conditions of the joining process KCCs which can deliver joint KPCs within their design tolerances. However, KCCs which are within the process

window and which maximize process efficiency related KPIs might not deliver maximum process quality such as maximum acceptance rate. For example, in RLW if process efficiency needs to be maximized then maximum welding speed within the process window will be preferred for running the process. However, maximum welding speed might not give maximum acceptance rate. Consequently there is a trade-off between KPIs related to process efficiency and quality.

The proposed methodology provides the capability to analytically address the trade-off between KPIs related to process efficiency and quality.

iii. *Scalable surrogate model driven corrective actions for product failures due to unwanted dimensional variations of KPCs –*

The main achievement of this methodology is a data-driven approach of addressing corrective action in a complex assembly without requiring in-depth understanding of the underlying physical process and experience based trial and error in KCC adjustment. The crucial element in this methodology is diagnosis of the assembly failure through dimensionality reduction of large number of KCCs found in complex assemblies. Overall, the proposed corrective action involves the following two approaches:

A. *Diagnosis via scalable surrogate modelling* of faulty KPCs to identify few critical KCCs and develop surrogate models of the faulty KPCs in terms of the identified critical KCCs

B. *Two step design adjustment* which takes as input the surrogate models of faulty KPCs and suggests optimal nominal change and tolerance reallocation of critical KCCs to minimize production yield of faulty

KPCs

The proposed methodology focuses on type-I assemblies for which though accurate VSA models exist to conduct forward analysis but there is lack of systematic approach of dimensionality reduction of KCCs required in tasks such as diagnosis of unwanted variations in KPCs. In complex type-I assembly products, dimensional variations of KPCs closely related to a failure mode can potentially be affected by variations in a large number KCCs. Due to numerical intractability of VSA models of complex assemblies involving a large number of KCCs, there is lack of information about critical KCCs closely related to the faulty KPC and a model of their specific relationship with the latter. This makes corrective action case specific and experience based trial-and-error reverse engineering. The proposed methodology reduces the dependency on case-by-case heuristic analysis by integrating failure modes with design models such as VSA via surrogate modelling of faulty KPCs in terms of few critical KCCs

The proposed approach is applied to reduce warranty failures related to an automotive ignition switch. Here, warranty failures caused by dimensional variations in KPCs of the switch are analyzed. Results show significant dimensionality reduction of KCCs. The number of critical KCCs identified for the faulty KPCs is on an average 83% less than the total number of KCCs present in the switch assembly. Moreover, the production yield of faulty switches can be reduced by 34 percentage points by following the KCC adjustments recommended in this study.

6.3 Critical Review

This section provides a critical review of the methodologies developed in this thesis. Firstly, advantages of the proposed approach are highlighted in Section 6.3.1. This is followed by a discussion about the limitations of the same in Section 6.3.2. Lastly, Section 6.3.3 discusses the positive and negative aspects related to computational effort required for developing surrogate models.

6.3.1 Advantages of scalable design synthesis

The advantages of the three scalable surrogate model driven design synthesis methods developed in this thesis are summarised as follows:

i. *Accurate surrogate models for deterministic VSA which provide computationally efficient approach of achieving quality design solutions within time constraints –*

This is demonstrated through a comparative study of time-constrained fixture layout optimization via direct integration of VSA with GA versus fixture layout optimization via surrogate modelling. For the two sheet metal assembly case studies described in Chapter 3, fixture layout optimization results are significantly better within given time constraints. Cost of quality is 80 % and 50% less when surrogate models are used for the doing the fixture layout optimization.

ii. *Identification of stochasticity in KPCs in absence of comprehensive and useful first-principle based models –* Design synthesis tasks lacking useful *first-principle* models rely on noisy experimentation data for developing KPC-KCC interrelations. Proposed scalable surrogate model allows accurate identification of the noise as KCC-independent/dependent variance through statistical hypothesis testing. This information is then used for characterising design synthesis requirements. Case study shows significant difference between results obtained via proposed approach and those obtained by state-of-the-art methods.

iii. Identification of critical KCCs closely related to a KPC of interest –For complex

assemblies identifying critical KCCs can be challenging because a large number of

KCCs can potentially affect a KPC. The proposed method of scalable surrogate

model identifies critical KCCs with least knowledge about the underlying physical

process governing the KPC-KCC interrelations.

Overall benefits of scalable design synthesis

The design synthesis tasks discussed in this thesis can be addressed by

trial-and-error approach whereby accurate results might be achieved through the

application of in-depth knowledge and experience of the physical processes. However,

experience-driven trial-and-error approach might not be feasible for design of

products and processes for at least the following two reasons: (i) product and process

design and requirements of design synthesis changes frequently and are case specific;

and (ii) knowledge and experience of the designer limits quality of design synthesis

solution.

Under the aforementioned conditions, scalable surrogate model driven

design synthesis provides an analytical and algorithmic approach of addressing design

synthesis requirements within time constraints.

6.3.2   Limitations of the proposed scalable design synthesis

Driven by requirements of the design synthesis tasks discussed in this

thesis, the proposed surrogate models individually address the following three

characteristics that are present in KPC-KCC interrelationships: (i) deterministic non-

linearity; (ii) stochasticity; and, (iii) KCC dimensionality. However, there might be

design synthesis tasks which require addressing more than one of the aforementioned

characteristics.

The limitation of the surrogate modelling methods (developed in Chapters 3, 4 and 5) is that they take into consideration each of the aforementioned three characteristics one at a time. Though the proposed methods are building blocks for the framework of Scalable Design Synthesis, they might not be sufficient for design synthesis tasks such as multi-station fixture layout optimization for batch of parts. Though deterministic VSA can be used to analyze fixture KCCs (for example clamp locations) and assembly KPCs (such as part-to-part gaps), multi-station fixture layout optimization for batch of parts introduces the following additional challenges:

- stochastic variation in KPCs due to variations of shape from one part to another

- potential high dimensionality of KCCs related to a KPC due coupling of KCCs between multiple stations

Under the aforementioned conditions, there is requirement to further enhance the proposed methods to address more than one of the three characteristics namely deterministic non-linearity, stochasticity and KCC dimensionality present in KPC-KCC interrelations.

Future work discussed in Section 6.4 outlines an approach to address multiple characteristics present in KPC-KCC interrelations.

6.3.3   Review of computational effort in scalable design synthesis

Computational effort is an important aspect for developing surrogate models. This section reviews the advantages and disadvantages with respect to computational effort required for developing scalable surrogate models. Moreover, overall benefit obtained via the scalability effort is also described. The discussion is based on the design synthesis task of fixture layout optimization for which computational time is a crucial aspect.

226

Let us introduce few notations followed by a brief recapitulation of the surrogate modelling approach for fixture layout optimization.

Notations

N   Number of iterations performed by the surrogate modelling process

$t_{\text{VSA}}^{(\text{N})}$ Computational time spent on running VSA till N^{th} iteration

$t_{\text{OK}}^{(\text{N})}$ Time taken to run OK till N^{th} iteration

$t_{\text{GPK}}^{(\text{N})}$ Time taken to run GPK till N^{th} iteration

$t_{\text{Total-OK}}^{(\text{N})}$ Total computational time taken for training OK models till N^{th} iteration

$t_{\text{Total-GPK}}^{(\text{N})}$ Total computational time taken for training GPK models till N^{th} iteration

For fixture layout optimization, a computationally expensive VSA is used to estimate assembly KPCs from given fixture KCCs. For the door inner panel-hinge assembly discussed in Chapter 3, one run of VSA takes on an average 22 minutes. Both OK (state-of-the-art method) and GPK (proposed method) are used to develop surrogate models of KPC-KCC interrelations based on VSA. The surrogate models are developed by the iterative process discussed in Section 3.3 of Chapter 3. In each iteration, <u>100 simulations</u> of VSA is ran. Therefore the computational time spent on running VSA till N^{th} iteration is given by

$$t_{\text{VSA}}^{(\text{N})} = 22 \times 100 + 22 \times 100 + ... \text{N time}$$ (6.1)

All the data generated till current iteration is used for training the surrogate models. Therefore, sample size of training data grows as $100, 2 \times 100, ..., N \times 100$. Due to increasing size of training data computational time required for running OK and GPK also increases. Let $t_{\text{OK}}^{(\text{N})}$ and $t_{\text{GPK}}^{(\text{N})}$ be the time taken to run OK and GPK till N^{th} iteration. Therefore total computational time till N^{th} iteration is the sum of $t_{\text{VSA}}^{(\text{N})}$ and time taken to build surrogate models till N^{th} iteration and is

given by

for *OK* as

$$t_{\text{Total-OK}}^{(N)} = t_{\text{VSA}}^{(N)} + t_{\text{OK}}^{(N)} \tag{6.2}$$

and for *GPK* as

$$t_{\text{Total-GPK}}^{(N)} = t_{\text{VSA}}^{(N)} + t_{\text{GPK}}^{(N)} \tag{6.3}$$

A key consideration is to run VSA till OK and GPK surrogate models attain degree of determination $R^2 \geq 0.90$. OK and GPK surrogate models reached the required R^2 in N=8 and N=2 iterations respectively. GPK has been ran for an additional two iterations to observe its performance with respect to R^2 and computational time.

Figure 6.1 and 6.2 shows R^2 and the computational time of OK and GPK models over N=1, 2…, 8 iterations.
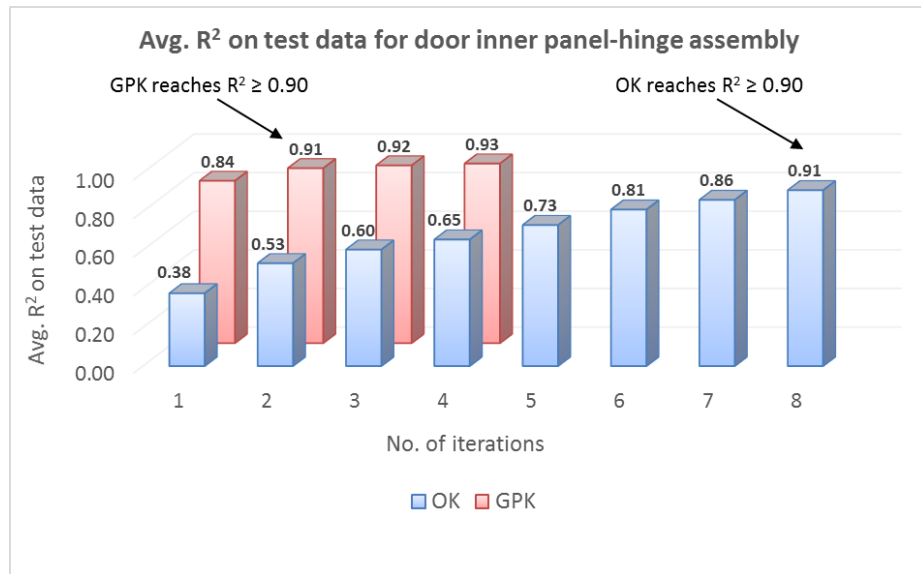
Figure 6.1: Comparison of degree of determination (R^2) of OK and GPK
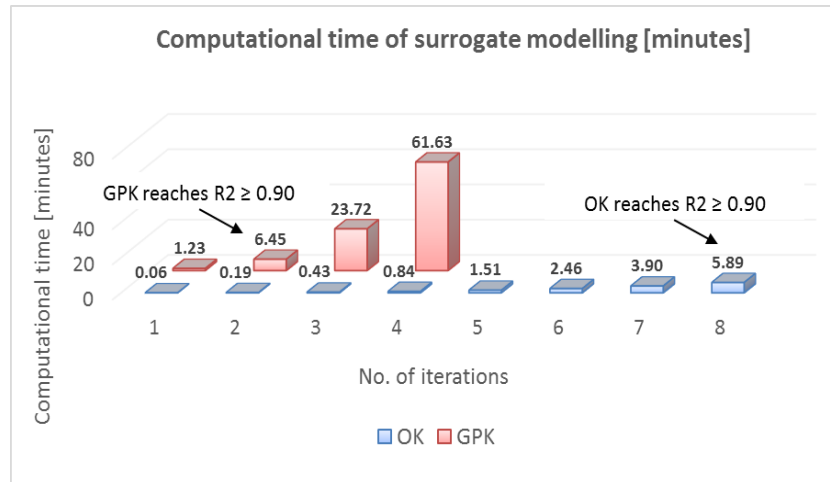
Figure 6.2: Comparison of computational time of surrogate modelling between OK and GPK

Figure 6.3 shows the total computational time of surrogate modelling which includes time taken by VSA and time taken by the surrogate modelling algorithms.
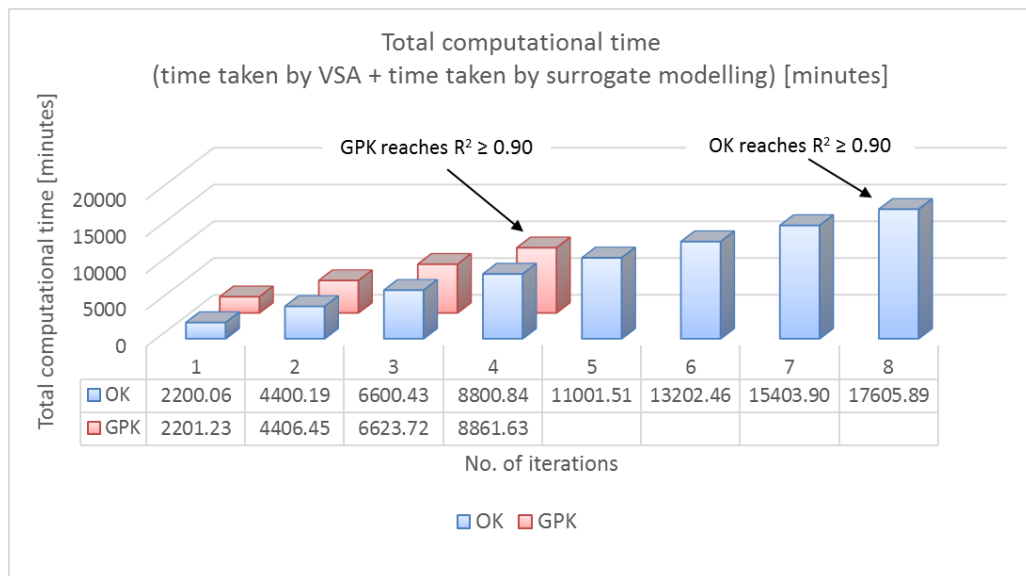

Figure 6.3: Comparison of total computational time of surrogate modelling between OK and GPK

Based on the results shown in Figures 6.1 and 6.2, the advantages and disadvantages with respect to computational time are as follows:

- Advantages: (i) GPK method reaches required accuracy in significantly less

229

number of iterations; and, (ii) a significant saving in total computational time is achieved through GPK which delivers surrogate models of desired accuracy in 4406.45 minutes which is appromimately $\frac{1}{4}$th of the total time taken by OK. Hence the main advantage is faster development of surrogate models.

- Disadvantages: (i) As shown in Figure 6.2, GPK takes significantly higher computational time than OK for the same number of samples in training data; and, (ii) rate of increase of computational time of GPK is higher than that of OK with increase in number of samples in training data. This disadvantage might be considerable if computational time of VSA is siginifcantly lower. However, for practical engnieering application, VSA with a low computational time might not be feasible.

Overall benefit of scalability

Despite higher computational time taken by GPK than OK for same number of samples in training data, the overall benefit achieved by GPK stems from the fact the total computational time taken by GPK is significantly less than that taken by OK. VSA models are computationally expensive. Therefore it is desirable to apply surrogate modelling methods such as GPK which can address the underlying non-linearity in the data and generate surrogate models of required accuracy in minimal total time of computation.

Minimising the total computational time is important for design synthesis tasks such as fixture layout optimization which rely on computationally expensive VSA.

A note on computational effort required for addressing stochasticity and KCC dimensionality

This thesis also addresses varying stochasticity and KCC dimensionality in the context of relevant design synthesis tasks discussed in Chapter 4 and 5 respectively. The primary objective of scalable surrogate models for varying stochasticity and KCC dimensionality have been to address limitations and challenges which state-of-the-art methods do not take into consideration such as effect of stochasticity in calculation of acceptance of joining process and identification of critical KCCs for corrective actions. Computational effort for design synthesis tasks such as joining process parameters selection and corrective actions of product failures as considered in the scope of this thesis might not be significant. However when similar design synthesis task will be needed over multiple assembly stations, a consideration of computational time will be required.

6.4 Future Work

In this thesis, methodologies have been developed to address the following three design synthesis tasks: (1) fixture layout optimization for sheet metal assemblies; (2) joining process parameters selection for automotive BIW assembly joining; and, (3) corrective actions of production failures due to unwanted dimensional variations in KPCs.

Future work related to the aforementioned three design synthesis tasks and requiring development of surrogate models is summarized as follows:

i. *Surrogate model driven robust fixture layout optimization* – In sheet metal assemblies, fixture KCCs such as clamp locating layout control KPCs such as part-

231

to-part gaps. The KPC-KCC interrelations are also affected by geometry of the parts. Due to variations in the stamping process, geometry of parts is subjected to variations and manifest as deviations from the nominal. This type of part variations is also called part shape error (Cai, *et al.*, 2009). The KPC-KCC interrelations depend on part shape errors. For a single part, fixture design analysis tool with negligible numerical error, gives deterministic estimates of KPCs for given KCCs. However, when a batch of parts is analysed, estimation of KPCs, subject to part shape errors, varies for given KCCs. The variations in KPCs due to shape error of parts can be treated as a stochastic noise. Therefore surrogate models for robust fixture layout optimization for a batch of parts would require addressing of KPC stochasticity originating from part shape errors.

To enable surrogate modelling driven robust fixture layout optimization, the proposed Greedy Polynomial Kriging (GPK) method can be extended to address stochastic KPCs. Depending upon requirements of the design synthesis task, the following two problem scenarios need to be addressed:

A. Magnitude of variation in KPCs due to part shape errors is comparable to KPC dimensions - In such cases, the design synthesis task might require estimation of the KPC variance. To address this need, GPK needs to be enhanced to predict both KPCs nominal as well as variance

B. Magnitude of variation in KPCs due to part shape errors is negligible compared to KPC dimensions – In such cases, KPC variation might be ignored without affecting the quality of the solution. To address this scenario, the negligible stochastic noise in KPCs can be eliminated through statistical methods such as Singular Value Decomposition.

232

After removal of the noise, the KPCs can be treated as deterministic and the GPK approach can be applied for surrogate model development.

ii. *Homo- and hetero-skedastic surrogate modelling of joint KPCs in multi material assemblies* – Joining processes such as Resistance Spot Welding, Remote Laser Welding etc. are applied for vehicle body assembly in industries such as automotive and aerospace. Vehicle bodies are made of sheet metal panels which are characterized by attributes such as material type, thickness and surface coating. A particular combination of these attributes is commonly known in the automotive industry as stack-up. Developing surrogate models for joint KPCs for different stack-up require conducting separate batches of experiments, which can be resource intensive. Future work needs to be done on methods which can provide the capability to reduce the number of experiments that need to be done to develop surrogate models of acceptable accuracy for a new stack-up. Existing data, surrogate models and similarity between stack-up attributes can be utilized to determine adaptive sample of KCCs required to run experiments for a new stack-up.

iii. *Design for service performance via surrogate modelling driven design optimization* – In this thesis, a scalable surrogate modelling driven corrective actions is proposed to address product service failures such as electrical malfunctioning caused by dimensional misalignment. The proposed methodology has been applied to the industrial case study on automotive ignition switch as a reactive approach of corrective action for warranty failures. In future, there is need to expand the proposed framework for developing methods which can proactively conduct product and process design optimization. Such methods will focus on

improving reliability of product performance in service. Warranty and other service related information from previous generations of products needs to be integrated with the design optimization during new product and process development. This should take into consideration the reliability and failure rate in design optimization to develop a comprehensive approach of *design for service performance*, which will go beyond currently existing methods of design for serviceability and maintenance which addresses design for ease of product maintenance and repair.

6.5 Broader Impact

Overall, the methodologies develop in this thesis are seen as building blocks of a broader engineering framework that seeks to create capabilities required for achieving shorter time-to-market with "*zero-defect*" production. Developing systematic approaches to achieving this target is important because in the face of growing market competition on a global scale manufacturers are often required to shorten time-to-market, which is closely dependent on integrated product and process design time and ramp-up time. To achieve this goal in a cost-efficient manner, manufacturers are also required to achieve "zero-defect" capabilities which entail (i) minimizing engineering changes after prototype release from design; and (ii) rapid identification and root cause analysis of production faults during ramp-up. Shorter time-to-market with "zero-defects-capabilities" allows a longer period of full production thereby generating higher return-on-investment.

Managing time-to-market with "zero-defect" capabilities is important especially for emerging manufacturing processes such as assembly of automotive body panels from remote laser welding (RLW). Successful integration of emerging

technologies with existing production systems requires understanding the capabilities and limitations of existing computer-aided engineering (CAE) tools and information and communications technologies (ICT) and developing systematic methodologies to complement CAE and ICT tools. The methodologies developed in this thesis contributes to developing a holistic research framework of *Lifecycle Analytics Development* (LAD) which includes research and development of tools to complete existing CAE and ICT tools.

LAD encompasses the ecosystem of research, development, verification & validation and implementation of key technical enablers required on top of and beyond current CAE and ICT tools to operationalize shorter time-to-market with "zero-defect" capabilities in product lifecycle. Under the framework of LAD, the key emphasis is given to development of approaches which allows integration of heterogeneous engineering models and data from different phases of product lifecycle such as design, manufacturing and field[2] through data exploration, visualization and machine learning to support or enable the application of CAE and ICT tools for different engineering tasks in the product lifecycle. Methods developed in the ecosystem of LAD are classified into two categories: (i) methods for *intra-loop* tasks; and, (ii) methods for *inter-loop* tasks (Ceglarek, *et al.* 2009).

Intra-loop tasks require data and models from the same phase of product lifecycle. Examples of *intra-loop* task include statistical process control (SPC) which uses manufacturing data for monitoring product quality. In design phase, design synthesis focusing on design optimization tasks such as fixture layout optimization, joining process parameters selection etc. uses simulation and experimentation data related to product and process design. Though necessary, simulation and

---

[2] Field phase starts in a product's lifecycle when it starts being used by the customer.

experimentation is not sufficient for achieving quality design synthesis results within time constraint. Therefore surrogate model such as those developed in this thesis are required to complement simulation/experimentation and enhance their practical applicability.

Inter-loop tasks require integration of data and models from more than one phase of the product lifecycle such as addressing warranty failures by using data from manufacturing and field phases of the product lifecycle (Mannar, *et al*., 2006). Inter-loop tasks such as root cause analysis and corrective actions of warranty failures creates a closed-loop product lifecycle management system which provides feedback from one phase to enable engineering task into another.

Methodologies related LAD act as crucial enablers to address *intra* and *inter* loop tasks such as the aforementioned ones. Scalable Design Synthesis proposed in this thesis fits into this broader framework of LAD and focusses particularly on integrated product and process design during the design phase

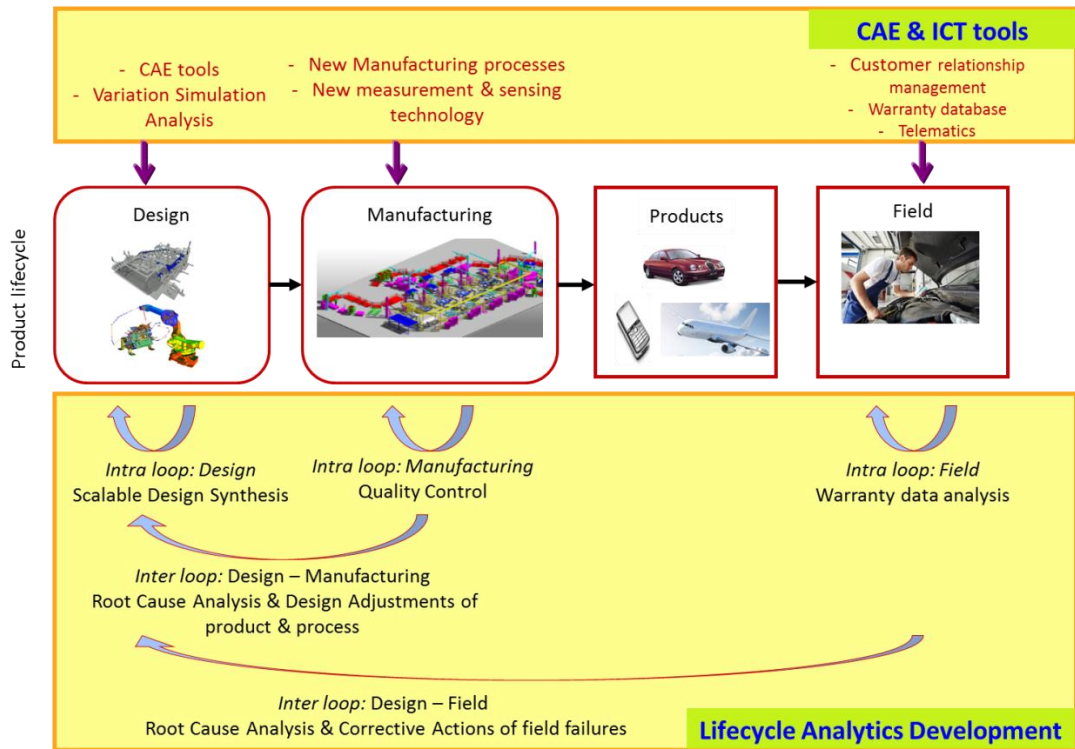Figure 6.1 shows the *intra* and *inter* loops under the research framework of LAD.

Figure 6.4: Lifecycle Analytics Development – intra and inter loop approaches

REFERENCES

Acherjee, B., Kuar, A. S., Mitra, S., Misra, D., & Acharyya, S., 2012. Experimental investigation on laser transmission welding of PMMA to ABS via response surface modeling. *Optics & Laser Technology,* 44(5), pp. 1372-1383.

Acherjee, B., Kuar, A. S., Mitra, S. & Misra, D., 2012. Modeling and analysis of simultaneous laser transmission welding of polycarbonates using an FEM and RSM combined approach. *Optics & Laser Technology,* 44(4), pp. 995-1006.

Acherjee, B., Misra, D., Bose, D. & Venkadeshwaran, K., 2009. Prediction of weld strength and seam width for laser transmission welding of thermoplastic using response surface methodology. *Optics & Laser Technology,* 41(8), pp. 956-967.

Antony, J., 2001. Simultaneous optimization of multiple quality characteristics. *International Journal of Advanced Manufacturing Technology,* Volume 17, p. 134–138.

Apley, D. W. & Shi., J., 1998. Diagnosis of multiple fixture faults in panel assembly. *Journal of Manufacturing Science and Engineering,* 120(4), pp. 793-801.

Apley, D. W. & Shi, J., 2001. A factor-analysis method for diagnosing variability in mulitvariate manufacturing processes. *Technometrics,* 43(1), pp. 84-95.

Aslanlar, S., Ogur, A., Ozsarac, U. & Ilhan, E., 2008. Welding time effect on mechanical properties of automotive sheets in electrical resistance spot welding. *Materials & Design,* 29(7), pp. 1427-1431.

Barton, R. R., 1998. *Simulation metamodel.* Washington, DC, USA, Proceedings of the 30th conference on Winter simulation, IEEE Computer Society Press .

Bea, M., Brockmann, R. & Havrilla, D., 2011. *Remote laser welding in automotive production.* [Online]
Available at: http://www.industrial-lasers.com/articles/print/volume-26/issue-5/features/remote-laser-welding-in-automotive-production.html
[Accessed 2014].

Ben-Ari, E. N. & Steinberg, D. M., 2007. Modeling data from computer experiments: an empirical comparison of kriging with MARS and projection pursuit regression. *Quality Engineering,* 19(4), pp. 327-338.

Benyounis, K. Y., Olabi, A. G. & Hashmi, M. S. J., 2005. Effect of laser welding parameters on the heat input and weld-bead profile. *Journal of Materials Processing Technology,* Volume 164, pp. 978-985.

Bilici, M. K. Y. A. İ. &. K. M., 2011. The optimization of welding parameters for friction stir spot welding of high density polyethylene sheets.. *Materials & Design,* 32(7), pp. 4074-4079.

Blight, B. J. N. & Ott, L., 1975. A Bayesian approach to model inadequacy for polynomial regression. *Biometrika,* 62(1), pp. 79-88.

Booker, A. J., 1996. *Case studies in design and analysis of computer experiments.* s.l., Proceedings of the Section on Physical and Engineering Sciences.

Cai, Z. Y., Wang, S. H., Xu, X. D. & Li, M. Z., 2009. Numerical simulation for the multi-point stretch forming process of sheet metal. *Journal of Materials Processing Technology,* 209(1), pp. 396-407.

Camelio, J. A. & Hu, S. J., 2002. Compliant assembly variation analysis using components geometric covariance. *In ASME 2002 International Mechanical Engineering Congress and Exposition,* pp. 431-437.

Camelio, J. A. & Hu, S. J., 2004. Multiple fault diagnosis for sheet metal fixtures using designated component analysis. *ASME Journal of Manufacturing Science and Engineering,* 126(1), pp. 91-97.

Camelio, J. A., Hu, S. J. & Ceglarek, D., 2004. *Impact of Fixture Design on Sheet Metal Assembly Variation.* s.l., In ASME 2002 International Design Engineering Technical Conferences and Computers and Information in Engineering Conference.

Camelio, J., Hu, S. J. & Ceglarek, D., 2003. Modeling variation propagation of multi-station assembly systems with compliant parts. *Journal of Mechanical Design,* 125(4), pp. 673-681.

Camelio, J., Hu, S. J. & Ceglarek, D., 2003. Modeling variation propagation of multi-station assembly systems with compliant parts. *Journal of Mechanical Design,* 125(4), pp. 673-681.

Carlson, J., 2001. Quadratic sensitivity analysis of fixtures and locating schemes for rigid part. *Journal of Manufacturing Science and Engineering,* Volume 123, p. 462–472.

Ceglarek, D. & Shi, J., 1995. Dimensional variation reduction for automotive body assembly. *Manufacturing Review,* 8(2), pp. 139-154.

Ceglarek, D. & Shi, J., 1996. Fixture failure diagnosis for autobody assembly using pattern recognition. *Journal of Manufacturing Science and Engineering,* 118(1), pp. 55-66.

Ceglarek, D. & Shi, J., 1999. Fixture failure diagnosis for sheet metal assembly with consideration of measurement noise. *ASME Journal of Manufacturing Science and Engineering,* 121(4), pp. 771-777.

Ceglarek, D., Huang, W., Zhou, S., Ding, Y., Kumar, R. & Zhou, Y., 2004. Time-based competition in multistage manufacturing: stream-of-variation analysis (SOVA) methodology-review. *International Journal of Flexible Manufacturing Systems,* 16(1), pp. 11-44.

Ceglarek, D., Prakash, Phoomboplab, Izquierdo L. E., 2009, Self-Resilient Production Systems: Going Beyong Design Robustness,
Keynote paper for the 2009 CIRP International Computer-Aided Tolerance Conference, March 26-27, Annecy, France.

Ceglarek, D., & Prakash, P. K. S., 2012. Enhanced piecewise least squares approach for diagnosis of ill-conditioned multistation assembly with compliant parts. In Proceedings of the Institution of Mechanical Engineers, Part B: Journal of Engineering Manufacture, 226(3), pp. 485-502.

Ceglarek, D., Colledani, M., Vancza, J. & Kim, D. Y., 2015. Rapid Deployment of Remote Laser Welding Processes in Automotive Assembly Systems. *CIRP Annals,* 64(1).

Chang, M. & Gossard, D., 1997. Modeling the assembly of compliant, non-ideal parts. *Computer-Aided Design,* 29(10), pp. 701–708.

Chang, M. & Gossard, D. C., 1998. Computational method for diagnosis of variation-related assembly problems. *International Journal of Production Research,* 36(11), pp. 2985-2995.

Chase, K. W., 1999. Tolerance allocation methods for designers.. *ADCATS Report,* 99(6), pp. 1-28.

Chase, K. W. & Parkinson, A. R., 1991. A survey of research in the application of tolerance analysis to the design of mechanical assemblies. *Research in Engineering design,* 3(1), pp. 23-37.

Chen, G., Zhou, J., Cai, W., Lai, X., Lin, Z. & Menassa, R., 2006. A framework for an automotive body assembly process design system. *Computer-Aided Design,* 38(5), pp. 531-539.

Chen, M. C., 2001. Tolerance synthesis by neural learning and nonlinear programming. *International Journal of Production Economics,* 70(1), pp. 55-65.

Chen, V. C., Tsui, K. L., Barton, R. R. & Meckesheimer, M., 2006. A review on design, modeling and applications of computer experiments. *IIE Transactions,* 38(4), pp. 273-291.

Chen, W. N. L. & Xue, J., 2008. Deformation control through fixture layout design and clamping force optimization. *International Journal of Advanced Manufacturing Technology,* 38(9-10), pp. 860-867.

Chen, X., Diez, M., Kandasamy, M., Zhang, Z., Campana, E. F. & Stern, F., 2014. High-fidelity global optimization of shape design by dimensionality reduction, metamodels and deterministic particle swarm. *Engineering Optimization,* 47(4), pp. 473-494.

Choi, H. G. R., Park, M. H. & Salisbury, E., 2000. Optimal tolerance allocation with loss functions. *Journal of Manufacturing Science and Engineering,* 122(3), pp. 529-535.

Couckuyt, I., Forrester, A., Gorissen, D., De Turck, F. & Dhaene, T., 2012. Blind Kriging: Implementation and performance analysis. *Advances in Engineering Software,* Volume 49, pp. 1-13.

Currin, C., Mitchell, T., Morris, M. & Ylvisaker, D., 1991. Bayesian prediction of deterministic functions, with applications to the design and analysis of computer experiments. *Journal of the American Statistical Association,* 86(416), pp. 953-963.

Darwish, S. M. & Al-Dekhial, S. D., 1999. Statistical models for spot welding of commercial aluminium sheets. *International Journal of Machine Tools and Manufacture,* 39(10), pp. 1589-1610.

Deb, K., Pratap, A., Agarwal, S. & Meyarivan, T. A. M. T., 2002. A fast and elitist multiobjective genetic algorithm: NSGA-II. *IEEE Transactions on Evolutionary Computation,* 6(2), pp. 182-197.

Ding, Y., Ceglarek, D., & Shi, J., 2000. Modeling and diagnosis of multistage manufacturing processes: part I: state space model. In Proceedings of the 2000 Japan/USA symposium on flexible automation, pp. 23-26.

Ding, Y., Ceglarek, D. & Shi, J., 2002. Design evaluation of multi-station assembly processes by using state space approach. *ASME Journal of Mechanical Design,* 124(3), pp. 408-418.

Ding, Y., Ceglarek, D., & Shi, J., 2002. Fault diagnosis of multistage manufacturing processes by using state space approach. *ASME Journal of Manufacturing Science and Engineering*, 124(2), 313-322.

Ding, Y., Jin, J., Ceglarek, D. & Shi, J., 2005. Process-oriented tolerancing for multi-station assembly systems. *IIE Transactions,* 37(6), pp. 493-508.

Dongxia, Y., Xiaoyan, L., Dingyong, H., Zuoren, N. & Hui, H., 2012. Optimization of weld bead geometry in laser welding with filler wire process using Taguchi's approach. *Optics and Laser Technology,* 44(7), pp. 2020-2025.

Dougherty, J., Kohavi, R. & Sahami, M., 1995. *Supervised and unsupervised discretization of continuous features.* s.l., Proceedings of the Machine Learning-International Workshop and Conference 1995.

Dubourg, V., Sudret, B. & Bourinet, J. M., 2011. Reliability-based design optimization using kriging surrogates and subset simulation. *Structural and Multidisciplinary Optimization,* 44(5), pp. 673-690.

ElMaraghy, H. A., 2005. Flexible and reconfigurable manufacturing systems paradigms. International Journal of Flexible Manufacturing Systems, 17(4), 261-276. Ford, 2010. *Engineering Specification-Laser Beam Welding-Stitch Welds,* s.l.: Ford Internal Document.

Forsberg, J. & Nilsson, L., 2005. On polynomial response surfaces and Kriging for use in structural optimization of crashworthiness. *Structural and multidisciplinary optimization,* 29(3), pp. 232-243.

Franciosa, P., Das, A., Ceglarek, D., 2014. *Design Synthesis Methodology for Dimensional Management of Assembly Process with Compliant non-Ideal Parts.* Toulouse, France, Joint Conference on Mechanical, Design Engineering & Advanced Manufacturing.

Franciosa, P., Gerbino, S. & Patalano, S., 2010. Variational modeling and assembly constraints in tolerance analysis of rigid part assemblies: planar and cylindrical features. *International Journal of Advanced Manufacturing Technology,* 49(1-4), pp. 239-251.

Franciosa, P., Gerbino, S. & Patalano, S., 2011. Simulation of variational compliant assemblies with shape errors based on morphing mesh approach. *The International Journal of Advanced Manufacturing Technology,* 53(1-4), pp. 47-61.

Fukumoto, S., Fujiwara, K., Toji, S. & Yamamoto, A., 2008. Small-scale resistance spot welding of austenitic stainless steels. *Materials Science and Engineering: A,* 492(1), pp. 243-249.

Gao, J., Chase, K. W. & Magleby, S. P., 1998. Generalized 3-D tolerance analysis of mechanical assemblies with small kinematic adjustments. *IIE Transactions,* 30(4), pp. 367-377.

Gao, Y. & Wang, X., 2008. An effective warpage optimization method in injection molding based on the Kriging model. *The International Journal of Advanced Manufacturing Technology,* 37(9-10), pp. 953-960.

Ghosal, A. & Manna, A., 2013. Response surface method based optimization of ytterbium fiber laser parameter during machining of Al/Al 2 O 3-MMC. *Optics & Laser Technology,* Volume 46, pp. 67-76.

Gorissen, D., Couckuyt, I., Demeester, P., Dhaene, T. & Crombecq, K., 2010. A surrogate modeling and adaptive sampling toolbox for computer based design. *The Journal of Machine Learning Research,* Volume 11, pp. 2051-2055.

Gu, H., 2010. Laser lap welding of zinc coated steel sheet with laser-dimple technology. *Journal of Laser Applications,* 22(3), pp. 87-91.

Gupta, A. & Apley, D. W., 2004. Singularity issues in fixture fault diagnosis for multi-station assembly processes. *Transactions of the ASME,* Volume 126, pp. 200-210.

Hamedi, M., Shariatpanahi, M. & Mansourzadeh, A., 2007. Optimizing spot welding parameters in a sheet metal assembly by neural networks and genetic algorithm. *Proceedings of the Institution of Mechanical Engineers, Part B: Journal of Engineering Manufacture,* 221(7), pp. 1175-1184.

Han, L., Thornton, M., Boomer, D. & Shergold, M., 2010. Effect of aluminium sheet surface conditions on feasibility and quality of resistance spot welding. *Journal of Materials Processing Technology,* 210(8), pp. 1076-1082.

Hartigan, J. A. & Wong, M. A., 1979. Algorithm AS 136: A k-means clustering algorithm. *Journal of the Royal Statistical Society. Series C,* 28(1), pp. 100-108.

He, X., Pearson, I. & Young, K., 2008. Self-pierce riveting for sheet materials: State of the art. *Journal of Material Processing Technology,* 199(1-3), pp. 27-36.

Hong, Y. S. & Chang, T. C., 2002. A comprehensive review of tolerancing research. *International Journal of Production Research,* 40(11), pp. 2425-2459.

Høst, G., 1999. Kriging by local polynomials. *Computational Statistics & Data Analysis,* 29(3), pp. 295-312.

Hu, M., Lin, Z., Lai, X. & Ni, J., 2001. Simulation and analysis of assembly processes considering compliant, non-ideal parts and tooling variations. *International Journal of Machine Tools and Manufacture,* 41(5), pp. 2233-2243.

Hu, S. J., 1997. Stream-of-variation theory for automotive body assembly. *CIRP Annals-Manufacturing Technology,* 46(1), pp. 1-6.

Huang, Q. & Shi, J., 2004. Stream of variation modeling and analysis of serial-parallel multistage manufacturing systems. *Journal of Manufacturing Science and Engineering,* 126(3), pp. 611-618.

Huang, W., Lin, J., Bezdecny, M., Kong, Z. & Ceglarek, D., 2007. Stream-of-Variation Modeling I: A Generic 3D Variation Model for Rigid Body Assembly in Single Station Assembly Processes. *ASME Transactions on Journal of Manufacturing Science and Engineering,* 129(4), pp. 821-831.

Huang, W., Lin, J., Kong, Z. & Ceglarek, D., 2007. Stream-of-Variation Modeling II: A Generic 3D Variation Model for Rigid Body Assembly in Multistation Assembly Processes. *ASME Transactions on Journal of Manufacturing Science and Engineering,* 129(4), pp. 832-842.

Huang, W., Phoomboplab, T. & Ceglarek, D., 2009. Process capability surrogate model-based tolerance synthesis for multi-station manufacturing systems. *IIE Transactions,* 41(4), pp. 309-322.

Huang, Z., Wang, C., Chen, J. & Tian, H., 2011. Optimal design of aeroengine turbine disc based on kriging surrogate models. *Computers & Structures,* 89(1), pp. 27-37.

Jakumeit, J., Herdy, M. & Nitsche, M., 2005. Parameter optimization of the sheet metal forming process using an iterative parallel Kriging algorithm. *Structural and Multidisciplinary Optimization,* 29(6), pp. 498-507.

Jayaprakash, G. & Sivakumar, K., 2010. Parametric Tolerance Analysis of Mechanical Assembly Using FEA and Cost Competent Tolerance Synthesis Using Neural Network. *Journal of Software Engineering and Applications,* 3(12), pp. 1148-1154.

Jeang, A., 1999. Optimal tolerance design by response surface methodology. *International Journal of Production Research,* 37(14), pp. 3275-3288.

Jin, J. & Shi, J., 1999. State space modeling of sheet metal assembly for dimensional control.. *Journal of Manufacturing Science and Engineering,* 121(4), pp. 756-762.

Jin, R., Chen, W. & Sudjianto, A., 2002. *On sequential sampling for global metamodeling in engineering design.* Montreal, Canada, ASME 2002 International Design Engineering Technical Conferences and Computers and Information in Engineering Conference.

Jou, M., 2003. Real time monitoring weld quality of resistance spot welding for the fabrication of sheet metal assemblies. *Journal of materials processing technology,* 132(1), pp. 102-113.

Kashyap, S. & DeVries, W. R., 1999. Finite element analysis and optimization in fixture design. *Structural optimization,* 18(2-3), pp. 193-201.

Khan, M. M. A., Romoli, L., Fiaschi, M., Dini, G. & Sarri, F., 2011. Experimental design approach to the process parameter optimization for laser welding of martensitic stainless steels in a constrained overlap configuration. *Optics & Laser Technology,* 43(1), pp. 158-172.

Kim, P. & Ding, Y., 2005. Optimal engineering system design guided by data-mining methods. *Technometrics,* 47(3), pp. 336-348.

Kim, T., Park, H. & Rhee, S., 2005. Optimization of welding parameters for resistance spot welding of TRIP steel with response surface methodology. *International Journal of Production Research,* 43(21), pp. 4643-4657.

Kim, Y. J. & Cho, B. R., 2001. The use of response surface designs in the selection of optimum tolerance allocation. *Quality Engineering,* 13(1), pp. 35-42.

Kleijnen, J., 2008. *Design and analysis of simulation experiments.* 15 ed. s.l.:Springer.

Kleijnen, J. P., 2009. Kriging metamodeling in simulation: A review. *European Journal of Operational Research,* 192(3), pp. 707-716.

Kleijnen, J. P. & Van Beers, W. C., 2004. Application-driven sequential designs for simulation experiments: Kriging metamodelling. *Journal of the Operational Research Society,* 55(8), pp. 876-883.

Koehler, J. & Owen, A., 1996. Computer Experiments. In: S. G. a. C. R. Rao, ed. *Handbook of Statistics.* New York: Elsevier Science, pp. 261-308.

Koenker, R., 1981. A note on studentizing a test for heteroscedasticity.. *Journal of Econometrics,* 17(1), pp. 107-112.

Koenker, R., 2005. *Quantile regression.* s.l.:Cambridge University Press.

Kohavi, R., 1995. A study of cross-validation and bootstrap for accuracy estimation and model selection. *Proceedings of International Joint Conference on Artificial Intelligence,* 14(2), pp. 1137-1145.

Kong, Z., Ceglarek, D. & Huang, W., 2008. Multiple fault diagnosis method in multistation assembly processes using orthogonal diagonalization analysis. *ASME Journal of Manufacturing Science and Engineering,* 130(1), pp. 773-780.

Koren, Y., & Shpitalni, M., 2010. Design of reconfigurable manufacturing systems. *Journal of Manufacturing Systems*, 29(4), 130-141.

Lai, X. M., Luo, A. H., Zhang, Y. S. & Chen, G. L., 2009. Optimal design of electrode cooling system for resistance spot welding with the response surface method. *The International Journal of Advanced Manufacturing Technology,* 41(3-4), pp. 226-233.

Lee, D. T. & Schachter, B. J., 1980. Two algorithms for constructing a Delaunay triangulation. *International Journal of Computer & Information Sciences,* 9(3), pp. 219-242.

Lee, K. H., 2005. Optimization of a driver-side airbag using kriging based approximation model. *Journal of Mechanical Science and Technology,* 19(1), pp. 116-126.

Liao, X. & Wang, G. G., 2005. Employing fractals and FEM for detailed variation analysis of non-rigid assemblies. *International Journal of Machine Tools and Manufacture,* 45(4), pp. 445-454.

Liao, X. & Wang, G. G., 2007. Non-linear dimensional variation analysis for sheet metal assemblies by contact modeling. *Finite Elements in Analysis and Design,* 44(1), pp. 34-44.

Li, B., Shui, B. W., & Lau, K. J., 2002. Fixture Configuration Design for Sheet Metal Assembly with Laser Welding : A Case Study. *International Journal of Advanced Manufacturing,* 19(7), pp. 501-509.

Li, B., Shiu, B. & Lau, K., 2001. Principle and Simulation of Fixture Configuration Design for Sheet Metal Assembly with Laser Welding. Part 1: Finite Element Modelling and a Prediction and Correction Method. *International Journal of Advance Manufacturing Technologies,* 18(1), pp. 266-275.

Li, B. & Shiu, B., 2001. Principle and Simulation of Fixture Configuration Design for Sheet Metal Assembly with Laser Welding. Part 2: Optimal Configuration design with the Genetic Algorithm. *International Journal of Manufacturing Technologies,* 18(1), pp. 276-284.

Li, M., Li, G. & Azarm, S., 2008. A kriging metamodel assisted multi-objective genetic algorithm for design optimization. *Journal of Mechanical Design,* 130(3).

Linkletter, C., Bingham, D., Hengartner, N., Higdon, D. & Kenny, Q. Y., 2006. Variable selection for Gaussian process models in computer experiments. *Technometrics,* 48(4), pp. 478-490.

Liu, C. & Hu, J., 1997. Variation simulation for deformable sheet assemblies using finite element methods. *ASME Journal of Manufacturing Science and Engineering,* 119(3), p. 368–374.

Liu, Y. G. & Hu, S. J., 2005. Assembly fixture fault diagnosis using designated component analysis. *Journal of Manufacturing Science and Engineering,* 127(2), pp. 358-368.

Li, Y. F., Ng, S. H., Xie, M. & Goh, T. N., 2010. A systematic comparison of metamodeling techniques for simulation optimization in decision support systems. *Applied Soft Computing,* 10(4), pp. 1257-1273.

Loose, J. P., Chen, N. & Zhou, S., 2009. Surrogate modeling of dimensional variation propagation in multistage assembly processes.. *IIE Transactions,* 41(10), pp. 893-904.

Lovison, A. & Rigoni, E., 2011. Adaptive sampling with a Lipschitz criterion for accurate metamodeling. *Communications in Applied and Industrial Mathematics,* pp. 110-126.

Luo, X., Li, X., Zhou, J. & Cheng, T., 2012. A Kriging-based hybrid optimization algorithm for slope reliability analysis. *Structural Safety,* 34(1), pp. 401-406.

Majumdar, D. &. M. I., 2011. Laser material processing. *International Materials Reviews,* 56(5-6), pp. 341-388.

Mannar, K., Ceglarek, D., F., N. & Abifaraj, B., 2006. Fault Region Localization: Product and Process Improvement Based on Field Performance and Manufacturing

Measurements. *IEEE Transactions on Automation Science and Engineering,* 3(4), pp. 423-439.

Mantripragada, R. & Whitney, D. E., 1999. Modeling and controlling variation propagation in mechanical assemblies using state transition models. *IEEE Transactions on Robotics and Automation,* 15(1), pp. 124-140.

Martin, J. D. & Simpson, T. W., 2004. *On the use of kriging models to approximate deterministic computer models.* s.l., ASME 2004 International Design Engineering Technical Conferences and Computers and Information in Engineering Conference, American Society of Mechanical Engineers.

Michalos, G., Makris, S., Papakostas, N., Mourtzis, D. & Chryssolouris, G., 2010. Automotive assembly technologies review: challenges and outlook for a flexible and adaptive approach. *CIRP Journal of Manufacturing Science and Technology,* 2(2), pp. 81-91.

Muhammad, N., Manurung, Y. H., Jaafar, R., Abas, S. K., Tham, G. & Haruman, E., 2013. Model development for quality features of resistance spot welding using multi-objective Taguchi method and response surface methodology. *Journal of Intelligent Manufacturing,* 24(6), pp. 1175-1183.

Odeha, I. O. A., McBratney, A. B. & Chittleborough, D. J., 1994. Spatial prediction of soil properties from landform attributes derived from a digital elevation model. *Geoderma,* 63(3), pp. 197-214.

Olabi, A. G., Casalino, G., Benyounis, K. Y. & Hashmi, M. S. J., 2006. An ANN and Taguchi algorithms integrated approach to the optimization of CO2 laser welding. *Advances in Engineering Software,* 37(10), pp. 643-648.

Padmanaban, G. & Balasubramanian, V., 2010. Optimization of laser beam welding process parameters to attain maximum tensile strength in AZ31B magnesium alloy. *Optics & Laser Technology,* 42(8), pp. 1253-1260.

Pal, A., Franciosa, P., & Ceglarek, D., 2014. Root cause analysis of product service failures in design-A closed-loop lifecycle modelling approach. In Proceedings of 24th CIRP Design Conference, Milan, Italy, pp. 165-170.

Pal, A., Franciosa, P., & Ceglarek, D., 2014. Corrective Actions of Product Service Failures via Surrogate Modelling of Dimensional Variations. In Proceedings of the 2014 Industrial and Systems Engineering Research Conference, Institute of Industrial Engineers, Montreal, Canada, pp. 2271-2280.

Phoomboplab, T. & Ceglarek, D., 2007. Design synthesis framework for dimensional management in multistage assembly system. *CIRP Annals - Manufacturing Technology,* 56(1), pp. 153-158.

Phoomboplab, T. & Ceglarek, D., 2008. Process Yield Improvement through Optimal Design of Fixture Layout in 3D Multi-station Assembly Systems. *ASME Transactions on Journal of Manufacturing Science and Engineering,* 130/061005.

Quan, N., Yin, J., Ng, S. H. & Lee, L. H., 2013. Simulation optimization via kriging: a sequential search using expected improvement with computing budget constraints. *IIE Transactions,* 45(7), pp. 763-780.

Ren, Y., Ding, Y. & Zhou, S., 2006. A data mining approach to study the significance of nonlinearity in multistation assembly processes. *IIE Transactions,* 38(12), pp. 1069-1083.

Rong, Q., Ceglarek, D., & Shi, J., 2001. Dimensional fault diagnosis for compliant beam structure assemblies. *ASME Journal of Manufacturing Science and Engineering,* 122(4), pp. 773-780.

Rong, Q., Shi, J. & Ceglarek, D., 2001. Adjusted least squares approach for diagnosis of ill-conditioned compliant assemblies. *ASME Journal of Manufacturing Science and Engineering,* 123(3), pp. 453-461.

Sacks, J., Schiller, S. B. & Welch, W. J., 1989. Designs for computer experiments. *Technometrics,* 31(1), pp. 41-47.

Sacks, J. W., J., W., Mitchell, T. J. & Wynn, H. P., 1989. Design and analysis of computer experiments. *Statistical Science,* 4(4), pp. 409-423.

Sathiya, P., Jaleel, M. A., Katherasan, D. & Shanmugarajan, B., 2011. Optimization of laser butt welding parameters with multiple performance characteristics. *Optics & Laser Technology,* 43(3), pp. 660-673.

Sathiya, P., Panneerselvam, K. & Soundararajan, R., 2012. Optimal design for laser beam butt welding process parameter using artificial neural networks and genetic algorithm for super austenitic stainless steel. *Optics & Laser Technology,* 44(6), pp. 1905-1914.

Shao, J., 1993. Linear model selection by cross-validation. *Journal of the American Statistical Association,* 88(422), pp. 486-494.

Shi, J., 2006. *Stream of variation modeling and analysis for multistage manufacturing processes.* s.l.:CRC Press.

Shi, J. & Zhou, S., 2009. Quality control and improvement for multistage systems: A survey. *IIE Transactions,* 41(9), pp. 744-753.

Shiu, B. W., Apley, D., Ceglarek, D. & Shi, J., 2003. Tolerance allocation for sheet metal assembly using beam-based model. *Transactions of IIE, Design and Manufacturing,* 35(4), pp. 329-342.

Shiu, B. W., Ceglarek, D. & Shi, J., 1996. Multi-stations sheet metal assembly modeling and diagnostics. *Transactions of North American Manufacturing Research Institution of SME,* pp. 199-204.

Simpson, T. W., Mauery, T. M., Korte, J. J. & Mistree, F., 2001. Kriging models for global approximation in simulation-based multidisciplinary design optimization. *AIAA Journal,* 39(12), pp. 2233-2241.

Simpson, T. W., Poplinski, J. D., Koch, P. N. & Allen, J. K., 2001. Metamodels for computer-based engineering design: survey and recommendations. *Engineering with computers,* 17(2), pp. 129-150.

Skowronski, V. J. & Turner, J. U., 1996. Estimating gradients for statistical tolerance synthesis. *Computer-Aided Design,* 28(12), pp. 933-941.

Skowronski, V. J. & Turner, J. U., 1997. Using Monte-Carlo variance reduction in statistical tolerance synthesis. *Computer-Aided Design,* 29(1), pp. 63-69.

Society, A. W., 1989. *Standard Welding Terms and Definitions, ANSI/AWS A3.0-89,* Miami, USA: American Welding Society.

Surjanovic, S. & Bingham, D., 2013. *Virtual Library of Simulation Experiments: Test Functions and Datasets.* [Online]
Available at: http://www.sfu.ca/~ssurjano/optimization.html
[Accessed 06 05 2015].

Toal, D. J., Bressloff, N. W., Keane, A. J. & Holden, C. M. E., 2011. The development of a hybridized particle swarm for kriging hyperparameter tuning. *Engineering optimization,* 43(6), pp. 675-699.

Varghese, P., Braswell, R. N., Wang, B. & Zhang, C., 1996. Statistical tolerance analysis using FRPDF and numerical convolution. *Computer-Aided Design,* 28(9), pp. 723-732.

Veitschegger, W. & Wu, C. H., 1986. Robot accuracy analysis based on kinematics. *IEEE Journal of Robotics and Automation,* 2(3), pp. 171-179.

Wang, G. G. & Shan, S., 2007. Review of metamodeling techniques in support of engineering design optimization. *Journal of Mechanical Design,* 129(4), pp. 370-380.

Wang, H. & Ceglarek, D., 2005. Quality-driven Sequence Planning for Compliant Structure Assemblies. *Annals of CIRP-Manufacturing Technology,* 54(1), pp. 31-35.

Wang, H. & Ceglarek, D., 2009. Variation propagation modeling and analysis at preliminary design phase of multi-station assembly systems. *Assembly Automation,* 29(2), pp. 154-166.

Wang, M. Y., Liu, T. & Pelinescu, D. M., 2003. Fixture kinematic analysis based on the full contact model of rigid bodies. *Journal of Manufacturing Science and Engineering,* 125(2), pp. 316-324.

Wang, X., Hao Chen, H., Liu, P. L., Zhang Y., Chuang H., Zhenuan Z., and Yuxuan G., 2013. Simulation and optimization of continuous laser transmission welding between PET and titanium through FEM, RSM, GA and experiments. *Optics and Lasers in Engineering,* 51(11), pp. 1245-1254.

Wang, X., Zhang, C., Wang, K., Li, P., Hu, Y. & Liu, H., 2012. Multi-objective optimization of laser transmission joining of thermoplastics. *Optics & Laser Technology,* 44(8), pp. 2393-2402.

Welch, W. J., Buck, R. J., Sacks, J., Wynn, H. P., Mitchell, T. J., & Morris, M. D., 1992. Screening, predicting, and computer experiments. *Technometrics,* 34(1), pp. 15-25.

White, H., 1980. A heteroskedasticity-consistent covariance matrix estimator and a direct test for heteroskedasticity. *Econometrica: Journal of the Econometric Society,* pp. 817-838.

Whitney, D. E., 2004. *Mechanical assemblies: their design, manufacture, and role in product development.* New York, USA: Oxford University Press.

Whitney, D. E., Gilbert, O. L. & Jastrzebski, M., 1994. Representation of Geometric Variations Using Matrix Transforms for Statistical Tolerance Analysis in Assemblies. *Research in Engineering Design,* 6(4), pp. 191-210.

Wu, F., Dantan, J. Y., Etienne, A., Siadat, A. & Martin, P., 2009. Improved algorithm for tolerance allocation based on Monte Carlo simulation and discrete optimization. *Computers & Industrial Engineering,* 56(4), pp. 1402-1413.

Xie, K., Wells, L., Camelio, J. A. & Youn, B. D., 2007. Variation propagation analysis on compliant assemblies considering contact interaction. *ASME Journal of Manufacturing Science and Engineering,* 129(5), pp. 934-942.

Xiong, C., Rong, Y., Koganti, R. P., Zaluzec, M. J. & Wang, N., 2002. Geometric variation prediction in automotive assembling. *Assembly Automation,* 22(3), pp. 260-269.

Yang, Y. S. & Lee, S. H., 1999. A study on the joining strength of laser spot welding for automotive applications. *Journal of Materials Processing Technology,* 94(2), pp. 151-156.

Hong-Chao Zhang, 1997). Advanced tolerancing techniques (Vol. 5). John Wiley & Sons.

Zhao, D., Wang, Y., Sheng, S. & Lin, Z., 2014. Multi-objective optimal design of small scale resistance spot welding process with principal component analysis and response surface methodology.. *Journal of Intelligent Manufacturing,* 25(6), pp. 1335-1348.

Zhao, Y., Zhang, Y., Hu, W. & Lai, X., 2012. Optimization of laser welding thin-gage galvanized steel via response surface methodology. *Optics and Lasers in Engineering,* 50(9), pp. 1267-1273.

Zhou, Q., Qian, P. Z. & Zhou, S., 2012. Surrogate Modeling of Multistage Assembly Processes Using Integrated Emulation. *Journal of Mechanical Design,* 134(1).

APPENDIX A

K-FOLD CROSS VALIDATION

K-fold cross validation is commonly used to compute the generalized prediction error of a predictive model f, which is measure of its average predictive error on unseen test samples. It is motivated by two fundamental problems in machine learning:

i.   *Model selection* – Most statistical predictive models requires tuning of model parameters. Examples of models parameters include parameters of the correlation function of a Kriging surrogate model, number of hidden layers of a neural network, number of leaves in a decision tree and others. Feature selection which involves finding a subset of the explanatory variables ($\mathbf{x}$) to be used as predictors in a model is special case of model selection. The objective of model selection is to determine optimal model parameters $\boldsymbol{\theta}^{*}$ or subset of features $\mathbf{x}^{*} \subseteq \mathbf{x}$ in case of feature selection which minimize the model's prediction error which is also called model loss function L as it measures the discrepancy between actual y and predicted $f(\mathbf{x}, \boldsymbol{\theta})$ response/target.

ii. *Performance estimation* – The prediction error or loss function L of a model for given parameters and explanatory variables is a measure of the model's performance. It is used to compare performance of different statistical predictive models.

An essential requirement of both model selection and performance estimation is that the measured prediction error or loss function should reflect true prediction error of the model observed on the entire population. However, estimation

of model's true prediction error is possible only under availability of unlimited data, which seldom happens. Therefore an expected value of the true prediction error/loss function $\xi = \mathrm{E}[L]$ is to be estimated from a limited and observable data $\mathrm{S_T} = \{\mathbf{x}_i, y_i\}_{i=1}^{n}$. It is to be noted that for the expected loss ξ, to be a reliable estimate of the true model error, must be computed on unseen validation sample and not on the data used to train the model. Model selection and performance estimation, when done on the basis of ξ which is computed on unseen validation sample, ensure that the model generalizes well on unseen validation sample and does not overfit the training sample. Therefore it is desirable that ξ is the model's generalized prediction error or average prediction error observed on unseen validation sample.

The requirement of a generalized prediction error ξ is the motivation for k-fold cross validation which enables computation of ξ through repeated random sub-sampling of the training data $\mathrm{S_T}$. For given model parameters $\boldsymbol{\theta}$ and explanatory variables or features $\mathbf{x}$, estimation of ξ through k-fold cross validation involves the following three steps:

A. Randomly divide the training sample $\mathrm{S_T}$ into k folds or validation samples $\mathbf{S}_\mathrm{V}^{(1)}, \mathbf{S}_\mathrm{V}^{(2)}, \ldots, \mathbf{S}_\mathrm{V}^{(k)}$ each approximately of $m \approx n/k$ instances

B. For each $j = 1, 2, \ldots, k$ perform the following sub steps:

- Train the model $f^{(j)}$ using instances from $\{\mathbf{S}_T^{(g)}\}_{g \neq j}$

- Consider $\mathbf{S}_\mathrm{V}^{(j)}$ as the validation sample and predicted the response for instances in $\mathbf{S}_\mathrm{V}^{(j)}$

- Compute loss function $L^{(j)}$ using the actual and predicted values for fold $\mathbf{S}_\mathrm{V}^{(j)}$. For example, the mean squared error loss for the jth fold is

253

computed as $L^{(j)} = \dfrac{1}{m} \displaystyle\sum_{i=1}^{m} \left(y_i - f^{(j)}\left(\mathbf{x}_i, \boldsymbol{\theta}\right)\right)$

C. Compute the generalized prediction error ξ by taking average of 'k' fold

errors i.e. $\xi = \dfrac{1}{k} \displaystyle\sum_{j=1}^{k} L^{(j)}$.

The number of folds 'k' is set by the user and is usually kept at 3, 5, 10 etc. depending upon computational effort required to train the model f and number of instances in training sample S_T.

The k-fold cross validation technique is used in this thesis for polynomial feature selection and surrogate model parameter tuning (for example parameters of GPK correlation function).

Detailed research on k-fold cross validation is done by (Shao, 1993; Kohavi, 1995) and other authors.

APPENDIX B

BEST LINEAR UNBIASED ESTIMATOR OF KRIGING

The Gaussian Polynomial Kriging (GPK) surrogate model can be expressed

$$\hat{y} = \sum_{j=1}^{m} \beta_j h_j(\mathbf{x}) + Z(\mathbf{x}) \tag{B.1}$$

whereby the linear regression $\sum_{j=1}^{m} \beta_j h_j(\mathbf{x})$ provides a global approximation of the response over the domain of control parameters and the local non-linearities are modelled by the Gaussian process $Z(\mathbf{x})$. The regression component is based on polynomial features $\mathbf{h}(\mathbf{x}) = \{h_1(\mathbf{x}), h_2(\mathbf{x}), ..., h_m(\mathbf{x})\}$. The Gaussian process $Z(\mathbf{x})$ has mean $E[Z(\mathbf{x})] = 0$ and covariance, $\mathrm{cov}\big(Z(\mathbf{x}_i), Z(\mathbf{x}_k)\big) = \sigma^2 R(\mathbf{x}_i, \mathbf{x}_k; \boldsymbol{\theta})$. Here, σ^2 is the variance of the Gaussian process and $R(\cdot)$ is the exponential correlation function, which is described as

$$R(\mathbf{x}_i, \mathbf{x}_k) = \exp(-\sum_{j=1}^{d} \frac{\left| x_{ij} - x_{kj} \right|^{\alpha}}{\gamma_j}) \tag{B.2}$$

$R(\cdot)$ has parameters $\boldsymbol{\theta} = \{\gamma_1, \gamma_2, \ldots, \gamma_d; \alpha\}$. For given $\mathbf{h}(\mathbf{x})$ and $\boldsymbol{\theta}$, best linear unbiased estimators (BLUE) of variance of the Gaussian process σ^2 and coefficients of the regression component, $\boldsymbol{\beta} = \{\beta_1, \beta_2, ..., \beta_m\}$ and can be expressed as a function of the training data and $\boldsymbol{\theta}$. The process of determining BLUE for σ^2 and $\boldsymbol{\beta}$ is now described.

Given training sample $S_T = \{\mathbf{x}_i, y_i\}_{i=1}^n$, Eq. (B.3) suggests a linear predictor of the response $y(\mathbf{x}')$ at an unseen test point $\mathbf{x}'$.

$$\hat{y}(\mathbf{x}') = \mathbf{w}^T\mathbf{y} \tag{B.3}$$

where $\mathbf{y} = [y_1, y_2,..., y_n]^T$ is a $n\times 1$ vector of the response obtained from the training sample S_T and $\mathbf{w}$ is a $n\times 1$ weight vector. The expected mean squared error of the linear estimator prescribed in Eq. (B.3) as is

$$MSE[\hat{y}(\mathbf{x}')] = E[(\hat{y}(\mathbf{x}') - y(\mathbf{x}'))^2] = E[(\mathbf{w}^T\mathbf{y} - y(\mathbf{x}'))^2] \tag{B.4}$$

where $y(\mathbf{x}')$ is the actual response at the test point $\mathbf{x}'$.

The BLUE of $y(\mathbf{x}')$ is given by the weight vector $\mathbf{w}$ which minimizes $MSE[\hat{y}(\mathbf{x}')]$ subject to the unbiasedness constraint

$$E[\mathbf{w}^T\mathbf{y}] = E[y(\mathbf{x}')] \tag{B.5}$$

Let $\mathbf{H}$ denote the $n\times m$ design matrix of a set of 'm' polynomial features $\mathbf{h}(\mathbf{x})$ and $\mathbf{R}$ be the $n\times n$ correlation matrix based on training samples $S_T = \{\mathbf{x}_i, y_i\}_{i=1}^n$ for response y. The correlation between the untried design point $\mathbf{x}'$ and instances in the training sample S_T is $\mathbf{r}' = [R(\mathbf{x}',\mathbf{x}_1), R(\mathbf{x}',\mathbf{x}_2),..., R(\mathbf{x}',\mathbf{x}_n)]^T$. All correlations are computed based on the exponential correlation function $R((\mathbf{x}_i,\mathbf{x}_k);\boldsymbol{\theta})$, which has given parameters $\boldsymbol{\theta}$. Based on these definitions the MSE can be rewritten as

$$MSE[\hat{y}(\mathbf{x}')] = \sigma[1 + \mathbf{w}^T\mathbf{R}\mathbf{w} - 2\mathbf{w}^T\mathbf{r}'] \tag{B.6}$$

Moreover the unbiasedness constraint suggested in Eq. (B.5) implies that $\mathbf{H}^T\mathbf{w} = \mathbf{h}'$, where $\mathbf{h}' = [h_1(\mathbf{x}'), h_2(\mathbf{x}'),..., h_m(\mathbf{x}')]^T$ are the polynomial features at the point $\mathbf{x}'$. The weight vector $\mathbf{w}$ of the BLUE satisfies the following Langrangian formulation

$$\begin{pmatrix} 0 & \mathbf{H}^T \\ \mathbf{H} & \mathbf{R} \end{pmatrix} \begin{pmatrix} \lambda \\ \mathbf{w}^T \end{pmatrix} = \begin{pmatrix} \mathbf{h}' \\ \mathbf{r}' \end{pmatrix} \tag{B.7}$$

where λ is the Lagrange multiplier for the constrained minimization of $MSE[\hat{y}(\mathbf{x}')]$. The BLUP of $y(\mathbf{x}')$ obtained after inverting the partitioned matrix and is given by

$$\hat{y}(\mathbf{x}') = \mathbf{h}'(\mathbf{H}^{\mathrm{T}}\mathbf{R}^{-1}\mathbf{H})^{-1}\mathbf{H}^{\mathrm{T}}\mathbf{R}^{-1}\mathbf{y} + \mathbf{r}'\mathbf{R}^{-1}\left(\mathbf{y} - \mathbf{H}(\mathbf{H}^{\mathrm{T}}\mathbf{R}^{-1}\mathbf{H})^{-1}\mathbf{H}^{\mathrm{T}}\mathbf{R}^{-1}\mathbf{y}\right) \qquad \text{(B.8)}$$

It is noteworthy that the estimated coefficients $\hat{\boldsymbol{\beta}}$ of the polynomial features $\mathbf{h}(\mathbf{x})$ are the generalized least squares estimate $\hat{\boldsymbol{\beta}} = (\mathbf{H}^{\mathrm{T}}\mathbf{R}^{-1}\mathbf{H})^{-1}\mathbf{H}^{\mathrm{T}}\mathbf{R}^{-1}\mathbf{y}$ and hence Eq. (B.8) can be simplified as follows.

$$\hat{y}(\mathbf{x}') = \mathbf{h}'\hat{\boldsymbol{\beta}} + \mathbf{r}'\mathbf{R}^{-1}\left(\mathbf{y} - \mathbf{H}\hat{\boldsymbol{\beta}}\right) \qquad \text{(B.9)}$$

Moreover the maximum likelihood estimation (MLE) of the process variance σ^2 is

$$\hat{\sigma}^2 = \frac{1}{n}(\mathbf{y} - \mathbf{H}\hat{\boldsymbol{\beta}})^{\mathrm{T}}\mathbf{R}^{-1}(\mathbf{y} - \mathbf{H}\hat{\boldsymbol{\beta}}) \qquad \text{(B.10)}$$

At this stage it is important to note that both $\hat{\boldsymbol{\beta}}$ and $\hat{\sigma}^2$ have been derived as functions of the parameters $\boldsymbol{\theta}$ of the exponential correlation function $\mathrm{R}(\cdot)$. $\boldsymbol{\theta}$ are either set by the user $\mathbf{R}$ or can be determined by the method of MLE. The log likelihood is a function of the coefficients $\boldsymbol{\beta}$ of the regression model, the process variance σ^2 and parameters $\boldsymbol{\theta}$ of the correlation function $\mathbf{R}$. Now given the estimated regression coefficients $\hat{\boldsymbol{\beta}}$ and estimated process variance $\hat{\sigma}^2$, the MLE of $\boldsymbol{\theta}$ is obtained by minimizing $det(\mathbf{R})^{1/n}\hat{\sigma}^2$, which is a function of the correlation parameters $\boldsymbol{\theta}$ only. Hence using the given training sample $S_{\mathrm{T}} = \{\mathbf{x}_i, y_i\}_{i=1}^{n}$, the parameters of the correlation function can be determined by running an optimization algorithm such as conjugate gradient, Nelder-Mead, BFGS etc. which identifies optimal $\boldsymbol{\theta}$ which minimizes the log likelihood.

The correlation function $\mathrm{R}(\cdot)$ is also referred to as the kernel function. Kernel optimization for kriging refers to determining the correlation function/kernel

parameters θ and this can be done by MLE. In this thesis, a hybrid approach of kernel optimization bas been developed which integrates MLE with minimization of the kriging surrogate model's generalized prediction error which is estimated by *k*-fold cross validation. Using case studies on surrogate modeling for fixture design analysis tool, the proposed hybrid approach to kernel optimization has been shown to generate kriging surrogate models which have a better performance on unseen test samples than those for which kernel optimization is done by state of the art MLE. (Sacks, *et al*., 1989) describes the process of generating BLUE estimator for the regression coefficients and variance of Gaussian process.

APPENDIX C

ADDITIONAL CASE STUDY ON
OPTIMAL MULTI RESPONSE ADAPTIVE SAMPLING

C.1 Introduction

This appendix illustrates Optimal Multi Response Adaptive Sampling (O-MRAS) method using 2-D benchmark functions which are commonly used to evaluate surrogate modelling algorithms. The objectives of this appendix are (i) to describe the steps of O-MRAS using 2-D examples; and, (ii) to compare performance of O-MRAS with uniform random sampling.

The iterative surrogate modelling approach described in Chapter 3 is used to develop Greedy Polynomial Kriging (GPK) surrogate models of two well-known benchmark functions. Figure C.1 schematically describes the surrogate modelling approach used for the comparative study. To compare performance of O-MRAS versus uniform random sampling, the GPK surrogate models are built first using O-MRAS (process 1) and then by uniform random sampling (process 2).

In iteration one, the design matrix of control parameters ($\mathbf{x}$), for both process 1 and 2, is generated by 2 factor 5 level full-factorial design and therefore has 25 instances. During each subsequent iteration, the design matrix on $\mathbf{x}$ having 25 instances is generated by O-MRAS for process 1 and by uniform random sampling for process 2. Iterations are stopped when average degree of determination (R^2) of the surrogate models exceeds 0.90 on a test dataset from 200×200 regular grid of $\mathbf{x}$

In this appendix, selection of design matrix via O-MRAS (Step 5 of process 1) is described in details.
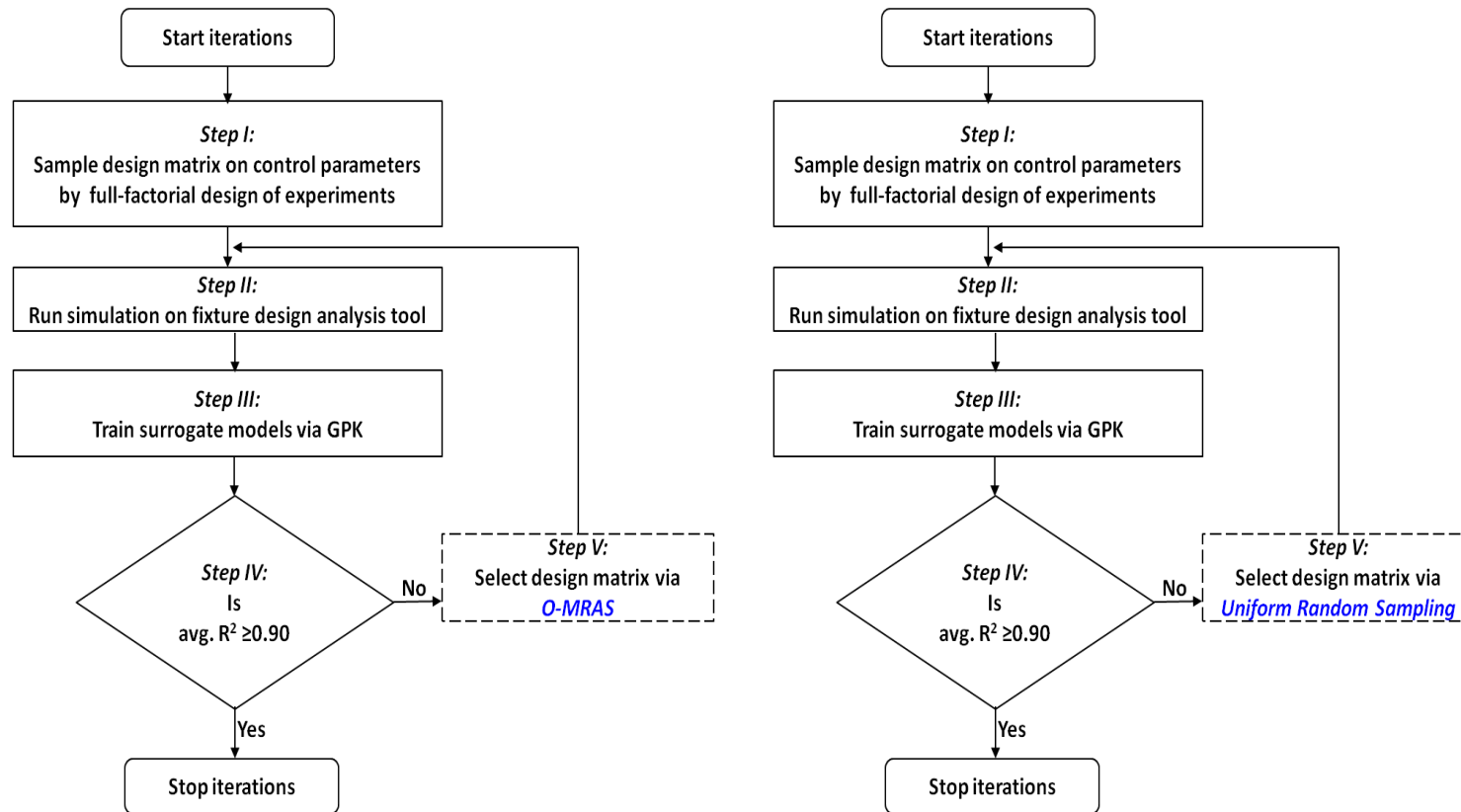
Figure C.1: Comparative study of surrogate modelling via O-MRAS versus Uniform Random Sampling

C.2 Optimal Multi Response Adaptive Sampling

This section illustrates using two bivariate benchmark functions how an adaptive sample for multiple responses is generated by O-MRAS. Details about benchmark functions are described by (Surjanovic & Bingham, 2013). The benchmark functions used for this comparative analysis are:

i. *Three hump camel function* − This bivariate function is evaluated in the domain $x_i \in [-2,2]$ for i=1 and 2. Eq. (C.1) shows this function.

$$y_1 = 2x_1^2 - 1.05x_1^4 + \frac{x_1^6}{6} + x_1 x_2 + x_2^2 \qquad (C.1)$$

Figure C.2 shows plot of the function in the aforementioned domain.
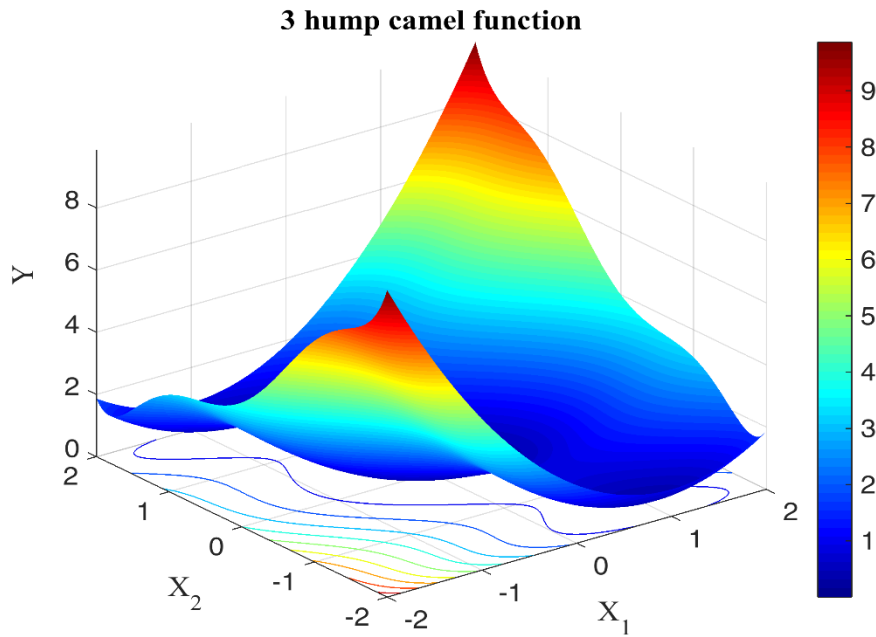
Figure C.2: 3 hump camel function

ii. *Shubert function* − This bivariate function is also evaluated in the domain $x_i \in [-2, 2]$ for i=1 and 2. Eq. (C.2) shows this function.

$$y_2 = \left(\sum_{i=1}^{5} i \cos\big((i+1)x_1 + i\big) \right)\left(\sum_{i=1}^{5} i \cos\big((i+1)x_2 + i\big) \right) \qquad (C.2)$$

Figure C.2 shows plot of the function in the aforementioned domain.
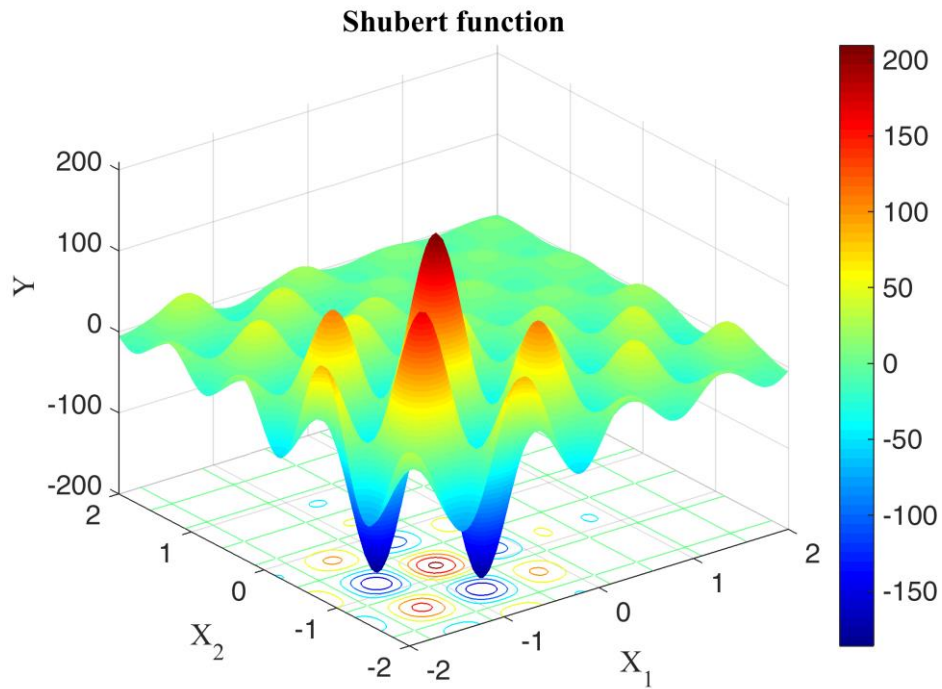
Figure C.3: Shubert function

GPK surrogate models of 3 hump camel function (y_1) and Shubert function (y_2) are developed through the iterative processes shown in Figure C.1. During each iteration in process 1, adaptive sample of the control parameters ($\mathbf{X}$) is generated by O-MRAS, which has three major steps. The steps of O-MRAS are illustrated using the bivariate examples as follows:

A. *Generate adaptive samples for individual responses* – Adaptive samples for individual responses (y_1 and y_2) are generated using Lipschitz criterion. This result in two design matrices $\mathbf{X}_C^{(1)}$ and $\mathbf{X}_C^{(2)}$ each having 25 instances or points from the domain of the control parameters. Each point has an associated merit υ_i which measures the goodness of the point for being selected in adaptive sample. Figure C.4 and C.5 show the 25 points selected

for 3 hump camel function and Shubert functions respectively. As expected, Lipschitz criterion based adaptive sampling has chosen points from regions where the functions are steep.
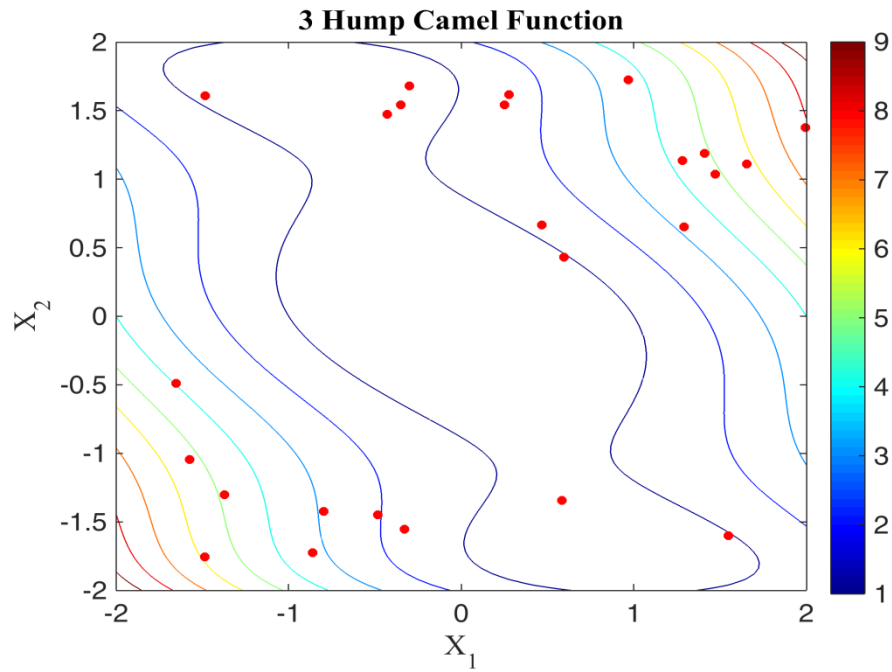
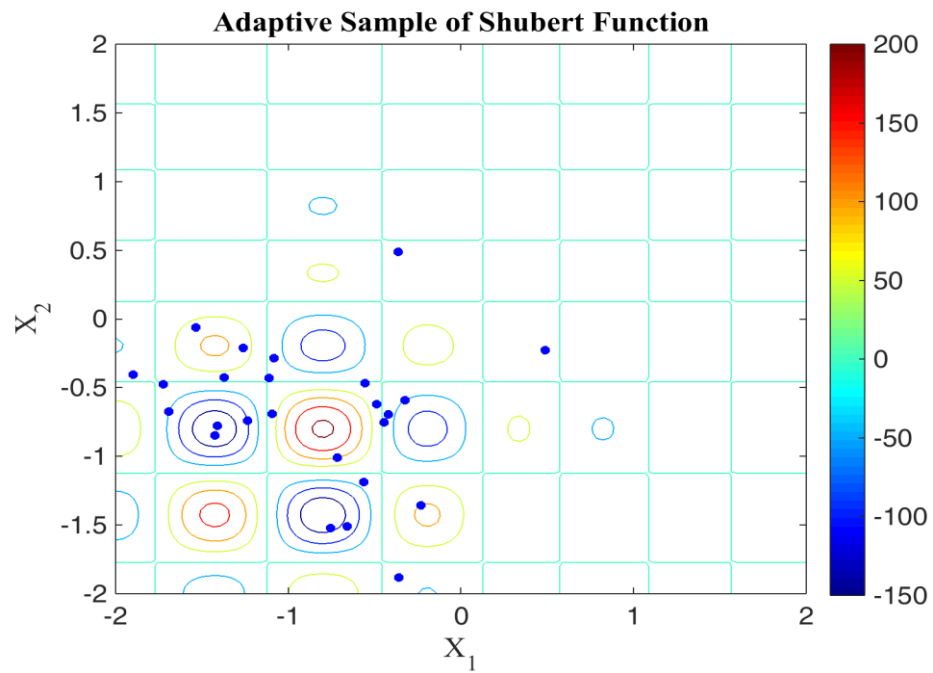**Figure C.4**: Adaptive sample of 3-Hump Camel function

Figure C.5: Adaptive sample of Shubert function

Adaptive samples of $\mathbf{X}_C^{(1)}$ and $\mathbf{X}_C^{(2)}$ have a total of 50 points which are shown on a 2-D grid in Figure C.6. To run the simulations, an optimal adaptive sample $\mathbf{X}_C^*$ of 25 points is identified from the union of $\mathbf{X}_C^{(1)}$ and $\mathbf{X}_C^{(2)}$ in steps *B* and *C*.
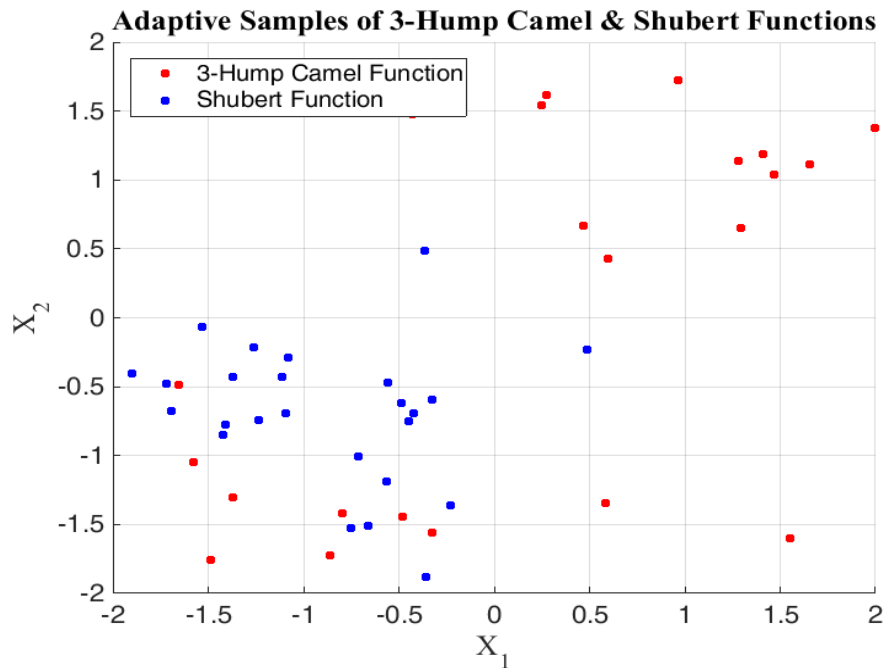
Figure C.6: 50 points from adaptive samples of 3-Hump of Shubert function

B. *K-means clustering to identify 25 groups* – The points generated by adaptive sampling on individual responses are clustered into 25 groups by *k*-means clustering. '*k*' represents number of clusters or groups to be identified hence in this case *k*=25. Figure C.7 shows the 25 clusters identified.
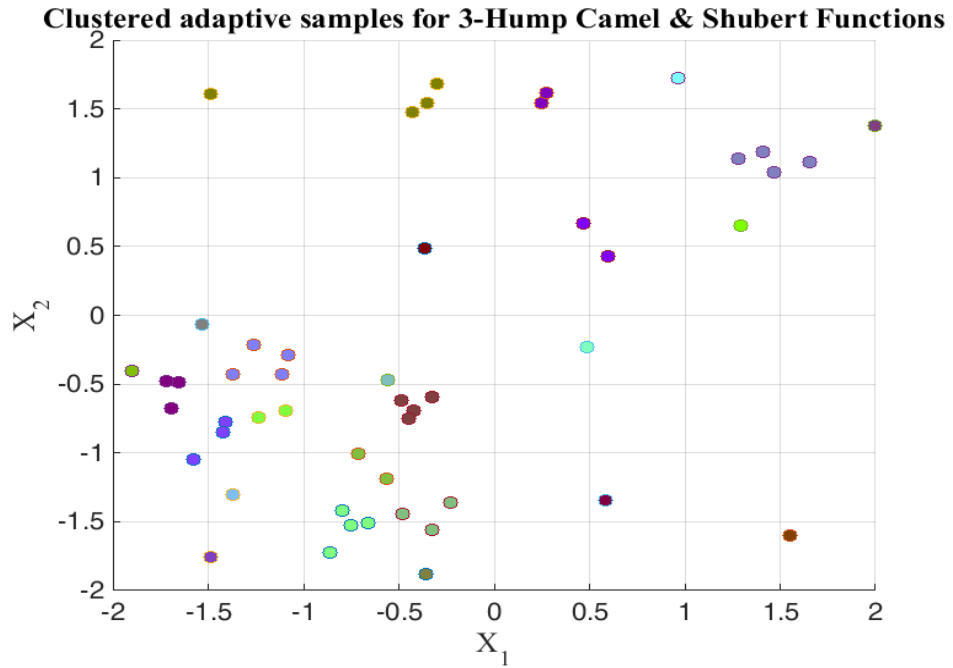
Figure C.7: 50 points grouped in 25 clusters

C. *Identify optimal point from each cluster* – Points in each cluster is analysed to identify an optimal point which is the best representative of the cluster. The optimal point is the one which maximizes a weighted average of merit and proximity to the cluster centroid. Figure C.8 illustrates the selection of an optimal point for a cluster which as 3 candidate points.
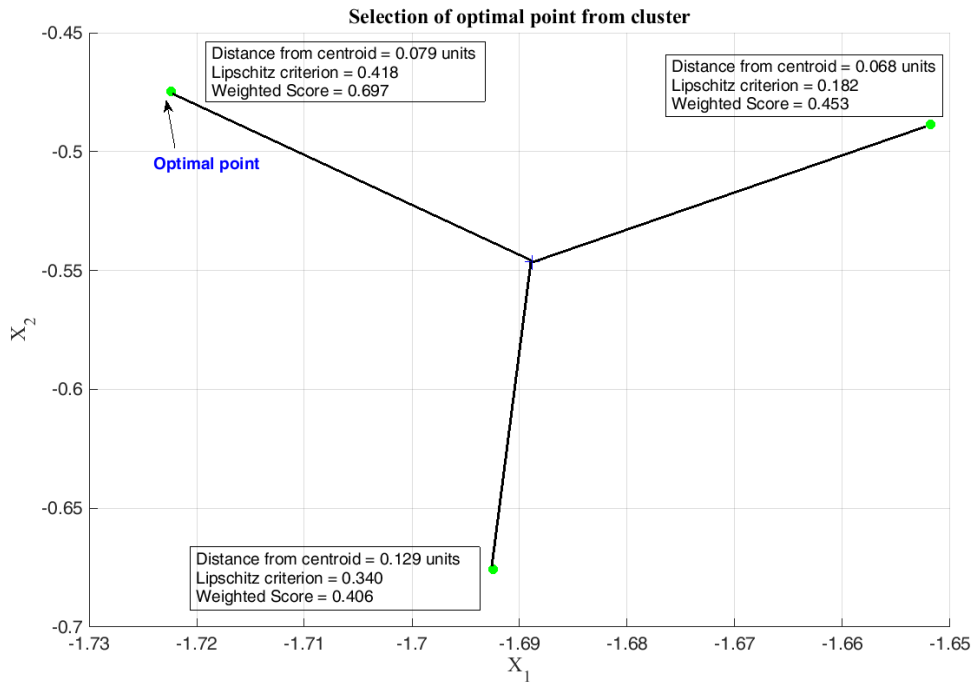
Figure C.8: Cluster-wise selection of optimal point

In summary, O-MRAS generates a single adaptive sample from individual adaptive samples of multiple responses. Merging individual adaptive samples and identifying a single adaptive sample which is an optimal representative of the individual adaptive samples is important for computationally expensive simulation routines such as fixture design analysis tools. Hence for practical applications O-MRAS drastically reduces time that would have been required to simulate 'r' individual responses separately.

C.2 Comparison of performance of O-MRAS and uniform random sampling

Surrogate models such as GPK are trained over multiple iterations of computer simulation. During each iteration adaptive sampling identifies the design matrix of control parameters ($\mathbf{x}$) which must be used as an input to computer

simulation. Data generated from simulation is then used to train the surrogate model during the current iteration. The objective of adaptive sampling is to identify the design matrix of **x** so that the resulting training data would be most informative in developing the surrogate models and hence accelerate achievement of the stopping criteria. In effect adaptive sampling reduces the number of computer simulations required to build surrogate models of desirable accuracy. A comparative study between O-MRAS and uniform random sampling is done by training GPK surrogate models for 3 hump camel function and Shubert function in an iterative manner. Each iteration adds 25 points to the training data. Design matrix for the 25 points is identified by O-MRAS and uniform random sampling. Figure C.9 shows the average R^2 of the GPK surrogate models over different iteration. It is evident that O-MRAS helps GPK surrogate models to achieve an average R^2 of more than 0.90 in lesser number of iterations than uniform random sampling.
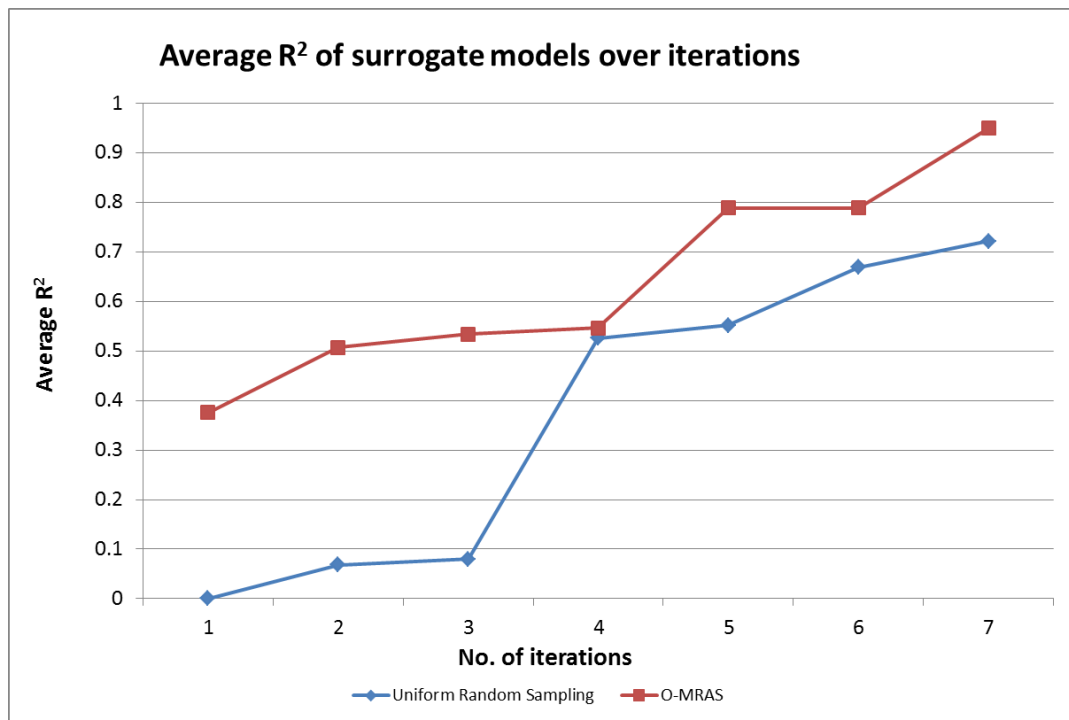

Figure C.9: Comparative analysis of O-MRAS and Uniform Random Sampling for developing GPK surrogate models

APPENDIX D
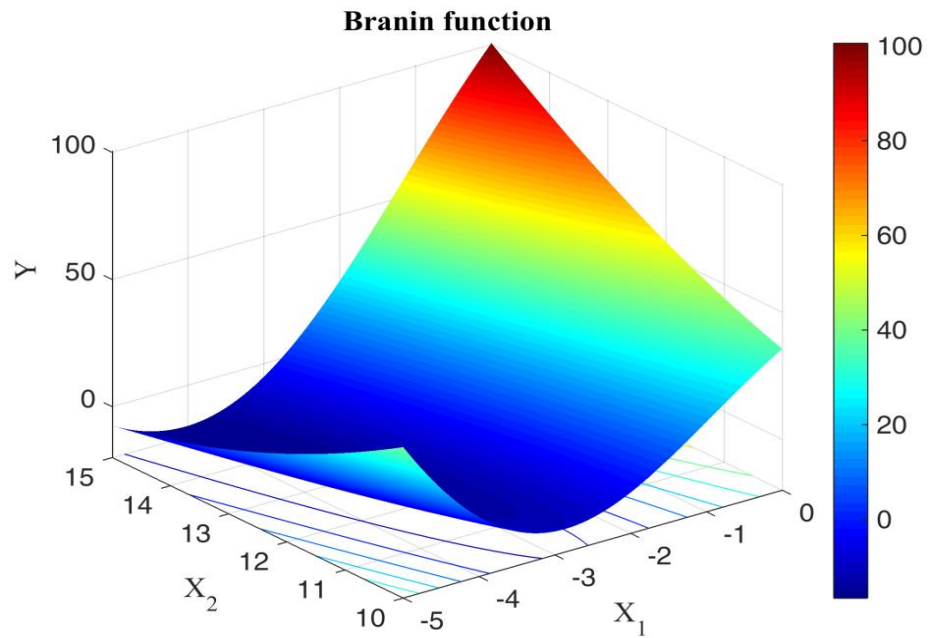
2D PLOTS OF BENCHMARK FUNCTIONS
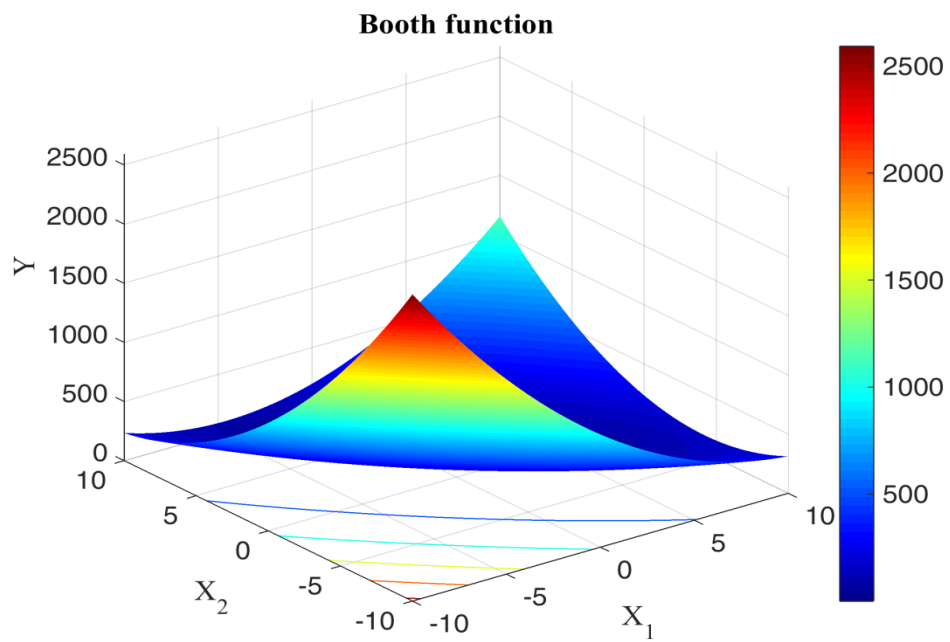

Figure D.1: 2D plot of Branin function

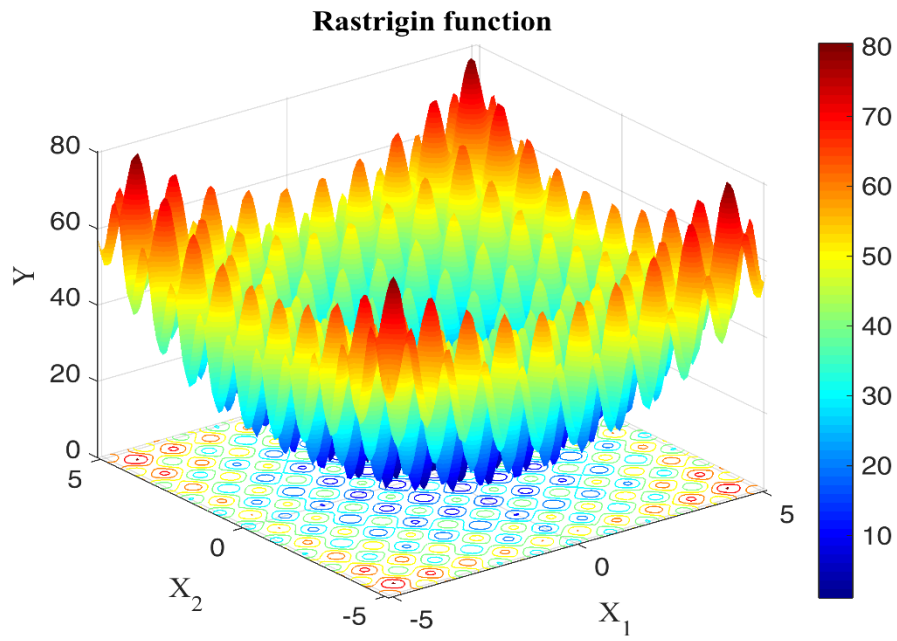**Figure D.2**: 2D plot of Booth function

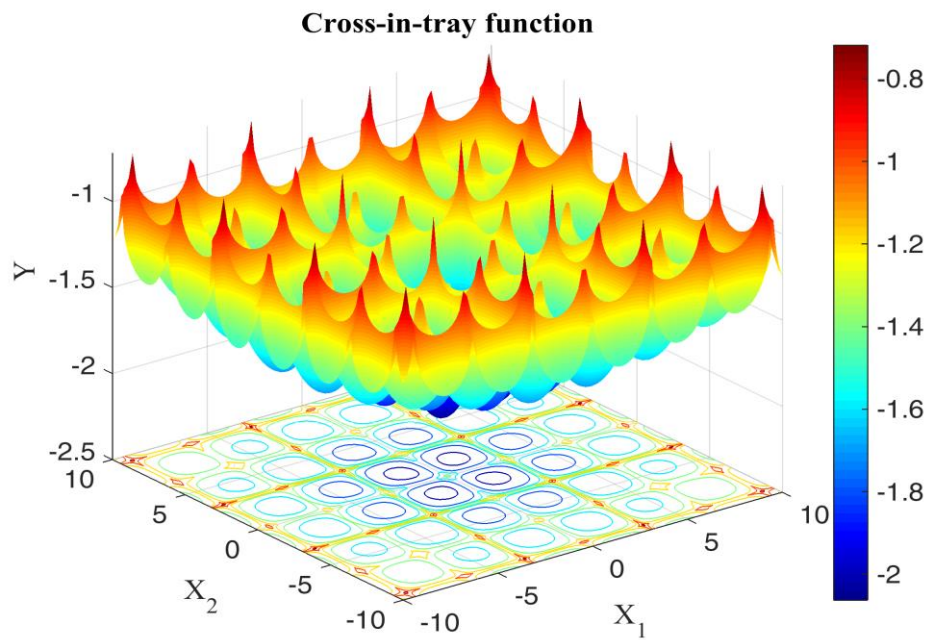**Figure D.3**: 2D plot of Rastrigin function

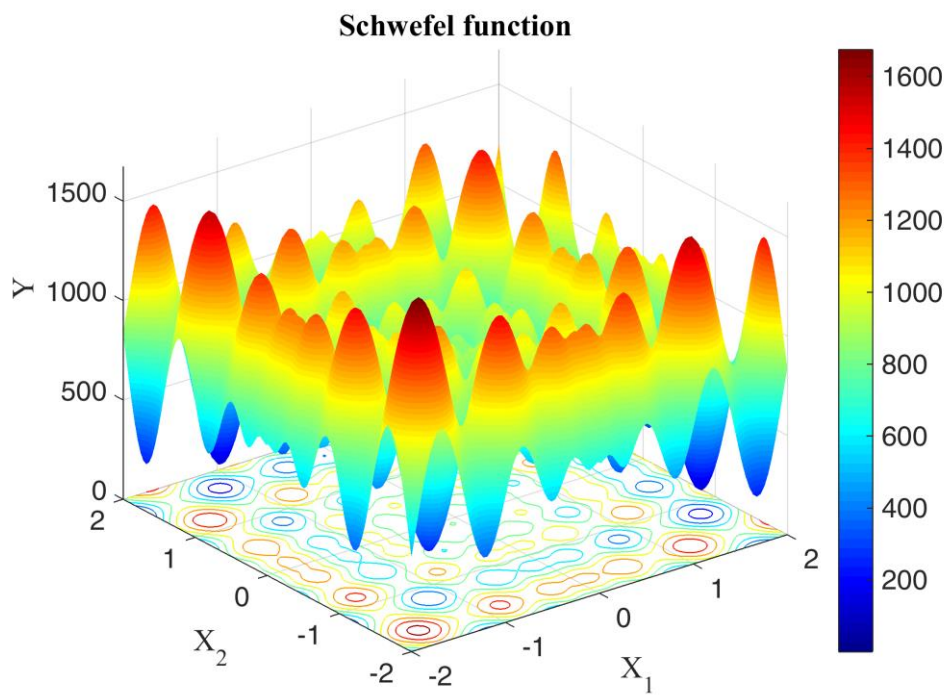**Figure D.4**: 2D plot of Cross-in-tray function
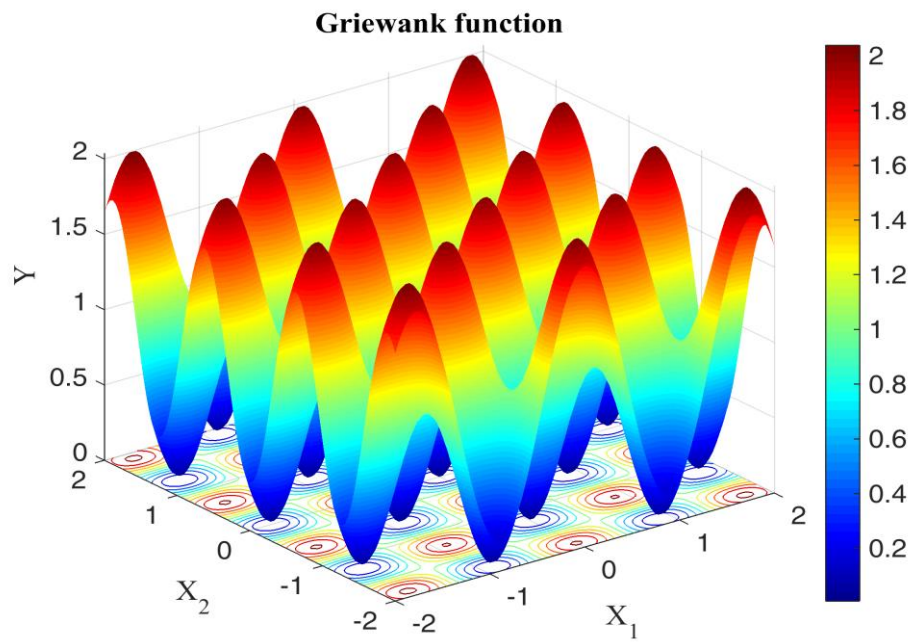
Figure D.5: 2D plot of Schwefel function

Figure D.6: 2D plot of Griewank function

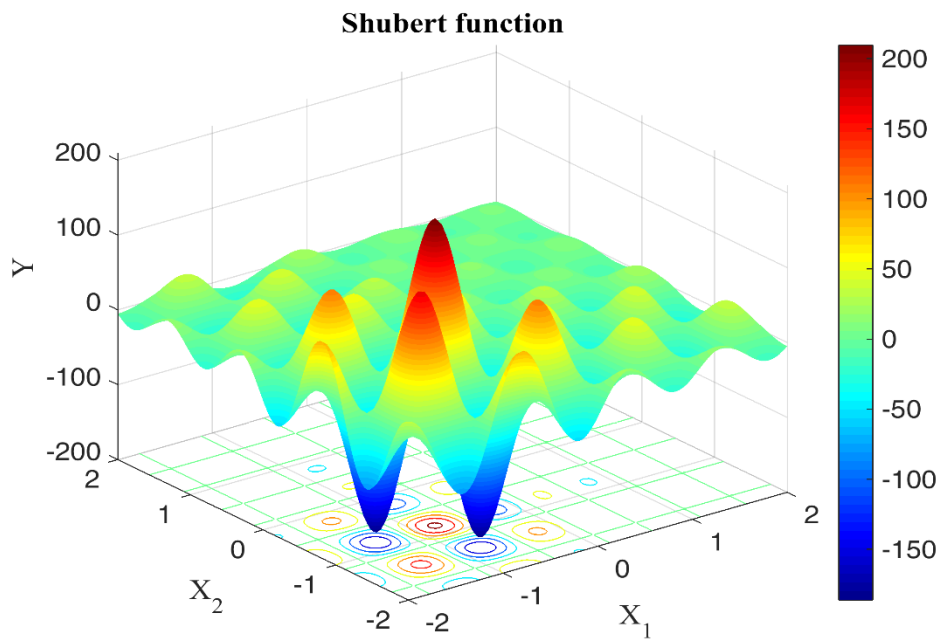**Figure D.7**: 2D plot of Shubert function

EXPERIMENTAL VERIFICATION OF SURROGATE MODELS FOR JOINING PROCESS PARAMETERS SELECTION

Chapter 4 has developed homo- and hetero-skedastic surrogate models of Key Product Characteristics (KPCs) in terms of Key Control Characteristics (KCCs) related to joining process parameters selection. The proposed surrogate models are developed based on data from physical experimentation in absence of comprehensive and useful *first-principle* based models of the joint KPCs.

This appendix presents experimental verification of the surrogate models developed in Chapter 4. Experimental verification for surrogate models of joint KPCs is necessary because of the lack of *first-principle* based models of the joint KPCs. This is in contrast to the surrogate models developed in Chapters 3 and 5 where data is taken from *first-principle* based Variation Simulation Analysis (VSA)[3].

To perform the experimental verification, physical experimentation on Remote Laser Welding (RLW) was performed at KCC_1=*welding speed*=2.8 m/min and KCC_2=*part-to-part gap*=0.2 mm. The *welding speed* was selected as 2.8 m/min as it is within the process window identified in Section 4.5.3 of Chapter 4. Each experimental sample was subjected to microscopic imaging (as described in Section 4.5.1 of Chapter 4) to measure the actual *part-to-part gap* and the following six KPCs related to the RLW process: (i) penetration; (ii) s-value; (iii) top surface concavity (TSC); (iv) bottom surface concavity (BSC); (v) top seam with (TSW); and, (vi) lower

---

[3] Accuracy of surrogate models developed in Chapters 3 and 5 are limited to the accuracy of VSA. Hence experimental verification of surrogate models developed in Chapter 3 and 5 are dependent on the experimental verification of VSA itself, which is beyond the scope of this thesis.

seam width (LSW).

The proposed homo- and hetero-skedastic surrogate models of the joint KPCs are used to predict the mean, variance, upper control limit and lower control limit of each experimental replication. The control limits are calculated at ± 3 sigma limits.

The objective of the experimental verification is to ascertain whether the observed (actual) KPCs are within the predicted upper and lower control limits.

Table E.1 shows the experimental data realted to KCCs and actual (observed) KPCs. Table E.2 shows predicted mean and predicted control limits of the KPCs for the five replications.

Table E.1: KCCs and actual (observed) KPCs for experimental verification

KCCs		Actual KPCs					
Welding speed	Part-to-part gap	Penetration	S-Value	TSC	BSC	TSW	LSW
2.8	0.09	1.04	1.04	0	0	1.33	0
2.8	0.155	0.97	1.21	0.13	0.05	1.26	0.5
2.8	0.205	0.96	1.29	0.18	0.01	1.14	0.41
2.8	0.13	1.06	1.12	0.15	0	1.14	0
2.8	0.205	0.96	1.29	0.18	0.01	1.14	0.43

Welding speed is measured in m/min and *part-to-part gaps* are measured in mm. All the six KPCs are measured in mm.

It is noteworthy that *welding speed* and *part-to-part gaps* listed in Table E.1 were not used to train the surrogate models. Hence the experimental verification described in this appendix provides verification on *unseen* test samples.

Table E.2: Predicted mean and predicted control limits of KPCs

Penetration		
Mean	UCL	LCL
0.898	1.510	0.286
0.888	1.501	0.276
0.873	1.485	0.261
0.893	1.506	0.281
0.873	1.485	0.261
S-Value		
Mean	UCL	LCL
0.732	1.142	0.322
0.935	1.494	0.376
1.053	1.704	0.402
0.863	1.370	0.356
1.053	1.704	0.402
TSC		
Mean	UCL	LCL
0.156	0.428	-0.116
0.198	0.470	-0.074
0.244	0.516	-0.028
0.179	0.451	-0.093
0.244	0.516	-0.028
BSC		
Mean	UCL	LCL
0.077	0.313	-0.158
0.077	0.313	-0.158
0.077	0.313	-0.158
0.077	0.313	-0.158
0.077	0.313	-0.158
TSW		
Mean	UCL	LCL
1.019	1.353	0.686
1.104	1.349	0.859
1.169	1.314	1.025
1.071	1.354	0.789
1.169	1.314	1.025
LSW		
Mean	UCL	LCL
0.227	0.575	-0.121
0.227	0.575	-0.121
0.227	0.575	-0.121
0.227	0.575	-0.121
0.227	0.575	-0.121

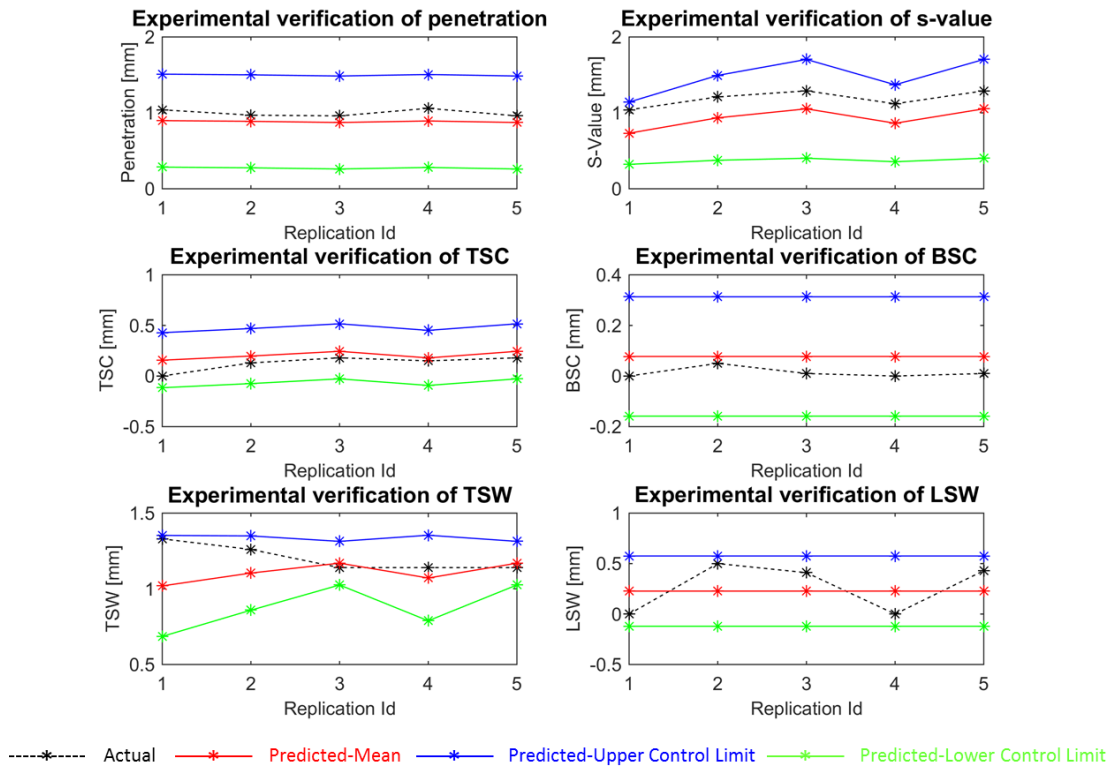Figure E.1 plots the actual and predicted KPCs.

Figure E.1: Visualisation of actual, predicted mean and predicted control limits of KPCs

Salient points about the results

The following salient points about the experimental verification are to be noted:

- In Table E.2, negative values in predicted LCL for TSC and BSC indicate change of weld surface curvature from *concavity* to *convexity*

- In Table E.2, negative values in predicted LCL for LSW indicate width of the lower surface of the weld when it is *convex* in shape

- Plots shown in Figure E.1 show that all joint KPCs are within the predicted UCL and LCL